UNIVERSITY OF SHEFFIELD

Department of Civil and Structural Engineering

SEMI-RIGID CONNECTIONS AND THEIR INFLUENCE ON STEEL COLUMN BEHAVIOUR

by

STEPHEN WYNFORD JONES

A thesis submitted to the University of Sheffield

for the Degree of Doctor of Philosophy

October, 1980

SUMMARY

A review of the development of the analysis of frames with semi-rigid end restraint is given, including the treatment of frame stability and effective lengths. The available experimental data relating to the moment versus in-plane rotational behaviour of practical beam-to-column connections, as used in steel frames, has also been reviewed. This data is found to be a non-linear function of connection deformation. Methods of mathematically modelling connection data have been reviewed and an improved representation based on the use of cubic B-spline curve fitting techniques is proposed.

An analytical procedure has been developed to investigate the influence of realistic end restraint on the strength and behaviour of "real" steel columns. A FORTRAN finite element computer program, which includes the effects of initial out-of-straightness, spread of yield and internal residual stresses is outlined. This is based on an incremental approach, with Newton-Raphson equilibrium iterations, to follow the load-deflection behaviour up to the maximum load level. The validity of the procedure is verified by comparison with available experimental data for an end restrained column test.

A parametric study was carried out to assess the behaviour of columns with semi-rigid end restraint.

The important parameters relating to the connection, the column section and the geometrical imperfections were studied. It was found that an increase in connection stiffness produces a corresponding reduction in column deflections and an increase in maximum load capacity, except in those cases where the column is so stocky that it can attain its full squash load.

Effective length factors calculated from these results indicate the column design economies that would be possible if the actual end restraint conditions were properly accounted for.

ACKNOWLEDGEMENTS

The author would like to express his appreciation and gratitude to Dr. D. A. Nethercot and Dr. P. A. Kirby, lecturers in the Department of Civil and Structural Engineering at the University of Sheffield, for their excellent guidance and supervision throughout. Words of appreciation are also extended to all other members of the academic and secretarial staff in the Department of Civil and Structural Engineering.

Thanks are due to Mrs. B. Green for her careful typing of this thesis.

The financial support of the Science Research Council is gratefully acknowledged.

CONTENTS

CONTENTS (Continued)(1)

CONTENTS (Continued)(2)

CONTENTS (Continued) (3)

CONTENTS (Continued)(4)

LIST OF FIGURES

LIST OF FIGURES (Continued)(1)

LIST OF FIGURES (Continued)(2)

LIST OF FIGURES (Continued)(3)

LIST OF TABLES

NOTATION

A	- Area of section
A_F, A_W	- Area of section's flange and web
A', B', C', D'	- Coefficients of generalised slope-deflection equation
a, b	- Extremes of spline function range
a_o	- Size of initial out-of-straightness
a_1, a_2, a_3, a_4	- Coefficients of single polynomial function
B	- Breadth of flange
C	- Connection size effects factor
C_{AB}, C_{BA}	- Moment-distribution carry over factors
C_e, C_p	- Modified alignment coefficient of reference 35
D_w	- Depth of web
d, g, t	- Variable connection dimensions
E	- Elastic modulus of material
E_{SH}	- Strain hardening elastic modulus
E_{ST}	- Elastic modulus of structural steel
E_t	- Tangent modulus
e	- Initial eccentricity
e_1, e_2	- End factors of reference 4
f	- Inverse of gradient of load-deflection curve
h	- Number of B-spline knots
I	- Moment of inertia of section
I_c, I_g	- Moment of inertia of column and beam section
j	- Joint ratio of reference 4
K_C	- Incremental rotational connection stiffness

NOTATION (Continued)(1)

K_s	- Linear spring stiffness
K_{ii}, K_{ii}'	- Initial and modified stiffness matrix leading diagonal terms
k	- Effective length factor
k_i	- B-Spline knot number i
L	- Real length of member
L_c, L_g	- Column and beam lengths
ℓ	- Effective length of member
M	- Moment at connection
M_p	- Fully plastic section moment
M_s	- Beam span moment
M_t	- Transition moment
M^F, M^F_{AB}, M^F_{BC}	- Fixed end moments
m	- Number of data points
n	- Order of spline function
P	- Axial load
P_{CR}	- Critical buckling load
P_E	- Euler buckling load
P_{MAX}	- Maximum load capacity of member
P_u	- Design load
P_Y	- Squash load
Δ_p	- Incremental load parameter
S_{AB}, S_{BA}	- Moment-distribution stiffness factors
W	- Uniformly distributed load
x	- Distance along member
x_f	- Distance along flange
x_r, f_r	- Moment-rotation data points
y_w	- Distance along web
Z, Z_A, Z_B	- Semi-rigid connection factors

Matrices:

$[B]$	- Strain-displacement matrix
$[K]$	- Overall stiffness matrix
$[K_G]$	- Geometrical stiffness matrix
$[K_S]$	- Normal stiffness matrix
$[K^e]$	- Element stiffness matrix
$[K_E^e]$	- Element elastic stiffness matrix
$[K_G^e]$	- Element geometrical stiffness matrix
$[\bar{K}_G]$	- Geometrical stiffness matrix for unit axial load

Vectors:

$\{E\}$	- Out-of-balance forces
$\{F\}$	- General loads
$\{F^e\}$	- Element loads
$\{F_{EXT}\}$	- Externally applied forces
$\{F_{INT}\}$	- Internal forces
$\{F_{ref}\}$	- Unit reference load vector
$\{P_o\}$	- Imaginary lateral loads
$\{\Delta F\}$	- Incremental loads
$\{\Delta\delta\}$	- Incremental deflection
$\{\delta\}$	- General member deflections
$\{\delta^e\}$	- Element deflections
$\{\varepsilon\}$	- Element strains

Greek terms:

α, β	- Semi-rigid slip factors
α_j, β_i	- B-Spline coefficients
γ	- Spline coefficients
δ	- Central deflection
δ_o	- Initial central deflection
ε	- Material strain
ε_{SH}, ε_y	- Strain hardening and yield strains
θ_A, θ_B	- Rotations at member ends
θ_o	- Initial rotational deflection
λ	- Slenderness ratio
λ'	- Modified slenderness ratio
σ	- Material stress
σ_F	- Residual stress at flange tips
σ_{FW}	- Residual stress at flange to web junction
σ_{RC}, σ_{RT}	- Compressive and tensile residual stresses
σ_{RF}, σ_{RW}	- General residual stresses in flange and web
σ_u	- Design stress
σ_{uy}, σ_{ult}	- Upper yield and ultimate stress of structural steel
σ_y	- Yield stress
σ_w	- Residual stress at centre of web
τ	- Estimate of automatic load increment truncation error
ϕ	- Connection rotation

CHAPTER 1

Introduction

1.1 Semi-Rigid Connections

Virtually all currently used methods for the design of steel frames (1, 2, 3) are based on the initial assumption that the joints will either behave as pin-connections or that they will provide full rotational continuity between adjacent members. Similar assumptions also form the basis of most methods of frame analysis. The Draft Standard for Structural Steelwork (4) continues to use these ideas with its consideration of "simple construction" and "continuous construction". The former approach is used most extensively in the design of steel frames. These two approaches have been used for many years despite the knowledge that real connections rarely behave in either manner. Experimental investigations of actual connection behaviour conducted at various times during the past fifty years have clearly shown that "simple" connections do possess a certain amount of rotational rigidity while nominally "rigid" connections have some degree of flexibility. Therefore it would be more correct to consider all real connections as "semi-rigid".

In the past, structural beam-to-column connections have been classified (5) with respect to their moment-rotation characteristics and the amount of end restraint provided. Three types of connection are illustrated in Figure 1.1 and are defined as follows:

1. Flexible connections are those which are capable of carrying the required end reaction, but which allow

relatively free rotation between the end of the beam and the column.

2. Rigid connections are those in which the rotation is reduced to a minimum by the use of heavy connection details.

3. Semi-rigid connections are those which transmit bending moment with some degree of rotation, thereby providing a degree of end restraint somewhere between complete rigidity and complete flexibility.

An obvious advantage of a design utilising semi-rigid connections is that beam moments are reduced leading to lighter beam sections. Figure 1.1 shows that for an isolated beam with simple connections the span moment is critical, whereas when rigid connections are assumed the end moments are critical for beam design. If semi-rigid end restraint is assumed the two moments may be more nearly balanced. Another source of economy lies in the design of the columns where a better understanding of actual end restraint should lead to more rationally based, less conservative methods of column design. All codes of practice rely heavily on the concept of effective length in the design of the column section, this being the length of a pin-ended column that has the same maximum load capacity as the restrained column. This effective column length is dependent upon the degree of end restraint present, so that if proper consideration of the actual restraint showed it to be

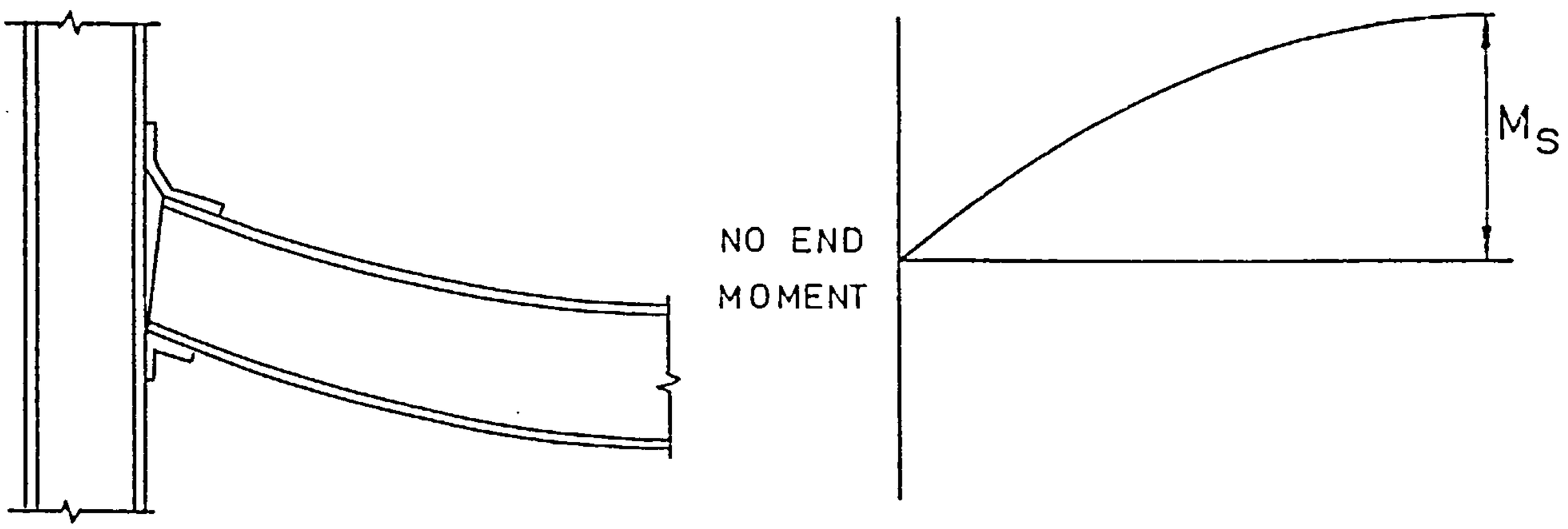

(a) Flexible Connection

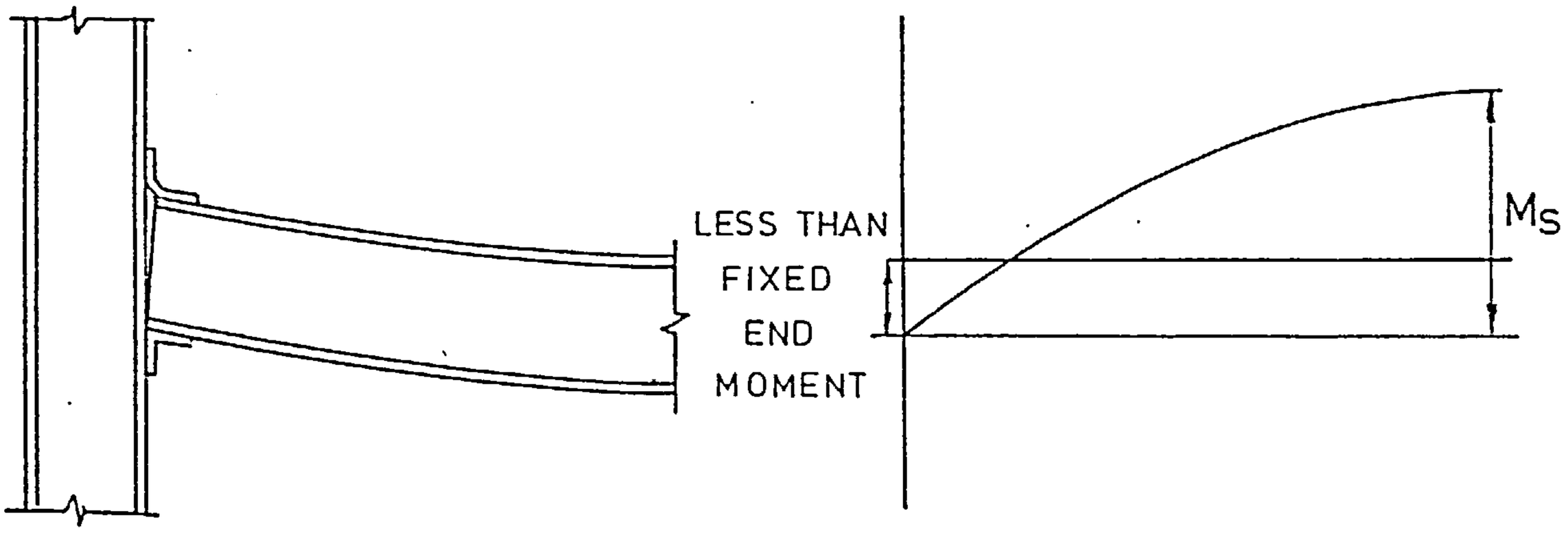

(b) Semi-Rigid Connection

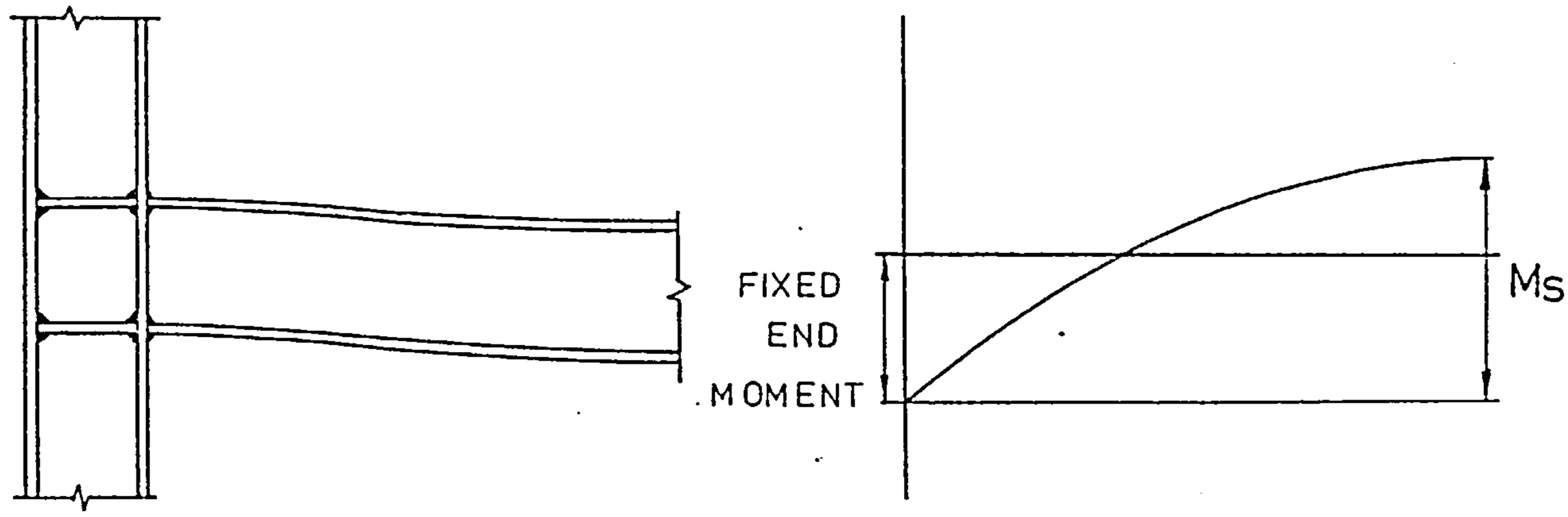

(c) Rigid Connection

FIGURE 1.1 - Classes of Beam-to-Column Connections

greater than commonly supposed it would be possible to use reduced effective lengths and hence lighter column sections would be required.

1.2 Objectives of the Investigation

The purpose of this investigation is to perform a general study of semi-rigid connections and their influence on the behaviour of end restrained steel columns. This general review is required since no complete study has been reported for forty years. The aims, therefore, of the present investigation are:

(i) to review methods of incorporating semi-rigid end restraint into conventional analytical methods,

(ii) to identify available experimental data on the behaviour of common types of structural connection,

(iii) to assess the suitability of methods of modelling this experimental data for use within analytical methods,

(iv) to develop an analytical technique to follow the load-deflection behaviour of an isolated "real" steel column with semi-rigid connections,

(v) to use this analysis to investigate the importance of the governing parameters such as:

a) type and size of connection,

b) type, size and bending axis of the column section,

c) initial out-of-straightness (geometrical imperfection),

d) initial residual stress pattern,

e) eccentricity of applied load, and

(iv) to assess the influence of realistic forms of end restraint on the effective length of columns.

1.3 Limitations of the Present Investigation

The present work is intended to study the nonlinear behaviour of an isolated column with realistic representations of the end restraint conditions. The column response is limited to in-plane bending, and so no flexural-torsional effects are considered. The load is assumed to be applied axially with possible end moments to represent any load eccentricity. During the analysis the load is assumed to be applied incrementally in a constantly increasing manner; loading is purely non-cyclic. Lateral loading has not been considered in the present investigation, although the analysis, as developed, permits these effects to be included. The response to be investigated is the load versus central deflection behaviour up to the maximum load level.

The column ends are connected by the semi-rigid end restraint to rigid supports, which represent beams with infinite stiffness. Any frame action due to the effects of rotations caused by beam bending is therefore neglected.

Comparison of results with experimental column tests, for which connection data is available, is very limited. Available connection data compatible with the column sections used in the parametric study is also limited.

This work rests on the assumption that the material has an elastic-perfectly plastic stress-strain characteristic, from which it follows that the effects of strain hardening are neglected.

CHAPTER 2

Literature Review of Semi-Rigid Analysis

2.1 Early Investigations into Semi-Rigid Connection Behaviour

The importance of the end restraint provided by semi-rigid connections, on the behaviour of beams and columns within structural frames, was realised over fifty years ago. The first investigation into the flexibility of riveted structural connections was reported by Wilson and Moore (6) in 1917.

Research workers in Britain (7, 8, 9), Canada (10) and the United States (11), in three separate investigations during the 1930's, measured the relations between moment transmitted by the connection and relative angle changes at beam-to-column connections in an attempt to provide data for semi-rigid connection design. Numerous tests on riveted, bolted and welded connections have since been reported. A review of available connection test data is given in Chapter 3. Early methods for predicting the end restraint provided by a connection for which the experimentally obtained moment-rotation relationship is known, using a graphical method, were proposed by Batho and Rowan (7). This method, known as the beam-line method, is discussed in more detail in Section 2.4. Young and Jackson (10) investigated

(i) the rotational capacity and end restraint provided by connections to reduce the beam moment due to gravity loads and also

(ii) the ability of connections in frames to resist horizontal deflections due to lateral or wind loads.

Methods of incorporating semi-rigid end restraint into classical methods of indeterminate frame analysis were proposed by both Baker (7) and Rathbun (11) independently. Both assumed a linear moment-rotation relationship and defined a semi-rigid connection factor Z (the angle change per unit moment) in order to perform the analysis.

From these early investigations into connection behaviour the possible economies were realised. According to British investigations (8) savings of as much as twenty per cent could be achieved on the design of beams in frames by taking advantage of semi-rigid end restraint.

2.2 Modified Methods of Indeterminate Frame Analysis to Allow for Semi-Rigid End Restraint

Conventional methods of indeterminate frame analysis have all been modified to allow for semi-rigid end restraint. The bases of these conventional methods are that frame deformations are due solely to the bending of members, but in practice extra deformation is caused by connection deformation. Slope-deflection, moment-distribution and matrix stiffness methods of analysis have been modified to allow for these extra connection deformations. Older methods such as the method of three moments and the deformeter method have also been modified.

The modification of all these methods uses the simplifying assumption that a linear moment-rotation

relationship exists, despite the fact that experiments have clearly shown that moment-rotation curves are non-linear over the full loading range, as shown in Figure 2.1. The linear assumption makes methods only strictly applicable for very low values of rotation, where the slope of the moment-rotation curve may be reasonably approximated by the inverse of the initial tangent connection factor Z.

2.2.1 Slope-deflection method

The slope-deflection method was first applied to frames with semi-rigid connections in 1936, by both Baker (8, 9, 12) and Rathbun (10) independently. The generalised slope-deflection equation for a beam of length L and flexural rigidity EI loaded by a uniformly distributed load W for the no-sway case can be written as:

$$M = \frac{2EI}{L} A'\left(B'\theta_A + C'\theta_B\right) - \frac{D'WL^2}{12} \qquad 2.1$$

The values of the coefficients A', B', C' and D' for both the conventional and modified methods are given in Table 2.1. The coefficients α and β used in Table 2.1 are defined as:

$$\alpha = \frac{2EI}{L}.Z_A \qquad \text{and} \qquad \beta = \frac{2EI}{L}.Z_B \qquad 2.2$$

where Z_A and Z_B are the semi-rigid connection factors for end A and B of the beam, respectively.

The slope-deflection method requires the solution of a series of simultaneous equations to determine

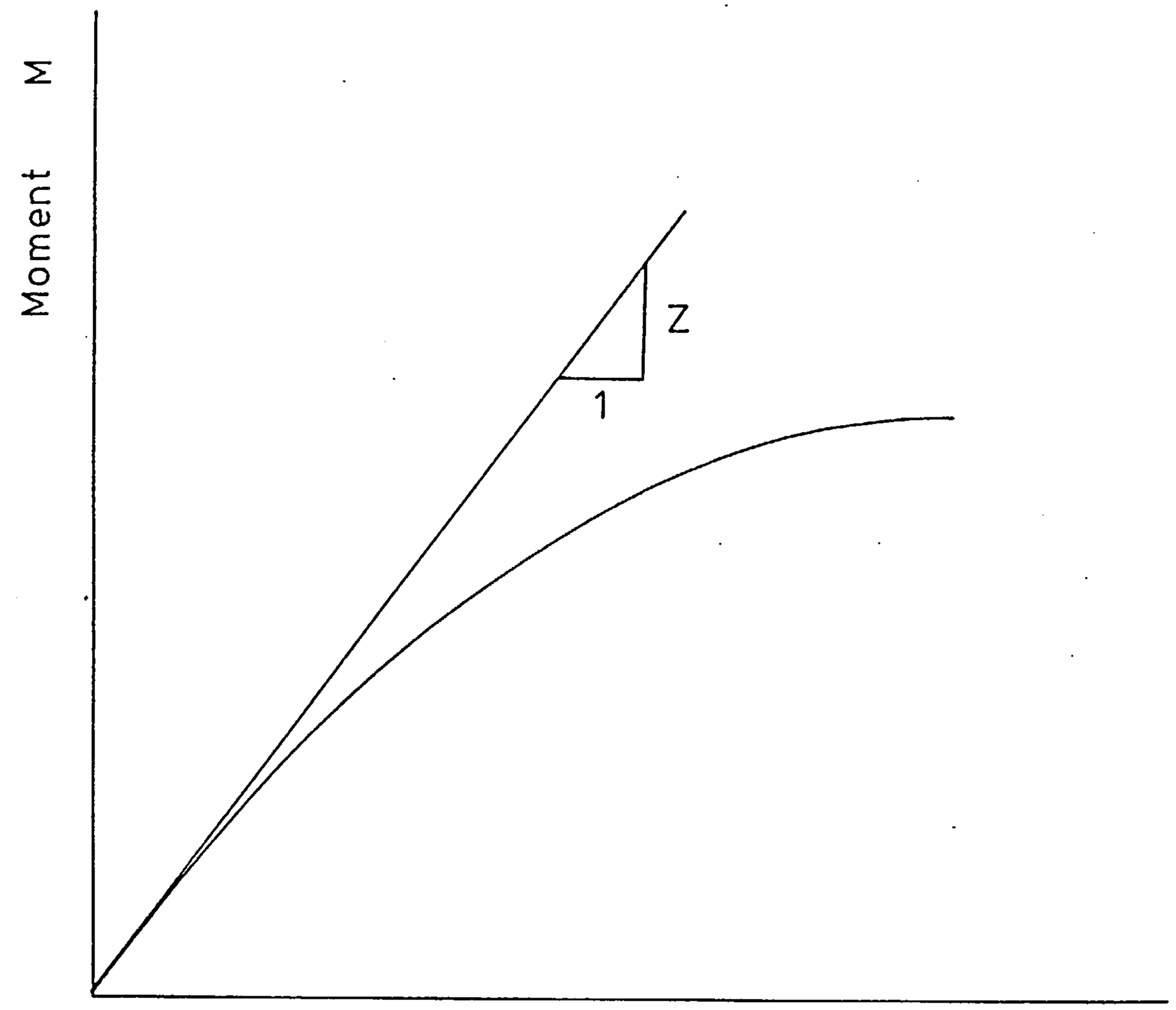

FIGURE 2.1 - Typical Moment-Rotation Curve of a Semi-Rigid Connection

TABLE 2.1 - Slope-Deflection Equation Coefficients

Coefficient	Conventional Slope - Deflection Method	Modified Slope - Deflection Method
A'_{AB}	1	$\frac{1}{(3\alpha\beta + 2\alpha + 2\beta + 1}$
B'_{AB}	2	$(3\beta + 2)$
C'_{AB}	1	1
D'_{AB}	1	$(3\beta + 1)$
A'_{BA}	1	$\frac{1}{(3\alpha\beta + 2\alpha + 2\beta + 1)}$
B'_{BA}	1	1
C'_{BA}	2	$(3\alpha + 2)$
D'_{BA}	-1	$-(3\alpha + 1)$

N.B. Factors α and β are defined in equation 2.2.

member end deflections. However, even for relatively small frames the number of equations to be solved is fairly large; in the days before electronic computers this method was very laborious for hand calculation.

2.2.2 Moment-distribution method

The moment-distribution method of analysis was modified to allow for flexible connections shortly after being first proposed by Hardy Cross (13) in 1930. Methods of incorporating the effects of semi-rigid connections into the analysis were proposed by Baker (8) and Rathbun (11). Johnston and Mount (14) developed the method to include the effects of the width of the column at the connection. More recently Gere (15) presented charts for easy evaluation of fixed-end moments, carry-overs and stiffness factors.

The original Hardy Cross method is confined to frames with perfectly rigid connections; the method when applied to frames with semi-rigid connections is performed in the same way. However, there are numerical differences in the values of fixed-end moments, carry-overs and stiffness factors. Table 2.2 gives a comparison of the conventional and semi-rigid moment-distribution factors for a beam of length L and flexural rigidity EI loaded by a uniformly distributed load W. For a semi-rigid frame, the factors of Table 2.2 can be evaluated and once obtained, the analysis is exactly the same as for a rigidly connected frame, the only extra work involved being the evaluation of the initial factors.

TABLE 2.2 - Comparison of Moment-Distribution Factors

Factor	Conventional M-D Method	Modified Method including Effects of Semi-Rigid Connections
Fixed-End Moment		
M_{AB}^{F}	$-\frac{WL^2}{12}$	$\frac{-(3\beta + 1)WL^2}{12(3\alpha\beta + 2\alpha + 2\beta + 1)}$
M_{BA}^{F}	$\frac{WL^2}{12}$	$\frac{(3\alpha + 1)WL^2}{12(3\alpha\beta + 2\alpha + 2\beta + 1)}$
Carry-Overs		
C_{AB}	$\frac{1}{2}$	$\frac{1}{(2 + 3\beta)}$
C_{BA}	$\frac{1}{2}$	$\frac{1}{(2 + 3\alpha)}$
Stiffness Factors		
S_{AB}	1	$\frac{(3\beta + 2)}{2(2\alpha\beta + 2\alpha + 2\beta + 1)}$
S_{BA}	1	$\frac{(3\alpha + 2)}{2(2\alpha\beta + 2\alpha + 2\beta + 1)}$

N.B. Factors α and β are defined in equation 2.2.

2.2.3 Some other analytical methods

The deformeter method, a method of mechanical structural analysis, uses a model of the structure made of celluloid sheet or other suitable elastic material. The model is proportioned so that the width of its members represent the relative rigidities of the members in the real frame. A modification of this method has been described by Baker (8) and Rathbun (11) in which the semi-rigid connection is represented by a local reduction in the width of the model at the connection positions.

Rathbun (11) described a modification to the theorem of three moments to account for the effects of elastic connections. Young and Jackson (10) first investigated the effects of semi-rigid connections on the sway deflections of frames in 1934. In the same year Baker (8) analysed a frame with side loads producing sway deflections using the moment-distribution method, this was later developed by Baker and Williams (9) in 1936. Stewart (16) applied the transverse method of analysis to a frame with elastic connections in 1947. Sourochnikoff (17) examined the behaviour of semi-rigidly connected frames subjected to combined gravity and horizontal wind loads and considered the behaviour of the connections due to moment reversals.

All the methods of analysis mentioned above are based on the assumption that structural connections have linear moment-rotation relationships.

2.2.4 Matrix stiffness methods

By 1960 the analysis of rigidly connected plane frames by matrix stiffness methods using electronic computers had become well established. In 1961 Lightfoot and Baker (18) produced a computer solution to the problem of plane frames with elastic connections, using the generalised slope-deflection equations in matrix form. The semi-rigid end restraint was incorporated into the analysis by the use of correction matrices to amend the initial assumption of fully rigid connections. Monforton and Wu (19) first incorporated the effects of semi-rigid connections into a matrix stiffness analysis program in 1963. Similar procedures were proposed by Livesley (20) and Gere and Weaver (21) at about the same time. The linear semi-rigid connection factor Z is used to modify the member stiffness matrices and the fixed-end forces vector. The stiffness matrices are modified by correction matrices and the resulting linear equations are solved as in the normal stiffness method. One particular advantage of the matrix stiffness method is that it can be programmed so that relatively large frames can be analysed with ease, and also improvements in the end restraint representation are possible using iterative correction techniques. Such a method will be developed in Chapter 4.

2.3 Investigations into Connection Behaviour to Provide Data for Design Methods

During the 1940's much experimental work was undertaken to provide moment-rotation data for bolted,

riveted and welded connections. A notable investigation by Hechtman and Johnston (5) at Lehigh University in 1947 considered the behaviour of 47 riveted connections. An extensive review of available connection moment-rotation data is given in Chapter 3.

Johnston and Hechtman (22) proposed a design procedure accounting for semi-rigid end restraint and suggested that economies of fifteen to twenty per cent of the weight of beams in a frame were possible by using their design procedures as opposed to assuming simple connections. In this method beams are first designed for the maximum moment assuming simple supports, then the ratio of beam stiffness to the sum of column stiffnesses at the joint is calculated. Charts equating this ratio to the percentage rigidity of the connection were provided from which a reduction factor, subsequently applied to the section modulus of the simply designed beam, may be obtained. A beam corresponding to this reduced section modulus is then used. Further design procedures were proposed by Johnston and Mount (14) and Hechtman and Johnston (5) as a result of their analytical and experimental investigations.

2.4 Early Methods of End Restraint Prediction

2.4.1 Beam line method

The Beam-line method is a graphical method which can be used to determine the actual end restraint provided by a connection using the actual measured moment-rotation curve.

The method was proposed by Batho and Rowan (8) and later developed by Batho (9) alone. Moment-area principles were used to derive the beam-line equation which gives the end restraining moment as a linear function of the angle of connection rotation, as shown in equation 2.3:

$$M = M^F - \frac{2EI\phi}{L} \qquad 2.3$$

This is for a beam of length L, of uniform section and of flexural rigidity EI. M^F is the calculated fixed-end moment due to the beam's applied loading. To determine the end restraint provided to the beam by a certain connection, this beam-line is drawn on the connection's moment-rotation curve, as shown in Figure 2.2.

The beam-line AB and the restraint line OQ intersect at a point P. The values of moment and angle of rotation at this intersection represent the end restraint conditions that would exist at the end of such a member when provided with the connection as described by the moment-rotation curve. An advantage of this method is that it uses the actual moment-rotation relationship and thus a more accurate value of the end restraint is found without the limitation of assuming linear moment-rotation behaviour. However, the method requires experimentally obtained moment-rotation data to be available for every connection analysed.

2.4.2 Elastic restraint equations

By the 1950's, methods of analysis for frames with semi-rigid connections were available. However,

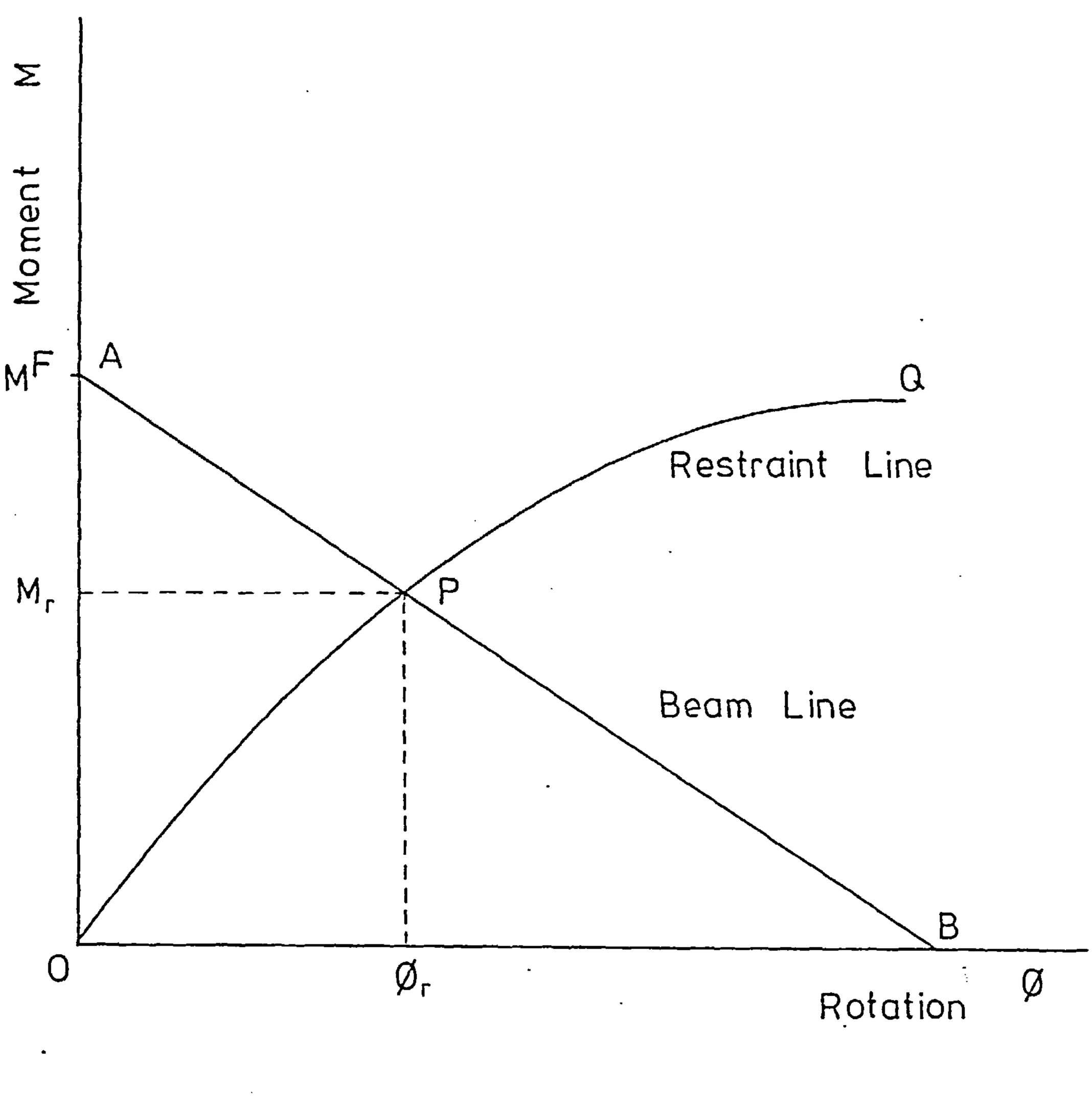

FIGURE 2.2 - Beam-Line Method

these methods could only be used to provide economy in frame design if data in the form of moment-rotation curves were available. If this data was not available expensive and time consuming laboratory tests had to be performed if semi-rigid design was to be considered. In an attempt to by-pass this experimental effort, methods for the prediction of the initial tangent semi-rigid connection factor Z were proposed by Lothers (23) in 1951. He derived elastic restraint equations which were applied to the analysis of web cleated connections. This work was extended to other connection types at Oklahoma State University (24, 25, 26) during the 1950's. These elastic restraint equations predicted values of the initial tangent connection factor which were shown to be in close agreement to the initial tangents of Rathbun's experimental results (11) for similar connections. The elastic restraint equation produces a single connection factor value and so represents a linear moment-rotation relationship subject to the usual limitations of this simplifying assumption. This initial tangent is, in practice, an upper bound of the connection stiffness, and this must be taken into account when used in semi-rigid design.

2.5 Developments in Structural Engineering Affecting Semi-Rigid Connection Analysis

2.5.1 Fasteners

The past fifty years have seen the strength of steel available to the structural engineer increase by a factor

of up to three, which has led to the development of the high strength friction grip (H.S.F.G.) bolt. During the period of the 1950's development of structural fasteners occurred as a result of two factors (27), firstly, the development of this H.S.F.G. bolt and secondly as a result of extensive research into fastening techniques.

Before 1950 riveting was the most common form of fastening used in structural connections. Most of the reported early investigations are on this type of connection. These have now generally been replaced by H.S.F.G. bolts as the principal type of fastener. The clamping force developed by a rivet is due to the shrinkage forces as a result of cooling, which are often inconsistent. The clamping force of an H.S.F.G. bolt is developed by the amount of torque applied to the bolt, this tightening processis much more controllable and so more consistent clamping forces are achieved. The main advantages of H.S.F.G. bolting over riveting may be summarised as follows:-

(1) Provides a more consistent clamping force (18, 28),

(2) Installation does not require expensive heating equipment,

(3) Reduces site fire risk,

(4) Bolting crews require less training to operate simpler equipment,

(5) Field erection costs are lower.

For these reasons the H.S.F.G. bolt became more competitive than the rivet and so to a large extent replaced it.

Welded methods have also advanced during the past fifty years due to developments into welding techniques. Very little welding was used in steel structures before 1930 and its acceptance was initially very slow. Research has provided new materials and many new welding processes for use in the steel industry, thereby making welded connections very popular in recent years. The welded end plate connection became more common after the 1950's.

These developments in fasteners and in the methods of using them provided more consistent and predictable beam-to-column connection behaviour. This enables the structural engineer to be more confident in the end restraint provided by connections for use in semi-rigid analysis and design. Detailed discussion of the behaviour of various fastener types is given by Fisher and Struik (29).

2.5.2 Electronic Digital Computers

Existing methods of incorporating semi-rigid end restraint into a structural analysis become tedious and cumbersome by hand calculation for even medium sized frames. The analysis of a large frame becomes far too arduous and virtually impossible for practical uses. For these reasons semi-rigid design and analysis was very unpopular and design practice continued to use the simplifying assumptions of either pinned or fully fixed connections.

The electronic digital computer was developed during the early 1950's and was applied to the analysis of structures in the late 1950's and early 1960's. The application of computers to matrix stiffness methods for the analysis of large structural frames became well known and many standard package programs now exist to perform the analysis. Computers also made it possible to incorporate systematic procedures into matrix stiffness methods to give a better representation of connection behaviour. Iterative methods of correcting connection stiffness and end restraint values can be used to produce better representations of real connection behaviour.

2.6 Stability Analysis of Frames with Semi-Rigid Connections

The stability of rigidly connected frames using matrix methods has been analysed by many authors, notably Halldorsson and Wang (30) and Przemieniecki (31). The stability of a frame can be measured by the determinant of the overall stiffness matrix of the structure. The stiffness matrix of a member is composed of two separate member stiffness matrices; (i) the normal stiffness matrix depending on the physical properties of the member and (ii) the geometrical stiffness matrix depending on the member length and the axial load alone. The geometrical stiffness matrix allows for the destabilising effect of the axial load. The overall stiffness

matrix for the complete frame, summed for all members, is the sum of the normal and geometrical stiffness matrices:

$$[K] = [K_S + K_G] \qquad 2.4$$

The point of frame instability occurs when the determinant of this overall stiffness matrix becomes equal to zero:

$$\text{Det} \quad |K| = 0 \qquad 2.5$$

In 1970, Romstad and Subramanian (32) investigated the effects of semi-rigid end restraint on the buckling capacity of simple frames. They incorporated modified end connection stiffnesses into the matrix stiffness analysis and used computer techniques to determine loads creating the instability condition of equation 2.5. However, they utilised the classical approach of stability analysis, whereby the deformations due to loading are neglected and the procedure searches for loads creating the condition of bifurcation. The procedure developed was used to study the behaviour of a single-storey single-bay frame with semi-rigid beam-to-column connections, both with and without sidesway. A bilinear model of a connection moment-rotation characteristic was assumed. Computational procedures for locating eigenvalues of the stiffness matrix were used, the load being applied incrementally with successive calculations being performed to detect determinant sign changes with a Regula-Falsi interpolation procedure to find the critical load. The bifurcation approach meant that they

were unable to determine the effect of a nonlinear moment-rotation characteristic on the buckling capacity of frames. It was concluded that significant increases in the buckling capacity of simple frames could be achieved by using connections with fifteen to twenty-five per cent of the fully fixed rigidity.

2.7 The Effective Length of Columns with Semi-Rigid End Restraint

The effective length of a column in compression depends on the end restraining conditions at the ends of its unbraced length. In structural frames these end restraint conditions depend on the stiffness of connecting members as well as the stiffness of the connections. The Column Research Council's alignment charts (33) can be used to find the effective length of columns with rigid connections taking into account the relative stiffness of adjoining members. These alignment charts provide a quick and convenient method for evaluating the effective length factor of a column with rigid end connections. Methods of modifying the alignment charts for use with semi-rigid end restraint were first proposed by De Falco and Marino (34) in 1966. They derived an equation for the determination of the relative stiffness of a member with semi-rigid connections. This equation was plotted in the form of an alignment chart for the ease of its determination. A value of the connection's initial tangent factor Z is required before the modified alignment chart can be used. De Falco and Marino used Lother's (23) elastic

restraint equations to calculate Z which means a linear moment-rotation relationship is assumed. Driscoll (35) developed this work to allow for frames both with and without sidesway.

Driscoll also conducted a theoretical study to determine the effect of semi-rigid end restraint on the effective length of columns in framed structures. From this it was found that the relative stiffness of connected beams range from ten to eighty-five per cent of that of rigidly connected beams. It was also found that the Column Research Council's 'G' nomograph parameter for a semi-rigid web cleated connection was from eighteen to thirty-three per cent greater than the 'G' parameter for the same members when rigidly connected. However, the resulting difference in effective length factors for the column were too small to be detected in the usual alignment charts.

The initial tangent connection factor Z is used in this analysis which assumes linear connection behaviour. However, in practice the connection stiffness will be reduced under increasing load due to the nonlinearity of the connection behaviour, resulting in an upper bound of the connection stiffness being used in the analysis. Therefore the influence of semi-rigid connections should have more significance on the column's effective length factor than that found by Driscoll using the connection factor Z.

In 1974, Wood (36) also considered the effective length of members with semi-rigid connections. He suggested that the connection stiffness should be taken as the incremental stiffness, i.e. the tangential stiffness of the nonlinear moment-rotation curve at the current value of the moment. This concept of semi-rigid connection stiffness will be used in the analysis presented in Chapter 4.

The B20 draft proposals of the British Standards Institution (4) give an empirical method of determining the effective length of continuous columns in multi-storey frames. The effective length ℓ is calculated by:

$$\ell = L(1.0 - e_1 - e_2) \qquad 2.6$$

where L is the actual length of the column and e_1 and e_2 are the end factors at each end, which are determined from the equation:

$$e = \frac{0.25j}{(250 + j)} \qquad 2.7$$

where j is the joint ratio depending on the ratio of beam stiffness to column stiffness at the connection. Certain conditions for the proportioning of connections must be satisfied before this empirical method may be used. These proposals are based on the design recommendations of the final report of the Steel Structures Research Committee of Great Britain (9).

2.8 Other Connection Deformations to be Investigated

2.8.1 In-plane behaviour

All the experimental and analytical methods described so far have only considered the in-plane flexural deformations of a connection. Connections may also have flexible deformation characteristics relating to other degrees of freedom, such as axial or shear deformation. This topic was first investigated in 1974 by Lightfoot and Le Messurier (37) who extended the matrix stiffness analysis to allow for connections in which members are constrained elastically against axial and shear forces as well as flexural moments. Linear force-deformation relationships were assumed in all cases. This work was applied to the analysis of scaffold structures, but the principles are easily applied to multi-storey structural frames.

2.8.2 Out-of-plane behaviour

Very little work has been reported of investigations of semi-rigid end restraints for out-of-plane degrees of freedom such as lateral shears, twisting and lateral bending. The nature of the end restraint provided to a member in these degrees of freedom may be of importance to its three-dimensional behaviour. The twisting degree of freedom was introduced into Monforton and Wu's analysis (19) assuming a linear torque-twist relationship. Lightfoot and Le Messurier (37) also considered the

analysis of space frames incorporating all possible degrees of freedom in the form of linear elastic spring end restraint. Correction matrices were presented for use within rigid frame procedures. Numerous data have been reported for in-plane flexural behaviour of connections, whereas, very little experimental data is available for all other degrees of freedom.

CHAPTER 3

Connection, Data and Representations

3.1 Flexural Behaviour of Connections

3.1.1 Description of flexural behaviour

The best description of the flexural behaviour of a connection is its moment-rotation characteristic. This is the relationship between the moment transmitted by the connection (from the beam to the column) and the rotation of the beam relative to the column. Figure 3.1 shows typical moment-rotation curves which can be used to explain connection behaviour. The horizontal (rotation) axis represents an idealised pinned connection where zero moment is developed for all values of rotation. The vertical (moment) axis represents the idealised fully rigid connection where no joint rotation occurs for all values of moment developed. These are the two extreme idealisations and do, of course, describe the classical assumptions of pinned and fully rigid connections, respectively. In practice, the moment-rotation curves for all real connections will lie in the range between these extremes. Figure 3.1 includes the moment-rotation curves of three real connections of differing degrees of rigidity. The lowest of these moment-rotation curves represents a flexible connection such as where the web has double cleats. The top and seat cleated connections, shown as the middle curve represents a connection of intermediate rigidity. The most rigid connection illustrated is made of T-stubs, attached to the top and bottom flanges of the beam and the resulting relationship is shown as the upper curve.

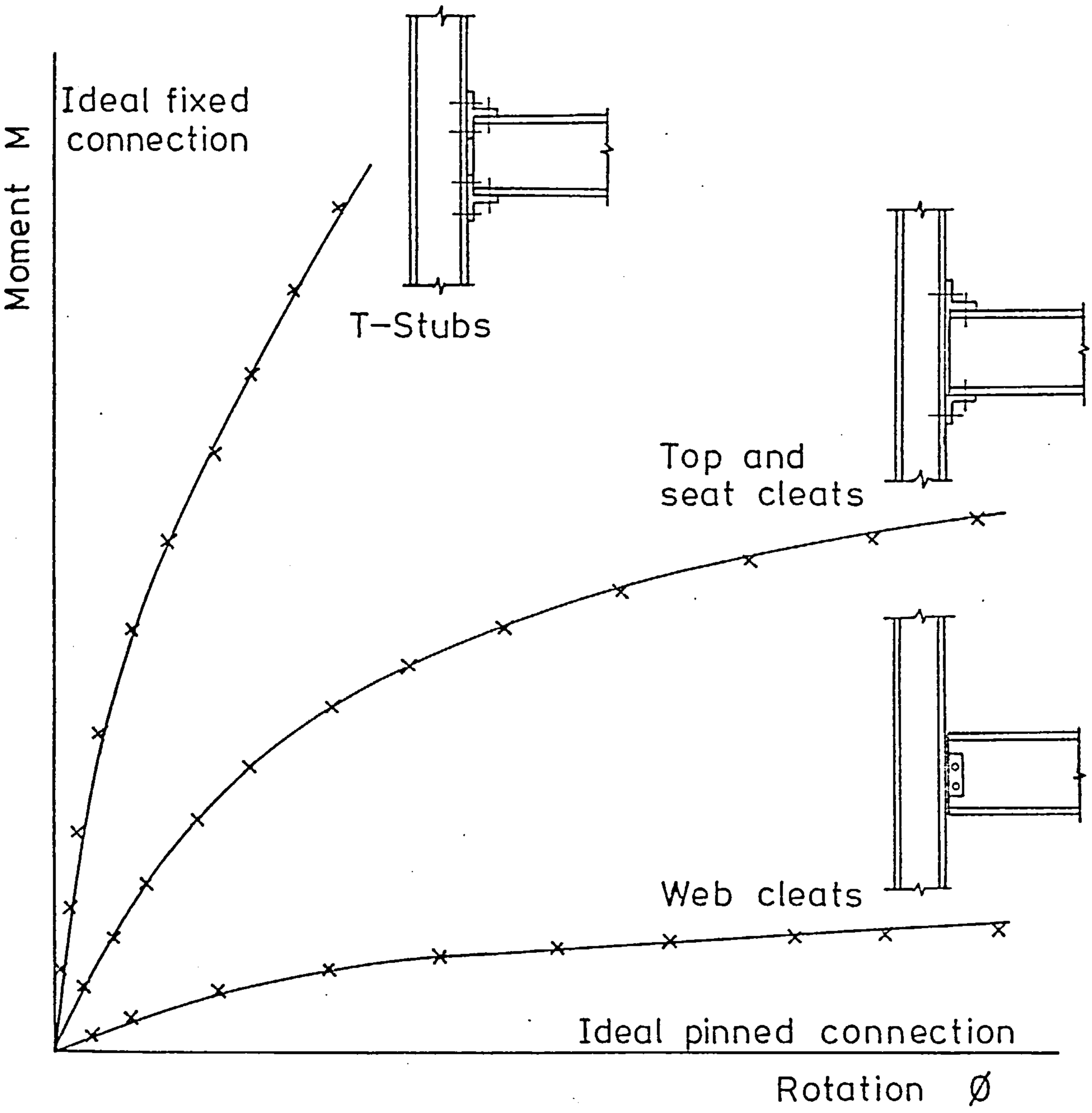

FIGURE 3.1 - Typical Moment-Rotation Curves

The slope of the moment-rotation curve is a measure of the rigidity or stiffness of the connection at any particular value of rotation. Thus moment-rotation curves may be used to compare the relative rigidities of differing connection types. Figure 3.1 shows graphically that T-stub connections are more rigid than top and seat cleated connections, which in turn are more rigid than double web cleated connections. It can also be seen that, in general, the rigidity of a connection decreases as joint rotation increases. Connections are most rigid in the initial stages of loading, after any slack due to lack of fit for the bolts has been taken up. As the moment transmitted through the connection increases the rigidity is reduced until the connection rigidity becomes zero.

3.1.2 Nonlinear connection behaviour

The moment-rotation characteristics of all real connections are nonlinear over the complete range of the curves, this is due to the complex nature and behaviour of joints. This complexity results from the fact that the connection components may have yielded in certain local positions, although the beam which is being supported may be carrying no more than its working load. As the connection deforms one part of the connection is pulled away from the supporting member while the other end of the same connection is pushed into the supporting member. The resultant of the forces

producing these deformations form the couple which resists the applied moment.

The moment-rotation relationship of the connection is nonlinear, even at relatively low applied moments. This lack of linearity exists in the elastic range of the component parts due to the change in stiffness of the compression side of the connection relative to the tension side as applied moment increases. This reduced stiffness is due to various factors as discussed by Lewitt, Chesson and Munse (38) and many other researchers as summarised in tabular form in the following section. Detailed explanations of reduced stiffness, connection behaviour and the various modes of failure have been described by these researchers. The important factors determining the rigidity of common types of connection can be listed as follows:-

1. Length and depth of connected beams

2. Connection gauge (Cross-centre Distance between Bolt Holes

3. Type and size of fastener

4. Thickness of connecting angles

5. Whether connection is to a column web, column flange or a girder web

6. Physical properties of angles, members and fastener material

7. End plate yield

8. Column stiffener yield

9. Local beam flange buckling

10. Column web yield

11. Beam and column contact during deformation

3.2 Experimental Data on Semi-Rigid Connections

3.2.1 Common connection types

Structural connections which join beams to columns are generally divided into three types, flexible, rigid and semi-rigid depending on their stiffness and degree of rotational restraint. Commonly used connection types are shown in Figure 3.2 and these can be classified into the three main categories.

Flexible connections are capable of carrying the full end shear force, but offer low rotational resistance to the end of the beam. Rotation can occur relatively freely between the end of the beam and the column. In design such connections are considered to be pinned and beams are designed to carry the full simple beam moment. In Figure 3.2 the single and double web cleated connections and the welded header plate connections would be considered as flexible.

Rigid connections are capable of carrying the full applied moment as well as the end shear force. The connection components are stiff so as to reduce the relative rotation of the beam to the column to a

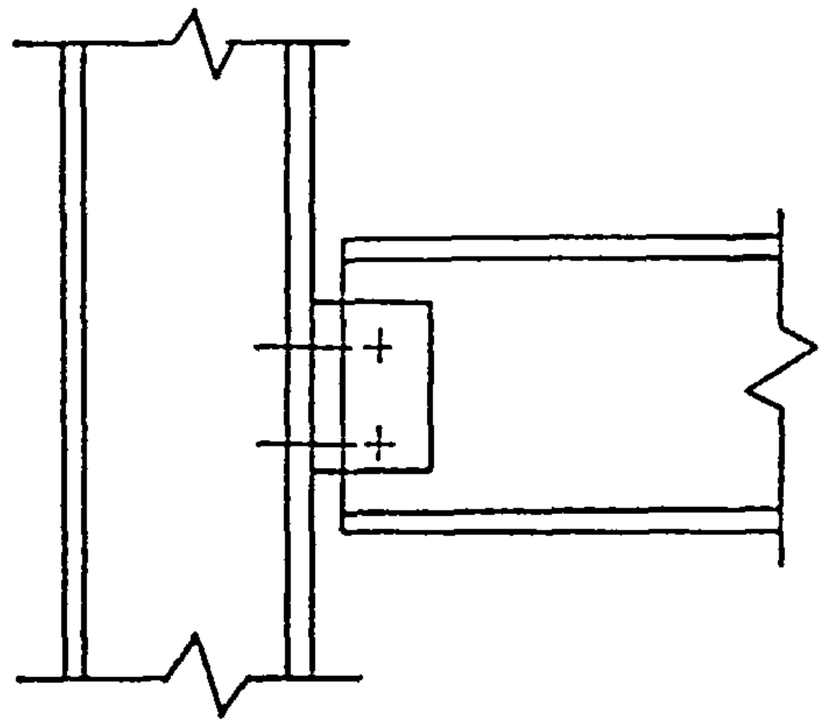

Single Web Angle

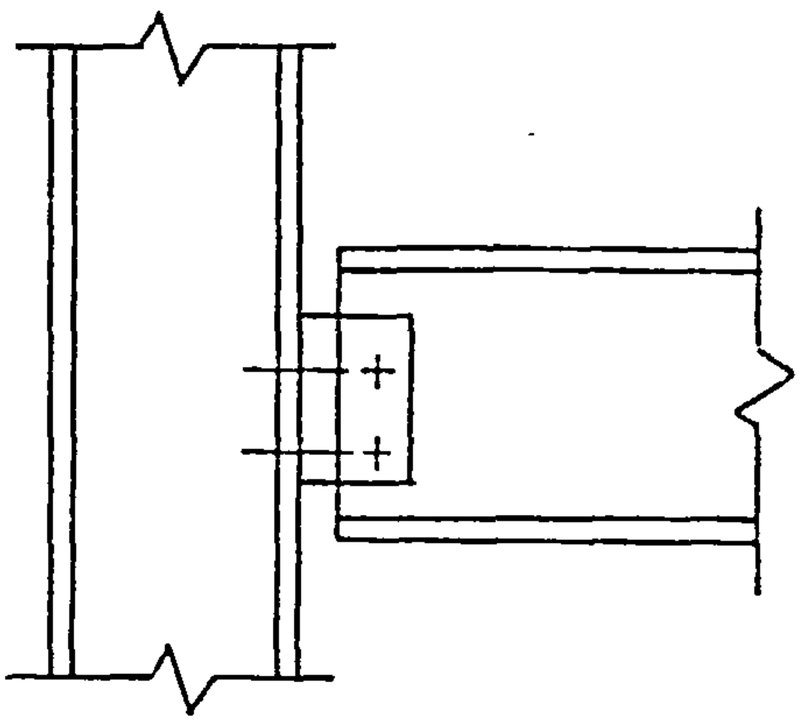

Double Web Angle

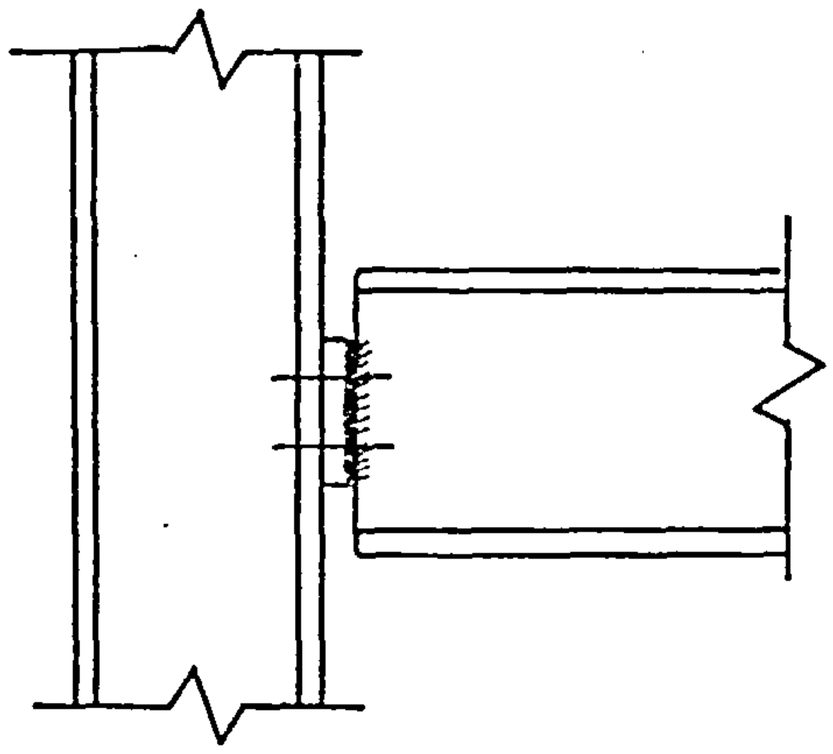

Header Plate

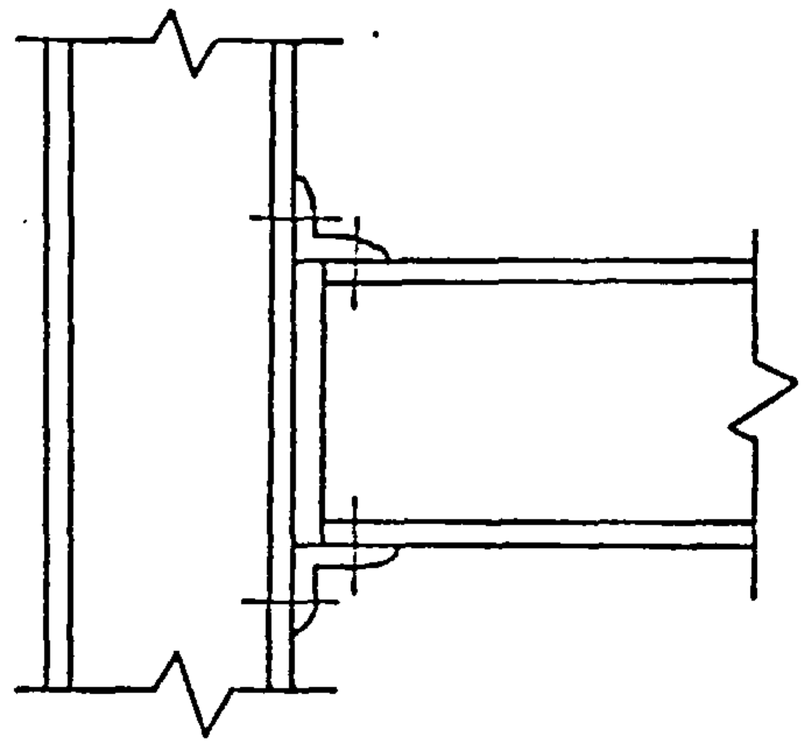

Top and Seat Cleats

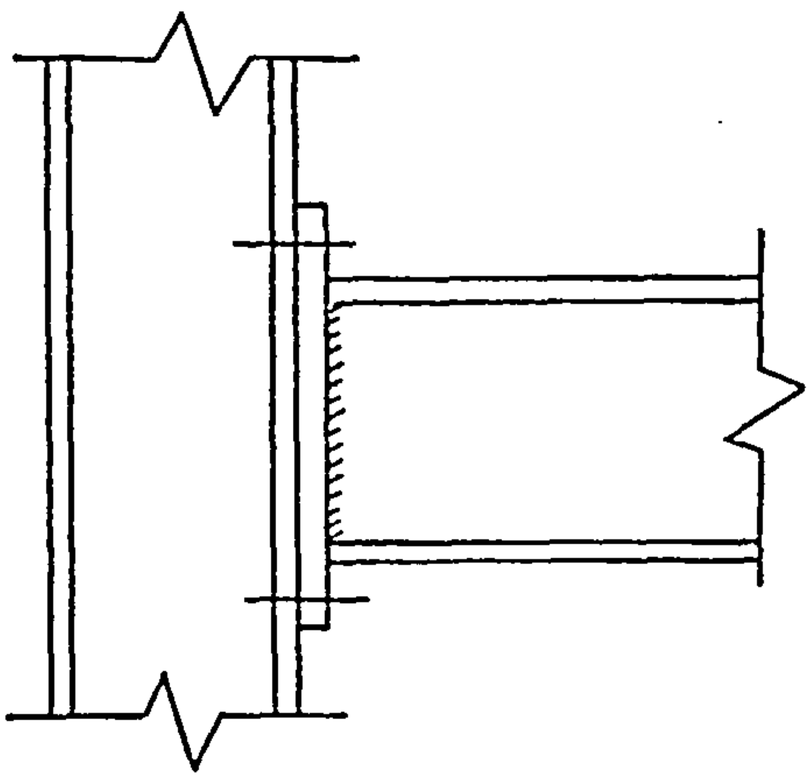

End Plate No Column Stiffeners

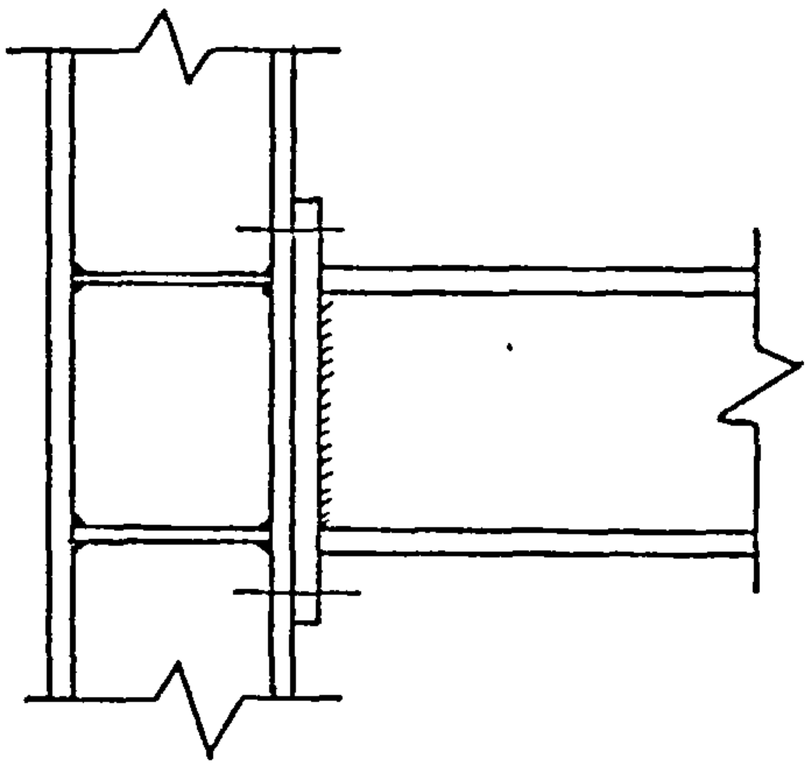

End Plate with Column Stiffeners

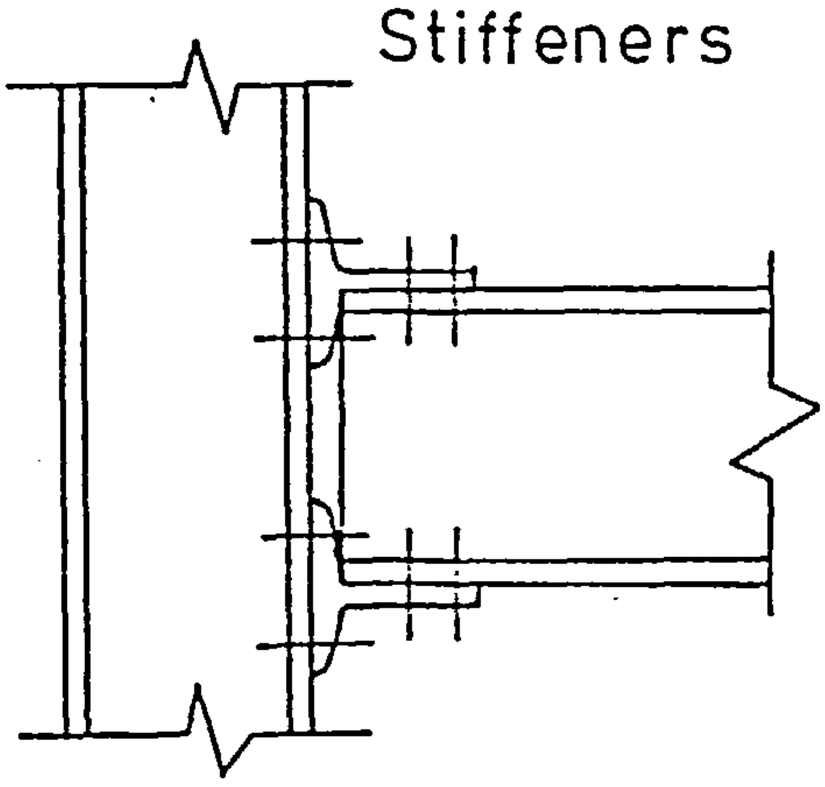

T-Stubs

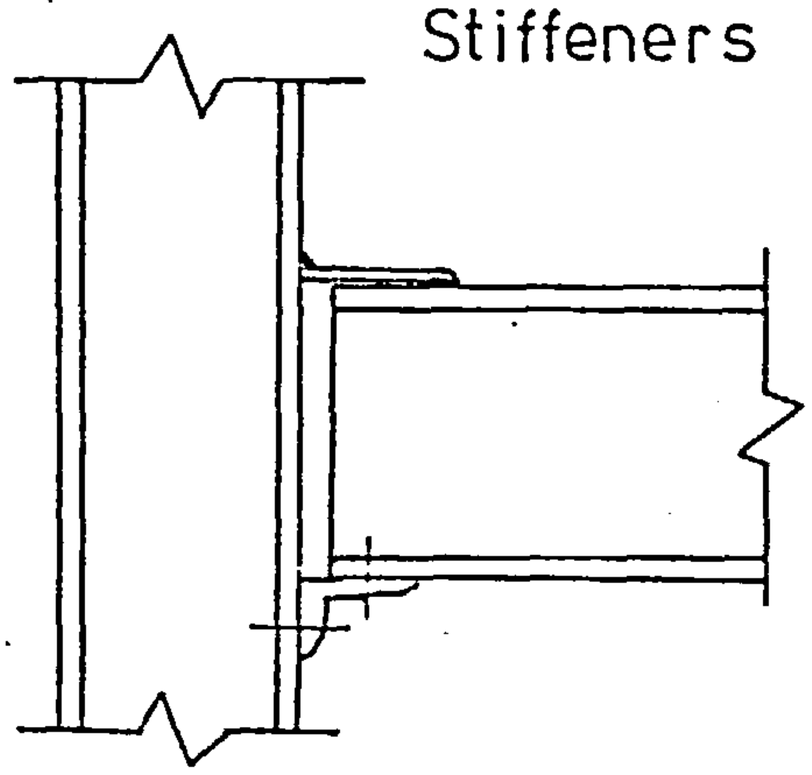

Top Plate and Seat Angle

FIGURE 3.2 - Common Connection Types

minimum. In design these connections are assumed to be fully rigid and would be expected to provide the full fixed end moment so that the beam may be designed as continuous. The T-stub connection of Figure 3.2 and the combined connections of Figure 3.3 would be considered as rigid connections. Combinations of two of the basic connection types are used to increase the rigidity of a connection, for example a combined top and seat angle connection with web cleats. Directly welded connections can also produce rigid connections.

Semi-rigid connections are capable of transmitting appreciable amounts of bending moment but with some relative rotation between the beam and the column. In design these connections have often been assumed to be flexible leading to simpler beam design. In fact many of the connections assumed to be flexible are inherently semi-rigid and do enable end moments to be developed which are not taken into consideration during design. The top and seat angle, welded top plate and seat angle and the end plates with and without column stiffeners, as shown in Figure 3.2, are all connection types that can be classified as semi-rigid.

Figure 3.4 shows typical moment-rotation curves for the common connection types shown in Figure 3.2. This figure illustrates graphically how the types of connection used in practice can be divided into the three main groupings. The divisions of connection range are drawn somewhat arbitrarily.

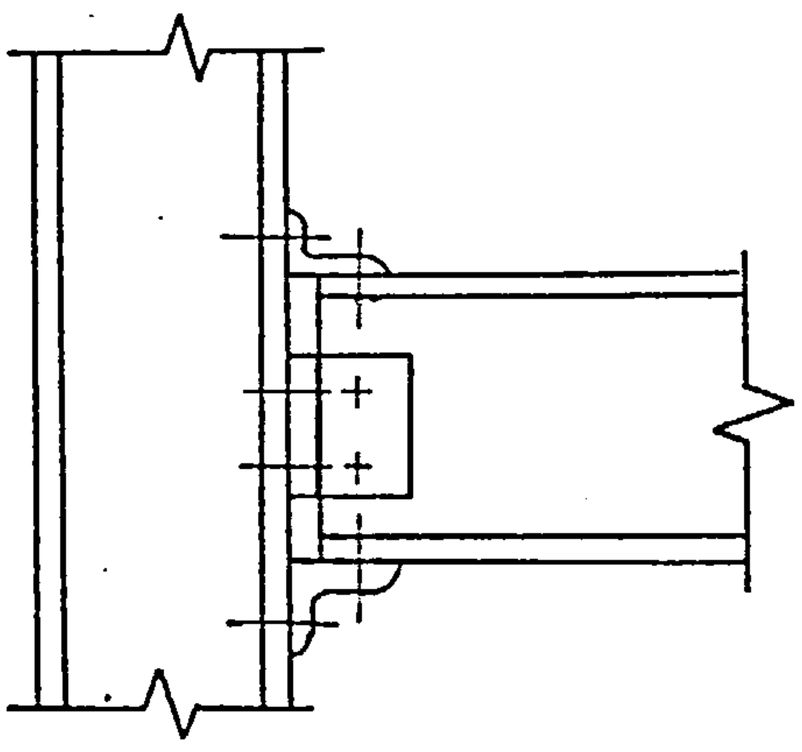

Combined Top and Seat Angles with Web Cleats

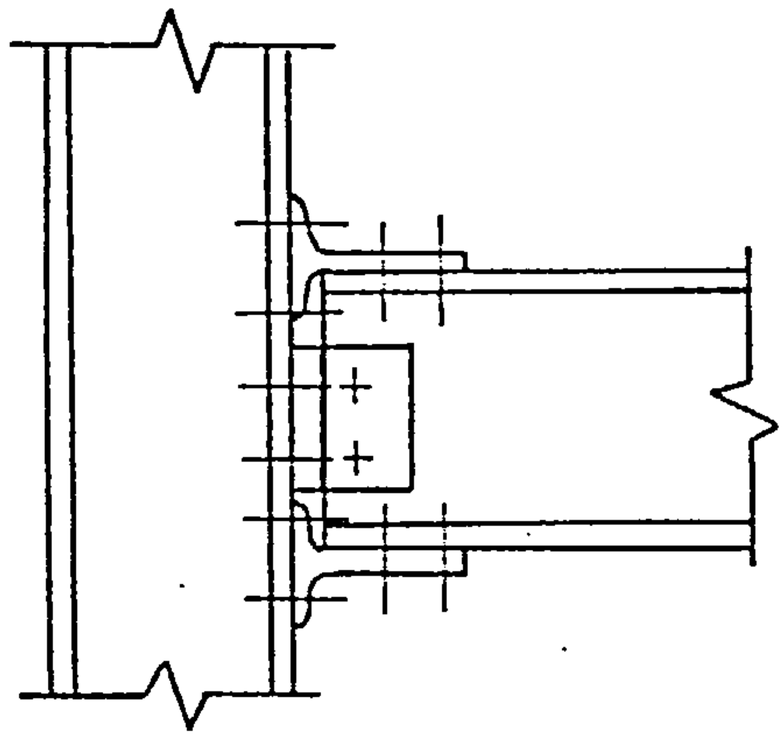

Combined T-Stubs with Web Cleats

FIGURE 3.3 - Combined Connections

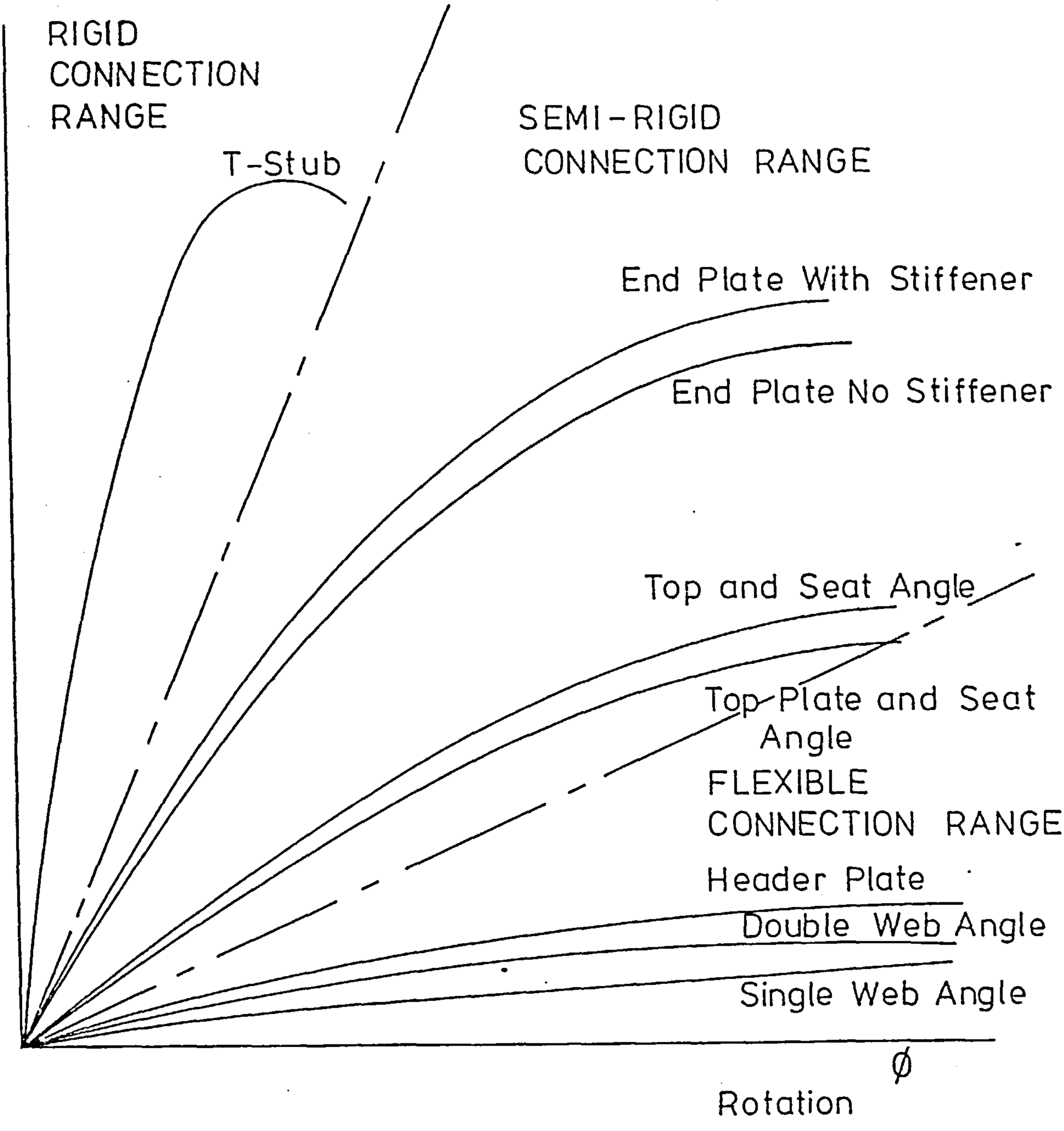

FIGURE 3.4 - Typical Moment-Rotation Curves for Common Connection Types

3.2.2 Available experimental data

Numerous tests on beam-to-column connections have been reported during the past fifty years. Investigations reporting moment-rotation data for flexible connections are summarised in Table 3.1. Table 3.2 summarises data for semi-rigid connections, while Table 3.3 summarises data for rigid connections including the combined connections. More detailed information relating to the attached beam and column sizes and the dimensions of the actual connections and fasteners is given in tabular form in Appendix A.

Unfortunately most of the available data are for types of connections which are no longer used in practice. Indeed much of the early data involves connections using rivets as the main fastener, techniques that have largely been superseded by high strength friction grip bolting and by welding. The majority of data reported are for connections of beams to column flanges, thus rotational restraint is provided in the plane of the column's major axis. However, since minor-axis buckling is normally more important, data for minor-axis restraint would be more useful when considering the behaviour of the column. In short, much of the available data is generally out-dated and does not include sufficient tests for minor axis bending to facilitate extensive restrained column analysis.

TABLE 3.1 - Available Data for Flexible Connections

Type of connection	Reference of experimental data	Date	Country of origin	No. of tests	Type of fastener	Column Axis restrained by connection
Single web cleats	Johnston + Deits (39)	1942	U.S.A.	4	Welded	Major
	Sommer (40)	1967	Canada	4	Bolts	Major
	Lipson (41)	1977	Canada	43	Bolts	Major
Double web cleats	Batho + Rowan (8)	1934	U.K.	3	Rivets	Major
	Rathbun (11)	1936	U.S.A.	7	Rivets	Major
	Munse, et. al. (28)	1959	U.S.A.	4	Rivets/Bolts	Major
	Mathison (42)	1959	Canada	4	Bolts	Major
	Howe (43)	1961	Canada	4	Bolts	Major
	Leon (44)	1961	Canada	6	Bolts	Major
	Lewitt, et. al. (38)	1969	U.S.A.	9	Rivets/Bolts	7-Major 2-Minor
	Bergquist (45)	1977	U.S.A.	3	Bolts	Minor
Header plate	Sommer (40)	1967	Canada	16	Bolts	Major

TABLE 3.2 - Available Data for Semi-Rigid Connections

Type of connection	Reference of experimental data	Date	Country of origin	No. of tests	Type of fastener	Column axis restrained by connection
Top and seat angle cleats	Batho + Rowan (8)	1934	U.K.	7	Rivets	Major
	Batho + Rowan (8)	1934	U.K.	3	Bolted	Major
	Rathbun (11)	1936	U.S.A.	3	Rivets	Minor*†
	Hechtman + Johnston (5)	1947	U.S.A	19	Rivets	14-Major 7-Minor
End plate - No Column Stiffener	Sherbourne (46)	1961	U.K.	1	Bolted	Major
	Ostrander (47)	1970	Canada	11	Bolted	Major
	Bailey (48)	1970	U.K.	3	Bolted	Major
	Surtees + Mann (49)	1970	U.K.	5	Bolted	Major
	Zoetemeijer (50)	1974	Holland	6	Bolted	Major
	Zoetemeijer + Kolstein (51)	1975	Holland	14	Bolted	6-Minor*‡ 8-Major
	Grundy, et. al. (52)	1980	Australia	2	Bolted	Major

* Plate used as column † Comment - beam-to-column ‡ Comment - beam-to-beam

Continued . . .

TABLE 3.2 (Continued)

Type of connection	Reference of experimental data	Date	Country of origin	No. of tests	Type of fastener	Column axis restrained by connection
End plate with column stiffener	Johnston, et. al. (53)	1960	U.K.	1	Bolted	Major
	Sherbourne (46)	1961	U.K.	4	Bolted	Major
	Ostrander (47)	1970	Canada	13	Bolted	Major
	Bailey (48)	1970	U.K.	10	Bolted	Major
	Surtees + Mann (49)	1970	U.K.	1	Bolted	Major
	Zoetemeijer + Kolstein (51)	1975	Holland	4	Bolted	Major
	Packer + Morris (54)	1977	U.K.	3	Bolted	Major
Welded top plate and seat	Young + Jackson (10)	1934	Canada	10	Welded	Minor*
	Johnston + Deits (39)	1942	U.S.A.	2	Welded	Major
	Brandes + Mains (55)	1944	U.S.A.	17	Welded	5-Major 12- Minor
	Pray + Jensen (56)	1956	U.S.A.	1	Welded	Major
	Johnson (57)	1959	U.K.	1	Welded	Major
	Johnson, et. al. (53)	1960	U.K.	1	Welded	Major

* Plate used as column

TABLE 3.3 - Available Data for Rigid Connections

Type of connection	Reference of experimental data	Date	Country of origin	No. of tests	Type of fastener	Column axis restrained by connection
T-Stub	Batho + Rowan (8)	1934	U.K.	2	Rivets	Major
	Rathbun (11)	1936	U.S.A.	6	Rivets	5-Minor*[1] 1-Major
	Douty (58)	1964	U.S.A.	3	Bolted	Major
	Bannister (59)	1966	U.K.	5	Bolted	Major
	Zoetemeijer (50)	1974	Holland	4	Bolted	Major
Combined web and top and seat cleats	Batho + Rowan (8)	1934	U.K.	2	Rivets	Major
	Young + Jackson (10)	1934	Canada	4	Welded	2-Major 2-Minor*[2]
	Rathbun (11)	1936	U.S.A.	2	Rivets	Minor*[3]

* Plate used as column

[1] Comment - 5 beam-to-beam [2] Comment - 2 beam-to-beam [3] Comment - beam-to-beam

Continued . . .

TABLE 3.3 (Continued)

Type of connection	Reference of experimental data	Date	Country of origin	No. of tests	Type of fastener	Column axis restrained by connection
Combined web cleats and T-stubs	Batho + Rowan (8)	1934	U.K.	1	Rivets	Major
	Young + Jackson (10)	1934	Canada	4	Rivets	2-Major 2-Minor*[2]
	Young + Jackson (10)	1934	Canada	4	Welded	2-Major 2-Minor*[2]
	Zoetemeijer (50)	1974	Holland	13	Bolted	Major[4]

* Plate used as column

[2] Comment - 2 beam-to-beam

[4] Comment - 1 with column stiffener

3.2.3 Joint rotation measurement

Analytical procedures are based on the ideal model of a system in which the structural members are represented by their centre-lines, with the connections being assumed to be at the intersection of these centre-lines. A comparison of the idealised model and the real structural arrangement is shown in Figure 3.5.

The total joint rotation ϕ_{TOTAL} is the relative rotation between point A and point C and has essentially three components; (i) that due to beam flexure for the length B to C (ϕ_{BC}), (ii) the flexural component of the half width of the column which is assumed to be part of the idealised system (ϕ_{AB}), and (iii) the additional rotation due to the connection itself ($\phi_{CONNECTION}$). The rotation of the connection includes deformations of the connection components, local distortions of the beam centre-line and distortions of the column face. Although not ideal the third of these three components should give a close representation of joint rotation in an analytical procedure and not the total rotation of point C relative to point A as has been assumed by many investigations.

$$\phi_{CONNECTION} = \phi_{TOTAL} - \phi_{AB} - \phi_{BC} \qquad 3.1$$

Equation 3.1 gives the rotation at point B whereas analytical procedures assume the joint rotation to occur at point A, this induces a source of error into the representation of joint rotation within these procedures.

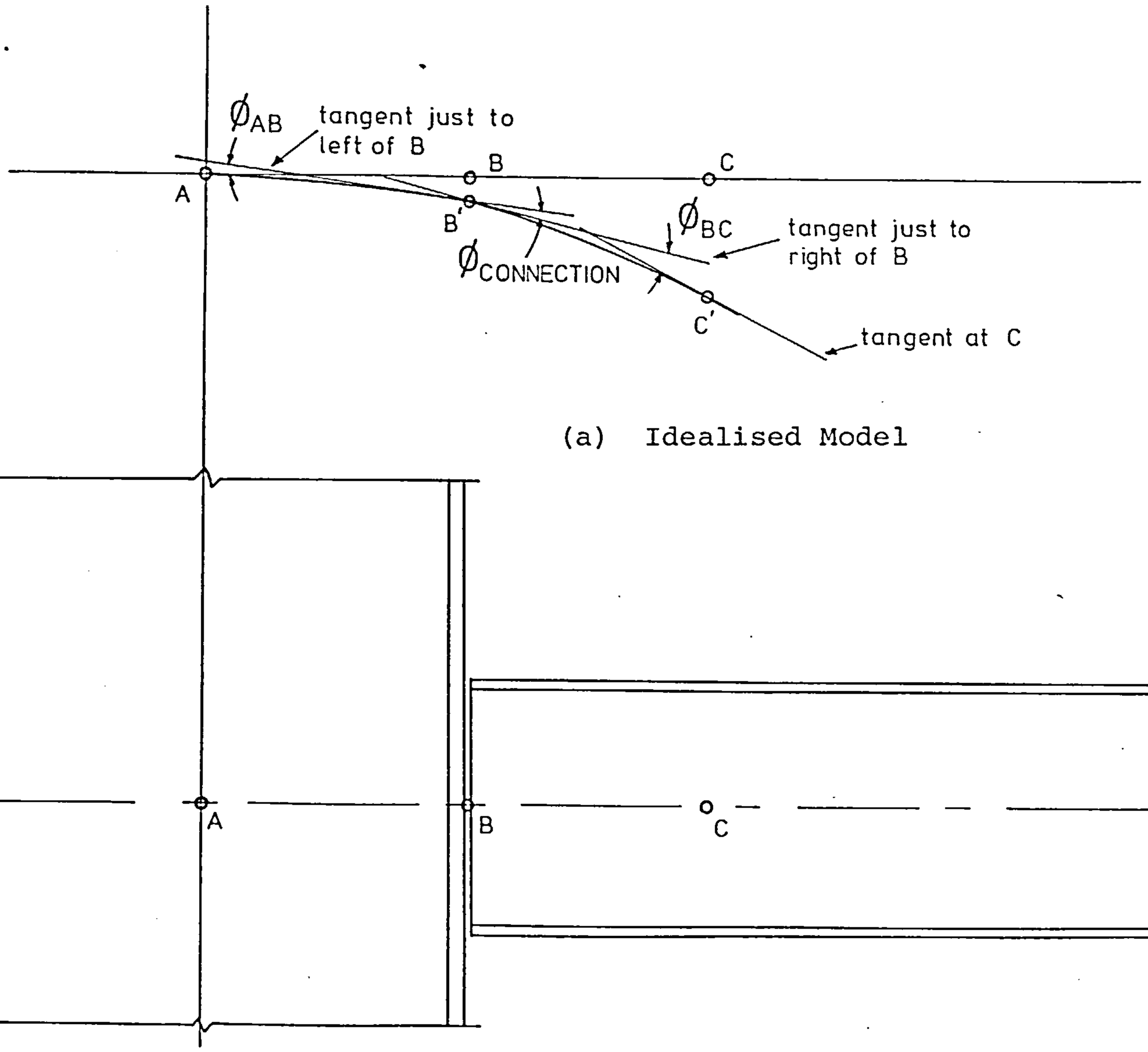

(a) Idealised Model

(b) Real Arrangement

Point A is the intersection of beam and column centre-lines

Point B is the beam/column interface on the beam centre-line

Point C is a point chosen as a convenient datum from which to measure rotation relative to point A

FIGURE 3.5 - Joint Rotation Measurement

Care must therefore be taken, before incorporating moment-rotation data into analytical procedures, to ensure that a sufficiently accurate representation of connection rotation is used. Rotation measurement equipment should be arranged so that flexural rotation may be allowed for and that sufficient mesurements are taken so as to enable the true relative rotation ($\phi_{CONNECTION}$) to be deduced. Much of the data reviewed in the previous section is incomplete in that insufficient data has been produced to allow for the flexural effects within the measurement zone.

3.2.4 Finite element connection analysis

The number of variables influencing the behaviour of structural connections makes an analysis to accurately predict the complete moment-rotation relationship very complex. Lothers (23) developed expressions to successfully predict the initial tangent semi-rigid connection factor for web cleated connections, but, this only gives the slope of the moment-rotation curve at zero moment.

It is accepted that the production of moment-rotation curves from actual tests can be time consuming and expensive. Moreover, the data obtained is limited to the particular arrangement tested. Recognising this Krishnamurthy et al (60, 61, 62, 63) have recently developed a finite element computer procedure for the numerical simulation of moment-rotation curves. This method has been used successfully to simulate the behaviour of bolted end plate connections. Lipson

and Haque (64) have adopted a similar approach for the analysis of single web cleated connections. The finite element method may be applied to the analysis of other types of connection, by redefining the mesh, to model any particular connection arrangement. To achieve reasonable accuracy, a fine finite element mesh must be used and this is fairly expensive on computer time and storage.

3.3 End Restraint Modelling

3.3.1 Linear models

Methods of modelling the moment-rotation relationships have been considered since the effects of semi-rigid connections on frame behaviour were first investigated in the early 1930's. The majority of early models assume a linear moment-rotation relationship, in which the structure as a whole is considered elastic including the connections. The connection may be thought of as a locally weakened section of the beam between the rest of the beam and the face of the column. Alternatively, the equivalent spring model may be assumed, in which the beam is assumed to be attached to rigid supports by elastic rotational coiled springs. These linear elastic connection models are illustrated in Figure 3.6.

These linear models have been applied to the modified slope-deflection, moment-distribution and matrix stiffness methods of analysis as described in Section 2.2. The linear model is usually assumed in the form of an initial

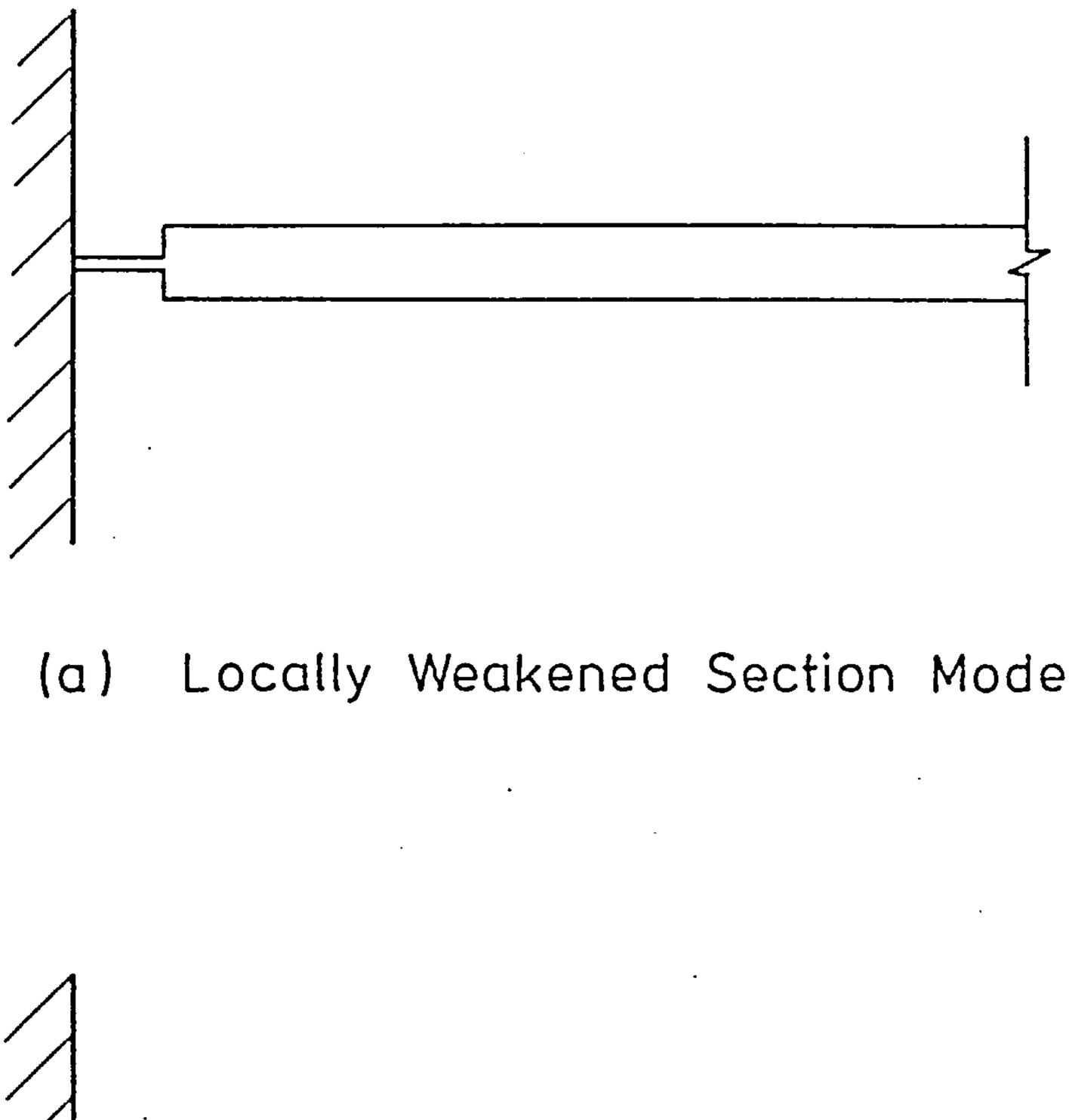

(a) Locally Weakened Section Model

(b) Equivalent Spring Model

FIGURE 3.6 - Linear Connection Models

tangent stiffness factor Z which is only strictly correct for zero end moment. As the bending moment applied to the connection is increased the initial tangent factor becomes less representative of connection stiffness. Driscoll (35) discusses the problems arising due to the use of the initial tangent semi-rigid connection factor when applied to effective length calculations. In bifurcation type buckling problems it is the instantaneous ability to resist deformation which must be determined and, if no moment exists at the connection until the point of bifurcation, then the initial tangent stiffness factor is applicable in this idealised case. In real frames moments do exist at connections before the bifurcation condition is attained and so the initial tangent factor is not representative of connection stiffness. This overestimate of connection stiffness would lead to an overestimate of frame buckling capacity in any analytical procedure using the simplifying assumption.

In an attempt to improve the straight line representation bilinear models were used by Lionberger (65, 66) and by Romstad and Subramanian (32) within matrix-stiffness analysis methods. Bilinear models are achieved by reducing the slope of the linear moment-rotation curve at a certain transition moment to follow the experimentally obtained curves more closely, as shown in Figure 3.7. However, the connection stiffness is still overestimated up to the transition moment level.

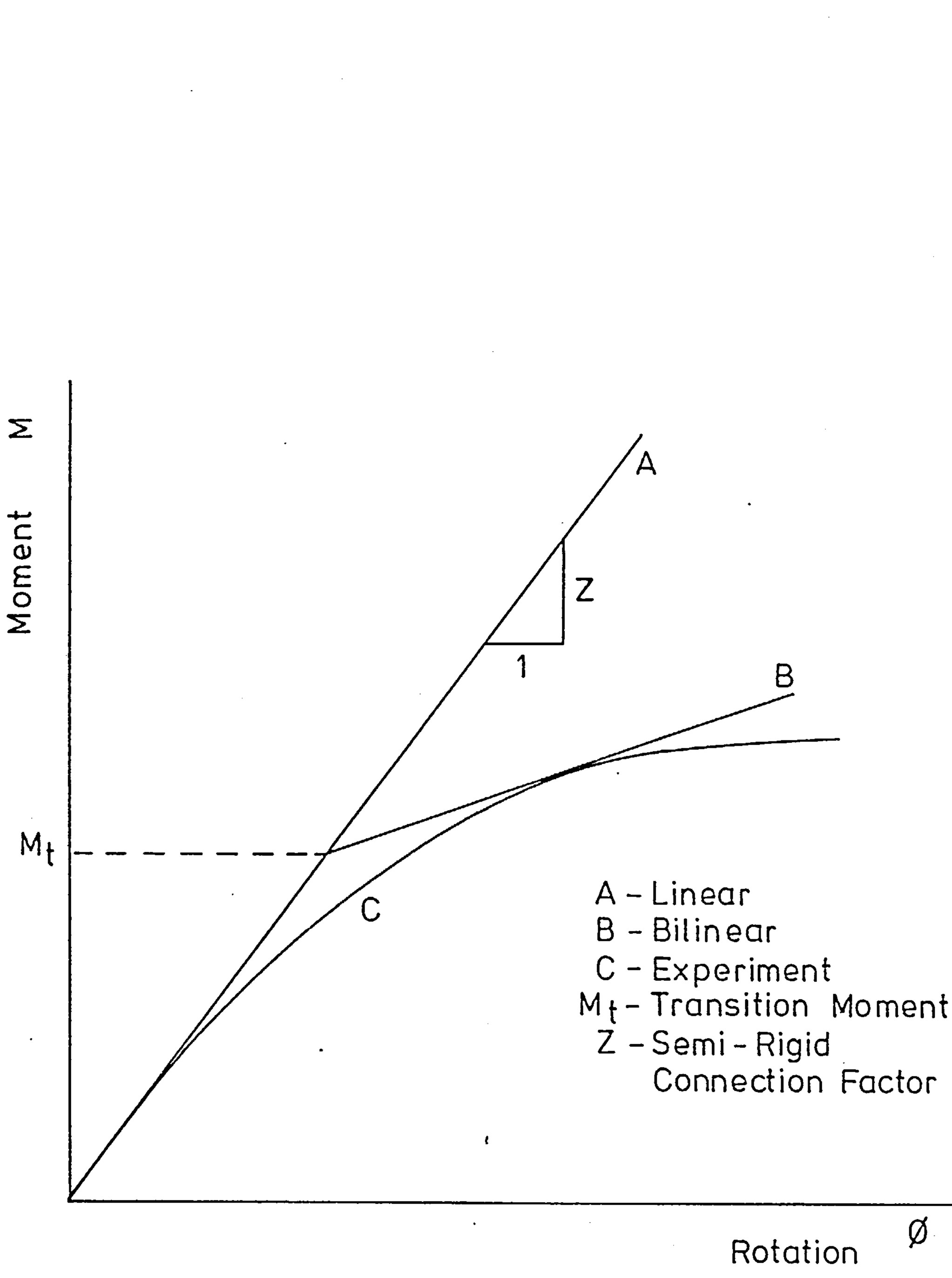

FIGURE 3.7 - Linear Moment-Rotation Functions

3.3.2 Polynomial curve-fitted models

3.3.2.1 Standardised moment-rotation equations

Experimental moment-rotation curves, although not following any simple mathematical function, may be approximated by polynomial type functions using curve fitting techniques. Sommer (40) in 1967, first fitted moment-rotation data to standardised moment-rotation curves in the form of non-dimensional polynomial series. Sommer applied this work to a study of header plate connections. The form of the polynomial series function is:

$$\phi = f(CM) \qquad 3.2$$

where C is a factor to allow for the size effects or dimensions of the connection. The terms M and ϕ are the connection's moment and rotation, respectively. The standardised moment-rotation function is applicable to all connections of the same type, the influence of different sizes and dimensions are accounted for by the size effect factor C. This eliminates the need to store moment-rotation data for every conceivable type of connection. The standardised moment-rotation relationship can be derived because all connections of a given type have similar moment-rotation curves. Thus the moment-rotation curve for any particular connection may be generated by substituting its size effect factor into the standardised function. Kennedy (67) extended this method to include end plate connections and compared

results with experimental data. The standardised function is shown to model the experimental data within a tolerance of ten per cent.

Frye (68) in 1971, and later with Morris (69), extended the work on standardised curve fits to allow for seven different types of connection. Using previously reported experimental data they produced standardised moment-rotation functions for the following types of connection:

1. Double web cleats

2. Single web cleats

3. Header plates

4. Top and seat angles

5. End plates - No column stiffeners

6. End plates - With column stiffeners

7. T-Stubs.

In all the functions produced for the above connections the variations in sizes of similar types of connection are allowed for by the term C. This size effect factor is the product of various size parameters raised to powers of constants, which have been determined by curve fitting processes using actual experimental data. For example for a double web cleated connection the size effect factor is:

$$C = d^{-2.4} t^{-0.23} g^{0.16} \qquad 3.3$$

where d is the depth of angle, t is the angle thickness and g is the connection gauge. This factor, when evaluated, may be substituted within the standardised moment-rotation equation which for this type of connection is given as:

$$\phi = 3.66(CM).10^{-4} + 1.15(CM)^{3}.10^{-6} + 4.57(CM)^{5}.10^{-8} \qquad 3.4$$

This equation was derived using Imperial units and care must be taken with the units of parameters before this equation is used. Similar expressions for all the above connections are given by Frye and Morris (69) and these were all shown to give close agreement to the corresponding original experimental curves.

Frye (68) successfully used these standardised equations within a matrix stiffness program for the analysis of multibay-multistorey frames. The analysis is used to calculate the extra overall frame deformations due to the flexibility of the connections when compared with the perfectly rigid connection. It is shown that, when certain types of semi-rigid connection are used, the overall frame sway may be increased by as much as twenty-one per cent.

3.3.2.2 Limitations of polynomial curve fits

Polynomial curve fitting methods were first considered by the Author for the representation of the end restraint to be used in the analysis, as will be

described in the next chapter. Firstly, a single polynomial series expression was used of the form:

$$M = a_1\phi + a_2\phi^2 + a_3\phi^3 + a_4\phi^4 \qquad 3.5$$

The best fit of the coefficients of equation 3.5 was found using a least squares routine in a computer analysis. The single polynomial curve when fitted to the experimental data of a top and seat flange cleated connection is shown in Figure 3.8. A good approximation to the shape of the data is produced, but the slope of the function is unsatisfactory as a description of connection stiffness. The nature of such a single polynomial function is to peak and trough within the range of the function as it seeks to produce a line as close as possible to a number of given points. End restraint modelling however, when applied to frame analysis requires values of connection stiffness at various stages of loading. This connection stiffness may be measured by the slope of the moment-rotation relationship and thus the first derivative of the function is vitally important. Polynomial functions do not give good approximations to the first derivative of moment-rotation data, and may in extreme cases become negative within the range of the function. This, of course, would represent an incorrect negative connection stiffness, such errors would be unsatisfactory in any analytical procedure.

The second end restraint representations to be investigated were the standardised moment-rotation

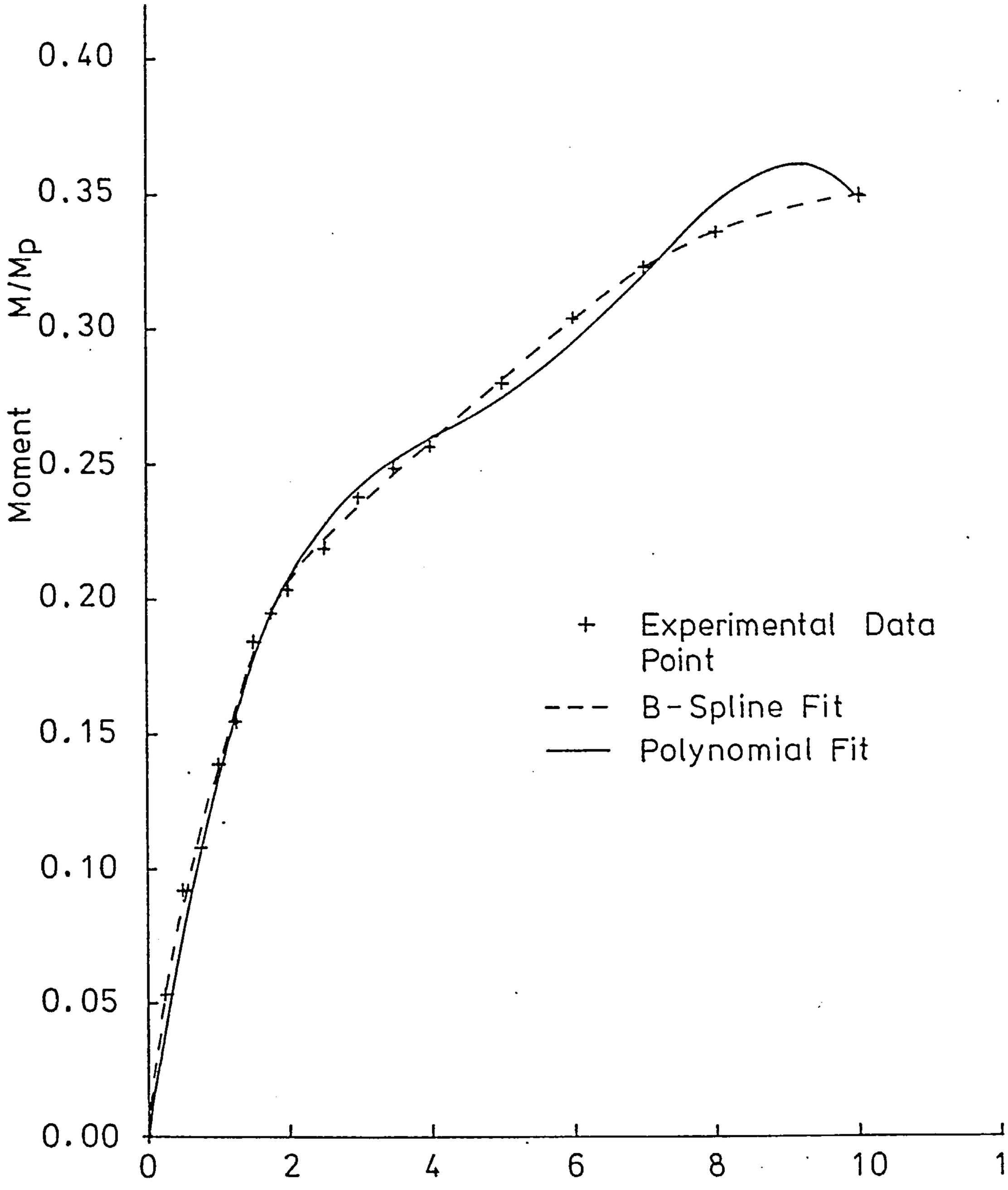

FIGURE 3.8 - Comparison of B-Spline and Polynomial Curve Fits

equations of Frye and Morris (69). These were found to be simple and easy to use, as the equations may be incorporated directly in the analysis provided that care is taken with the units of the various parameters. However, the deviation of the standardised curves from the experimental observations was found to be much greater than that claimed by Frye and Morris (69). Experimental data reported by Batho and Rowan (8) for a double web cleated, a top and seat flange cleated and a T-stub connection are compared with the appropriate standardised curves in Figures 3.9, 3.10 and 3.11, respectively. A comparison of the measured maximum deviations with the values claimed by Frye and Morris is given in Table 3.4. The accuracy of the representation of the web cleated connection is less than three times that claimed. The maximum difference between the generated curve and the experimental observations is forty-three per cent for the top and seat flange cleated connection, which is four times less accurate than that claimed. Even though the maximum deviation for the T-stub connection is twelve per cent, which does correspond closely to the value claimed by Frye and Morris, the standardised moment-rotation equation method was not considered to be accurate enough for use within the end restrained column analysis. A more accurate representation of the true connection behaviour may be achieved by using cubic B-spline curve fitting techniques (70, 71).

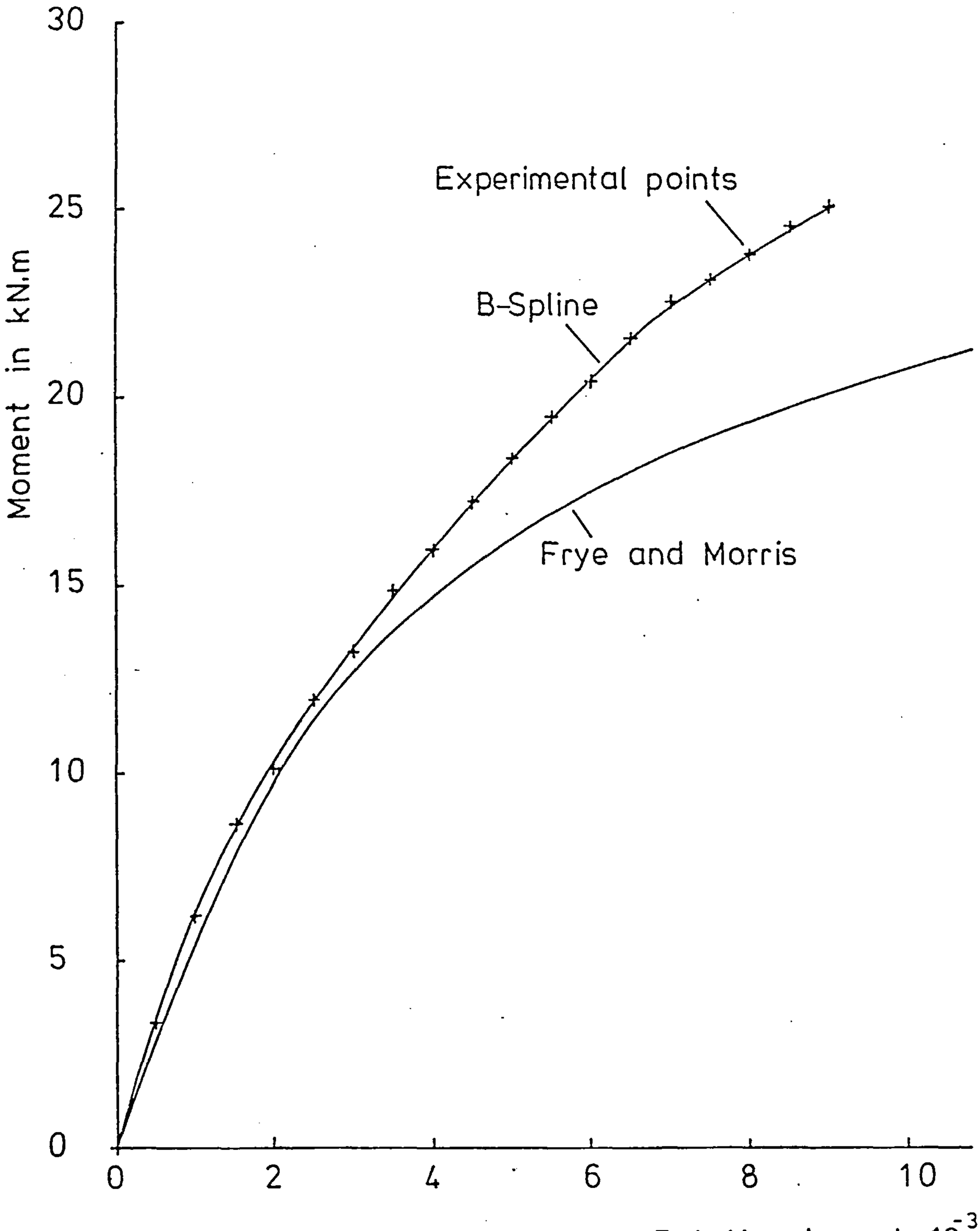

FIGURE 3.9 - Comparison of Standardised and Experimental Moment-Rotation Curves for Web Cleated Connections

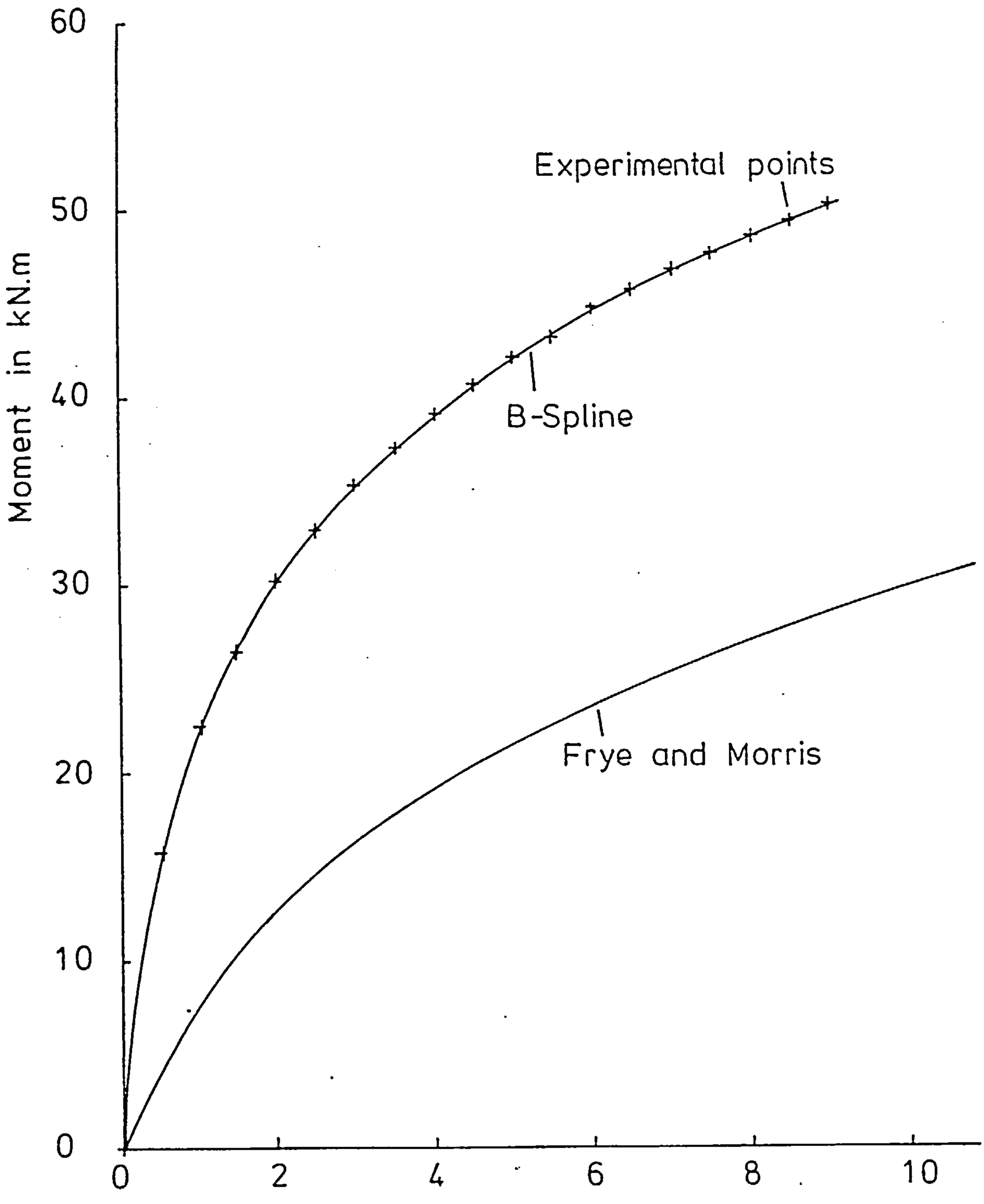

FIGURE 3.10 - Comparison of Standardised and Experimental Moment-Rotation Curves for Top and Seat Cleated Connections

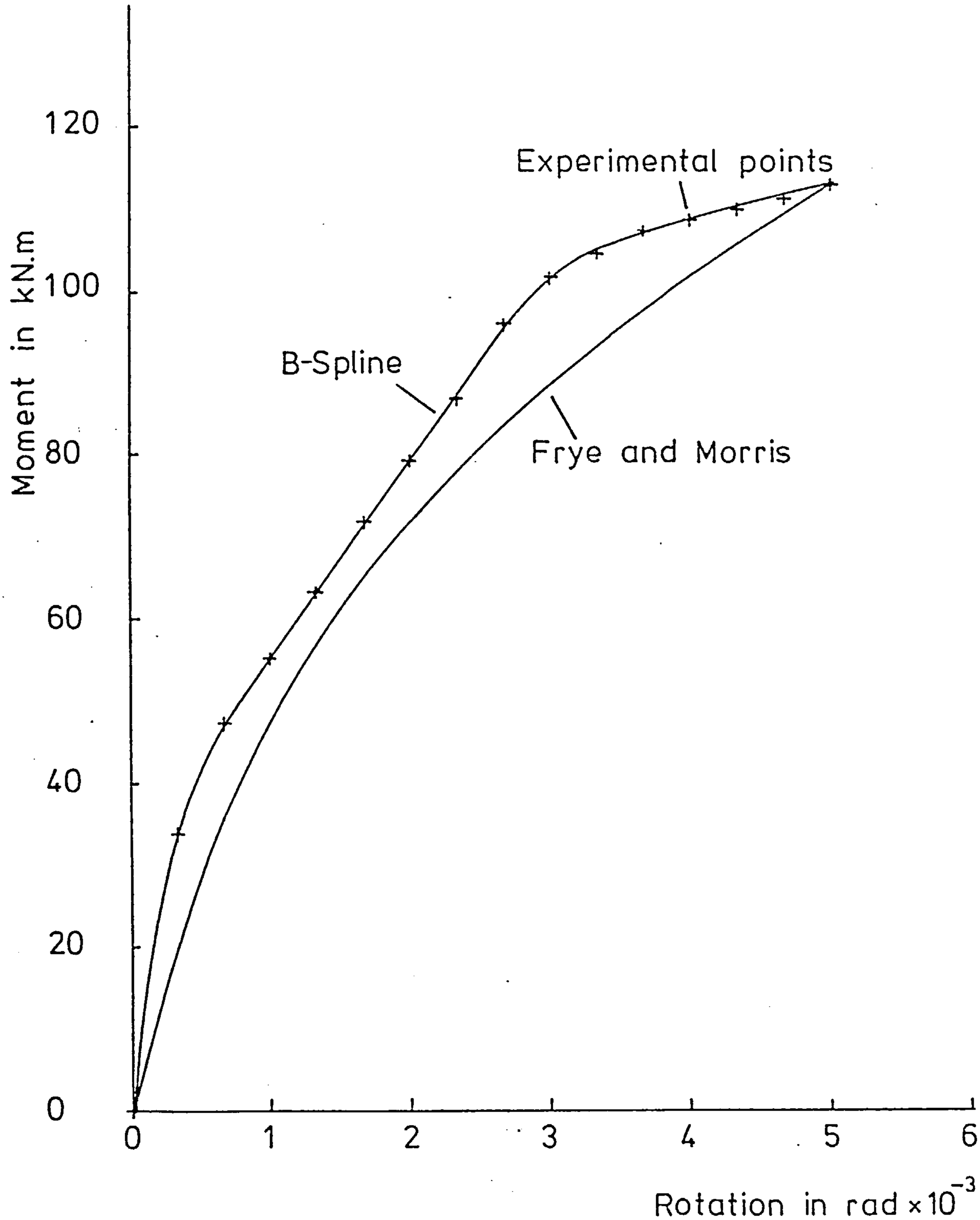

FIGURE 3.11 - Comparison of Standardised and Experimental Moment-Rotation Curves for T-Stub Connections

TABLE 3.4 - Comparison of Measured and Claimed Maximum Deviation of Standardised Moment-Rotation Equations

Type of Connection	Maximum deviation measured when compared with experimental data	Maximum deviation claimed by Frye and Morris
Double web cleats	20%	6%
Top and seat cleats	43%	11%
T-stubs	12%	12%

3.3.3 B-Spline curve fitting techniques

3.3.3.1 Cubic B-Splines

Spline functions, although only recently introduced to data fitting, have become very useful. They are adaptable to a wider variety of shapes than are single polynomial functions. The best fit to the spline functions is obtained using least square routines in much the same way as when used with single polynomials.

A spline function S(x) of order n (degree n-1), with knots k_1, k_2, k_3, . . ., k_h, (where $k_1 < k_2 < \ldots < k_h$) is a function with the following properties.

(i) In each of the intervals:

$$x \leq k_1 \qquad 3.6$$

$$k_{i-1} \leq x \leq k_i, \text{ for } i = 2, 3, 4, \ldots, h \qquad 3.7$$

and

$$k_h \leq x \qquad 3.8$$

S(x) is a polynomial function of degree n-1.

(ii) S(x) and its derivatives up to order n-2 are continuous. A knot k_i is a convenient data point which is used as the boundary between two adjacent intervals, there are h knots in all.

The function is a cubic spline when the order n is equal to 4 and this is considered to be a satisfactory function for curve fitting. The continuity of the second order derivative makes it adequate for most

practical problems. The above definition means that the cubic spline consists of a set of h + 1 cubic polynomials joined smoothly end to end. Practical problems normally require the approximation of a set of m data points (x_r, f_r), for r = 1, 2, . . ., m, by a cubic spline confined to a finite range, $a \leq x \leq b$. The first and last knots are chosen so that $a \leq k_1$ and $b \geq k_h$. This makes the cubic polynomials of finite length and a and b are normally set equal to the smallest and largest x_r, respectively.

A cubic spline which has knots $k_1, k_2, \ldots, k_h$ has a unique representation in the form (71):

$$S(x) = \sum_{j=0}^{3} \alpha_j x^j + \sum_{i=1}^{h} \beta_i (x - k_i)_+^3 \qquad 3.9$$

where

$$(x - k_i)_+ = \begin{cases} (x - k_i), & \text{when } (x - k_i) \geq 0 \\ 0, & \text{when } (x - k_i) \leq 0 \end{cases} \qquad 3.10$$

This representation contains h + 4 basic functions, 4 power terms and h one-sided cubics. This is the minimum number of terms in which the general cubic spline with h knots can be expressed. This general function when used in curve-fitting becomes a problem of minimising the squares of the deviations of this function from the data points:

$$\sum_{r=1}^{m} [S(x_r) - f_r]^2 \qquad 3.11$$

A least squares routine is used to minimise the values of α_j and β_i. This results in the least squares solution of an overdetermined system of linear equations:

$$\sum_{j=0}^{3} \alpha_j x_r^j + \sum_{i=1}^{h} \beta_i (x_r - \lambda_i)_+^3 = f_r, \text{ for } r = 1, 2, \ldots, m \qquad 3.12$$

It is assumed that the number of data points m is greater than or equal to h + 4.

The spline function represented by equation 3.9 is computationally unsatisfactory in that the m linear equations 3.12 for determining α_j and β_i tend to be ill conditioned (71). A better representation is obtained by using B-splines. A cubic B-spline is a cubic spline that is non-zero only over 4 adjacent intervals between knots. That is the cubic B-spline, which has knots $k_1, k_2, \ldots, k_h$, is zero everywhere except in the range $k_{i-4} < x < k_i$. to define the full set of B-spline functions for a curve fit it is necessary to introduce eight additional knots k_{-3}, k_{-2}, k_{-1}, k_0, k_{h+2}, k_{h+3} and k_{h+1}, k_{h+4}, which must satisfy the conditions:

$$k_{-3} < k_{-2} < k_{-1} < k_0 \leq a \qquad 3.13$$

and $$k_{h+4} > k_{h+3} > k_{h+2} > k_{h+1} \geq b$$

With this increased set of knots the h + 4 B-splines $M_i(x)$, i = 1, 2, . . ., h + 4 can be defined. The representation of the data in the range $a \leq x \leq b$ then has the form (71):

$$S(x) = \sum_{i=1}^{h+4} \gamma_i M_i(x) \qquad 3.14$$

The curve fitting problem then reduces to finding the h + 4 coefficients γ_i as the least squares of the m equations:

$$\sum_{i=1}^{h+4} \gamma_i M_i(x_r) = f_r, \text{ for } r = 1, 2, \ldots, m. \qquad 3.15$$

In practice these coefficients are determined using matrix notation and most scientific computer packages have routines for the determination and evaluation of B-spline functions.

3.3.3.2 Applications to connection representation

Cubic B-spline curve fitting methods are used to achieve more accurate representaions of the true moment-rotation behaviour of a connection. This method requires the range of connection rotations to be divided into a finite number of smaller ranges. These smaller ranges are divided by convenient data points being chosen as the knots for the B-spline routines. Computer package routines only require the experimental data points and a list of conveniently chosen knots to determine the cubic B-spline coefficients. This method has been shown to produce close and smooth representations of experimental moment-rotation data as can be seen in Figure 3.8, which shows the B-spline approximation and the set of experimental data from which it was derived.

B-spline curve fitting routines yield a numerical description of the moment-rotation behaviour of the connection and this numerical description may be used

directly within numerical differentiation procedures to give a measure of connection stiffness at any given value of rotation. The corrected value of connection stiffness can then be used in the modified matrix stiffness method for semi-rigid frame analysis. This enables column or frame analysis to be performed using very close representations to the true connection behaviour.

CHAPTER 4

An Analysis of Columns with Semi-Rigid End Restraint

4.1 Stability Analysis of Columns

The analysis of steel columns may be approached by two fundamentally different methods. Classical methods of analysis assume the column to be "ideal" in shape, properties and end restraint. The maximum load is determined using a direct eigenvalue method. In recent years attempts have been made to develop mathematical models of a "real" column, which include material and geometrical nonlinearities. The solution is found by tracing the complete load versus lateral deflection curve of the column with the maximum load being the peak point of this curve.

4.1.1 Eigenvalue approach

The column problem has historically been approached by the eigenvalue method in which a critical load is found without calculating any deflections. The first analysis to consider the buckling of slender columns, instead of material failure, was proposed by Euler in 1759. The well known Euler elastic buckling load, given by the expression:

$$P_E = \frac{\pi^2 EI}{L^2} \qquad 4.1$$

gives the maximum load capacity of an ideal slender column of length L, material elastic modulus E and moment of inertia I. An ideal column is one which has no geometric or material imperfections, the end restraint is perfectly pinned and loading is perfectly axial, so

that the only deflections to occur at low loads are those in the direction of loading. This critical load is found by mathematically testing the equilibrium of the column; the critical load is reached when the equilibrium path separates into two possible configurations. This load is known as the buckling or bifurcation load. The point of bufurcation for the ideal column is shown in Figure 4.1. At the critical load P_E the equilibrium path may either continue on the vertical axis or the lateral deflections may suddenly become indetermined. This simple analysis overestimates the maximum load capacity of real columns, which are not perfectly straight and for which the material is not perfectly elastic nor free of residual stress. Also, loading is not perfectly axial and in practice end moments often exist, for example, due to load eccentricity. On the other hand, these ideal end restraint assumptions underestimate the maximum load, because, as shown in Chapter 3, even the most flexible of real connections offer considerable rotational restraint to the column ends.

The limitations of the Euler analysis were recognised by Engesser, who in 1889 proposed the tangent modulus method to allow for the inelastic behaviour of the column material. This effect is introduced by replacing the material's elastic modulus E of equation 4.1, by the tangent modulus E_t, which is the slope of the material's stress-strain curve. The effects of material yield on the cross-section were later accounted

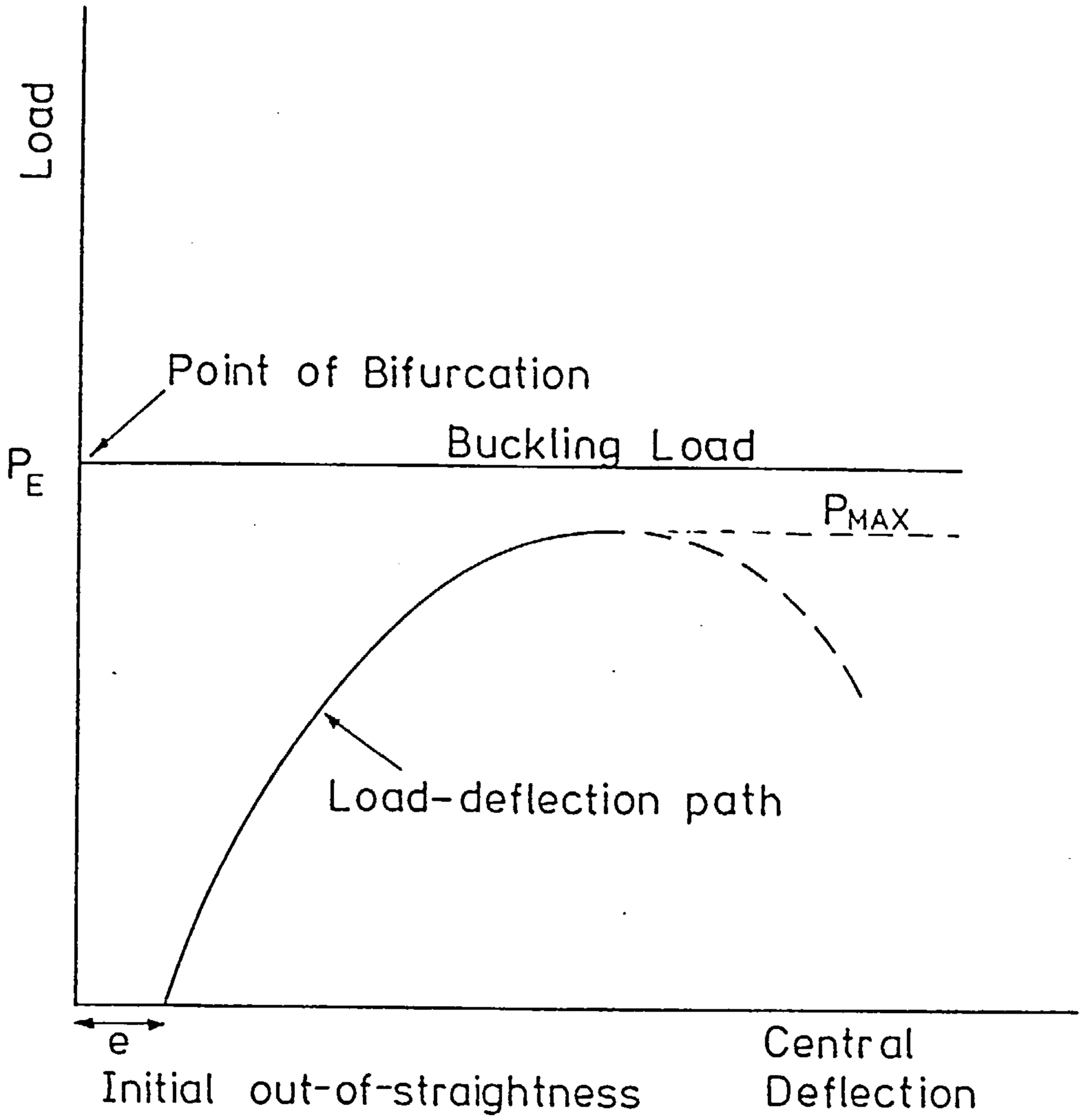

FIGURE 4.1 - Comparison of Classical Eigenvalue and Load-Deflection Methods

for by the reduced modulus approach. This assumes a reduced modulus, between E and E_t, to allow for partial plastification of the section. Again, the reduced modulus is substituted into the Euler expression to give a critical load value. These modifications to the original Euler analysis can account for the effect of residual stress and other material nonlinearities, but geometrical imperfections such as out-of-straightness and end restraint cannot be incorporated.

Modern matrix methods also adopt an eigenvalue approach to the column problem. The stiffness matrix of a member can be modified by the incorporation of stability functions to become the stability matrix (20), the determinant of which gives a measure of stability. The stability functions are dependent upon the level of applied axial load, and in turn this makes the determinant of the stability matrix load dependent. Axial load becomes critical when it causes the determinant of the stability matrix to equal zero. So the analysis becomes a matter of searching for the first eigenvalue of the column's stability matrix.

4.1.2 Load-deflection approach

The load-deflection method attempts to solve the stability problems by determining the load versus lateral deflection curve of the column over its entire loading range, including the post-maximum descending part of the curve. The solution technique is performed by applying

load incrementally and calculating resulting deflections. Equilibrium iterations are usually performed until the internal forces balance the externally applied loads. The calculation of deflections in the elastic-plastic range of materials is usually complex, so numerical computer procedures are often used to obtain a solution. The load-deflection approach must be used to obtain an accurate solution for a real column in a structural frame.

The real column is not perfectly straight but is assumed to have an initial out-of-straightness, which causes lateral deflections to occur throughout the full loading range. These deflections in turn produce secondary moments which cause further lateral deflections to occur. Real columns also have nonlinear material imperfections due to elastic-plastic stress-strain behaviour and also the presence of initial residual stresses. A geometrical imperfection of the column which has received very little attention is that of end restraint,which can have an important stiffening effect. Loading conditions on real colums are usually not perfectly axial, load is often applied at some eccentricity due to the geometry of structural connections and often columns are subject to additional lateral loads.

The column analysis described in this chapter adopts a load-deflection approach and includes the

material and geometrical imperfections discussed above. Particular attention is given to the inclusion of real end restraint conditions in the analysis.

Column theory has developed from consideration of an "ideal" column to the detailed study of the behaviour of a complex "real" column model. This change in approach has been made possible by increased knowledge of the effects which parameters such as: residual stress, initial out-of-straightness and end restraint, have on the strength of columns. These effects have all been incorporated into column models to make them more representative of the real column. As the column models become more sophisticated the load-deflection method of analysis becomes a better representation of true column behaviour.

The type of curve that results from a load-deflection analysis is shown in Figure 4.1, which illustrates the difference between the two approaches. A comparison of the assumption made about the column model in the two approaches is given in Table 4.1.

4.2 The Finite Element Method of Analysis

The Finite Element Method is a well-known structural analysis technique and is fully described in many standard textbooks (72, 73, 74). A detailed discussion of the Finite Element Method is beyond the scope of this thesis; for this reason only a brief outline of the method is given. Attention is concentrated upon the

TABLE 4.1 - Comparison of Real and Ideal Analysis Assumptions

Eigenvalue Analysis	Load-Deflection Analysis
Perfectly straight	Initial out-of-straightness
Elastic material	Elastic-perfectly plastic stress-strain curve
Initially stress free	Residual stresses
Ideally pinned connection	Actual connection behaviour

application of the method to the end restrained column problem.

To solve the column problem by the Finite Element Method, a general procedure must be followed. This may be summarised as follows:

1. The column is divided into a finite number of elements along its length. The divisions between these elements are marked by nodes. The ends of the elements on either side of these nodes are compatible in position and direction, so that the behaviour of the complete assemblage of elements approximates to the physical behaviour of the column. The material and physical properties are chosen to closely model the column's properties. The chosen length of the elements depends on the required accuracy of solution; the accuracy generally increases with an increased number of elements.

2. The element stiffness matrix to describe the properties of a typical element is chosen and relates the elements' nodal displacements to the forces that exist at the nodes. This relationship is described by the expression:

$$\{F^e\} = [K^e]\{\delta^e\} \qquad 4.2$$

in which $[K^e]$ is the element stiffness matrix, $\{F^e\}$ is the vector of loads applied at the nodes and $\{\delta^e\}$ is the vector of unknown nodal displacements.

3. The overall stiffness matrix [K] for the whole column is assembled by adding together all the individual element stiffness matrices. In the isolated column problem no transformation of coordinates is required. The resulting overall stiffness matrix relates the displacements at all nodes of the column {δ} to the vector of all applied forces {F}:

$$\{F\} = [K]\{\delta\} \qquad 4.3$$

4. The boundary conditions relating to fixed supports and end restraint are applied to equations 4.3 by modification of the overall stiffness matrix [K] and the applied load vector {F}. Boundary conditions must be applied to relate all displacements to a fixed datum. The overall stiffness matrix would be indeterminate if insufficient of these conditions were applied.

5. The vector of unknown displacements {δ} may then be found from the solution of the modified set of equations 4.3.

6. The internal stresses and strains within the elements may then be calculated from the nodal deflections determined in the previous step.

4.3 Column Model used in Analysis

The theoretical column model, used in the analysis, is shown in Figure 4.2a. The model consists of a member with a provided initial out-of-straightness

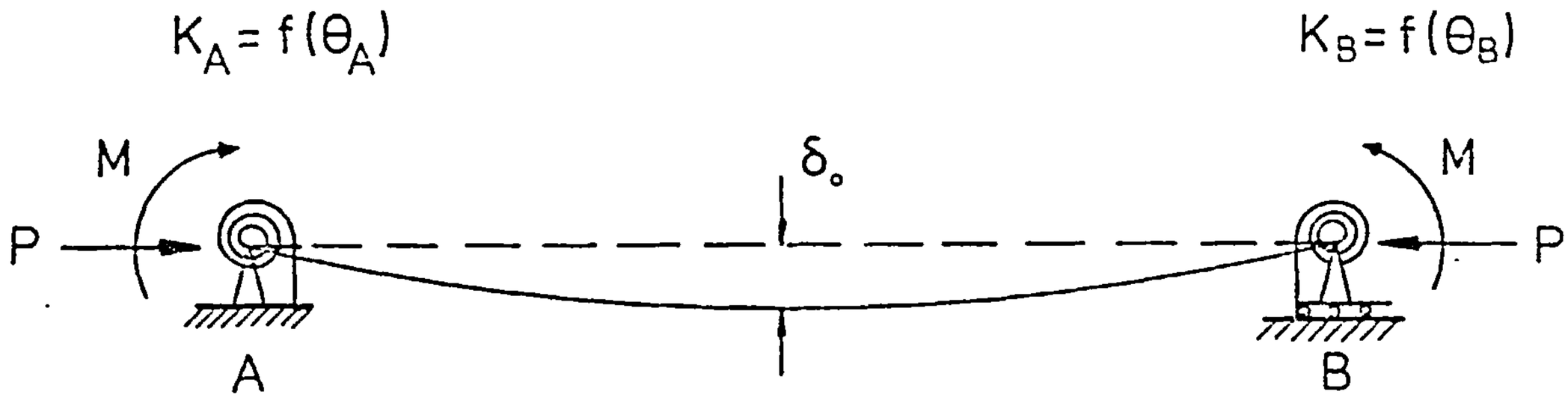

(a) Theoretical Column Model

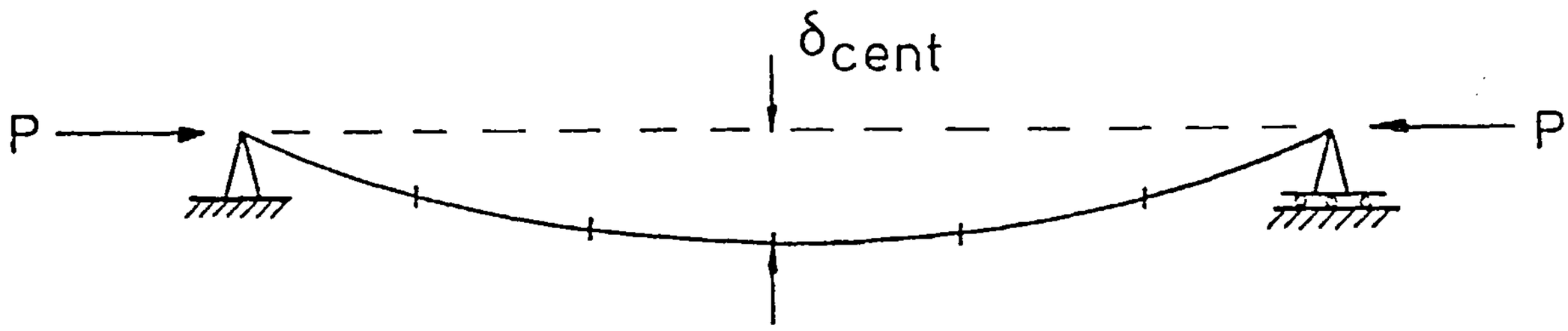

(b) Finite Element Column Model

FIGURE 4.2 - Column Models used in Analysis

between two pinned supports. The semi-rigid restraints at these supports are represented by rotational springs connected to the perfectly rigid datum. Realistic modelling of real connections requires that the stiffness of these rotational springs be a nonlinear function of rotation at the column ends. This may be expressed as:

$$K_c = f(\theta) \qquad 4.4$$

where K_c is the connection's rotational stiffness at a rotation of θ. Axial loading is applied at the column ends, where bending moment may also be applied. Eccentric loading can be represented by a combination of axial loads and bending moments. Although the column model shown in Figure 4.2a is for the sway prevented case, sway may be introduced into the analysis simply by changing boundary conditions.

The finite element column model is shown in Figure 4.2b. Nodes divide the column into a finite number of one dimensional beam elements. The analysis is restricted to in-plane deformations, so the beam elements have three degrees of freedom at each node; namely axial, lateral and rotational deformation. Therefore each beam element has six degrees of freedom and is represented by a 6×6 stiffness matrix. The number of elements used to represent the column depends on the required accuracy; an increase in the number of elements generally produces a corresponding increase in accuracy. All supports, apart from the rotational end restraint, are assumed to be perfectly rigid.

4.4 Column Stiffness

4.4.1 Element stiffness matrix

The column is represented in the analysis by a series of in-plane beam elements. Each of these elements has three degrees of freedom at each of its two nodes, as shown in Figure 4.3. The vectors of nodal forces and nodal displacements can be expressed as:

$$\{F^e\} = \begin{Bmatrix} F_{x1} \\ F_{y1} \\ M_{z1} \\ F_{x2} \\ F_{y2} \\ M_{z2} \end{Bmatrix}, \quad \text{and} \quad \{\delta^e\} = \begin{Bmatrix} u_1 \\ v_1 \\ \theta_1 \\ u_2 \\ v_2 \\ \theta_2 \end{Bmatrix} \qquad 4.5$$

These two vectors are related to each other, in the material's elastic range by the equations 4.3, in which $[K^e]$ is the element stiffness matrix. The element stiffness matrix for a straight beam element with uniform cross-section is derived by Przemieniecki (31), and may be expressed as:

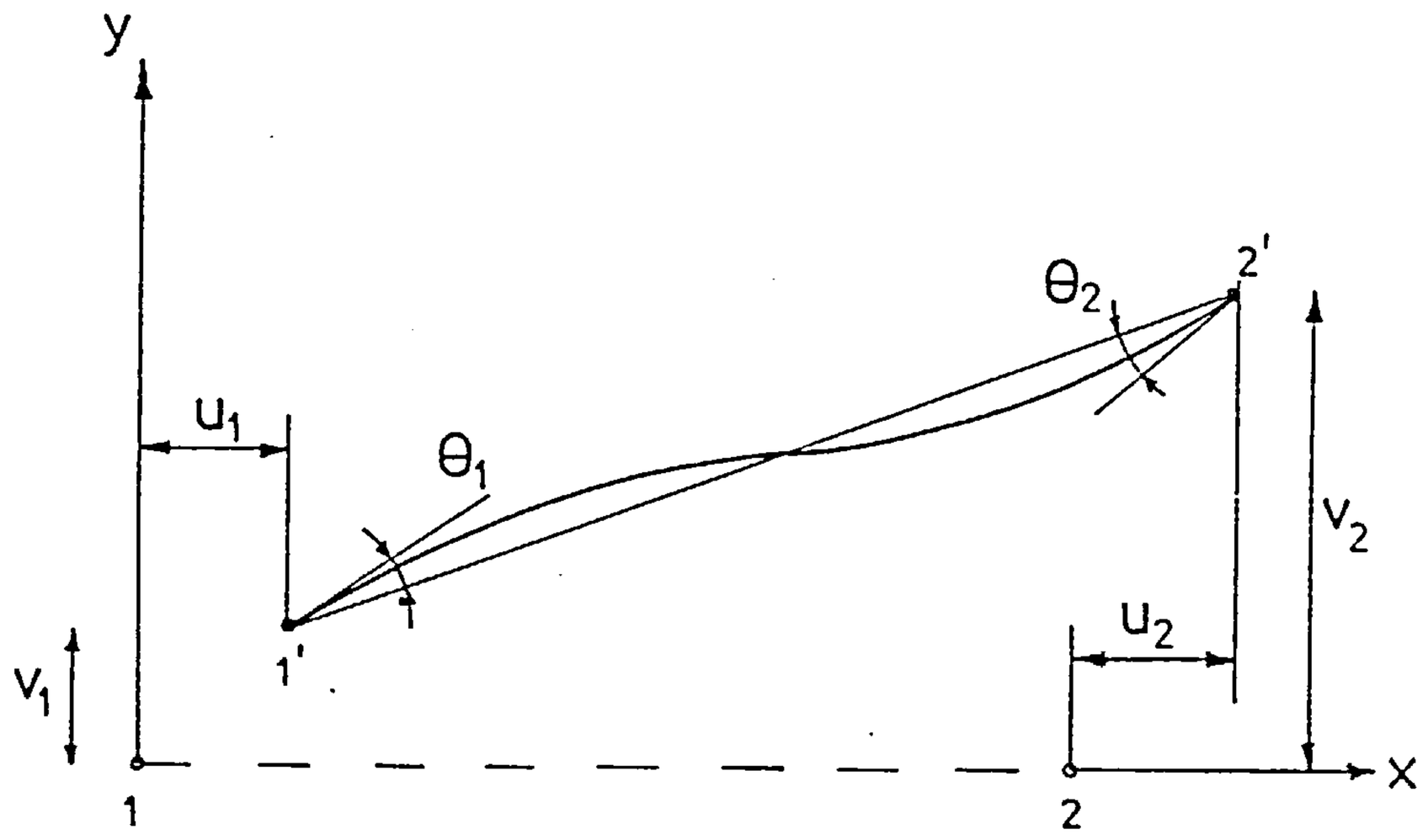

(a) Displacement

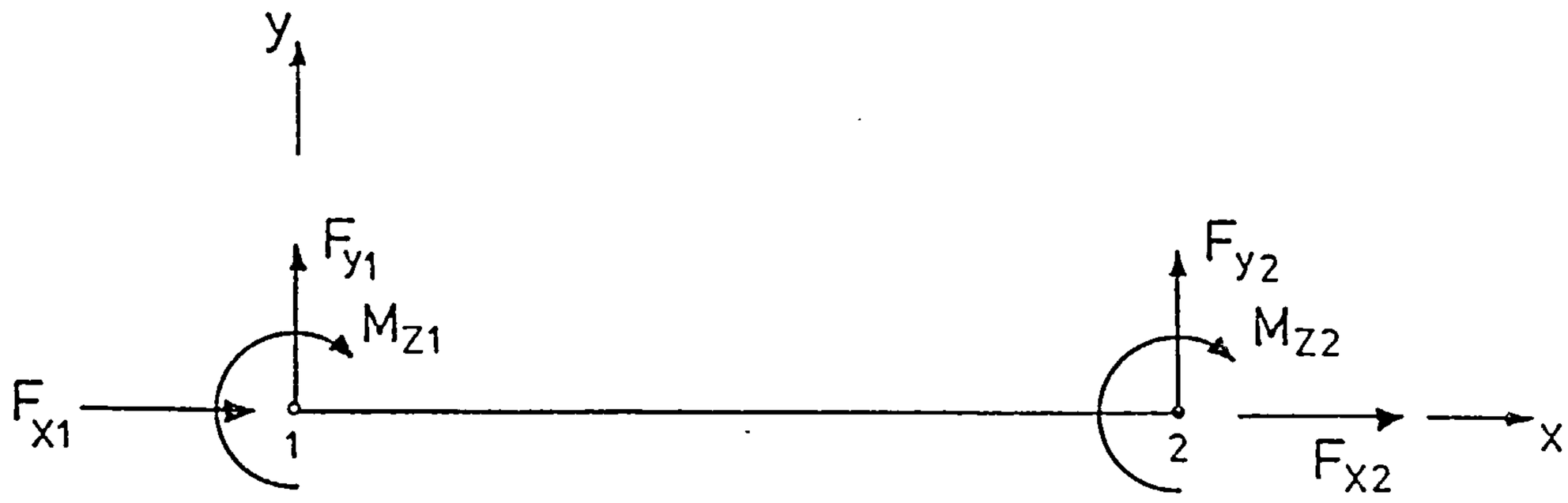

(b) Force

FIGURE 4.3 - Single Element Displacement and Force Components

$$[K_E^e] = \begin{bmatrix} \frac{EA}{L} & 0 & 0 & -\frac{EA}{L} & 0 & 0 \\ 0 & \frac{12EI}{L^3} & \frac{6EI}{L^2} & 0 & -\frac{12EI}{L^2} & \frac{6EI}{L^2} \\ 0 & \frac{6EI}{L^2} & \frac{4EI}{L} & 0 & -\frac{6EI}{L^2} & \frac{2EI}{L} \\ -\frac{EA}{L} & 0 & 0 & \frac{EA}{L} & 0 & 0 \\ 0 & -\frac{12EI}{L^3} & -\frac{6EI}{L^2} & 0 & \frac{12EI}{L^3} & -\frac{6EI}{L^2} \\ 0 & \frac{6EI}{L^2} & \frac{2EI}{L} & 0 & -\frac{6EI}{L^2} & \frac{4EI}{L} \end{bmatrix} \quad 4.6$$

where L is the length of the element, A is the cross-sectional area, I is the moment of inertia and E is the material's elastic modulus. This matrix may be derived by assuming a linear axial displacement function and cubic lateral and rotational displacement functions. A linear elastic stress-strain relationship is assumed in which the elastic modulus E is constant and the material is completely elastic. The element stiffness matrix is a measure of the element's stiffness due to its material properties. Nonlinear material properties may be accounted for, in an incremental analysis, by the use of reduced axial and flexural rigidities.

4.4.2 Element geometrical stiffness matrix

The element geometrical stiffness matrix is used to account for the effects of axial load and changes in element geometry. The geometrical stiffness matrix was derived by Gallagher and Padlog (75) to include the effects of large displacements in the calculation of the

element's stiffness matrix. Large displacements cause the strain-displacement functions to contain nonlinear terms. The large displacement strain-displacement functions are used to derive the element geometrical stiffness matrix, which is expressed as:

$$[K_G^e] = P \begin{bmatrix} 0 & 0 & 0 & 0 & 0 & 0 \\ 0 & \frac{6}{5L} & \frac{1}{10} & 0 & \frac{-6}{5L} & \frac{1}{10} \\ 0 & \frac{1}{10} & \frac{2L}{15} & 0 & \frac{-1}{10} & \frac{-L}{30} \\ 0 & 0 & 0 & 0 & 0 & 0 \\ 0 & \frac{-6}{5L} & \frac{-1}{10} & 0 & \frac{6}{5L} & \frac{-1}{10} \\ 0 & \frac{1}{10} & \frac{-L}{30} & 0 & \frac{-1}{10} & \frac{2L}{15} \end{bmatrix} \qquad 4.7$$

where L is the length of the element and P is the axial load with tension positive. Compressive axial loads reduce column stiffness and this is accounted for by adding the geometrical stiffness matrix to the element stiffness matrix:

$$[K^e] = [K_E^e] + [K_G^e] \qquad 4.8$$

4.4.3 Overall stiffness matrix

Once the individual element stiffness matrices have been established it is necessary to assemble the overall stiffness matrix of the whole column. This results in an equilibrium equation for each degree of freedom of the column, so that, if the column has been divided into eight elements with nine nodes, the overall stiffness

matrix will have 27 rows and columns. The individual elements are assembled to form the overall stiffness matrix to ensure that displacement compatibility is satisfied at each node of the column. Computational methods for the assembly of the overall stiffness matrix are given in standard textbooks (73, 74). The overall stiffness matrix is found, in the present analysis, by assembling all the element elastic stiffness matrices into the overall elastic stiffness matrix $[K_E]$ and all the element geometrical stiffness matrices into the overall geometrical stiffness matrix $[K_G]$, these are then added together to give:

$$[K] = [K_E] + [K_G] \qquad 4.9$$

In order to save computational effort the overall geometrical stiffness matrix need only be assembled once for unit axial load; this can then be stored and multiplied by the total axial load level for use in the incremental analysis. Due to changing column cross-sectional properties as loading increases, the overall elastic stiffness matrix has to be reassembled after each iteration. Equations 4.9 may then be expressed as:

$$[K] = [K_E] - P[\bar{K}_G] \qquad 4.10$$

where $[\bar{K}_G]$ is the overall geometrical stiffness matrix for unit axial load.

4.5 The Influence of Geometrical Imperfections

4.5.1 Initial out-of-straightness

Real columns are not perfectly straight due to the

initial curvature produced during the hot rolling process of manufacture. This initial curvature causes the column to bend throughout its loading range and this produces increases in member stresses. The greater the initial curvature the greater will be the bending effect. The initial out-of-straightness of a range of column sizes has been measured (76); and can be reasonably approximated by a half sine wave with a maximum central deflection given by:

$$\delta_o = a_o \text{Sin} \frac{\pi x}{L} \qquad 4.11$$

where a_o is the initial central deflection, L is the length of the column and δ_o is the initial lateral deflection at a distance x along the column. The value of the initial central deflection ranges from zero to a maximum of about 0.004L. Design and analytical procedures usually assume a value of 0.001L.

The finite element column model is initially straight and the effect of initial curvature is included in the analysis by the use of imaginary lateral loads $\{P_o\}$, which increase in the same proportion as the applied axial load P. Their purpose is to increase lateral deflections as column bending increases due to axial loads acting through the initial out-of-straightness. For zero axial load the initial deflection shape is assumed; initial lateral deflections δ_o are given by equation 4.11 and initial rotational deflections θ_o are given by the first derivative of equation 4.11 with respect to length x along the column:

$$\theta_o = \frac{d}{dx}(\delta_o) = a_o\frac{\pi}{L} \text{ Cos } \frac{\pi x}{L}, \qquad 4.12$$

initial axial deflections are zero. Equations 4.11 and 4.12 define the initial shape of the column from which additional deflections δ due to applied axial loads are measured. The imaginary lateral loads are calculated by multiplying the vector of initial deflections by the overall geometrical stiffness matrix (31):

$$\{P_o\} = [K_G]\{\delta_o\} \qquad 4.13$$

The load vector assumed in the analysis is the sum of the actual applied loads $\{F\}$ and the imaginary lateral loads $\{P_o\}$, this is applied incrementally and $\{P_o\}$ is calculated assuming the axial load level at the start of the load increment.

4.5.2 Destabilising effect of axial loads

An axial load acting through the initial out-of-straightness of the column affects its stability. A tensile axial load tends to straighten the column and so increases its stiffness. However, when a compressive axial load acts through an initial curvature the effects of the load acting at an eccentricity (due to the lateral deflection) cause secondary moments, which increase lateral deflections and reduce column stiffness. This reduced stiffness in turn reduces the stability of the column. A measure of the column's stability is given by the determinant of the overall stiffness matrix, the determinant being zero at the point of instability,when

displacements tend to infinity. The instability condition is then expressed as:

$$\det |K_E + K_G| = 0 \qquad 4.14$$

The geometrical stiffness matrix modifies the equilibrium equations to allow for the destabilising effect of axial loads. In the notation of the geometrical stiffness matrix for unit applied load, the instability condition may be expressed as:

$$\det |K_E - P.\bar{K}_G| = 0 \qquad 4.15$$

where P is the compressive axial load.

4.6 Inclusion of End Restraint into Analysis

The effects of semi-rigid end restraint are included in the analysis by modification of the column's assembled overall stiffness matrix. The stiffness matrix terms relating to the end nodes of the column model represent the column's inherent stiffness and do not include any external stiffness. Semi-rigid connections provide an additional external stiffness to the end node rotational degrees of freedom. This additional stiffness is the slope of the connection's moment-rotation characteristic for any particular connection rotation value. The column stiffness matrix can be modified by adding the connection stiffness to the relevant stiffness matrix terms which relate end moment to end rotation.

As the moment-rotation curve of a connection is a nonlinear function, the connection stiffness terms are calculated within an incremental loading procedure. The connection stiffness used in a load increment is assumed to be that which exists for the displacements at the start of that load increment. The moment-rotation curve for the connection is introduced into the analysis in the form of a cubic B-spline function which can be evaluated for any given end rotation. The tangent of this moment-rotation curve, representing the connection's rotational stiffness, is found by using the cubic B-spline function within a numerical differentiation routine. For a symmetrical column with identical connections at each end, the calculated rotational stiffness value K_c is added to the rotational stiffness terms in the column stiffness matrix. If the nodes of the finite element model are numbered in a regular pattern, so that each node has three consecutive degrees of freedom and the third degree is the rotational component, then the connection stiffness term has to be added to the third and last leading diagonal terms of the stiffness matrix. This can be expressed as:

$$K_{ii}' = K_{ii} + K_c, \quad \text{for } i = 3 \text{ and NDF} \qquad 4.16$$

where K_c is the connection stiffness, K_{ii} is the original stiffness matrix component for degree of freedom i which is modified to give K_{ii}'. NDF is the total number of degrees of freedom, and is equal to three times the number of nodes.

4.7 Evaluation of Section Properties

4.7.1 The stress-strain relationship

The important material properties of a structural material are given by its stress-strain relationship. Figure 4.4 compares the actual stress-strain curve for a structural steel with an assumed idealised elastic-perfectly plastic stress-strain relationship. The present analysis assumes the stress-strain behaviour of Figure 4.4b, in which the material has a linear stress-strain curve whose slope is the Young's modulus of elasticity E. The values of E vary within a fairly narrow range of 200-210 kN/mm^2, for most types of structural steel. The steel remains elastic while in this linear range. The limit for this elastic range is reached when the strain becomes equal to the yield strain ε_y, beyond this point the material flows plastically without any increase in stress. The maximum stress level achieved is the yield stress, which is the most important property in determining the strength of a structural steel. The yield stress varies significantly with the grade and chemical composition of the structural steel. The stress-strain relations assumed in the analysis may be expressed as:

$$\sigma = \begin{cases} E.\varepsilon, & \text{when } \varepsilon < \varepsilon_y \\ \sigma_y, & \text{when } \varepsilon > \varepsilon_y \end{cases} \qquad 4.17$$

It is assumed that steel flows plastically until the strain-hardening strain ε_{SH} is reached, after which the stress increases until the ultimate tensile strength

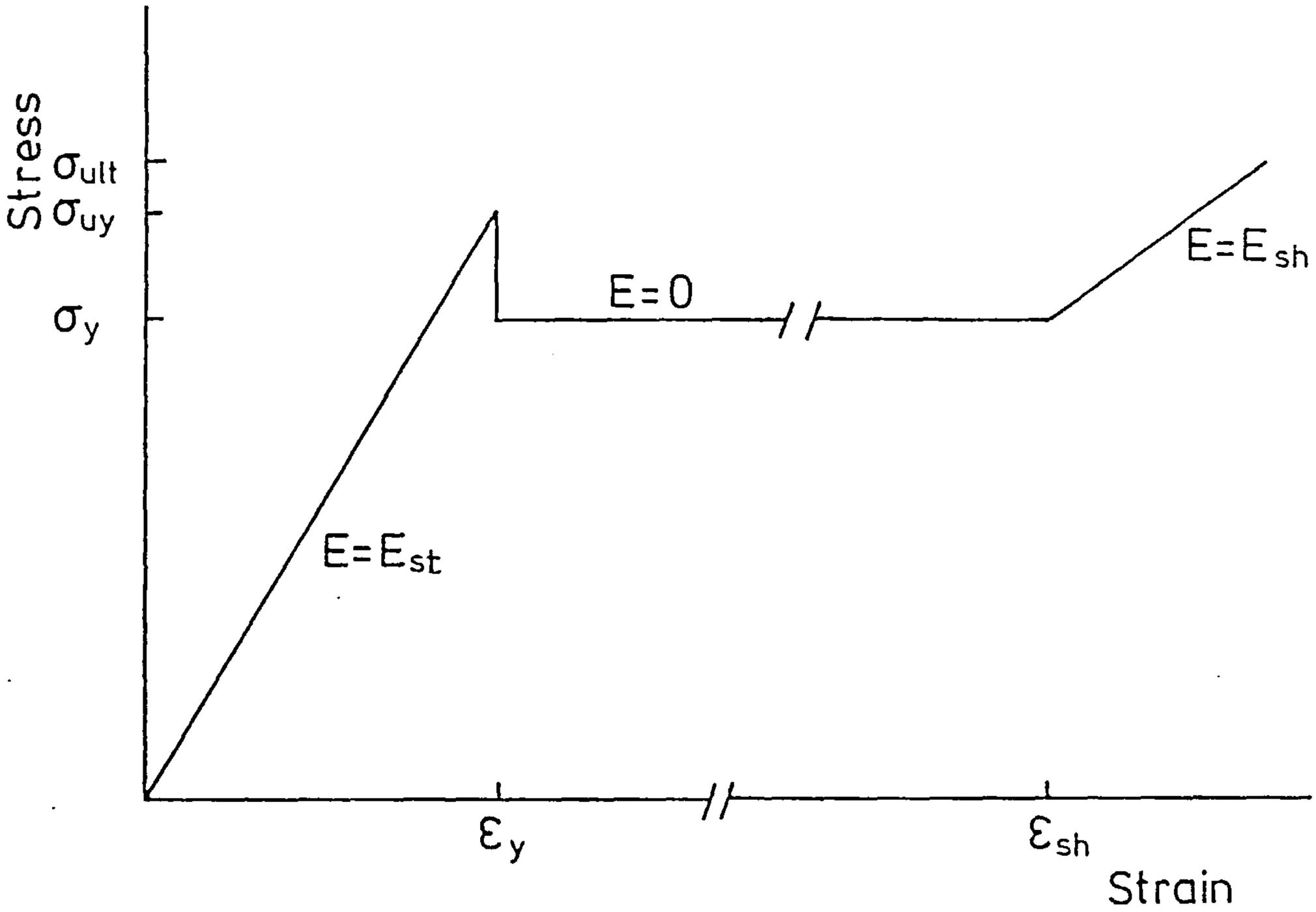

(a) Actual Stress-Strain Curve

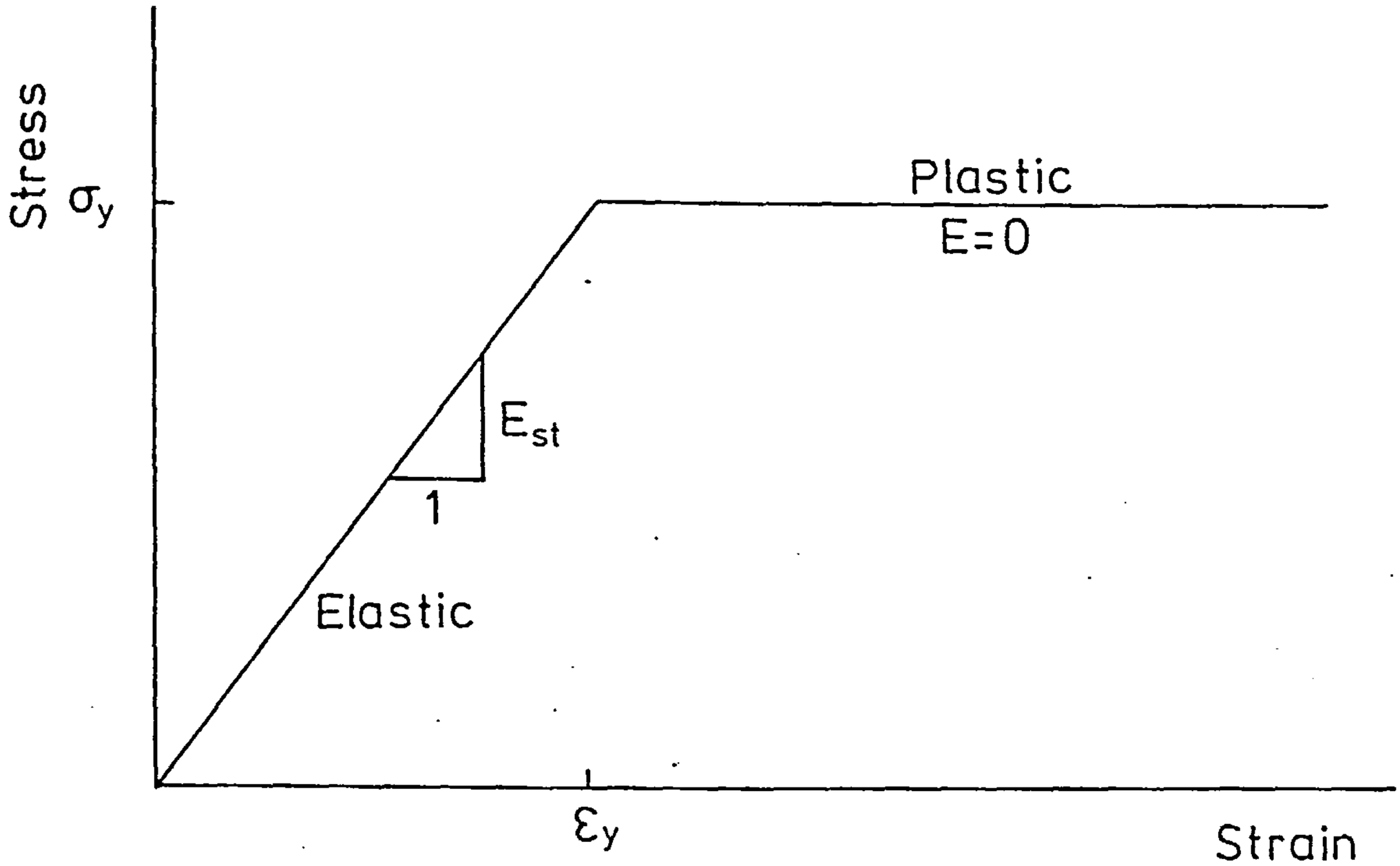

(b) Idealised Elastic Perfectly-Plastic Stress-Strain Curve

FIGURE 4.4 - Stress-Strain Relationships for Structural Steel

is reached. The elastic-perfectly plastic curve neglects this strain-hardening effect and is not included in the present analysis. However, strain-hardening could be introduced into the analysis by assuming a new elastic modulus E_{SH} for the material when the initial strain-hardening strain is exceeded:

$$E = E_{SH}, \text{ when } \varepsilon > \varepsilon_{SH} \qquad 4.18$$

4.7.2 Spread of yield within the member cross-section

The stiffness properties of a column are not affected while the material remains within its elastic range. The presence of bending strains cause a gradual change from an elastic state to the fully plastic state. From the load level of first yield, as yield spreads through the section there is a gradual reduction in the effective axial and flexural rigidities of the column. The effective axial and flexural rigidities of a column cross-section may be estimated by considering the contribution of elastic zones of the section only, where the current value of strain is less than the strain at yield.

The calculation of the effective section properties of a general cross-section is shown in Figure 4.5a, in which dA is an infinitely small area of section at a distance x from the neutral axis of the section. The effective axial and flexural rigidities may be expressed as:

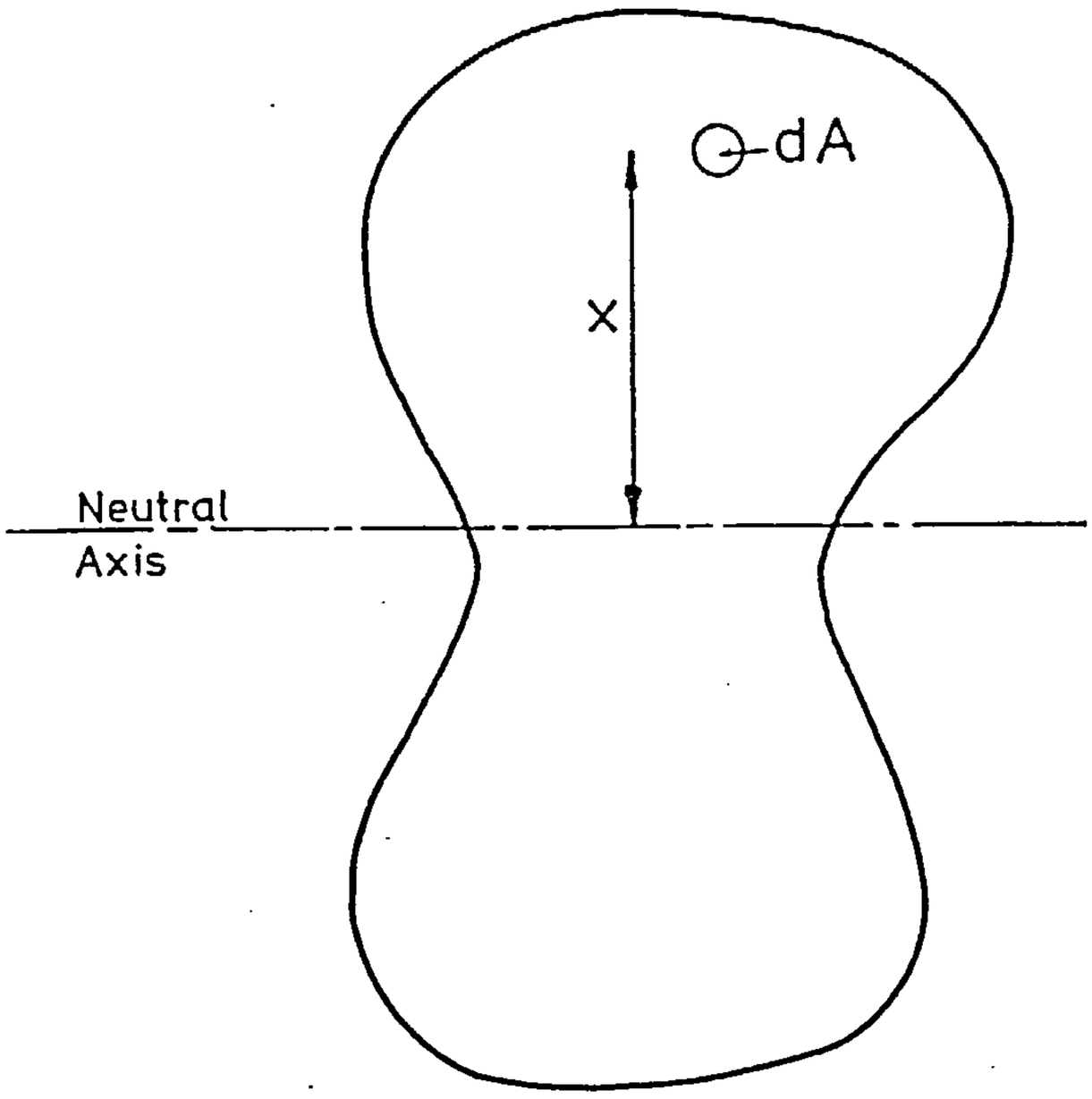

$$\text{Effective } EA = \int^{A} E\,dA$$

$$\text{Effective } EI = \int^{A} E x^2\,dA$$

Where if:

$\varepsilon < \varepsilon_y \quad E = E_{ST}$

$\varepsilon > \varepsilon_y \quad E = 0$

(a) Generalised Model

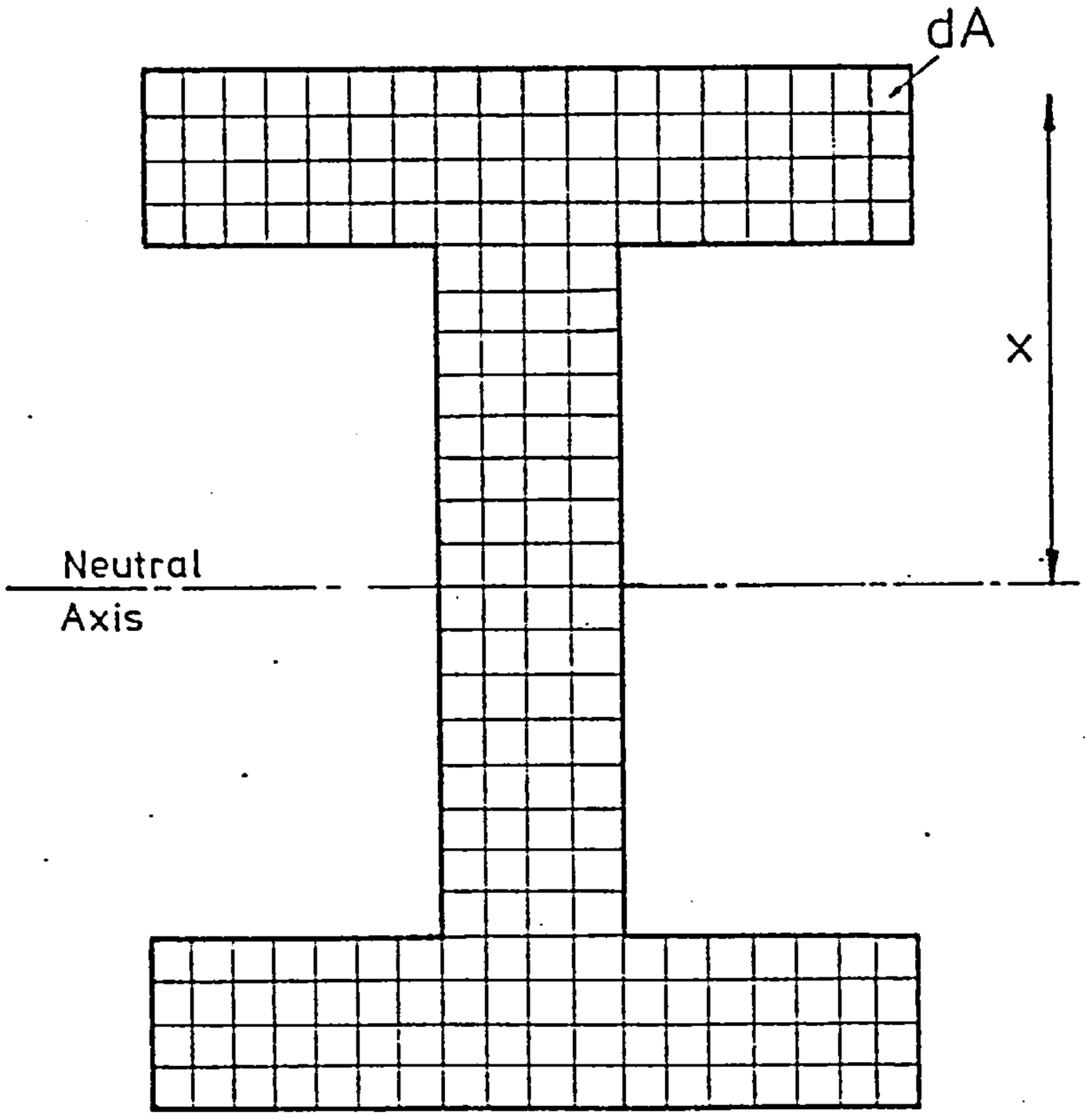

$$\text{Effective } EA = \Sigma E\,dA$$

$$\text{Effective } EI = \Sigma E x^2\,dA$$

Where if:

$\varepsilon < \varepsilon_y \quad E = E_{ST}$

$\varepsilon > \varepsilon_y \quad E = 0$

(b) Model used in Analysis

FIGURE 4.5 - Effective Section Calculation

$$EA_{eff} = \int_{A} E.dA \qquad 4.19$$

$$EI_{eff} = \int_{A} E.x^2.dA \qquad 4.20$$

where

$$E = \begin{cases} E_{ST}, & \text{when } \varepsilon < \varepsilon_y \\ 0, & \text{when } \varepsilon > \varepsilon_y \end{cases} \qquad 4.21$$

and equations 4.19 and 4.20 are integrals over the full area of the section.

The above method for calculating the effective section properties is not suitable for use within a numerical analysis procedure due to the use of infinitely small areas. An approximate method (77) to include the effects of material yield on section stiffness properties has been incorporated into the analysis, this requires the column cross-section to be divided into a number of rectangular regions as shown in Figure 4.5b. The axial and flexural rigidity contributions of each of these regions are calculated; each is assumed to be either completely elastic or completely plastic depending on the total strain that is applied to its centroid. This total strain consists of three components as shown in Figure 4.6. The rectangular axial strain distribution is due to axial deflections caused by direct axial load. The triangular strain distribution is due to curvature, along the length of the column, caused by lateral deflection due to initial out-of-straightness, end moments and eccentric or lateral

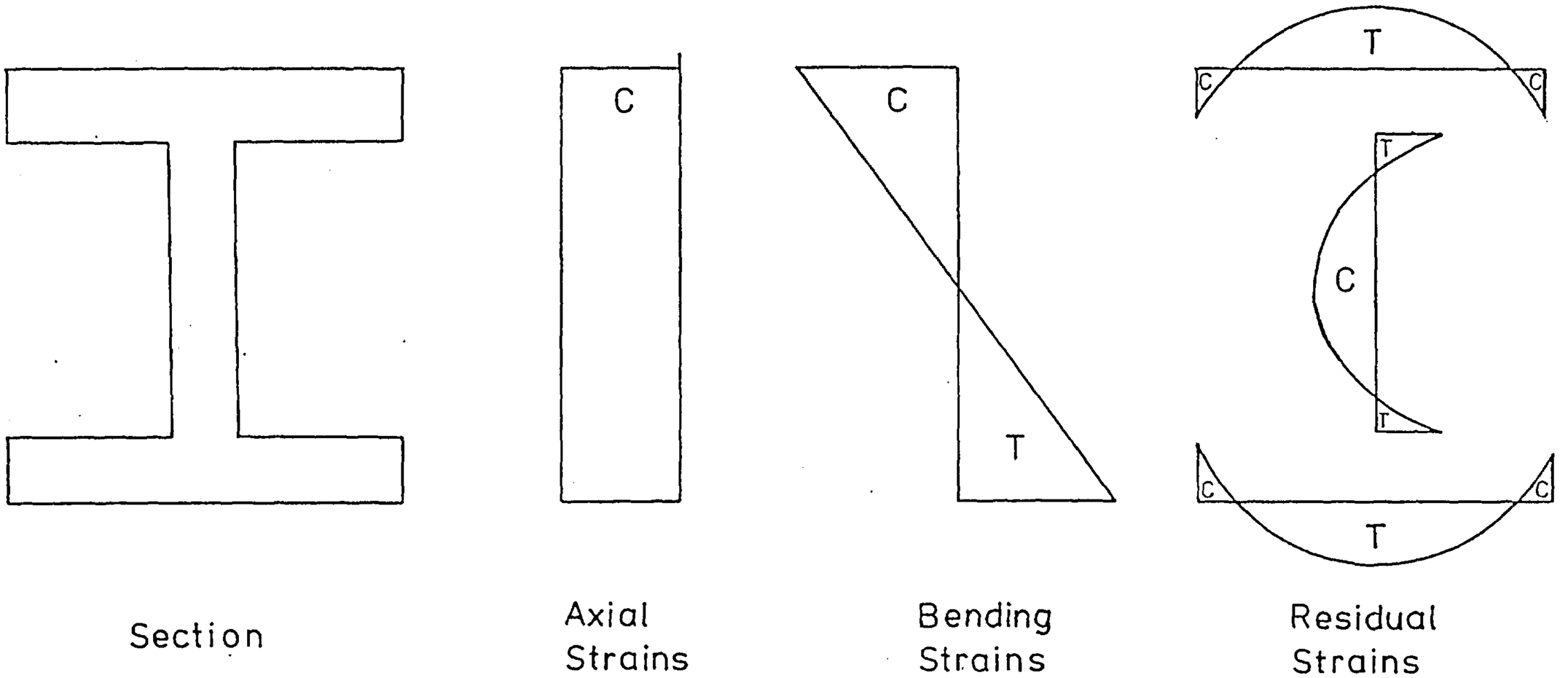

FIGURE 4.6 - Strains Applied to a Column Section

loads. Residual strain distributions are discussed in the following section. The three strain components existing at the centroid of each rectangular region are added together; if the total exceeds the yield strain then the effective modulus of the region is assumed to be zero. The effective section properties are found by summing the contributions of the individual regions over the whole section, the effective axial rigidity is:

$$EA_{eff} = \sum E.\Delta A \qquad 4.22$$

and the effective flexural rigidity is:

$$EI_{eff} = \sum E.x^2.\Delta A \qquad 4.23$$

where

$$E = \begin{cases} E_{ST}, & \text{when centroidal } \varepsilon < \varepsilon_y \\ 0, & \text{when centroidal } \varepsilon > \varepsilon_y \end{cases} \qquad 4.24$$

ΔA is the area of the rectangular region and x is the distance from the region's centroid to the section's neutral axial.

The resulting effective section properties represent the stiffness that exists at the nodes of the finite element model. The properties of a column finite element may be determined by averaging the rigidities that exist at its ends. The section properties, which are calculated from total deflections during each equilibrium iteration,

are substituted into the element elastic stiffness matrices. These are used to reassemble the overall stiffness matrix and so include the effects of material yield within the column analysis.

This method of determining the section properties may be used with any thin walled column section. The section is assumed to consist of a number of rectangular plates which are divided into four regions through the thickness of the plate and up to forty regions along its length. For a structural I section, subject to in-plane bending and neglecting the effects of residual stress, computational effort may be saved by having only one region along the width of the column for either vertical or horizontal plates. If residual stresses are assumed to be present, then the full number of regions across the width of flanges must be used. The method is readily programmed for computer analysis procedures and permits any cross-sectional shape or residual stress distribution to be assumed.

4.7.3 Inclusion of residual stresses

Residual stresses, which can exert a significant influence on the way in which yield spreads through the cross-section, should be included in any analysis attempting to model real column behaviour. These stresses, which result from differential cooling after hot rolling, can have a significant effect on column

behaviour. Flange tips which cool rapidly are usually left in residual compression, while regions which cool more slowly, such as the web to flange junction, are normally in residual tension (77). Residual stresses are also present in welded-up sections, high residual tension is normally present in the regions around the welds, while the remaining regions are in residual compression maintaining equilibrium within the section.

Residual stresses are included in the analysis by superimposing their strain distributions on the axial and bending strain distributions. This is done by assigning a residual strain value to the centroid of each cross-sectional region described in the previous section. The program includes two possible rolled residual stress patterns and a welded stress pattern. These three patterns are shown in Figure 4.7. The program can call any of these patterns automatically, or alternatively any other pattern may be input as data.

The parabolic strain distribution of sections used in British practice as described by Young (78) is shown in Figure 4.7a. This distribution may be represented by simple parabolic functions in both the web and the flange. Young gives the residual stress values for a steel I section at the flange tips σ_F, the flange to web junction σ_{FW} and the centre of the web σ_W as:

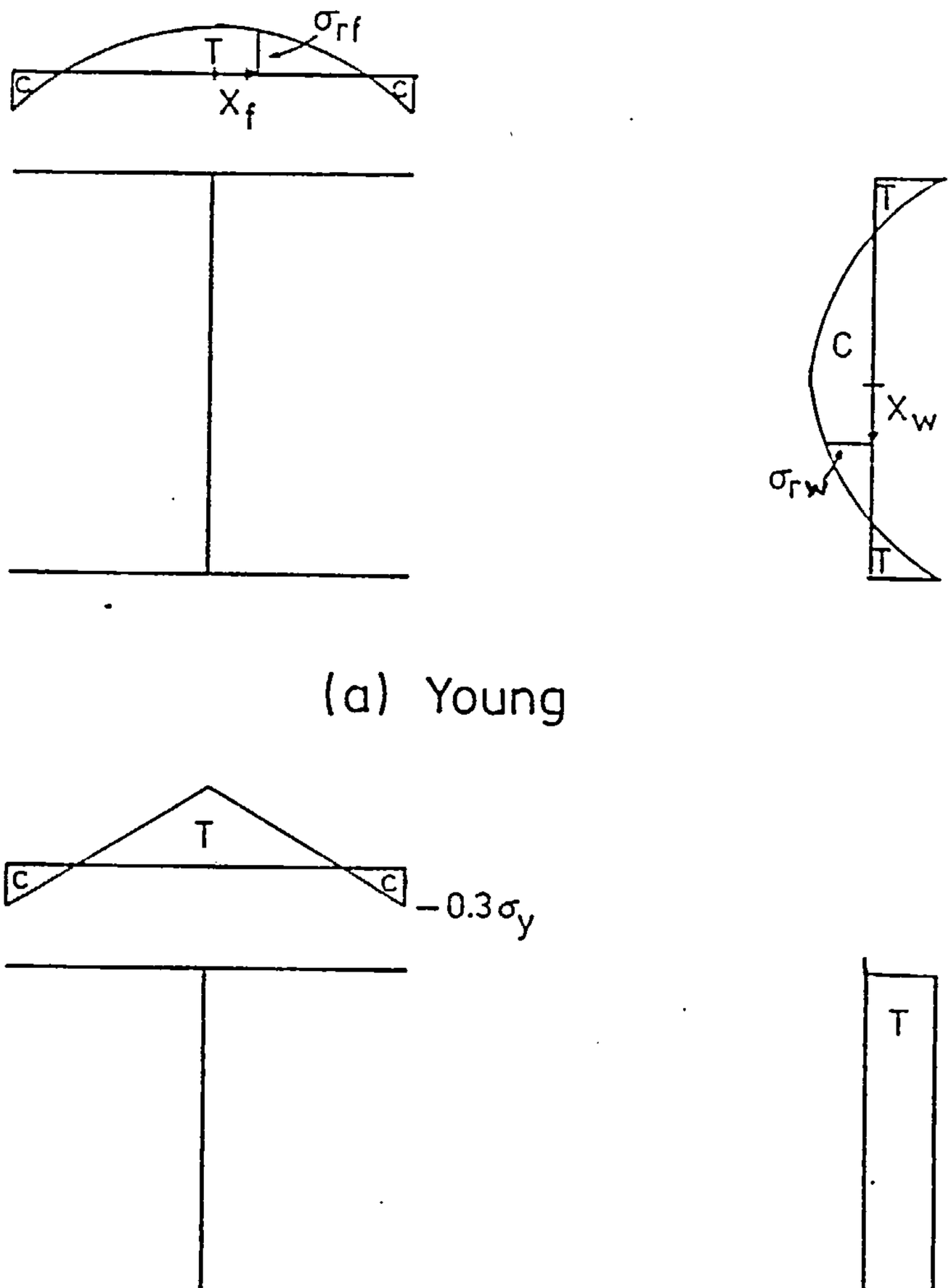

FIGURE 4.7 - Residual Stress Patterns

$$\sigma_F = 165\left(1 - \frac{A_W}{1.2A_F}\right) \quad N/mm^2, \qquad 4.25$$

$$\sigma_{FW} = -100\left(0.7 + \frac{A_W}{A_F}\right) \quad N/mm^2, \qquad 4.26$$

and $$\sigma_W = 100\left(1.5 + \frac{A_W}{1.2A_F}\right) \quad N/mm^2, \qquad 4.27$$

where A_W is the web area and A_F is the flange area. The residual stress level at any point along the flange may be represented by the simple parabolic equation:

$$\sigma_{RF} = a_1 x_f^2 + c_1 \qquad 4.28$$

in which σ_{RF} is the residual stress level at a distance x_f from the flange centroid, and a_1 and c_1 are constants to be determined from boundary conditions. At the flange to web junctions:

$$x_f = 0 \quad \text{and so} \quad \sigma_{RF} = c_1 \qquad 4.29$$

but the residual stress is known to be σ_{FW} at this point, therefore:

$$c_1 = \sigma_{FW}, \qquad 4.30$$

At the flange tip:

$$x_f = \pm\frac{B}{2} \quad \text{and so} \quad \sigma_{RF} = a_1\frac{B^2}{4} + \sigma_{FW} \qquad 4.31$$

where B is the width of the flange, but at these points the stress level is known to be σ_F, therefore:

$$a_1 = \frac{4(\sigma_F - \sigma_{FW})}{B^2} \qquad 4.32$$

The residual stress distribution in the flange is then fully defined by the equation:

$$\sigma_{RF} = \frac{4(\sigma_F - \sigma_{FW})}{B^2} x_f^2 + \sigma_{FW} \qquad 4.33$$

Similarly, the residual stress distribution along the length of the web may be represented by the parabolic equation:

$$\sigma_{RW} = a_2 y_W^2 + c_2 \qquad 4.34$$

in which σ_{RW} is the residual stress level at a distance y_W from the web centroid. Constants a_2 and c_2 are again determined from boundary conditions. At the web centroid:

$$y_W = 0 \qquad \text{and} \qquad \sigma_{RW} = c_2 \qquad 4.35$$

which is known to be equal to σ_W, therefore:

$$c_2 = \sigma_W \qquad 4.36$$

At the web to flange junction:

$$y_W = \pm\frac{D_W}{2} \qquad \text{and so} \qquad \sigma_{RW} = a_2 \frac{D_W^2}{2} + \sigma_W \qquad 4.37$$

where D_W is the depth of the web, but the stress level at this point is known to be σ_{FW}, therefore:

$$a_2 \frac{D_W^2}{2} + \sigma_W = \sigma_{FW} \qquad 4.38$$

and rearranging gives:

$$a_2 = \frac{4(\sigma_{FW} - \sigma_W)}{D_W^2} \qquad 4.39$$

This fully defines the residual stress distribution in the web as:

$$\sigma_{RW} = \frac{4(\sigma_{FW} - \sigma_W)}{D_W^2} y_W^2 + \sigma_W \qquad 4.40$$

Residual stresses are assumed to be constant throughout the thickness of both the flange and the web. Compressive stresses are assumed to be positive. The total stress pattern over the whole section should be in equilibrium; if the total compressive and tensile force components do not balance then the maximum web residual stress is modified until a balanced pattern is achieved.

The triangular stress distribution as described by many research workers at Lehigh University in the U.S.A., is shown in Figure 4.7b. The distribution in the flange is given by a linear function of distance from the centre of the flange. The residual stress values for a steel I section at the flange tips σ_F and at the flange to web junction σ_{FW} are given as

$$\sigma_F = 0.3\sigma_y \qquad 4.41$$

and

$$\sigma_{FW} = -0.3 \frac{\sigma_y A_F}{(A_W + A_F)} \qquad 4.42$$

where σ_y is the material yield stress. A_F and A_W are the areas of the flange and web, respectively. The residual stress at any point along the flange may be represented by the linear equation:

$$\sigma_{RF} = a_1 |x_f| + c_1 \qquad 4.43$$

Application of boundary conditions gives:

$$c_1 = \sigma_{FW} \qquad 4.44$$

and

$$a_1 = \frac{2(\sigma_F - \sigma_{FW})}{B} \qquad 4.45$$

therefore, the residual stress distribution in the flange is fully defined by the equation:

$$\sigma_{RF} = \frac{2(\sigma_F - \sigma_{FW})}{B} \cdot |x_f| + \sigma_{FW} \qquad 4.46$$

The distribution in the web of the section is assumed to be a constant tensile distribution σ_W, which is equal to the flange to web junction residual stress value:

$$\sigma_{RW} = \sigma_{FW} \qquad 4.47$$

The welded section has two residual stress components, in the areas around the weld the material is assumed to be in high residual tension σ_{RT}, which is equal to:

$$\sigma_{RT} = -0.9\sigma_y \qquad 4.48$$

and elsewhere in low residual compression σ_{RC} equal to:

$$\sigma_{RC} = 0.1\sigma_y \qquad 4.49$$

This width of the heat affected zone around the weld is chosen to maintain equilibrium over the complete section. The welded residual stress distribution is shown in Figure 4.7c.

4.8 Solution of Nonlinear Equilibrium Equations

4.8.1 Load incrementation

The geometrical and material nonlinearities, of the previous three sections, result in a system of nonlinear equilibrium equations:

$$\{F\} = [K]\{\delta\} \qquad 4.50$$

The overall stiffness matrix $[K]$ is nonlinear because it is dependent on the current configuration of the column during loading. Equation 4.5 states the member's equilibrium condition, in which the externally applied force $\{F\}$ should balance the internal forces resulting from member deformation. These nonlinear equations are solved in the analysis using an incremental method with iterative equilibrium corrections.

The incremental method is a numerical technique in which the nonlinear problem is solved in a step-wise fashion. In structural problems this is implemented by applying external loading as a sequence of sufficiently small increments so that the structure may be assumed to behave linearly within each increment. The equilibrium equations are then solved for each load increment resulting in an increment of displacement which can be added to the sum of all previous displacement increments to give the current deflected configuration of the column. The incremental external loading is applied proportionately using a unit reference load vector $\{F_{ref}\}$ and an incremental load parameter Δp so that:

$$\{\Delta F\} = \Delta p.\{F_{ref}\} \qquad 4.51$$

This method reduces the problem of solving the set of nonlinear equations 4.50 to the solving of a series of linear equations of the form:

$$\{\Delta F_i\} = [K]_{i-1}\{\Delta\delta\}_i \qquad 4.52$$

where i is the increment number. The stiffness matrix used in each linear calculation is that based on the column configuration at the beginning of the current increment, depending on displacement state $\{\delta\}_{i-1}$. The incremental displacements $\{\Delta\delta\}_i$ are found by solving equations 4.52, which are then added to the previous displacement state $\{\delta\}_{i-1}$ to give the displacement at the new load level:

$$\{\delta\}_i = \{\delta\}_{i-1} + \{\Delta\delta\}_i \qquad 4.53$$

This procedure is illustrated in Figure 4.8a.

The pure incremental procedure, as described above, has a basic disadvantage in that equilibrium is generally not satisfied after each increment and so the solution will tend to diverge from the true deformation path. This gives no estimate of the accuracy of the solution. Correction to the true equilibrium path is achieved by performing equilibrium iterations after each increment step.

4.8.2 Load incrementation with equilibrium iterations

The solution of equations 4.52 may be corrected to the true equilibrium path by the use of Newton-Raphson

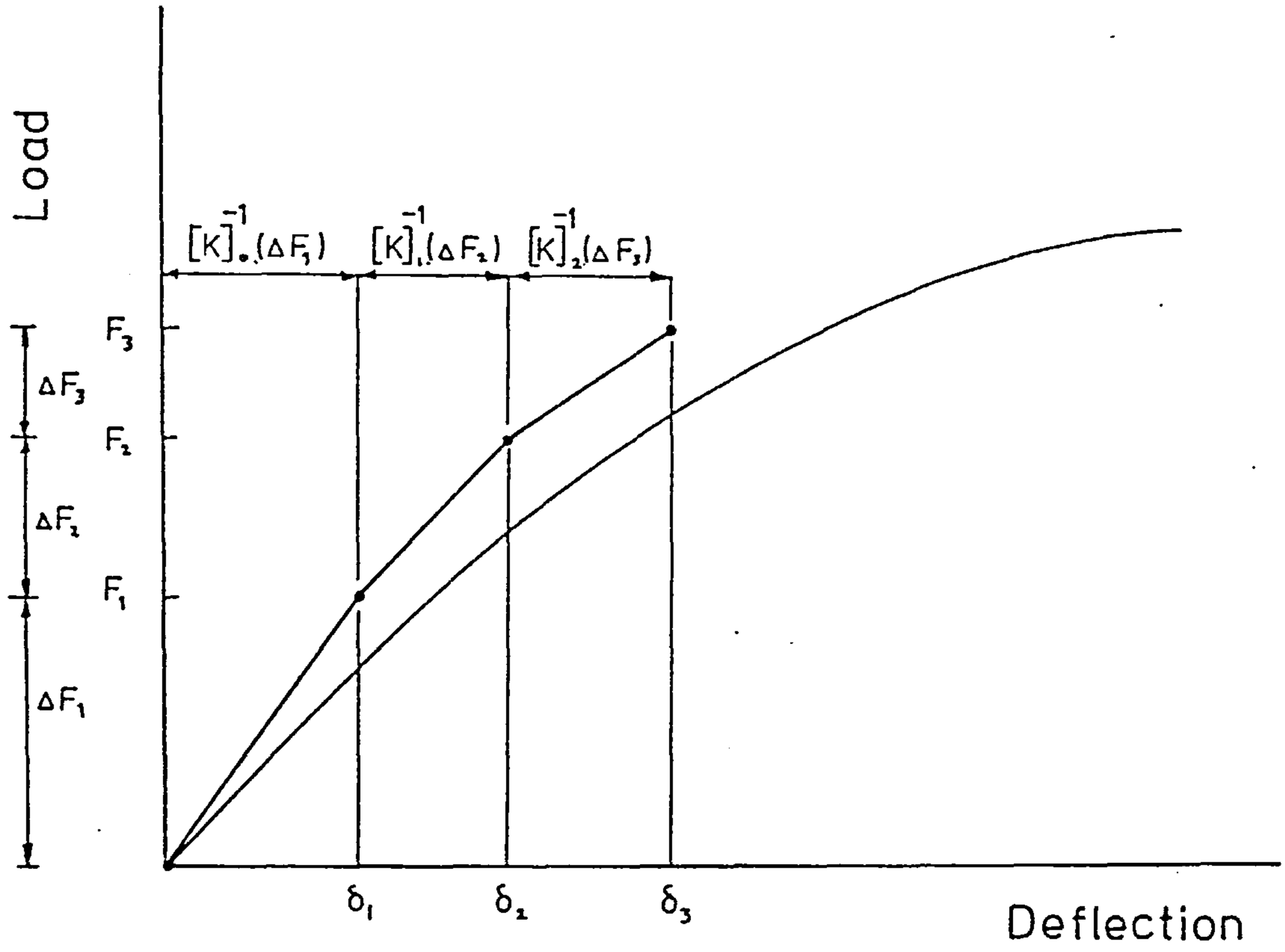

(a) Pure Incrementation

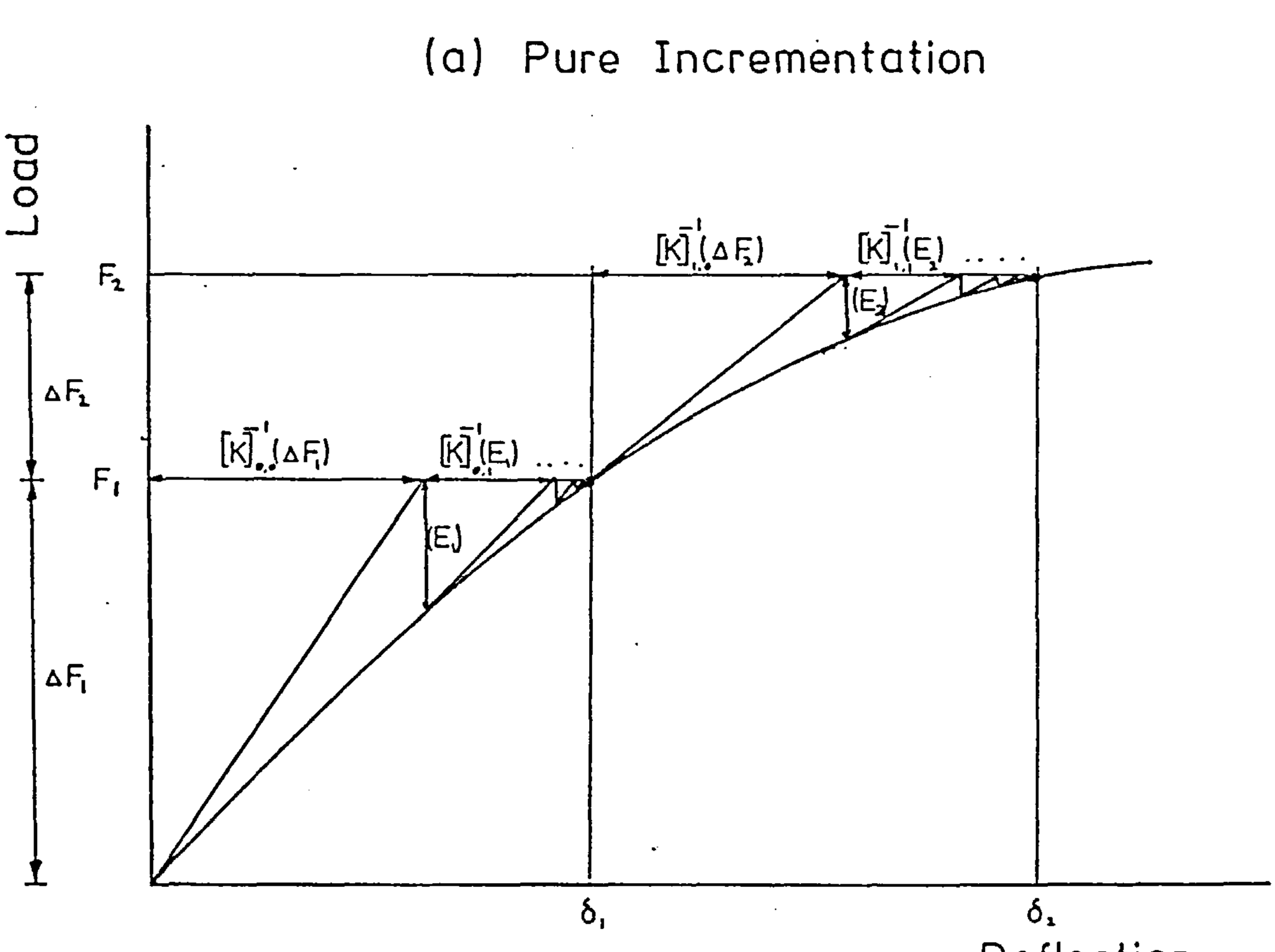

(b) Load Increments with Equilibrium Iterations

FIGURE 4.8 - Incremental and Iterative Techniques

equilibrium iterations. After each load step a series of iterative cycles are performed until the solution converges to the true path within a specified tolerance. The column stiffness matrix is now recalculated after each iteration, and the linear equilibrium equation can now be expressed as:

$$\{\Delta F\}_{i,j} = [K]_{i,j-1}\{\Delta\delta\}_{i,j} \qquad 4.54$$

where j is the iteration number, $\{\Delta F\}_{i,j}$ are the current out-of-balance forces and $\{\Delta\delta\}_{i,j}$ are incremental deflections resulting from the iterative cycle. The out-of-balance forces are the difference between the currently applied external forces $\{F_{EXT}\}_i$ and the current internal forces $\{F_{INT}\}_{i,j}$ as calculated from the currently displaced configuration of the column, this can be expressed as:

$$\{\Delta F\}_{i,j} = \{F_{EXT}\}_i - \{F_{INT}\}_{i,j} \qquad 4.55$$

The improved solution of column deflections resulting from the equilibrium iterations of equations 4.54 are:

$$\{\delta\}_{i,j} = \{\delta\}_{i,j-1} + \{\Delta\delta\}_{i,j} \qquad 4.56$$

These iteration cycles are performed after each load increment, as illustrated in Figure 4.8b.

4.8.3 Solution of equilibrium equations

The finite element method eventually reduces the column problem to the solutions of a large set of linear simultaneous equations which are expressed in

the matrix forms of equations 4.50, 4.52 or 4.54. In the analysis these equations are solved using the Gaussian elimination method (79), whereby the terms of the overall stiffness matrix [K] are systematically eliminated until the matrix is left in upper triangular form. This upper triangular matrix may then be used both for solving the system of equations and for the calculation of the determinant of the stiffness matrix. The system of equations is solved by back substitution to give the deflection values, and the determinant is found by calculating the product of all leading diagonal terms of the upper triangular matrix.

The resulting column deflections can be used in determining the stresses, strains and internal forces at the currently applied external load level. Methods of determining these quantities are discussed in the following section.

4.9 Determination of Internal Stresses and Forces

4.9.1 Internal stresses

In order to calculate the internal stresses that occur at the nodes of an element, it is first necessary to determine the nodal strains. When in-plane behaviour is being considered, only two quantities are required to express the nodal strains; the axial strain and the flexural curvature. These strains are related to the nodal displacements by the element's strain-displacement relationship, which is part of the derivation of the

element stiffness matrix (73). The axial strains are the first derivative of the axial displacement function while the curvature is the second derivative of the lateral displacement function. These strain-displacement functions may be expressed as:

$$\begin{Bmatrix} \varepsilon_1 \\ \phi_1 \\ \varepsilon_2 \\ \phi_2 \end{Bmatrix} = \begin{bmatrix} \frac{1}{L} & 0 & 0 & \frac{-1}{L} & 0 & 0 \\ 0 & \frac{6}{L^2} & \frac{4}{L} & 0 & \frac{-6}{L^2} & \frac{2}{L} \\ \frac{1}{L} & 0 & 0 & \frac{-1}{L} & 0 & 0 \\ 0 & \frac{-6}{L^2} & \frac{-2}{L} & 0 & \frac{6}{L^2} & \frac{-4}{L} \end{bmatrix} \begin{Bmatrix} u_1 \\ v_1 \\ \theta_1 \\ u_2 \\ v_2 \\ \theta_2 \end{Bmatrix} \qquad 4.57$$

or in the simplified notation of:

$$\{\varepsilon\} = [B]\{\delta^e\} \qquad 4.58$$

In equations 4.57 ε and ϕ are the axial strain and flexural curvature relating to each node, L is the length of the element and u, v, θ are the axial, lateral and rotational deflections, respectively. In the same equations expressed in the simplified form of equations 4.58 [B] is the strain-displacement matrix.

Once the overall member deflections have been calculated, as described in the previous section, the element nodal displacements can be found. These are then substituted into equations 4.57 to give the internal nodal strains. The maximum and minimum cross-section strains occur at the extreme fibres of the

section, these can be found for each node from the equations:

$$\varepsilon_{MAX} = \varepsilon + \frac{\phi D}{2} \qquad 4.59$$

and

$$\varepsilon_{MIN} = \varepsilon - \frac{\phi D}{2} \qquad 4.60$$

where D is the overall depth of the section.

These extreme fibre strains can then be used to calculate the maximum and minimum stresses occurring in the section. The stresses are found using the material stress-strain relationship:

$$\sigma = \begin{cases} -\sigma_y, & \text{if } \varepsilon \leq -\varepsilon_y \\ \varepsilon.E, & \text{if } -\varepsilon_y < \varepsilon < \varepsilon_y \\ \sigma_y, & \text{if } \varepsilon \geq \varepsilon_y \end{cases} \qquad 4.61$$

where σ_y and ε_y are the material's yield stress and strain, respectively.

4.9.2 Internal forces

The nodal end forces for each element can be found using the element stiffness matrix $[K^e]$ and the element nodal displacements $\{\delta^e\}$. The internal forces $\{F_{INT}\}$ can be found by substituting the nodal displacements into the equations:

$$\{F_{INT}\} = [K^e]\{\delta^e\} \qquad 4.62$$

where

$$[K^e] = [K_E^e] - P[\bar{K}_G^e] \qquad 4.63$$

in which P is the current axial load level.

4.10 Criteria of Column Failure

The load incrementation, within the analytical procedure, is terminated when either the section becomes fully yielded or the determinant of the overall stiffness matrix becomes negative. These two conditions are assumed to indicate column failure. A fully yielded section is assumed to exist when the combined effects of axial strain and flexural curvature at both of the section's extreme fibres exceed the material yield strain. This corresponds to the material failure mode and would be expected to occur for fairly stocky columns.

A negative determinant of the stiffness matrix is an indication that the initial buckling load has been exceeded and the column is in a state of instability. This will occur as a result of the destabilising effect of axial loads, usually acting through geometric imperfections. However, material yield within the column reduces the flexural rigidity EI of the section which also influences column stability. Instability would be expected to occur due to geometrical conditions for very slender columns, and a combination of both

geometrical and material conditions for more stocky columns.

Thus failure criteria correspond to the column's maximum load carrying capacity which is applicable to an isolated column with increasing applied load. However, for a column within a frame or an isolated column which has applied increments of deflection the maximum load capacity is not a suitable criteria of failure. For these cases the full load-deflection curve would be required in which the load carrying capacity reduces with increased deflection. Little is known about the descending part of the curve due to the numerical ill-conditioning that occurs in the analysis after the maximum load has been achieved. A routine to trace the full load-deflection curve is not included in the analysis, however, a numerical approach to the problem is discussed in the next chapter.

CHAPTER 5

Computer Program Development and Verification

5.1 Program Layout and Organisation

5.1.1 General Program details and flow diagram

A source program was written in FORTRAN IV to perform the analysis described in the previous chapter. This was developed using the ICL-1906S computer of the University of Sheffield. The core-image program requires 35K words of storage for a possible maximum of ten beam elements and to fully compile into binary form requires 30 seconds of central processing unit time.

The program consists of 18 routines which perform the following tasks:

1) Control the order of the analysis.

2) Control the load increment step size.

3) Read and print input data.

4) Generate element stiffness matrices.

5) Generate element geometrical stiffness matrices.

6) Assemble the overall stiffness matrices.

7) Apply rigid boundary conditions.

8) Allow for connection stiffness.

9) Impose initial out-of-straightness.

10) Apply load at an initial eccentricity.

11) Perform equilibrium iterations.

12) Calculated nodal stresses and strains.

13) Calculated internal forces.

14) Impose initial residual stresses.

15) Calculate section properties.

16) Solve simultaneous equations and evaluate the determinant of the overall stiffness matrix.

17) Program restart facility.

18) Terminate program after column failure and print results.

The restart facility is discussed in Section 5.2.1, while the theory of all other routines has been discussed in Chapter 4. A summary of the main features of the finite element column analysis program is given in Table 5.1.

A flow diagram is shown in Figure 5.1. Initially, input data is both read and printed; this is used to calculate the initial residual stress distribution, to generate the geometrical stiffness matrix for unit axial load $[\bar{K}_G]$ and to set up the initially curved shape of the column. After calculating the first load step the analysis enters the main incremental load stepping loop. The elastic stiffness matrix is calculated allowing for any reduced stiffness due to yield within the cross-section,

TABLE 5.1 - Summary of Main Features of the End Restrained Column Analysis

1. Traces full load-deflection behaviour up to maximum load level.
2. Within the limitation of uniflexural behaviour can handle any cross-sectional shape.
3. Allowance for spread of material yield.
4. Permits any pattern of residual stresses to be assumed.
5. Permits any initial out-of-straightness to be assumed.
6. Any connection moment-rotation data that has previously been fitted by a B-spline function may be used.

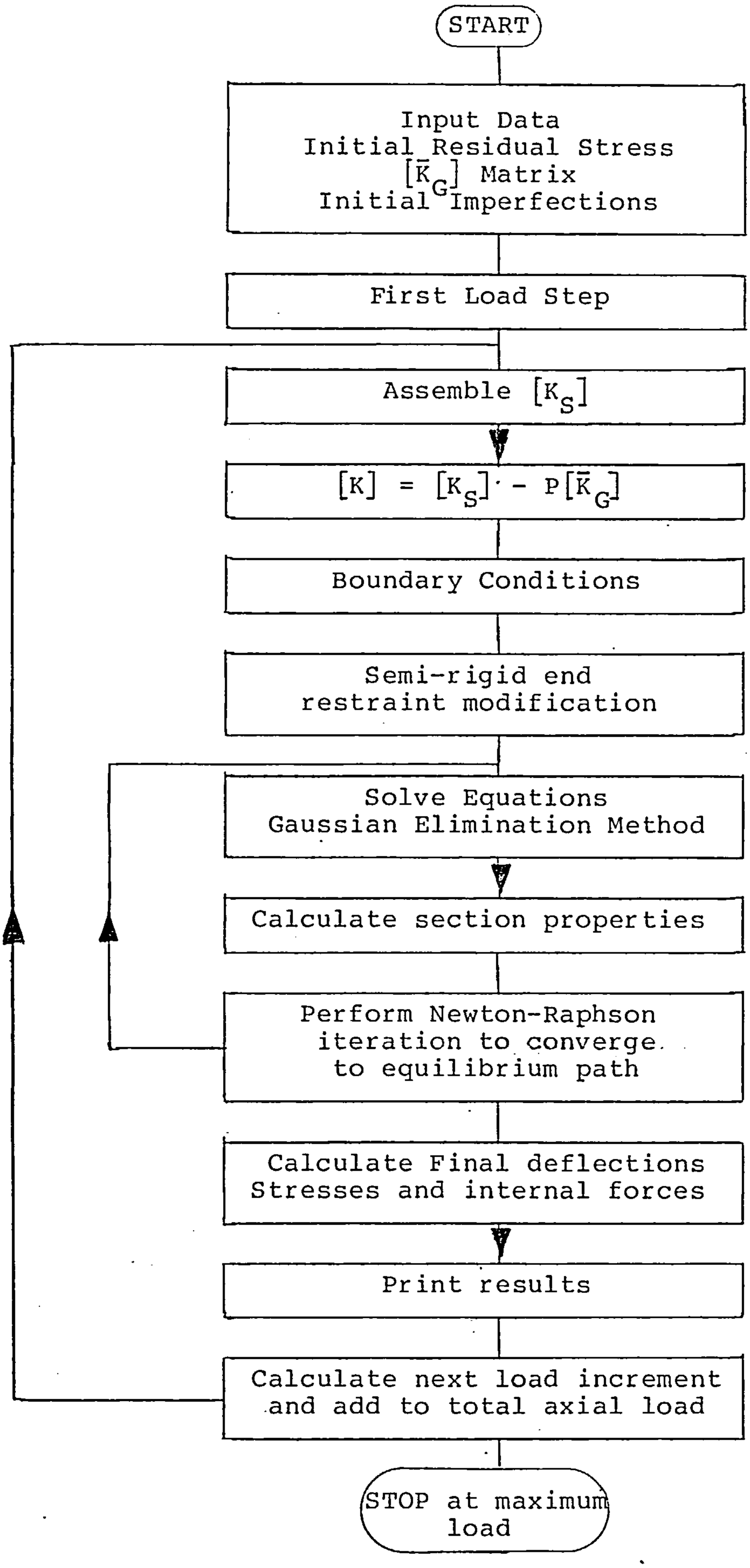

FIGURE 5.1 Column Analysis Flow Diagram

which is then added to the load corrected geometrical stiffness matrix to form the overall stiffness matrix. After the application of boundary conditions, including both fixed and semi-rigid end restraints the system of equilibrium equations is solved using the Gaussian elimination routine. These equations are assumed to be linear over the incremental load step and Newton-Raphson equilibrium iterations are performed until the external and internal forces balance to an accuracy of within one per cent. After convergence to this specified accuracy, total deflections, stresses and internal forces are calculated and printed. The next load increment is calculated at the end of each loop and this is added to the total column loads until the maximum load capacity has been exceeded. When this is achieved, due to either excessive yield or instability, the program is terminated and the overall load-deflection results are printed as well as the cause of failure. Details of the input and output method are expanded upon in the next sections.

A full listing and user manual of the above program is given in reference 80.

5.1.2 Input of data

The George IV filestore system on the ICL-1906S computer allows a very convenient data input system, as more than one input channel may be used by the program. The developed program uses three channels of data for each job. These three different channels are used for the input of the following information into the analysis:

1) The general control data file contains general information relating to the whole column problem to be analysed. The finite element column model details are input, including the number of elements, number of nodes, nodal coordinates and the node numbering system. Boundary conditions are input specifying rigid supports and any laterally applied loading. Types of initial residual stress and initial out-of-straightness are declared as well as the column's slenderness ratio and load eccentricity.

2) The section data file contains information relating to the type of member section being used. This contains a) the section's material properties, such as the elastic modulus E and the yield stress σ_y; and b) the shape properties of the section including the cross-sectional area, the moment of inertia and the section dimensions.

3) The connection data file contains information related to the type of connection that provides the end restraint. The cubic B-spline function coefficients are contained in these files.

The input of data using the three above files is particularly useful when running a parametric study in which some of the main column parameters are being varied within a series of tests. This allows general control programs (macros) to be written to start a series of column tests whilst picking up different data file

combinations for individual tests. A parametric study of the behaviour of columns is given in the next chapter.

5.1.3 Output of data

The George IV filestore system also allows the use of more than one output channel from the program. The program uses three channels for the output of results and information from the analysis. These are used for the following tasks:

1) The general lineprinter output file contains general information related to the various steps of the analysis such as general deflection, internal stresses, internal forces, the determinant values, reduced flexural rigidities, connection stiffness values and out-of-balance forces calculated during equilibrium iterations.

2) The load-deflection output file contains a list of the axially applied load and the central lateral deflection at each increment level. This file may then be used directly for the graphical presentation of results.

3) The restart output file is a direct access unformatted file containing all the important variables of the program. Once all the current values of variables have been written to a restart file, the program may be restarted from that point at any time. A more detailed discussion of the restart facility is given in the next section.

5.2 Some Computational Techniques

5.2.1 Program restarting routine

The restart facility enables the program to be stopped at the end of any increment with all the important analysis variables stored in one unformatted direct access file. At any time later, the program may be restarted from the same point by reading all the variables from this unformatted file. This technique is very useful during program development, when considerable computer time may be saved in the development of certain program features. For instance, at the point of first yield, a number of incremental steps are usually performed in the elastic range of the material before yield occurs and it is very wasteful to run an analysis from zero to study the effects at first yield. So, initially the program is run up to the last fully elastic increment and then all relevant parameters are stored in an unformatted file before the program is terminated. Subsequent runs initially read in the data stored in this unformatted file and then continue the analysis from the point at which the first program was terminated. This has the advantage that if program errors occur at the analysis event being developed, the program can be corrected and run again from that load level without having to run the whole analysis from the start of the load-deflection curve.

The restart is performed by declaring all important variables within a large common statement; this also

reduces program storage when transferring variables between the main routines of the program. When the restart is required within the program the complete statement is made equivalent to one large one-dimensional array. The contents of this array are then simply written to a permanent unformatted file before the program is terminated. When the subsequent program is started the contents of this file are read into the same large array and the equivalence statement reassigns all the analysis information back into the common statement. This then enables the analysis to continue until column failure or until another restart is required.

5.2.2 Load incrementation

Load increments are applied in a simple two level system. More sophisticated automatic increment generation (81) routines were tested. However, these were found to be expensive on computer time as they required the solution of the system of equations. A discussion of this automatic increment method is given in Section 5.6.

In the simple approach adopted a suitable load level is chosen and load increments are then made equal to a proportion of this load. This load level, P_{CR} is made equal to squash load P_y, or for a slender column whose Euler load P_E is less than the squash load, P_{CR} is made equal to P_E. This may be expressed as:

$$P_{CR} = \begin{cases} P_Y, \text{ if } P_Y < P_E \\ \\ P_E, \text{ if } P_Y > P_E \end{cases} \qquad 5.1$$

Initially, a coarse increment size of 0.1 P_{CR} is chosen and incrementation is allowed to continue until column failure. When failure is indicated the procedure steps back, through one increment, to the previous load level. The increment step size is then reduced to 0.01 P_{CR} and the procedure is allowed to continue until the column fails. The maximum load capacity of the column is then found to be that load level existing before the final increment step was taken. This method should predict the point of maximum load capacity to an accuracy of less than one per cent.

The step back technique is performed using a similar procedure to the information storage in the restart facility. After each load increment all important program variable values are written to an unformatted file; this may be retrieved when the step back is required. This method first finds a coarse approximation of the maximum load and then, using finer load increments, a more accurate solution is found.

5.2.3 Column symmetry

If the column to be analysed is perfectly symmetrical about its centre, only half of the column need be analysed because the resulting nodal deflections are also symmetrical about the centre point. The use

of symmetry reduces the number of nodes and so reduces the number of simultaneous equilibrium equations required to solve the system. This considerably reduces the amount of computer time required for the complete analysis. However, this assumption may only be made if a) initial out-of-straightness is symmetrical, b) lateral loading is symmetrical, c) the column section is symmetrical and d) the end restraint conditions are identical. A comparison of the full column and symmetrical half column models are shown in Figure 5.2.

5.3 Program Development

The program performing the main analysis was developed in a systematic manner. The analysis was built up from a simple beam element model to the "real" column model described in Chapter 4. After each feature of the analysis was included tests were performed to check the validity of the program.

Initially a program was written to perform a static analysis of a straight elastic beam. Lateral loads only were applied (i.e. no axial load) and the resulting deflections were calculated. These deflections and the resulting internal stresses and forces were checked with values for the same member found from simple bending theory. Results were found to agree within an acceptable tolerance. The next stage was to include axial loads and geometrical imperfections into

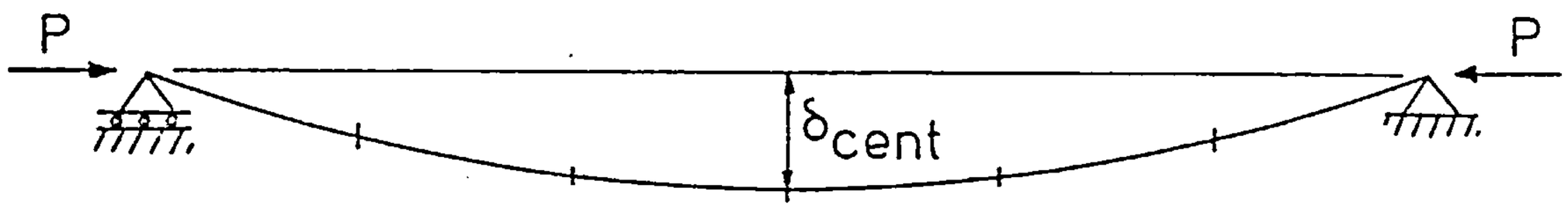

(a) Full Column Model

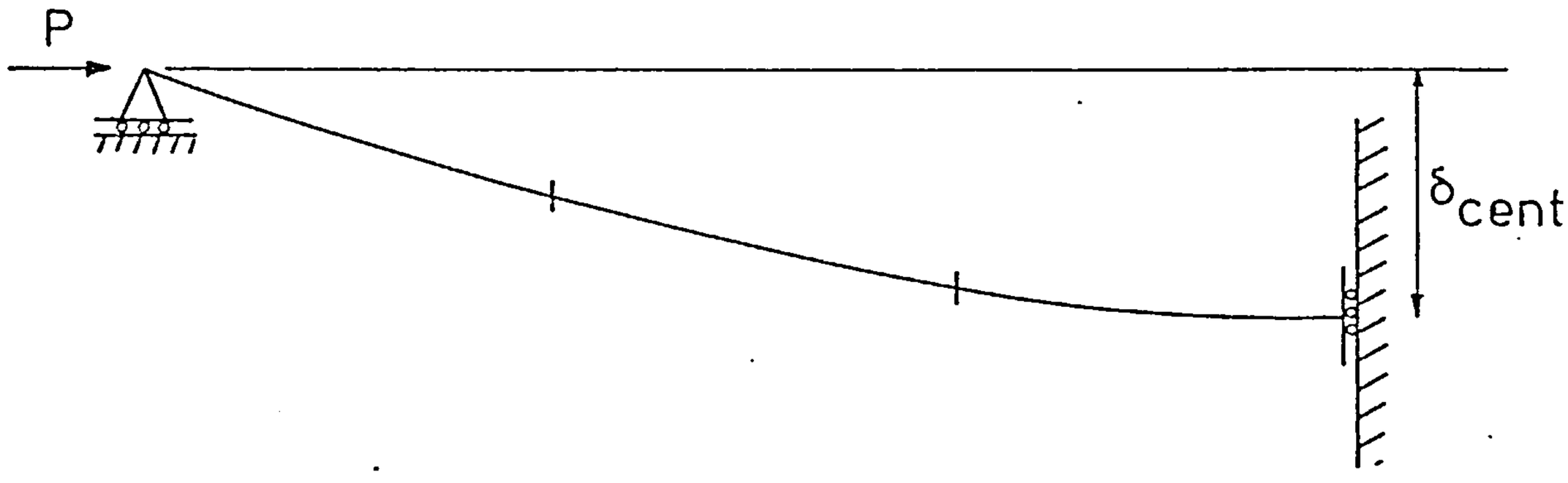

(b) Symmetrical Half Column Model

FIGURE 5.2 - The Use of Column Symmetry

the program so that the destabilising effects of these loads could be studied. This enabled an elastic pin-jointed column to be analysed and the resulting load-deflection curve compared with the Timoshenko (82) approximate formula:

$$\delta = \frac{\delta_o}{1 - P/P_E} \qquad 5.2$$

A comparison of the calculated and theoretical curves is shown in Figure 5.3. The calculated curve can be seen to closely follow the theoretical curve with a maximum deviation of 4.6 per cent of the theoretical load value which is considered to be acceptable.

The accuracy of the analysis is very dependent upon the number of beam elements used to model the column. The accuracy increases as the member is divided into an increasing number of smaller elements. However, as the number of member nodes increases so does the size of the system of equilibrium equations required to be solved. This increases the amount of computer time required, which becomes prohibitive beyond a certain number of nodes. Also, after the section has been divided into a certain number of elements, no significant increase in accuracy is achieved by dividing the member into still smaller elements. The number of elements into which the member must be divided to produce results of acceptable accuracy, within a reasonable amount of computer time, has to be optimised. To do this a series of

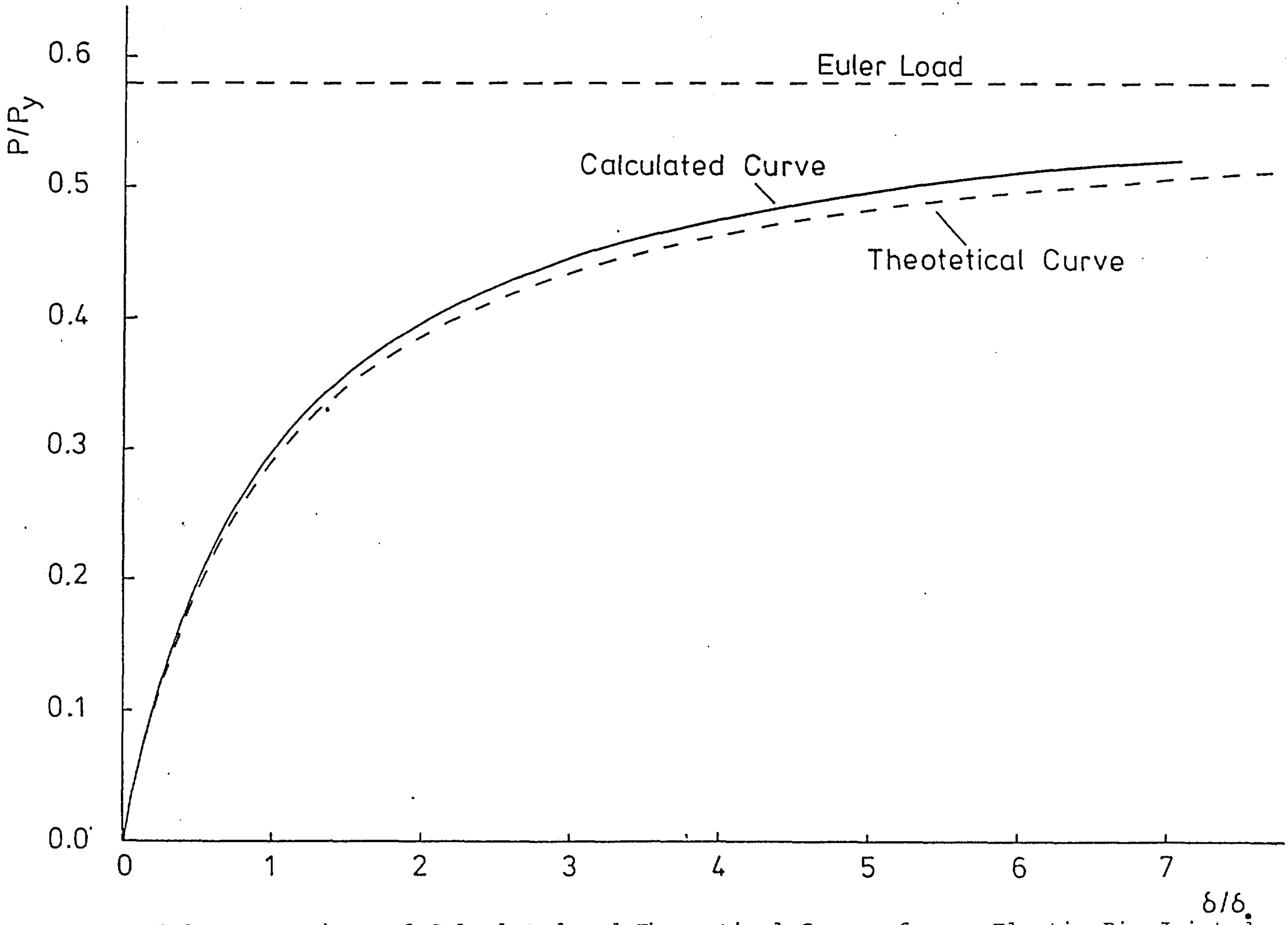

FIGURE 5.3 - Comparison of Calculated and Theoretical Curves for an Elastic Pin-Jointed Connection

tests were performed on a pin jointed 203×203UC60 column section with a slenderness ratio of 120. The column was first analysed with only two elements, then the number of elements were progressively increased through four, six, eight to finally ten elements. The resulting load-deflection curves are plotted in Figure 5.4 from which it can be seen that sufficiently accurate results are obtained with the column length divided into six elements. In all tests the column was assumed to be initially stress free, with perfectly pinned end connections. Therefore, in all subsequent work the column length will be divided into six elements.

Elastic-plastic material behaviour and initial residual stresses were next incorporated into the analysis, followed by the introduction of semi-rigid end restraint. No theoretical methods are available to check the validity of these routines, however, the complete analytical procedure may be checked against available data of experimental semi-rigidly end restrained columns as will be discussed in the next section.

5.4 Program Verification

Before any column analysis series could be performed, it was necessary to verify the validity of the analytical procedure against experimental results.

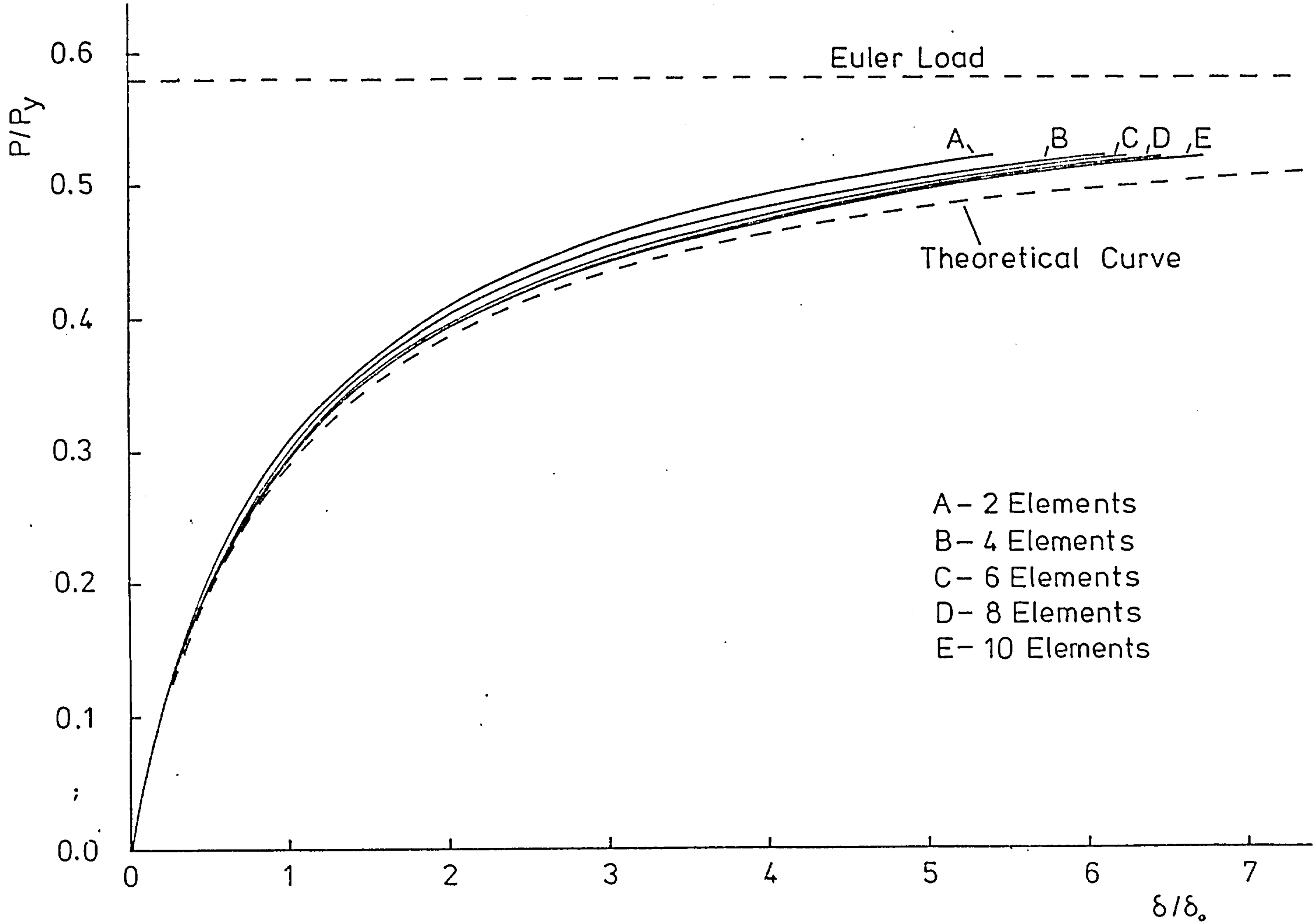

FIGURE 5.4 - Comparison of Load-Deflection Curves for the same Column Problem Analysed with Differing Numbers of Column Elements

The procedure was checked against the end-restrained column test reported by Bergquist (45), who experimentally measured connection moment-rotation curves and load-deflection curves for a W10×29 column section with a slenderness ratio of 189.7. Two W10×21 beams were attached to the column's minor-axis using web cleats fastened with A.325 bolts. The B-spline fit of the experimentally obtained connection characteristic used in the analysis is shown in Figure 5.5, whilst the computed load-deflection curve for the column assembly is compared with Bergquist's test results in Figure 5.6.

In performing these calculations the column was assumed to possess an initial deflected shape in the form of a half sine wave with a maximum central deflection of L/1000; this compares with a measured initial central deflection of L/1280 reported by Bergquist. Since no data relating to the initial residual stress pattern was reported the parabolic pattern proposed by Young (78) has been used; it is possible that this slightly underestimates the initial stress values typically found in North American W-series sections.

From Figure 5.6 it can be seen that agreement between the two sets of results is generally quite good. The calculated load-deflection curve slightly overestimates the actual stiffness, leading to a failure load some 8.6 per cent higher than that measured by Bergquist. The assumption made in the

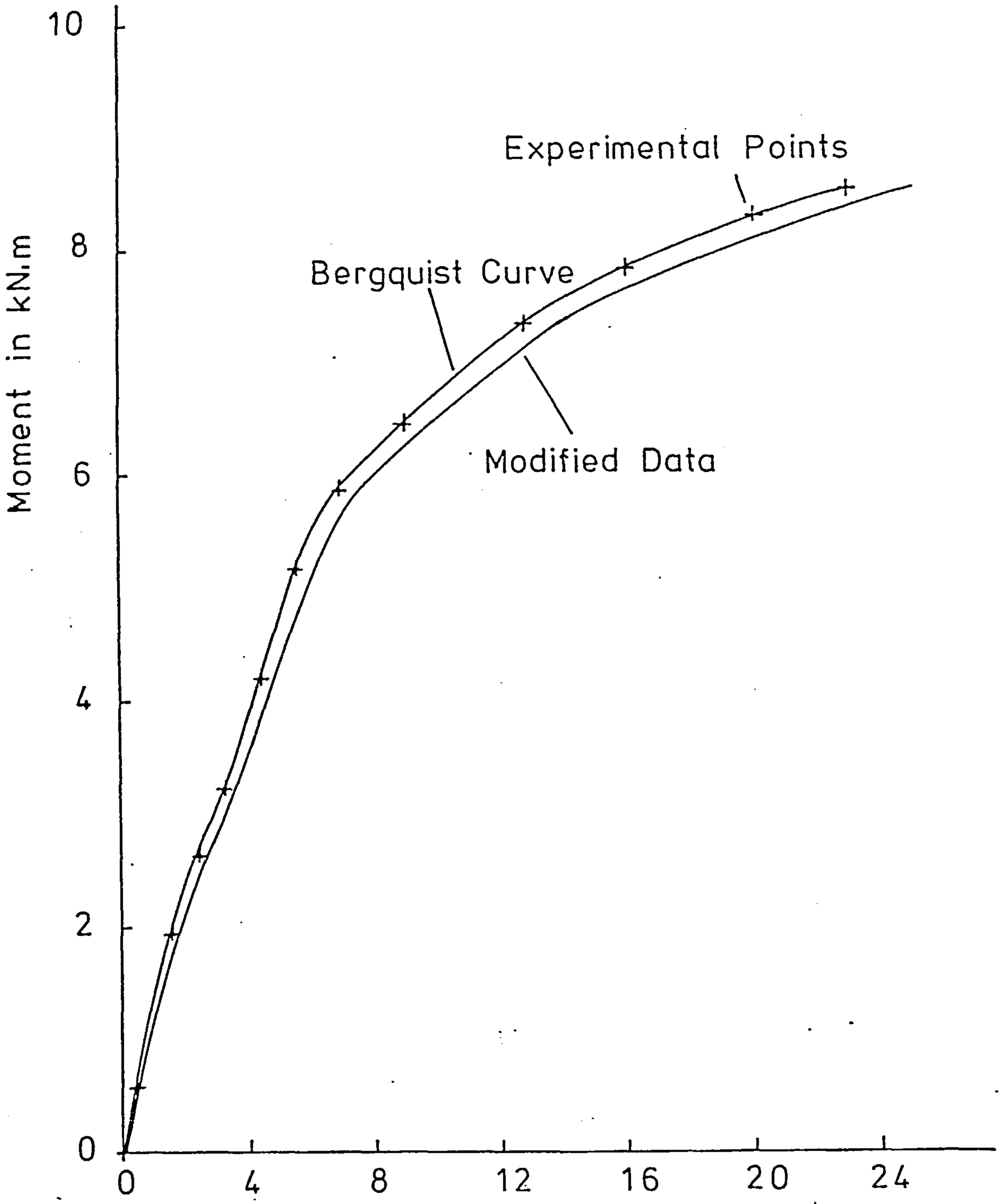

FIGURE 5.5 - Moment-Rotation Data Used in Program Verification

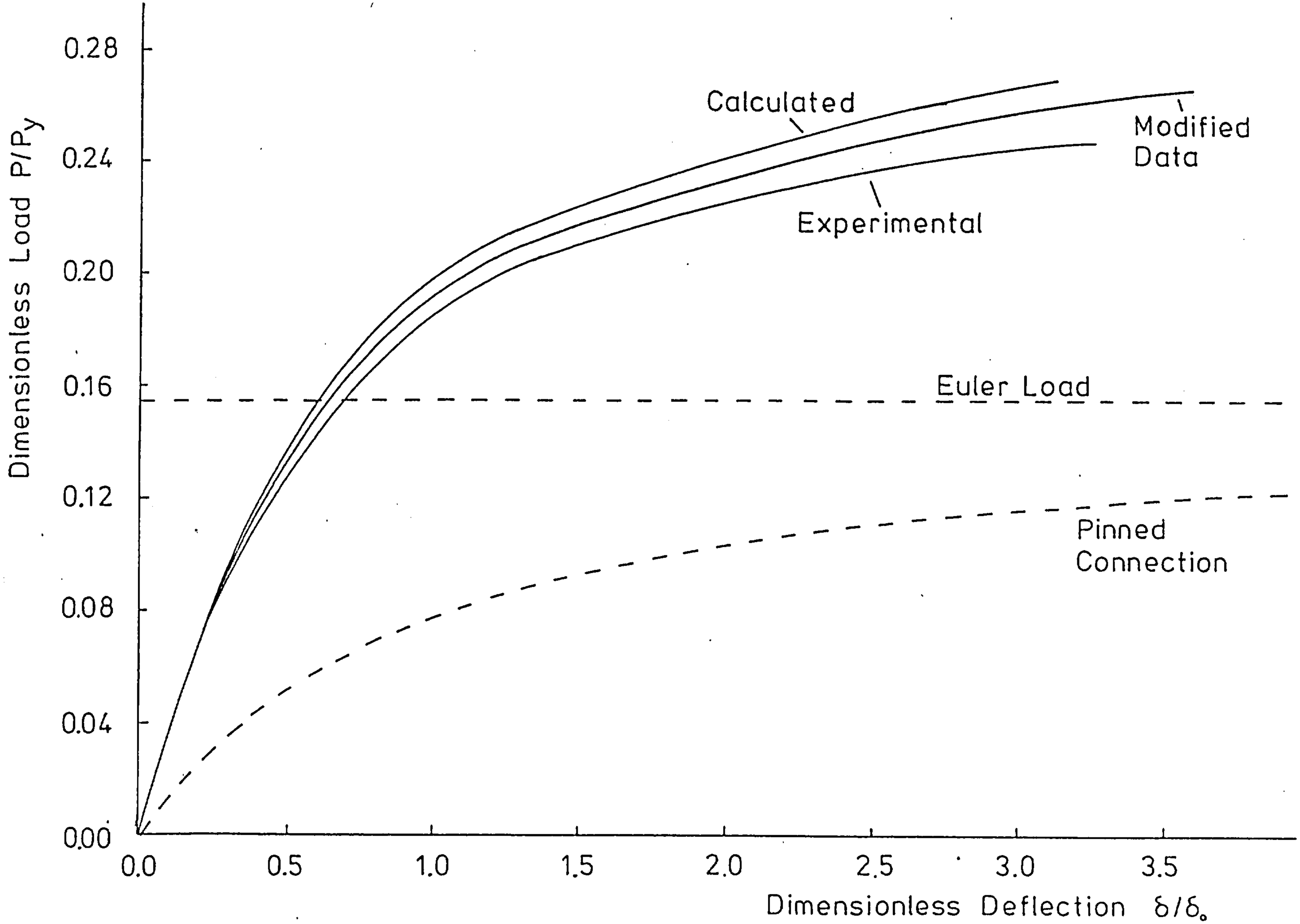

FIGURE 5.6 - Comparison of Calculated and Experimental Load-Deflection Curves in Program Verification

analysis that the column is connected to beams of infinite stiffness, whereas the experimental column is connected to beams of finite stiffness, contributes to this overestimate in actual column stiffness.

In order to test the sensitivity of the results to variations in the moment-rotation data used, a second analysis was performed using the modified moment-rotation curve shown in Figure 5.5. This modified data assumes a ten per cent overestimate of all rotational measurements. Although the use of this more flexible moment-rotation data moves the column load-deflection curve nearer to the experimental results, the magnitude of the change is sufficiently small to suggest that the analysis is not unduly sensitive to the exact form of the moment-rotation data used. Bearing in mind the difficulty of precisely duplicating the experiment arrangements, e.g. uncertainties associated with such factors as cross-sectional dimensions and properties, methods of measuring connection stiffness, values of residual stress, etc., it is considered that the accuracy of the analysis is quite acceptable.

5.5 Main Features of the Developed Computer Program

The main features of the developed finite element computer program in its completed form may be summarised as below:

1. The program uses one-dimensional beam elements to model an axially loaded structural column.

2. The analysis traces the full load-deflection behaviour of the column up to the maximum load.

3. Within the limitation of uniaxial flexural behaviour the program can handle any cross-sectional shape.

4. An elastic-perfectly plastic stress-strain characteristic is assumed for the column material and an accurate allowance for the spread of yield through the section is made.

5. The program allows any pattern of residual stress to be assumed.

6. Any initial out-of-straightness may be assumed.

7. The moment-rotation characteristic for any connection data that has previously been fitted by a B-spline function may be used.

5.6 Full Load-Deflection Behaviour

The load-deflection approach to the analysis attempts to trace the full load-deflection curve of the column including the post-maximum descending part of the curve. Little information is available for the full load-deflection behaviour of members both with and without semi-rigid end restraint. This

information is only of academic interest for the isolated column case. However, in the frame context the full load-deflection behaviour of a component column is important because, after the column has reached its maximum load, it will start to unload. The amount by which the column unloads is important because its load will be redistributed to other columns within the frame.

During the development of the column analysis program, as described in previous sections, two methods of tracing the full load-deflection path were investigated. Both of these methods developed ill-conditioning of the system of equilibrium equations after the maximum load had been obtained. The post-maximum descending part of the curve is highly nonlinear due to negative member stiffness and so it is very difficult to follow mathematically. At the maximum load the increment stiffness matrix is singular, this is the normal instability condition at which member deflections increase without any change in applied loading. Also, in the vicinity of this maximum load value the load-deflection curve is relatively 'flat' which causes ill-conditioning due to computational numerical instabilities of solutions in this region. For these reasons the developed computer program is presently restricted to tracing the load-deflection behaviour up to and including the maximum load level.

The first method which attempted to follow the full curve and avoid the problems associated with stiffness matrix singularities involved changing from load increments to deflection increments at the maximum load level. An incremental value is given to a single deflection component and the corresponding force reaction is evaluated along with the other deflection components. This method requires complex manipulation of the system of incremental equilibrium equations and ill-conditioning often still occurred. The matrix manipulation is made even more complicated when the force reaction does not correspond to the deflection component being incremented, for example if the lateral deflection component is being incremented and the resulting axial force reaction has to be evaluated.

The second method uses a variable load increment which becomes negative after the maximum load capacity has been determined. These load increments can be calculated using the automatic load increment generation equation proposed by Bergan and Soreide (81) and may be expressed as:

$$\Delta P^{i} = \Delta P^{i-1} \left[\frac{\tau}{f^{i-1} . \Delta P^{i-1} - ||\Delta \delta^{i-1}||} \right]^{\frac{1}{2}} \qquad 5.3$$

in which ΔP^{i} and ΔP^{i-1} are the calculated load increment and the previous load increment, respectively. τ is an estimate of the truncation error between the end of the linear load increment and the true equilibrium path, f^{i-1} is the inverse of the gradient of

the load-deflection curve at the previous load level and $||\Delta\delta^{i-1}||$ is some norm of the deflections during the previous increment. At low load levels equation 5.3 produces large increment steps, but these are gradually reduced as the maximum load level is approached due to the reduced gradient of the load deflection curve. The load increment will become negative as the curve passes through its maximum value. The method, again, is subject to numerical ill-conditioning in the region of the maximum load level. Lack of convergence of equilibrium iterations also occurs on the post-maximum part of the load-deflection curve.

CHAPTER 6

A Parametric Study of the Behaviour of Columns with Semi-Rigid End Restraint

6.1 Introduction

In order to investigate those parameters which can be expected to have most effect on the behaviour of columns with semi-rigid end restraint it is necessary to carry out a parametric study. This is useful to the designer in that it provides information which will help the understanding of the column behaviour subject to a range of different conditions. It also identifies those parameters which have the greatest influence on the behaviour of the column. However, when comparisons are made to design curves it must be remembered that in all cases the beams to which the semi-rigid connections are made are assumed to have infinite stiffness.

For the parametric study to be of greatest value it must be performed in a systematic manner. The most convenient approach is to start with the analysis of a basic problem, which is here chosen so that it represents typical practical conditions and dimensions. The investigation of the variation of chosen parameters may then be performed and comparison can be made with the basic problem, which serves as a datum for the whole parametric study. Therefore when a chosen parameter is being varied in a series of tests all other parameters are given the values they have in the basic problem.

6.2 The Basic Problem

6.2.1 Description of the basic problem

The basic problem chosen as a datum for the parametric study is a rolled universal column section with top and seat flange cleats. The column section is a medium range British rolled section, of serial size 203×203UC60, which is assumed to bend about its major axis. It is assumed to have an initial residual stress state corresponding to the parabolic stress pattern as described in Section 4.7.3. The column is made of mild steel with a yield stress of 240 N/mm^2 and an elastic modulus of 205 kN/mm^2. Semi-rigid end restraint is provided by top and seat flange cleats at both ends of the column, the connections being made from 152×152×12.6 angles with a length of 125 mm and connected to the column flanges by 20 mm rivets. The moment-rotation data for this connection was reported by Batho and Rowan (8) and a cubic B-spline curve fit to this data is shown in Figure 6.1.

Load is applied axially to the column, assuming no eccentricity of loading in the basic problem. Initial out-of-straightness is assumed in the form of a half sine-wave with a maximum central deflection of L/1000. The axial load is applied incrementally, as described in Section 5.2.2, so that the load-deflection curve is traced.

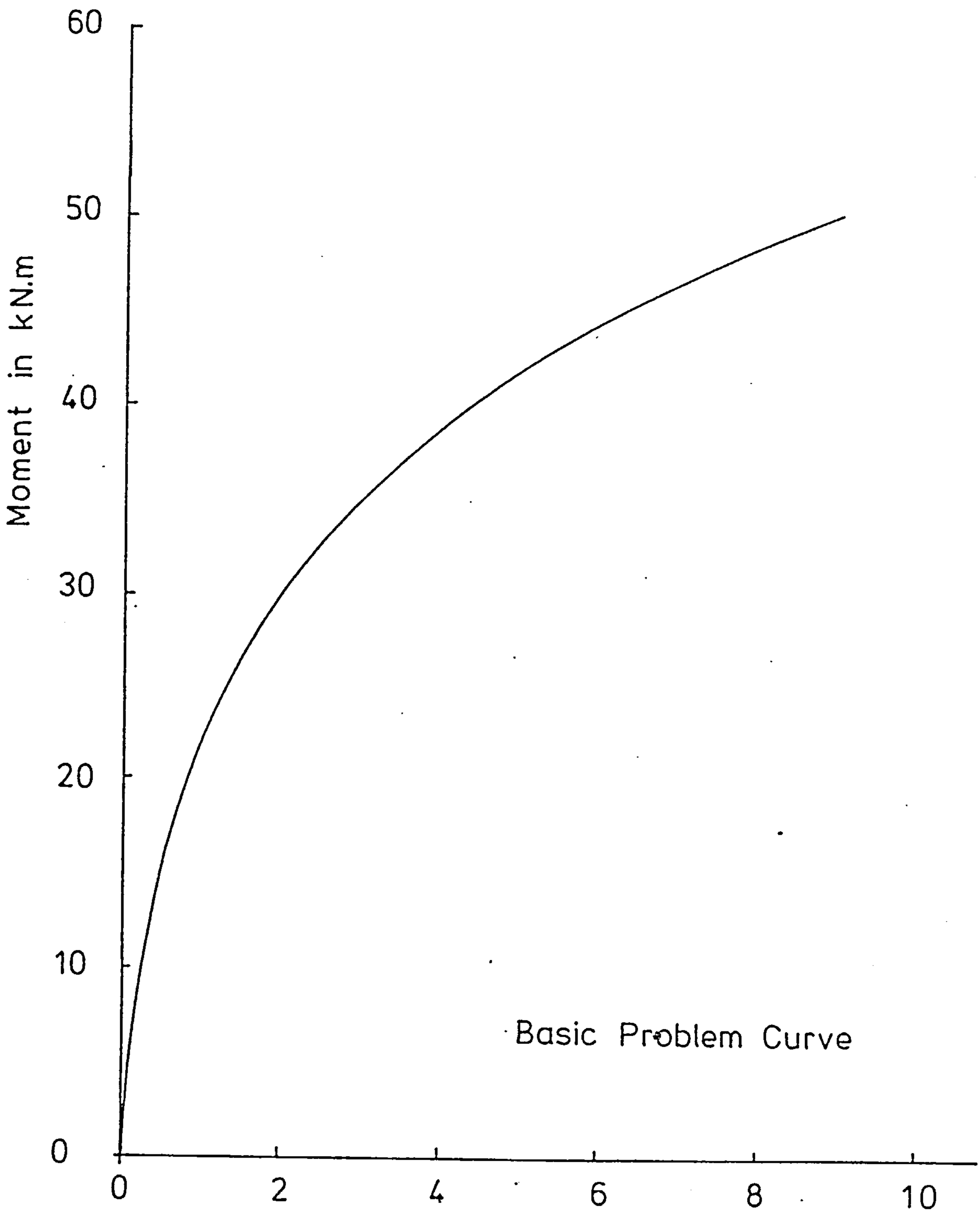

FIGURE 6.1 - Moment-Rotation Curve of Top Seat Flange Cleated Connection (Basic Problem)

In the basic problem the column analysis is performed over a full range of column slendernesses so that results are presented in the form of a "column curve", that is a plot of maximum load versus slenderness ratio. The range of slendernesses used extends from 20, for which the full squash load may be expected, to 240 at which failure occurs essentially by elastic buckling. The analysis is performed at 12 different slendernesses in this range, at intervals of 20. Load-deflection behaviour is calculated at each column slenderness ratio, however, load-deflection curves need only be presented at three typical slenderness values; 40 to illustrate behaviour in the stocky range, at a medium slenderness of 120 and for the very slender column where the value is 240.

6.2.2 Results of the basic problem analysis

The resulting column curve from the basic problem is shown in Figure 6.2; this gives a plot of the maximum load capacity of the column over the full slenderness range. The column curve is compared with the European Strut Curve 'b' (83) from which it can be seen that the effects of the top and seat flange cleated connection is to considerably increase the column's maximum load capacity above the value that it would normally be designed to carry. A plot of the load difference (between the European Strut

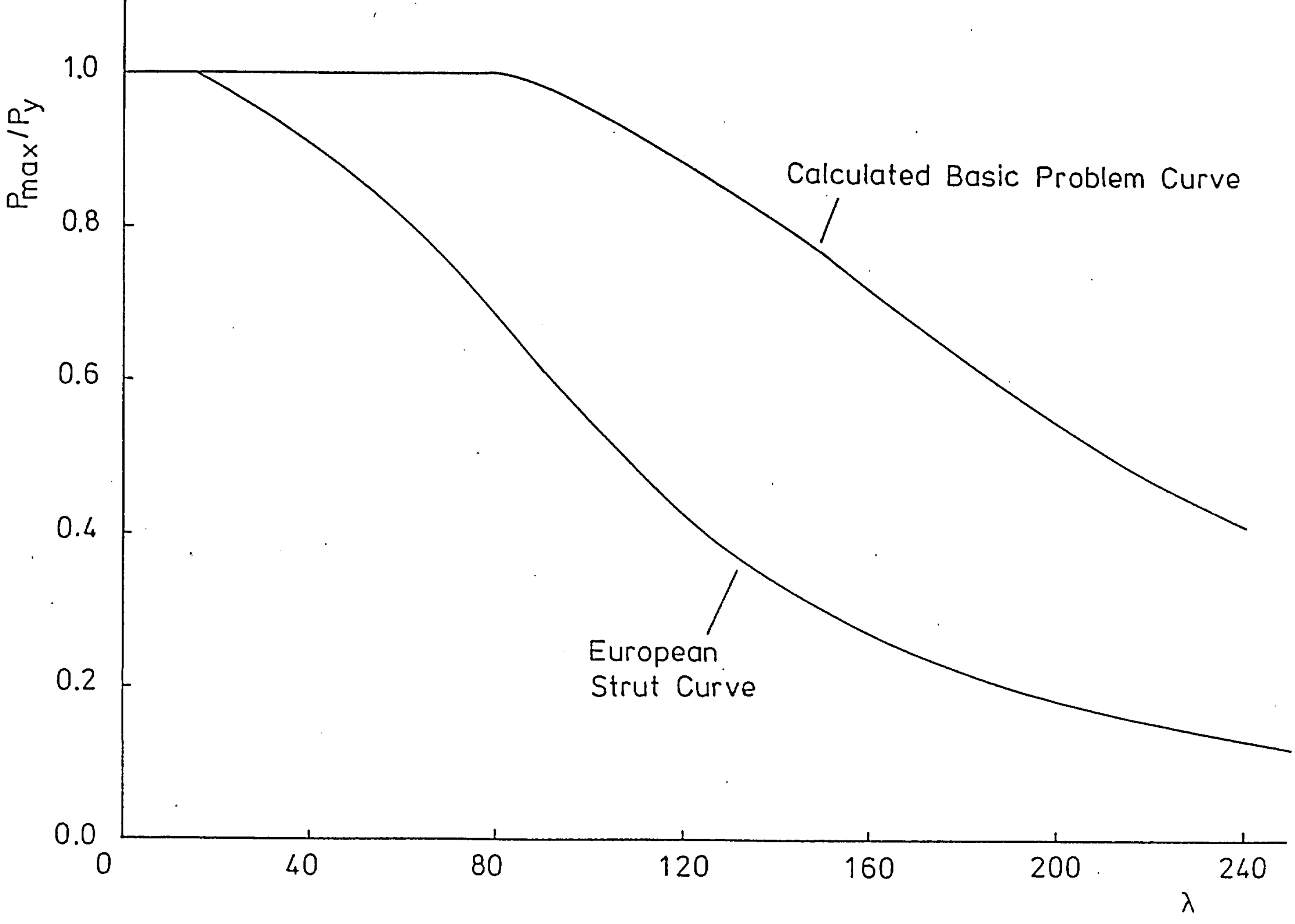

FIGURE 6.2 - Column Curve for Basic Problem

curve and the calculated basic problem curve) against slenderness ratio is shown in Figure 6.3. This shows how the semi-rigid connection influences column strength over the full slenderness range. For low slendernesses the effect of the end restraint is small, with failure occurring due to the full squash load being reached or due to excessive material yield in the section. As slenderness increases the influence of the stiffening effect of the connection becomes more important as column stability becomes more critical. A maximum increase in load capacity of 48 per cent of P_y is observed at a slenderness ratio of 140; this increase in load capacity is slightly reduced for higher slenderness ratios. From this it can be seen that semi-rigid end restraint has a significant influence on load capacity for slendernesses greater than 40.

Typical load-deflection curves are shown in Figure 6.4, which include the curve of the equivalent ideally pinned elastic column (dotted) for comparison. Figure 6.4a shows the behaviour of a stocky column with a slenderness of 40, in which the load capacity is not increased significantly, but the end restraint does reduce member deflections. Figures 6.4b and 6.4c show the load-deflection curves for columns with slenderness ratios of 120 and 240, respectively; both illustrate the reduction in deflections at particular load levels as well as the increase in maximum load capacity.

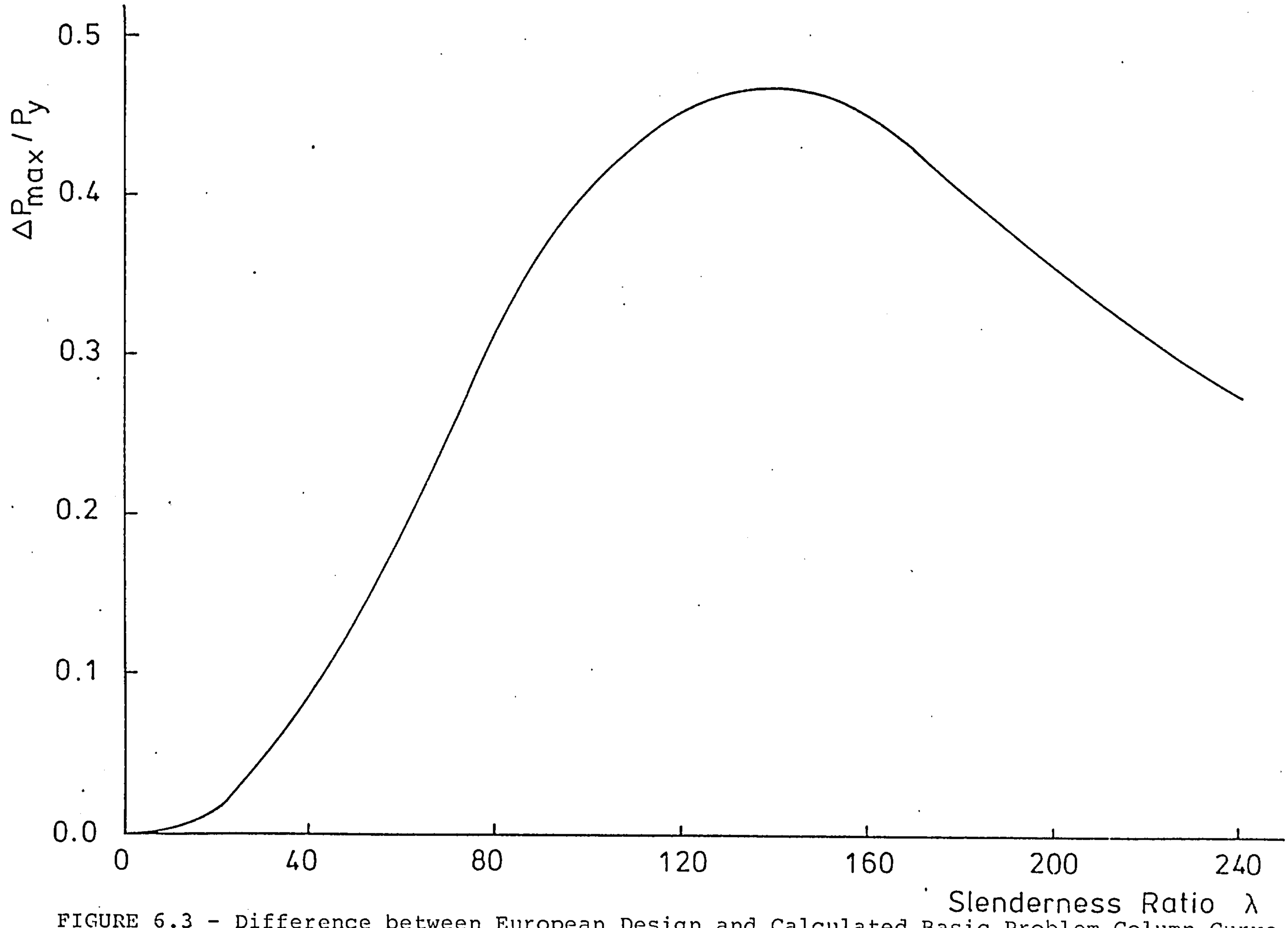

FIGURE 6.3 - Difference between European Design and Calculated Basic Problem Column Curve

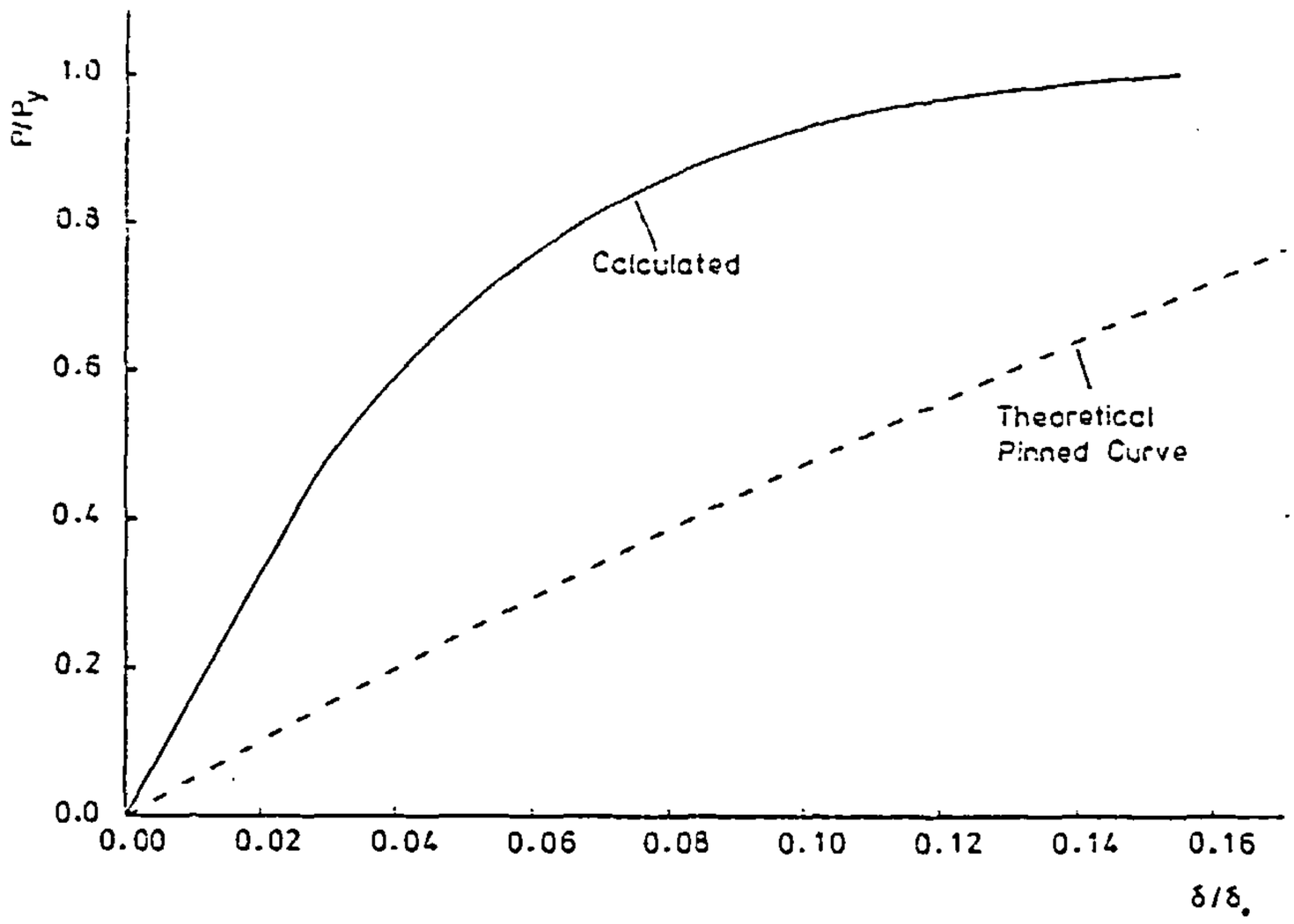

(a) $\lambda = 40$

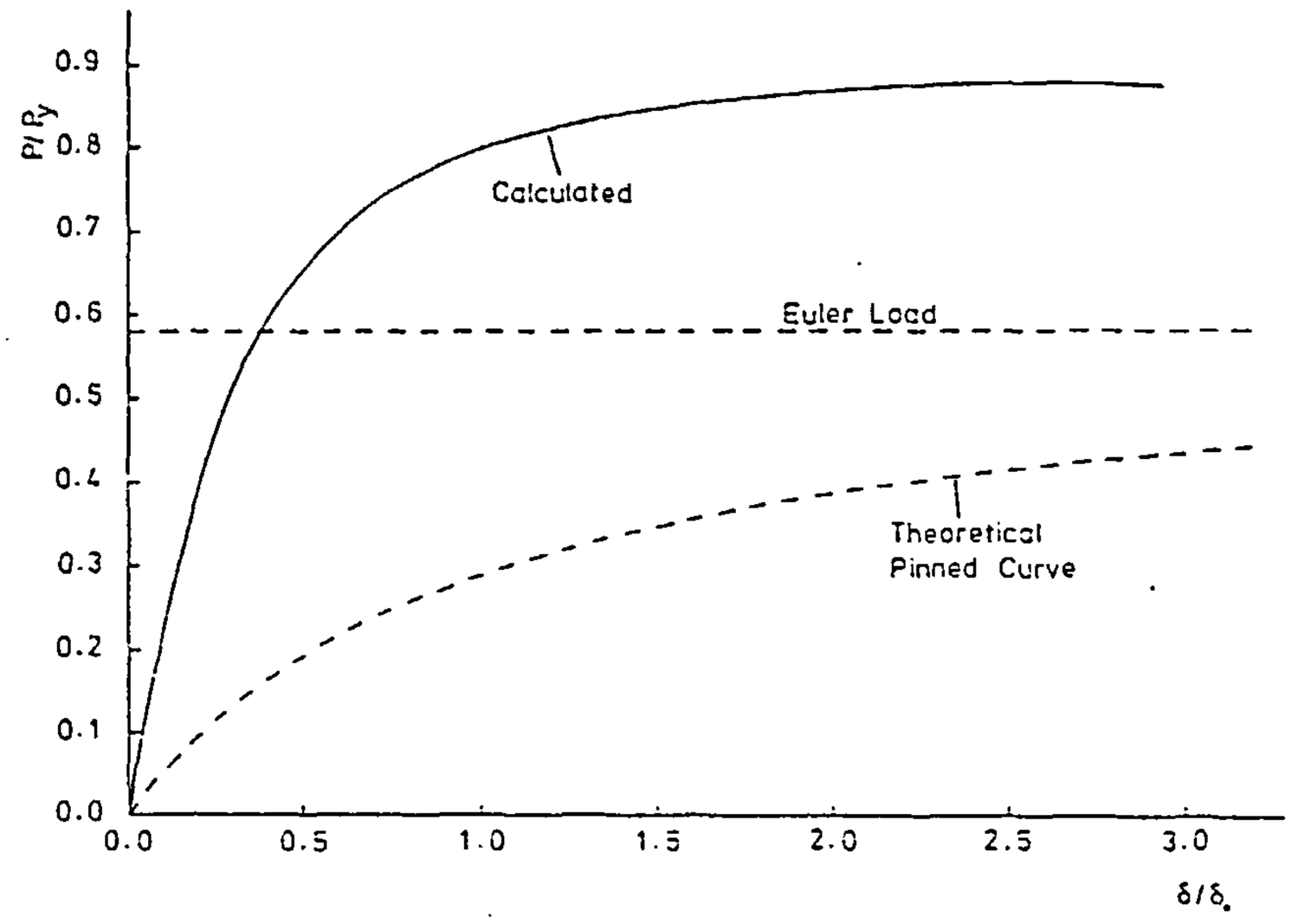

(b) $\lambda = 120$

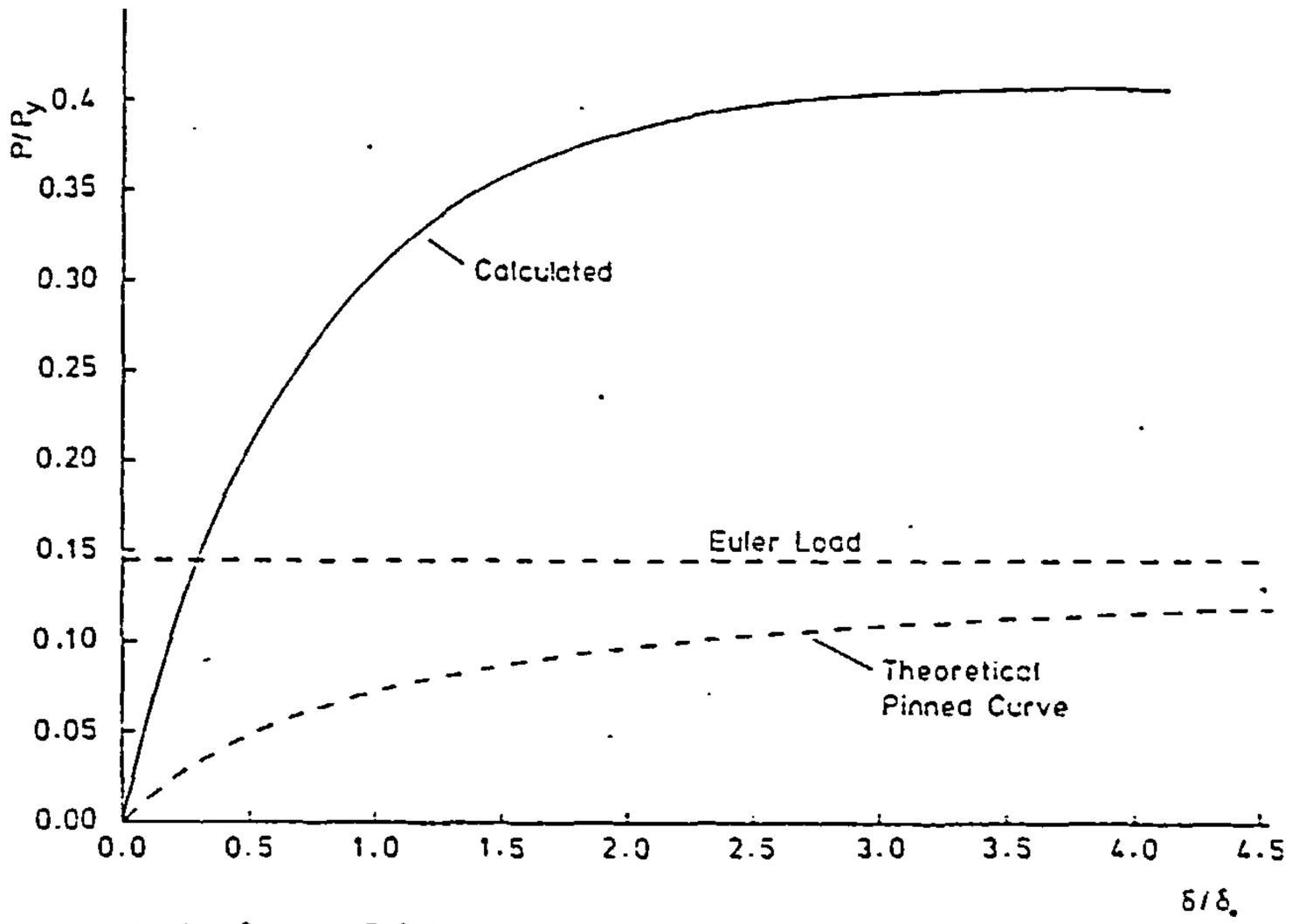

(c) $\lambda = 240$

FIGURE 6.4 - Typical Load-Deflection Curves for Basic Problem

The results of the basic problem show that semi-rigid end restraint increases the column stiffness, which reduces deflections for all slendernesses and increases column strength where failure is normally due to instability.

6.3 Description of the Parametric Study

In the rest of this chapter the results of the parametric study are presented; these are discussed briefly but a more general discussion is given in the following chapter. The parameters chosen for study, and their range of variation, are shown in Table 6.1. These parameters are arranged into three main categories. The first investigates the influence of the type and size of end restraint on the behaviour of the column. Secondly, variations in the type of column section are investigated, this includes the effects of section type, size, whether bending is about the major or minor axis and the type of initial residual stresses. The third category deals with geometrical considerations in which the effects of initial out-of-straightness and eccentricity of applied load are investigated.

The finite element model and the material properties, an elastic modulus of 205 kN/mm^2 and a yield stress of 240 N/mm^2, are the same as those used in the basic problem.

Normally, only one parameter is varied at a time and results are compared with those of the basic problem. However, in some cases extra results are

TABLE 6.1 - Parameter Variations of Parametric Study

Parameter Type	Basic Problem Value	Variations
<u>Characteristics of End Restraint</u>		
Connection type	Top and seat flange cleats	- Ideally pinned - Single web cleat - Double web cleats - End plate - T-stubs
Connection size	Medium angles	- Light angles - Heavy angles
<u>Characteristics of Column Section</u>		
Section type	Universal column	Universal beam
Bending axis	Major	Minor
Section size	203x203UC60	- Light: 152x152UC23 - Heavy: 305x305UC158
Residual stress pattern	Parabolic	- Initially stress free - Lehigh distribution - Welding stresses
<u>Characteristis of Geometrical Considerations</u>		
Initial out-of-straightness	δ_o = L/1000	- δ_o = L/250 - δ_o = L/500 - δ_o = L/2000 - δ_o = L/5000
Eccentricity	e = 0	- e = 10 mm - e = 25 mm - e = 50 mm - e = 100 mm

presented when, for example, it is useful to compare results for pinned connections or to investigate the effects of connection type in minor bending for beam sections.

6.4 Characteristics of End Restraint

6.4.1 Effects of connection type

In order to investigate the influence of end connection type on the strength and behaviour of the column, a series of tests were performed using, in addition to the flange cleated connection of the basic problem, three other connection types. These connection types were chosen to give the full range of connection stiffnesses. A T-stub connection, made from a split 381×152UC67 section of length 200 mm and connected by 22 mm rivets, represents the most rigid type of connection. The flange cleated connection of the basic problem represents a medium range semi-rigid connection, while a double web cleated connection, made from two 152×89×12.6 angles with 22 mm rivets, represents a flexible connection. An ideally pinned connection is also included, for the purpose of comparison. The moment-rotation curves for these three connections are shown in Figure 6.5, the horizontal axis again representing the pinned end condition. This data was reported by Batho and Rowan (8) who measured connection data experimentally, using the same column section as used in the analysis.

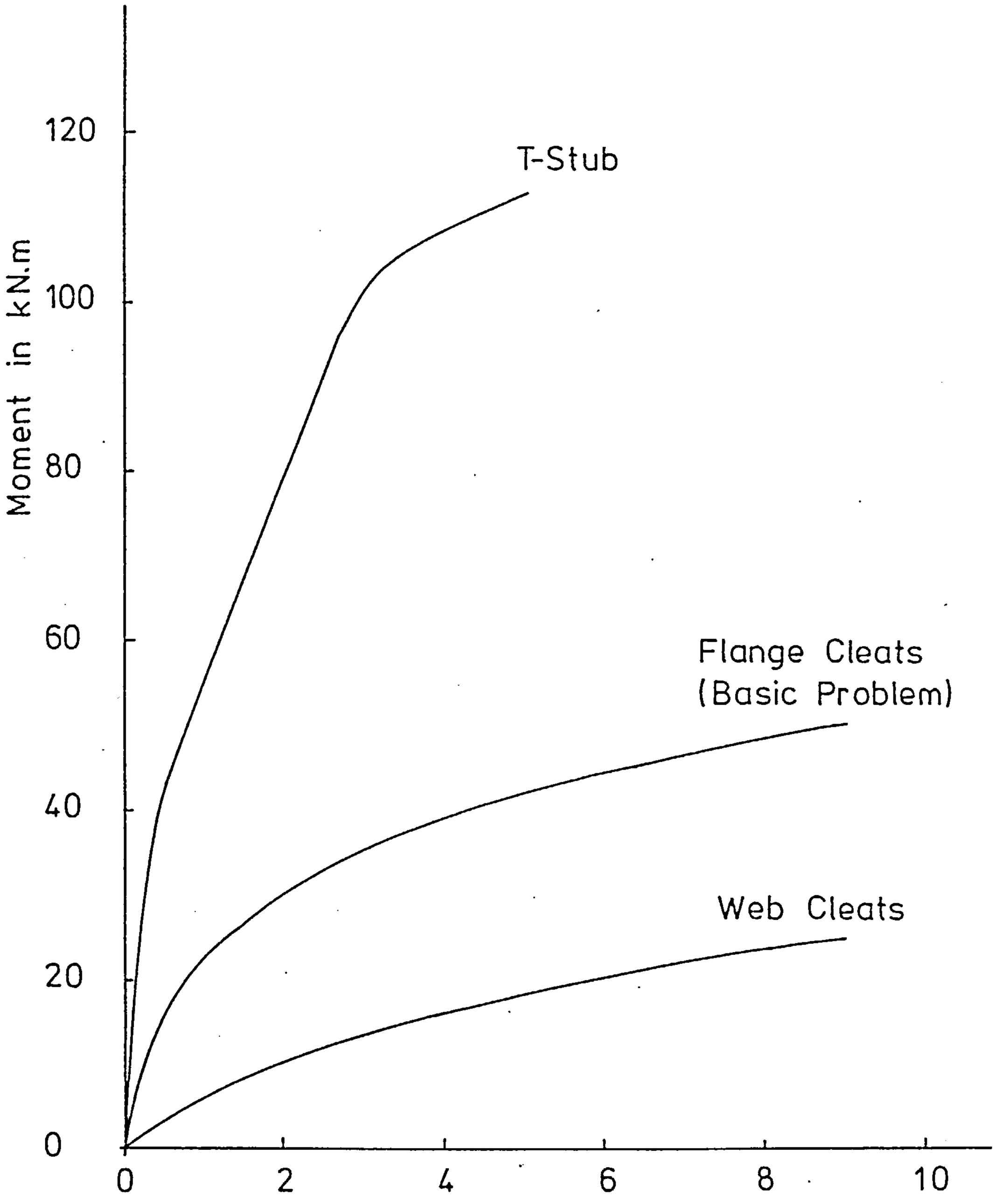

FIGURE 6.5 - Moment-Rotation Curves for Main Connection Types

Typical load-deflection curves at slenderness ratios of 40, 120 and 240 are shown in Figures 6.6a - c, respectively. In all cases the increase in connection stiffness produces a corresponding reduction in column deformation. This is accompanied by an increase in load carrying capacity, except in those cases where the column is so stocky that it can attain its full squash load, even when pin-ended. The benefits of increased end restraint become more significant as the column becomes more slender; the increases in strength, over the pinned column, at a slenderness of 140 are 26, 43 and 47 per cent of P_y for the web cleated, flange cleated and T-stub connections, respectively.

Column curves giving the complete set of results, Figure 6.7, show that load carrying capacity increases with more rigid connection stiffness. This increase in strength becomes most significant when the column slenderness exceeds 80. Also, the amount by which the column curve is raised depends on the connection stiffness.

The amount of actual connection data that is compatible with the above test series is restricted. In order to investigate the effects of other types of connection, moment-rotation curves have been generated using the standardised moment-rotation equations of Frye and Morris (69). In addition to the three

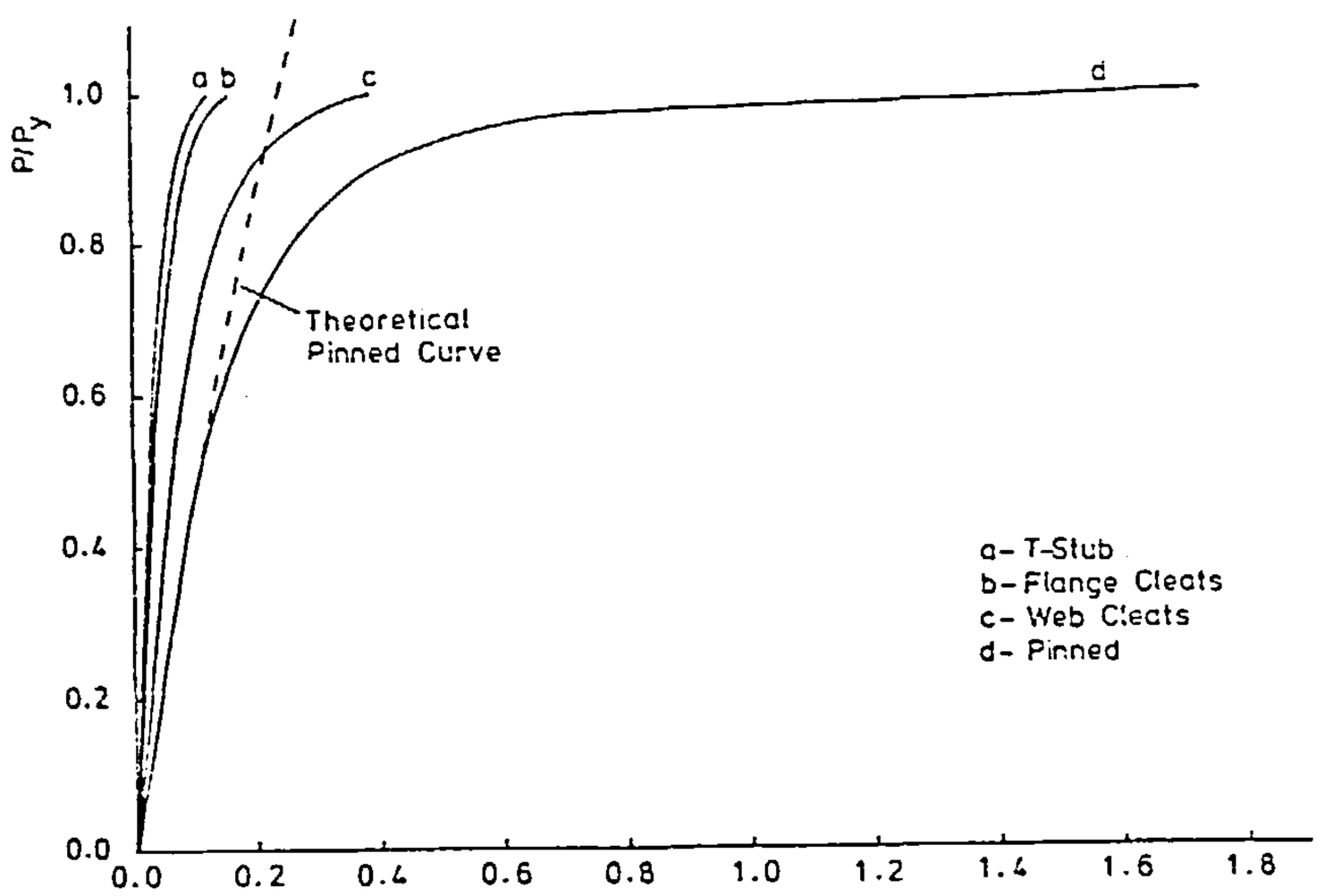

δ/δ.

(a) λ = 40

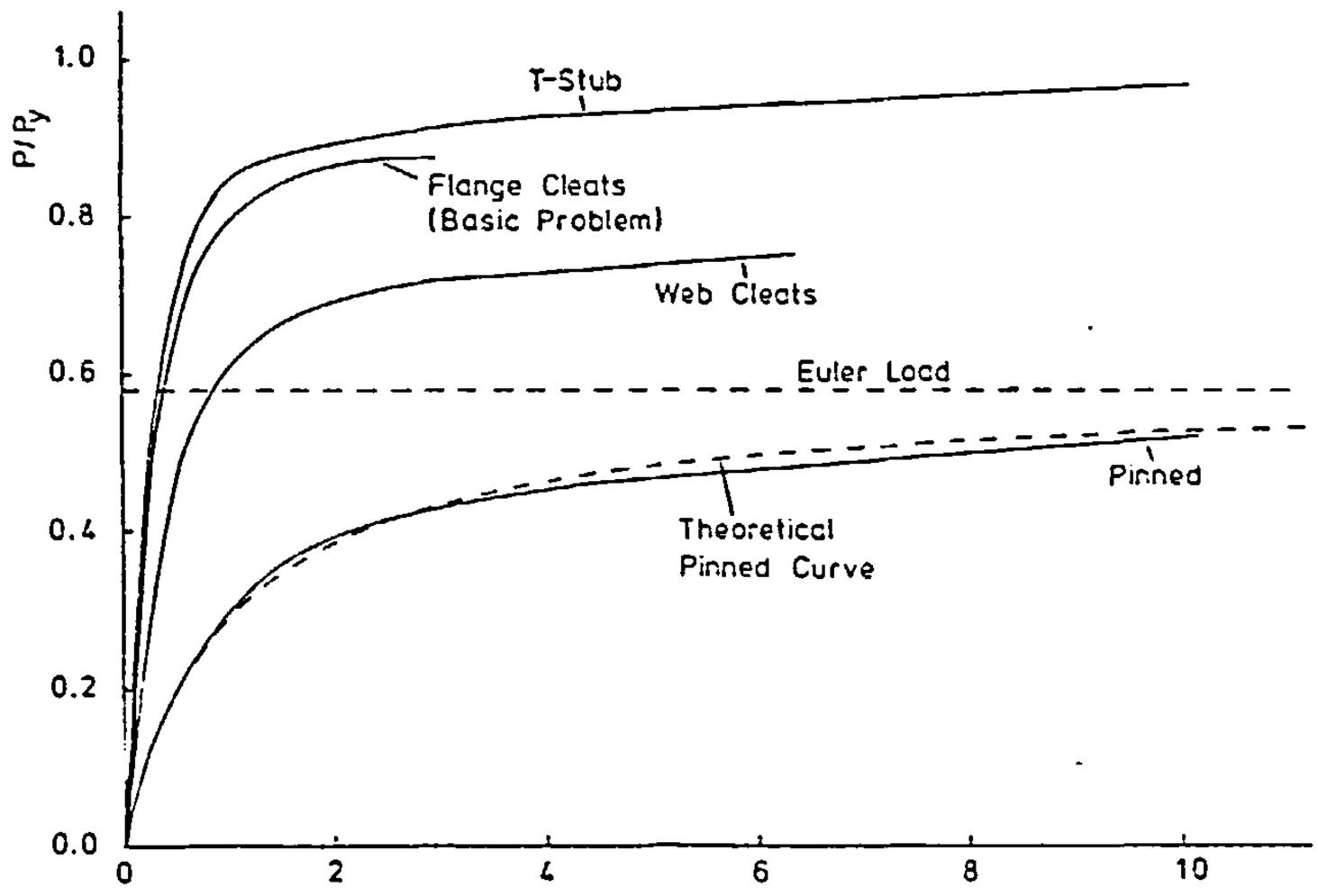

δ/δ.

(b) λ = 120

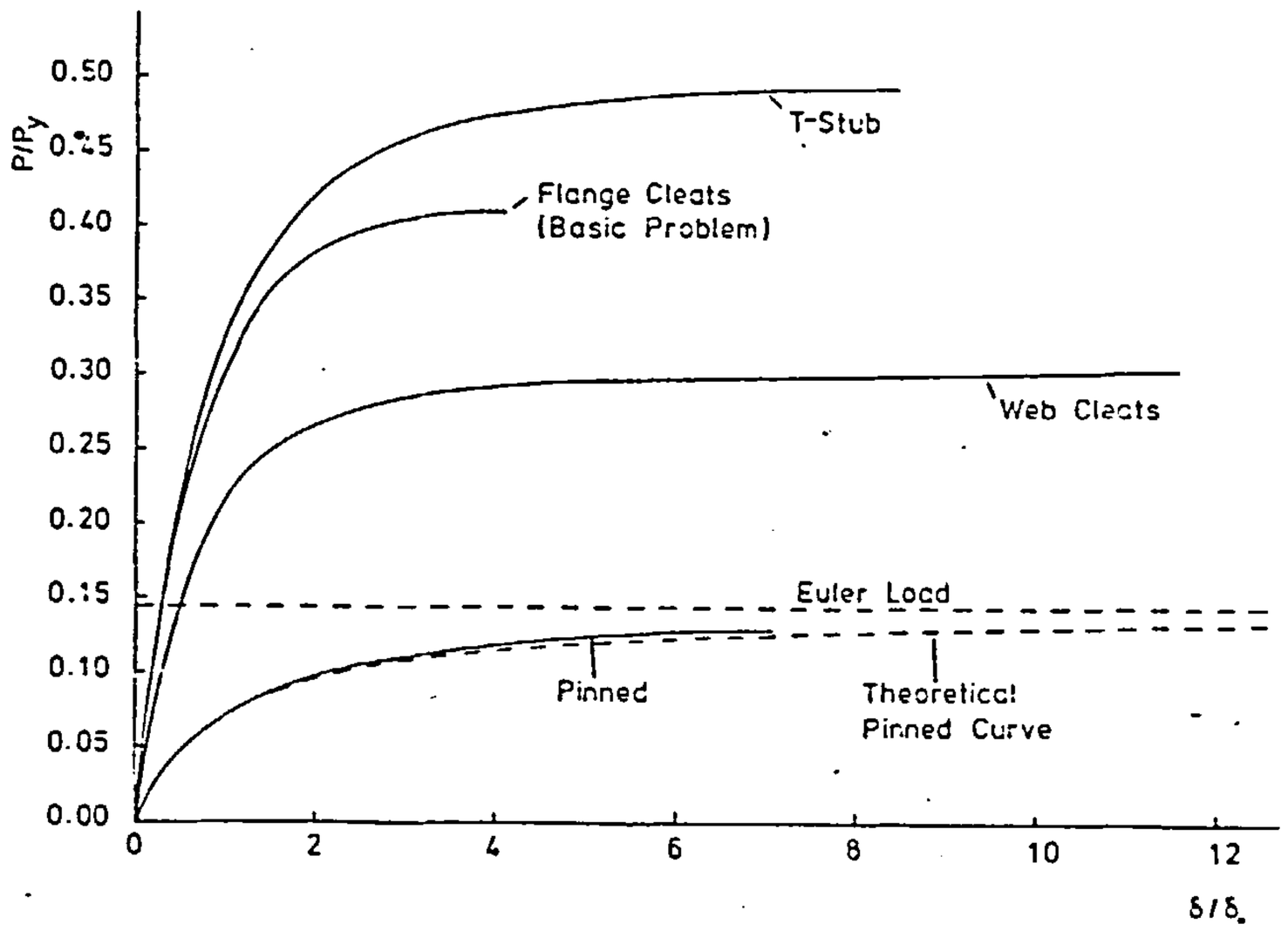

δ/δ.

(c) λ = 240

FIGURE 6.6 - Typical Load-Deflection Curves for Main Connection Types

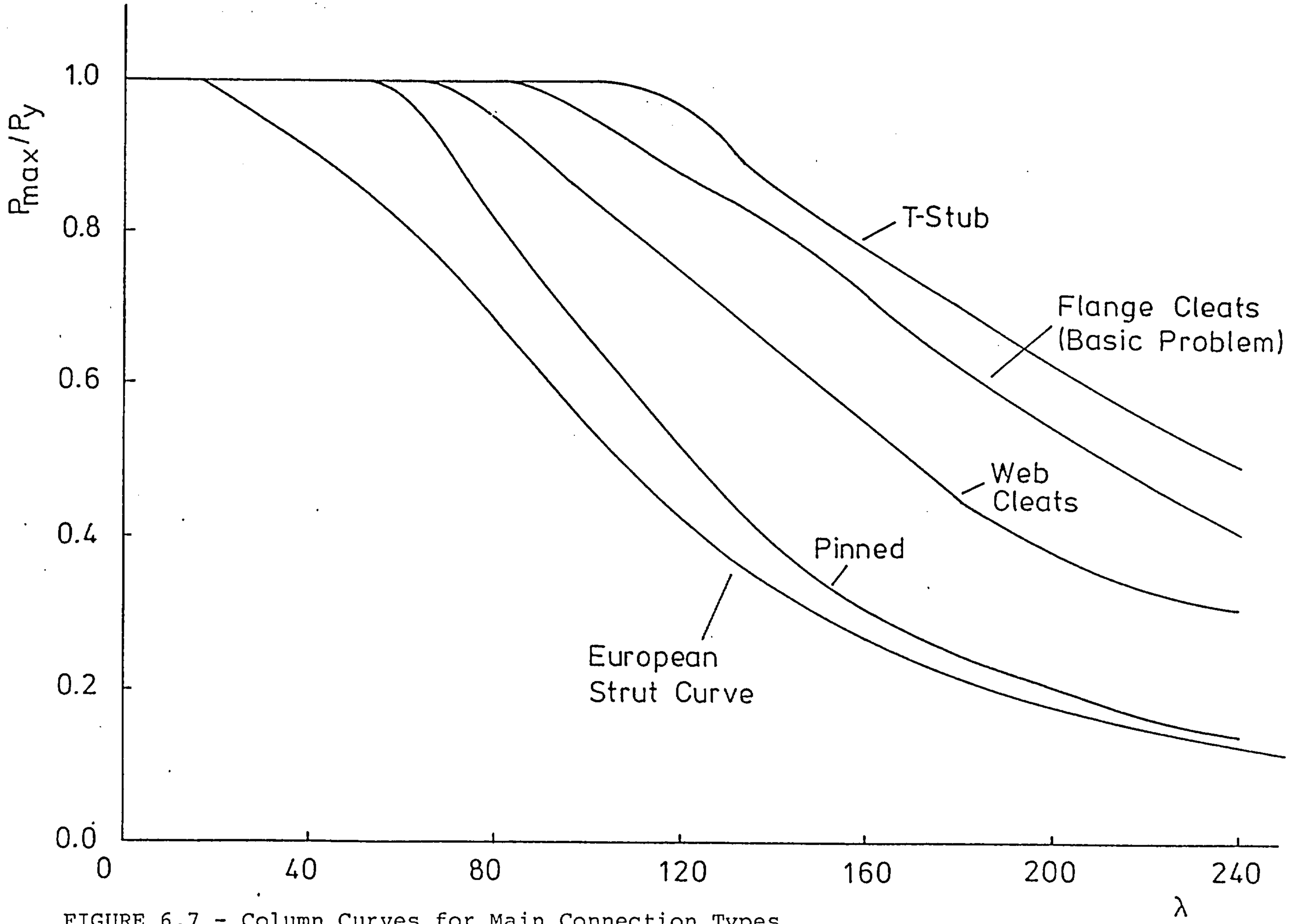

FIGURE 6.7 - Column Curves for Main Connection Types

connection types mentioned above, single web cleat and end plate connection data was also generated. The resulting moment-rotation curves for the five connection types are shown in Figure 6.8, showing the relative stiffness of each connection type.

This generated moment-rotation data was used in an additional test series to investigate the influence of connection type on column behaviour. Typical load-deflection curves are shown in Figures 6.9a - c and the full column curves are shown in Figure 6.10. These results, again, show that increases in connection rigidity produce corresponding reductions in column deformation and that load carrying capacities are increased, except in the case of the full squash load being attained. Although the tests using generated connection data produce similar results to the tests using actual connection data, care must be taken when using generated connection data. Comparisons of actual connection data and data generated by the Frye and Morris equations, using parameter sizes corresponding to the actual connection dimensions, were given in Section 3.3.2. For the web cleated and T-stub connections the agreement between the actual and generated curves is reasonably close, but for the flange cleated connection the moment values generated are almost half of the actual moment values. This of course, grossly underestimates the connection stiffness used in the analysis. The standardised

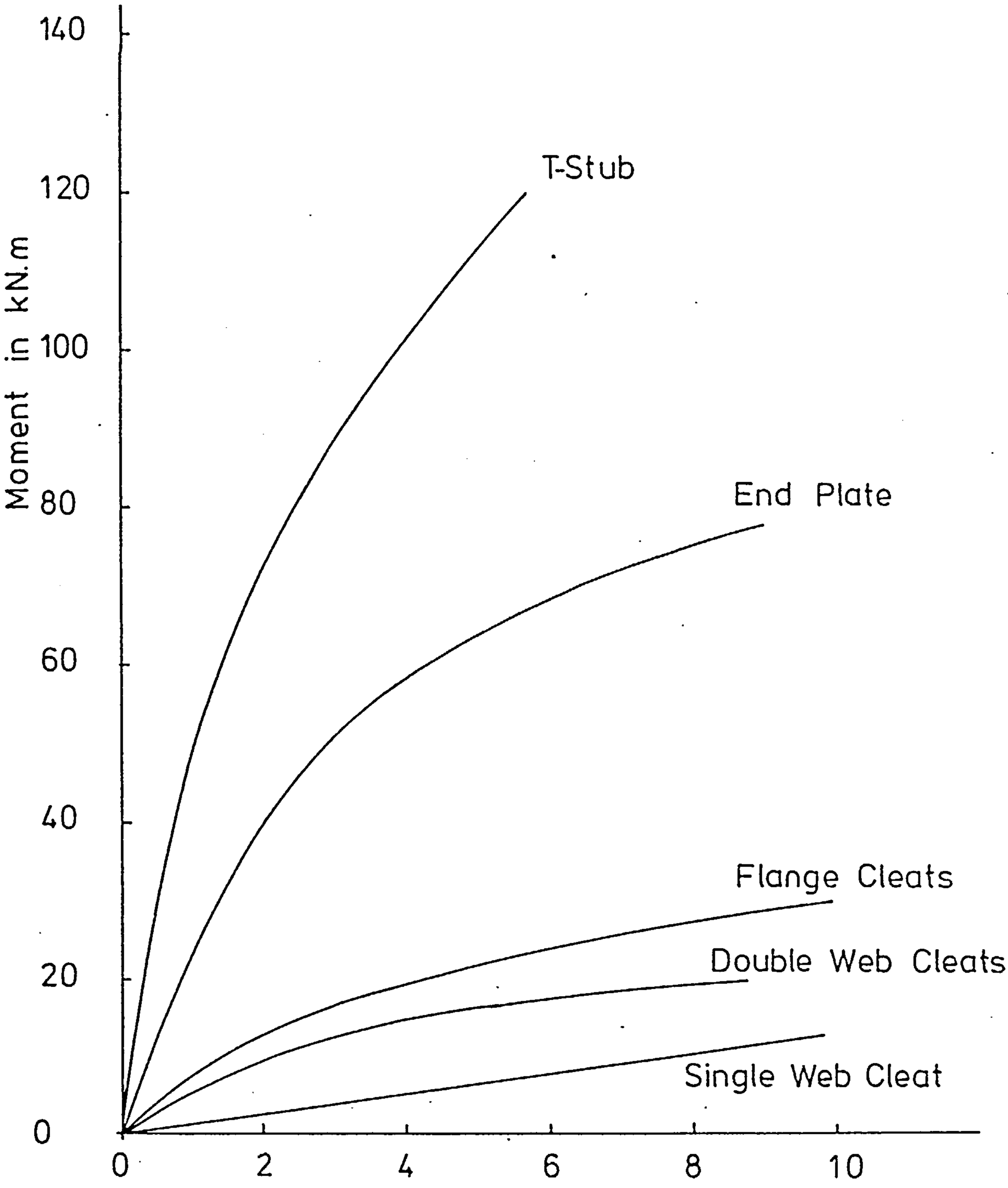

FIGURE 6.8 - Frye and Morris Equation Generated Moment-Rotation Curves

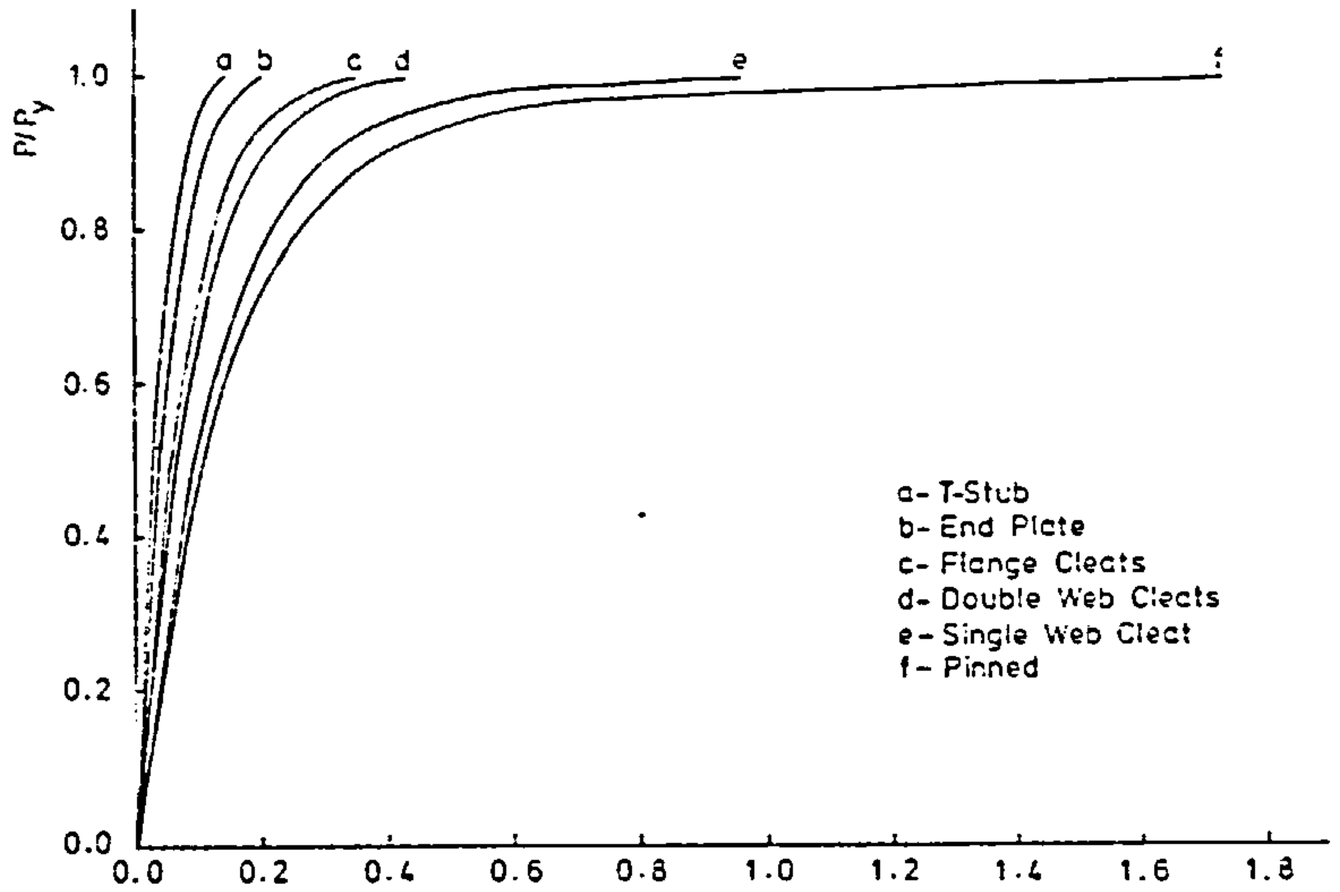

(a) λ = 40

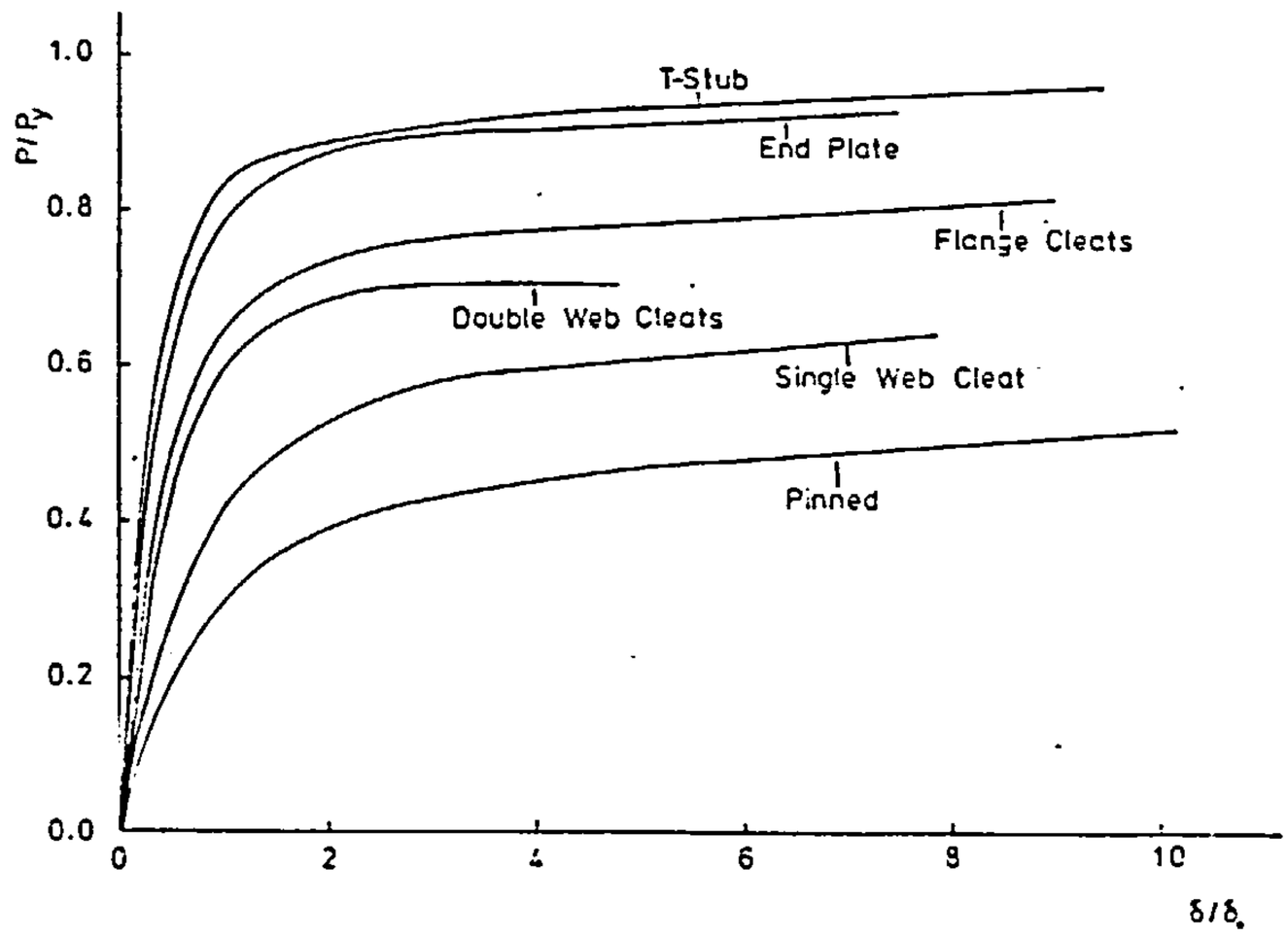

(b) λ = 120

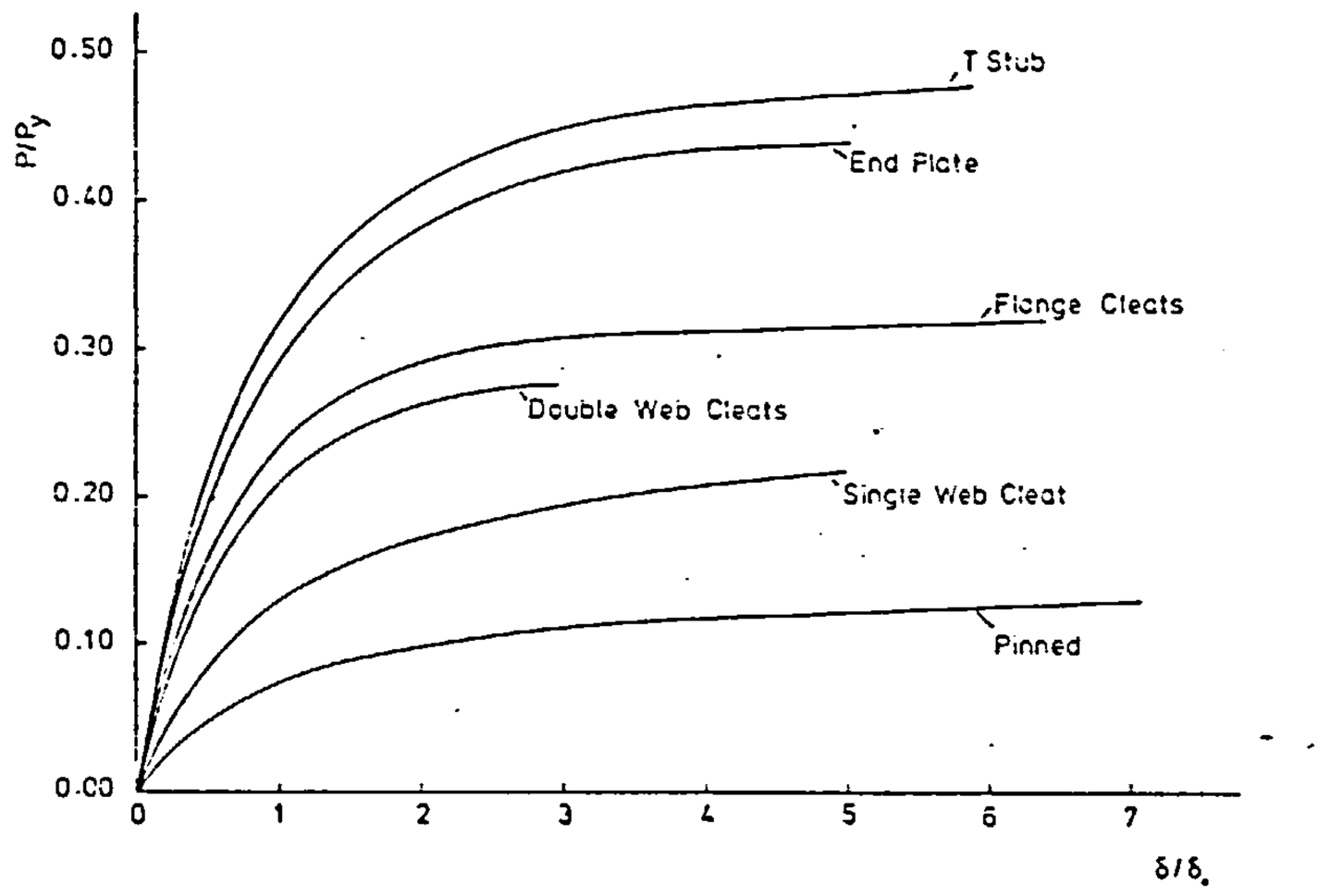

(c) λ = 240

FIGURE 6.9 - Typical Load-Deflection Curves for Generated Connection Data

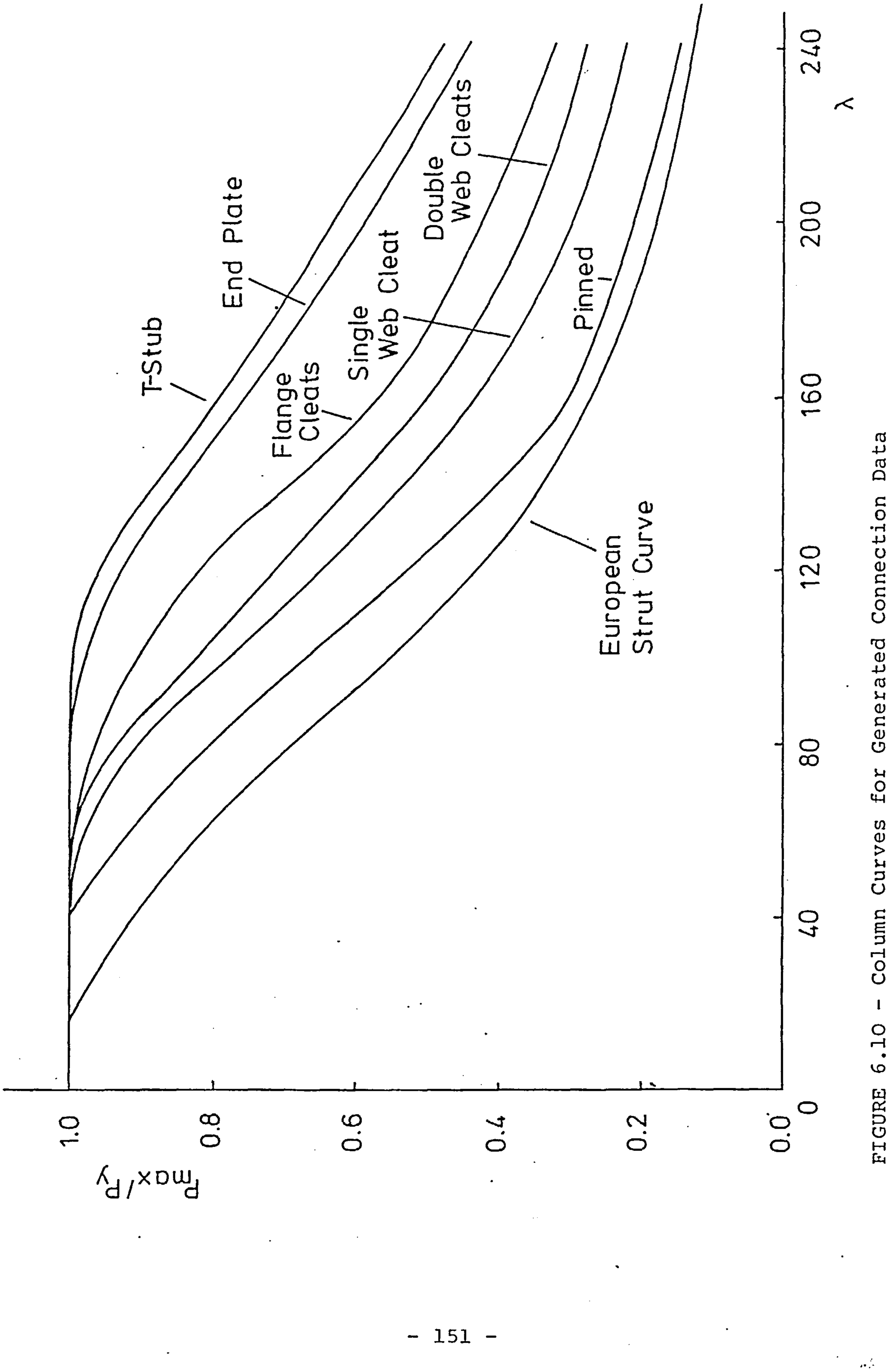

FIGURE 6.10 - Column Curves for Generated Connection Data

moment-rotation equation for the flange cleated connection is clearly in error, and should be updated before being used in analytical procedures.

6.4.2 Effect of connection size

In addition to an investigation into the effects of connection type, an investigation of variations in connection size was performed. The flange cleated connection dimensions of the basic problem were varied to have heavier and lighter connecting angles. The connection used for the basic problem is medium sized with 152×152×12.6 angles. In this study, a heavier connection using 152×152×25.3 angles and a lighter connection using 102×102×12.6 angles were also considered for comparison. The moment-rotation curves of the three connections are shown in Figure 6.11. As would be expected, an increase in component dimensions produces stiffer connections.

A series of tests were performed using this connection data with the column section used in the basic problem tests. Typical load-deflection curves, Figures 6.12a - c, show that the increased connection stiffness due to increased connecting angle size produces a corresponding reduction in column deformation. This, again, is accompanied by an increase in load carrying capacity for all but the most stocky columns. Column curves of the complete set of results, Figure 6.13, show that connection dimensions do have a significant effect in increasing load carrying capacity as connection size is increased. The effect of the

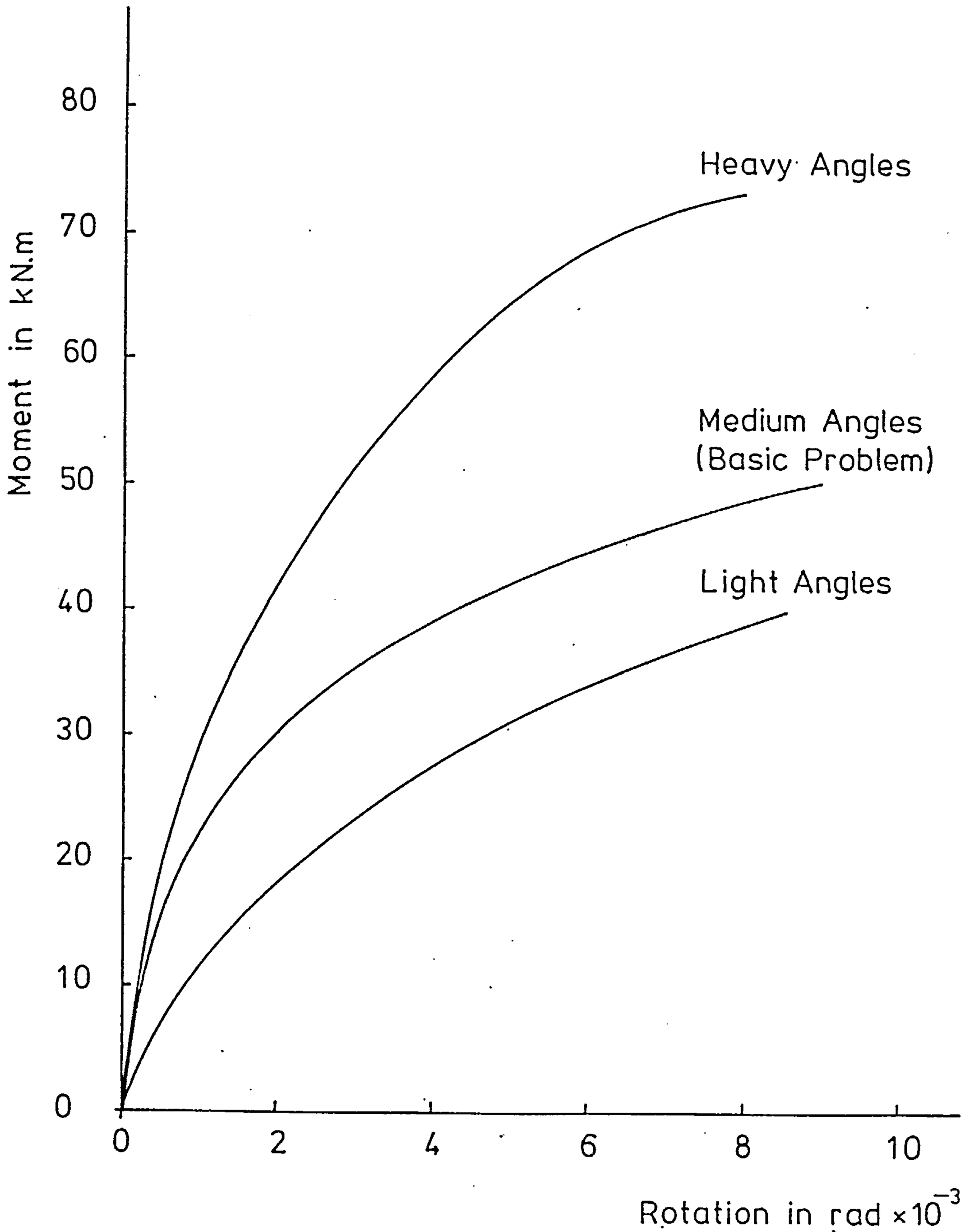

FIGURE 6.11 - Moment-Rotation Curves for Varied Dimension Flange Cleated Connections

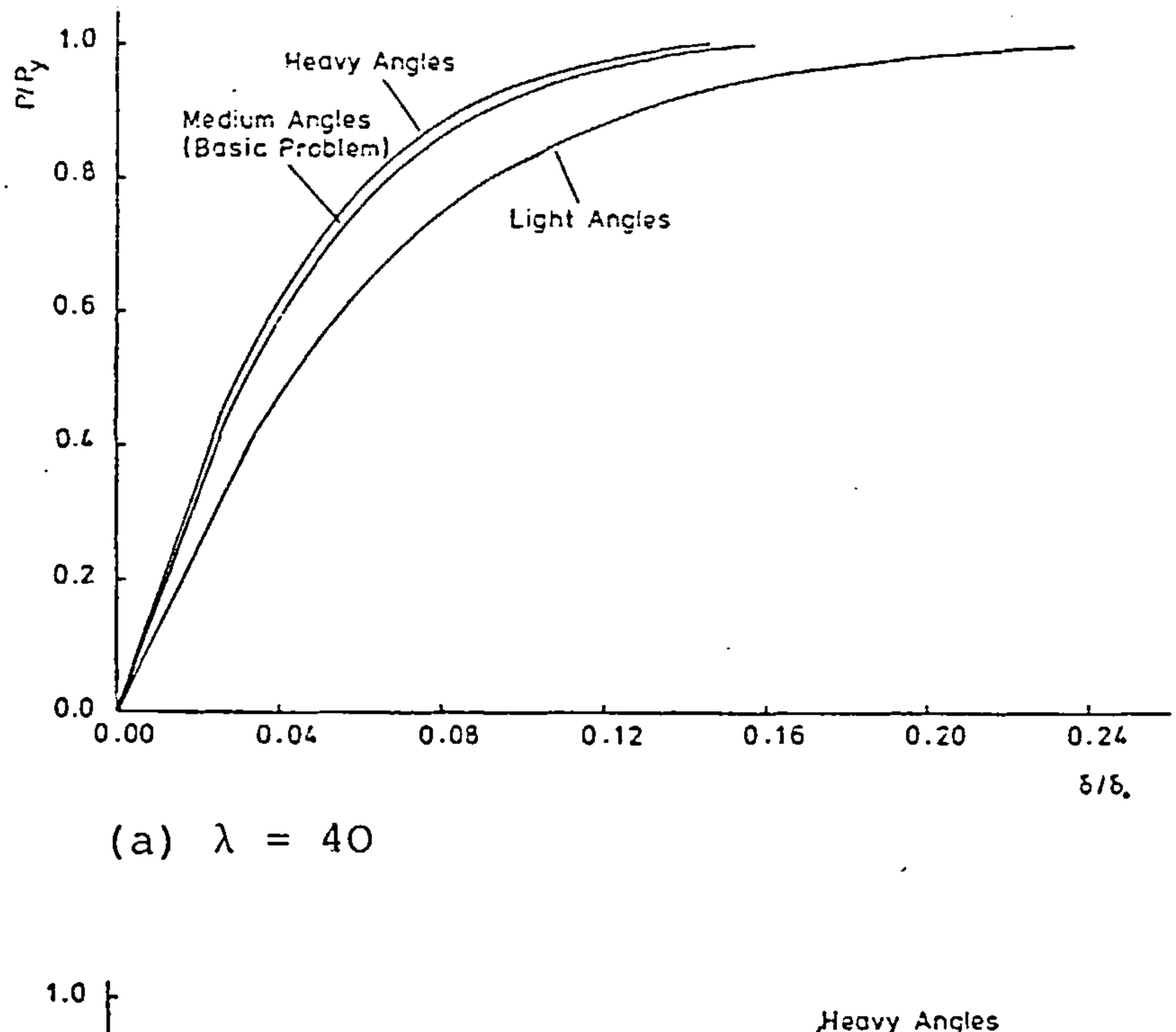

(a) $\lambda = 40$

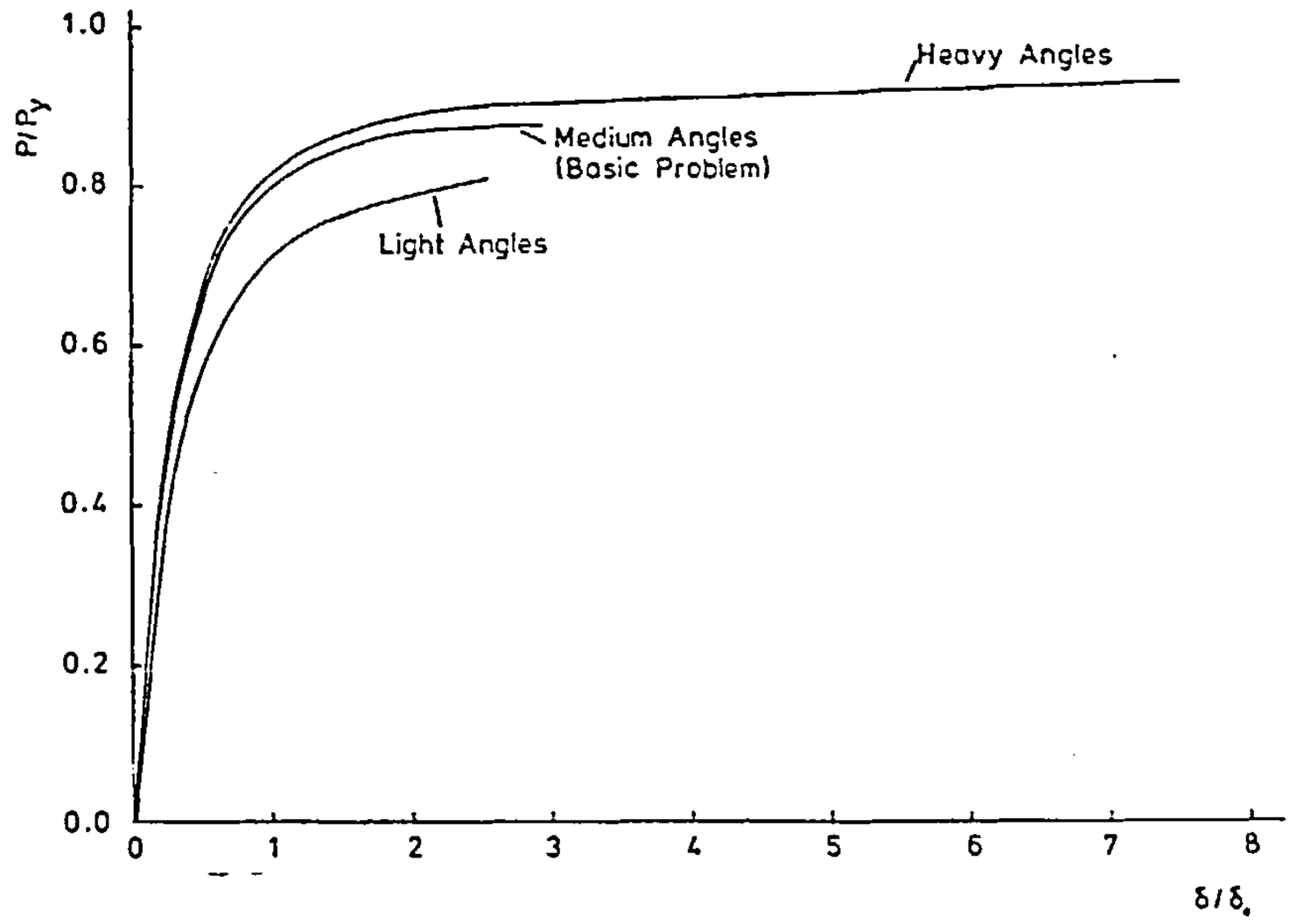

(b) $\lambda = 120$

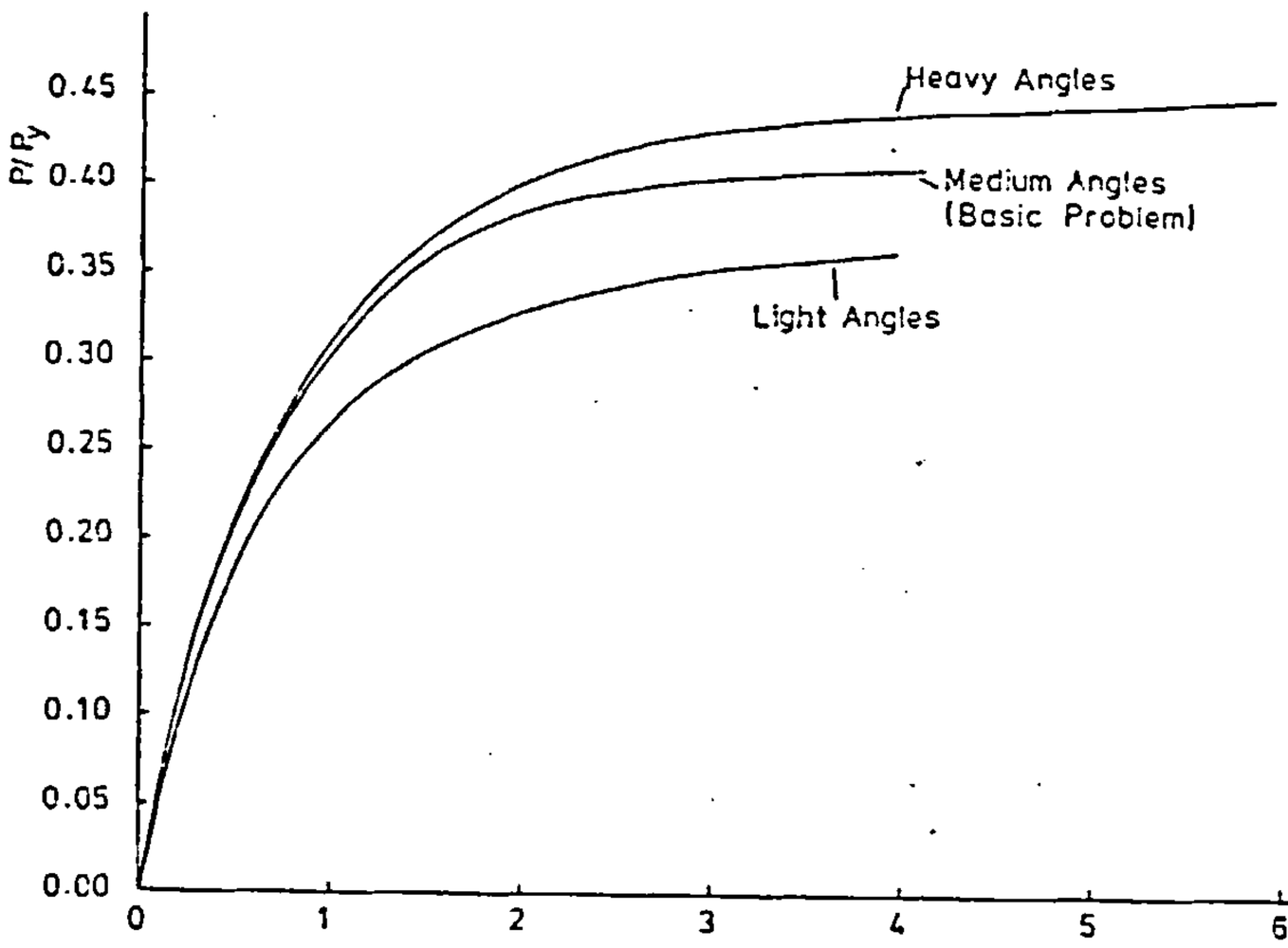

(c) $\lambda = 240$

FIGURE 6.12 - Typical Load-Deflection Curves for Varied Dimension Flange Cleated Connection

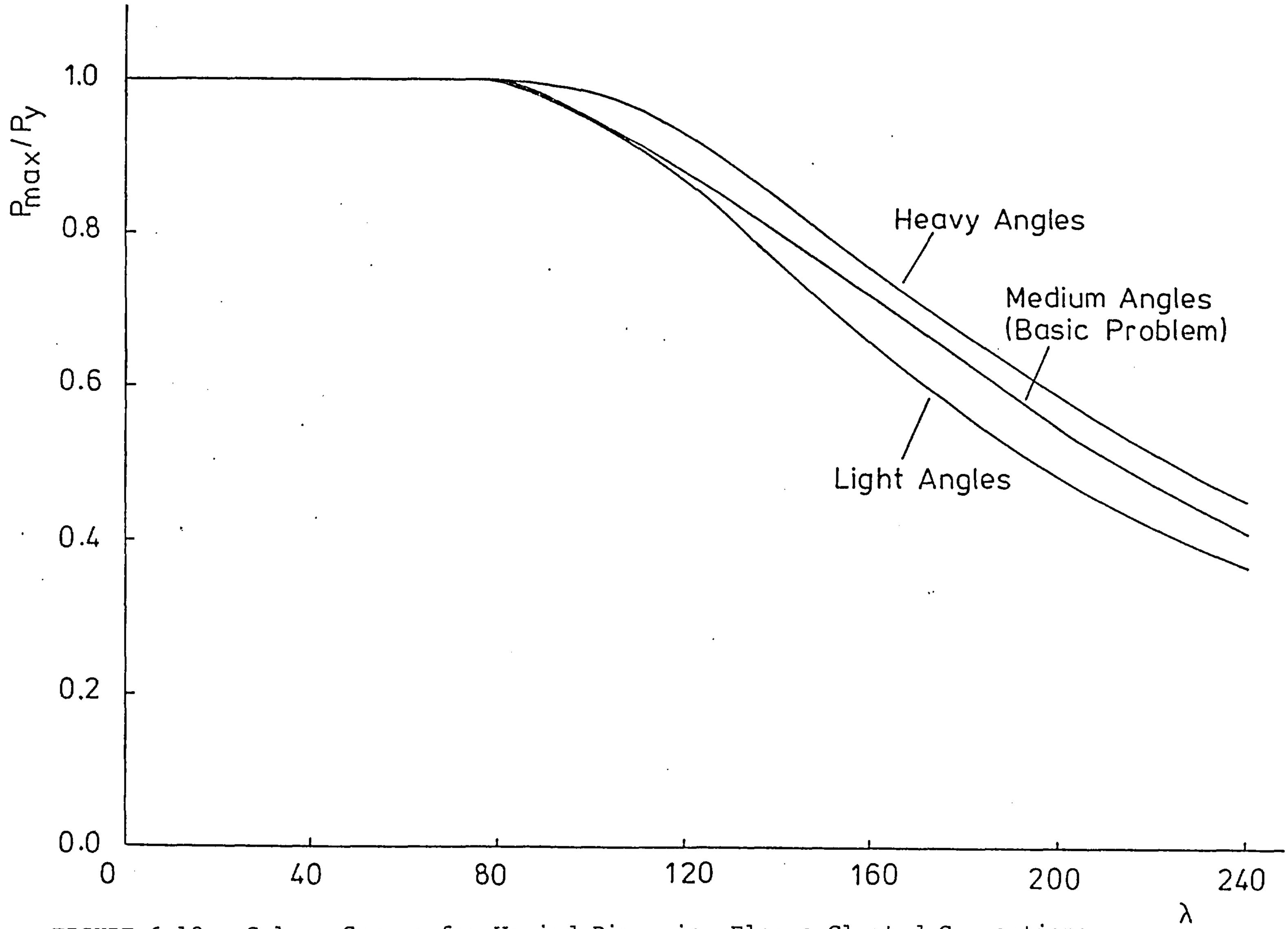

FIGURE 6.13 - Column Curves for Varied Dimension Flange Cleated Connections

connection size becomes most significant for columns with a slenderness greater than 120. For example, at a slenderness of 160 the heavier angles increase the column strength by three per cent of P_y, while the light angles decrease the column strength by 6.5 per cent of P_y compared to the value of the basic problem.

In addition to varying the dimensions of flange cleated connections, the influence of connection size of a more flexible (web cleated) connection and a more rigid (bolted flange cleated) connection were also investigated.

The double web cleated connection, used in Section 6.4.1, is compared with heavier and lighter angled connections in Figure 6.14. The heavier connection is made of 152×89×15.7 angles while the lighter connection is made of 152×89×9.4 angles. The resulting column curves for the flexible connection tests are shown in Figure 6.15. From these it can be seen that variation of a flexible connection's dimensions has little effect on the strength of the column.

To investigate the effects of varying the size of a more rigid type of connection a series of bolted flange cleated connections were used. Moment-rotation curves for heavy, medium and light connection using 152×152×19.0, 152×152×12.6 and 152×152×9.4 angles, respectively, are shown in Figure 6.16. This connection type was used due to a lack of compatible data for T-stub

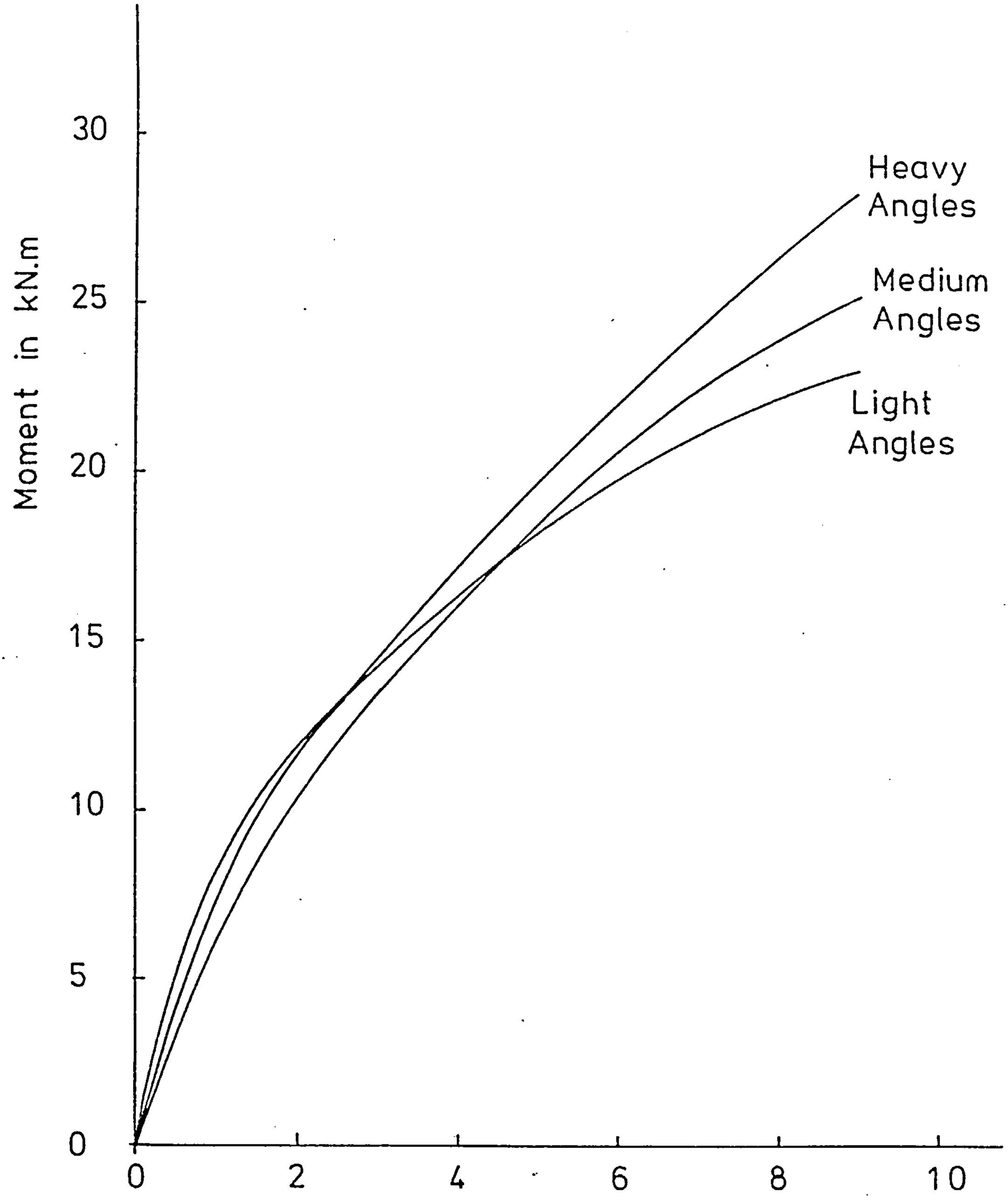

FIGURE 6.14 - Moment-Rotation Curves for Varied Dimension Web Cleated Connections

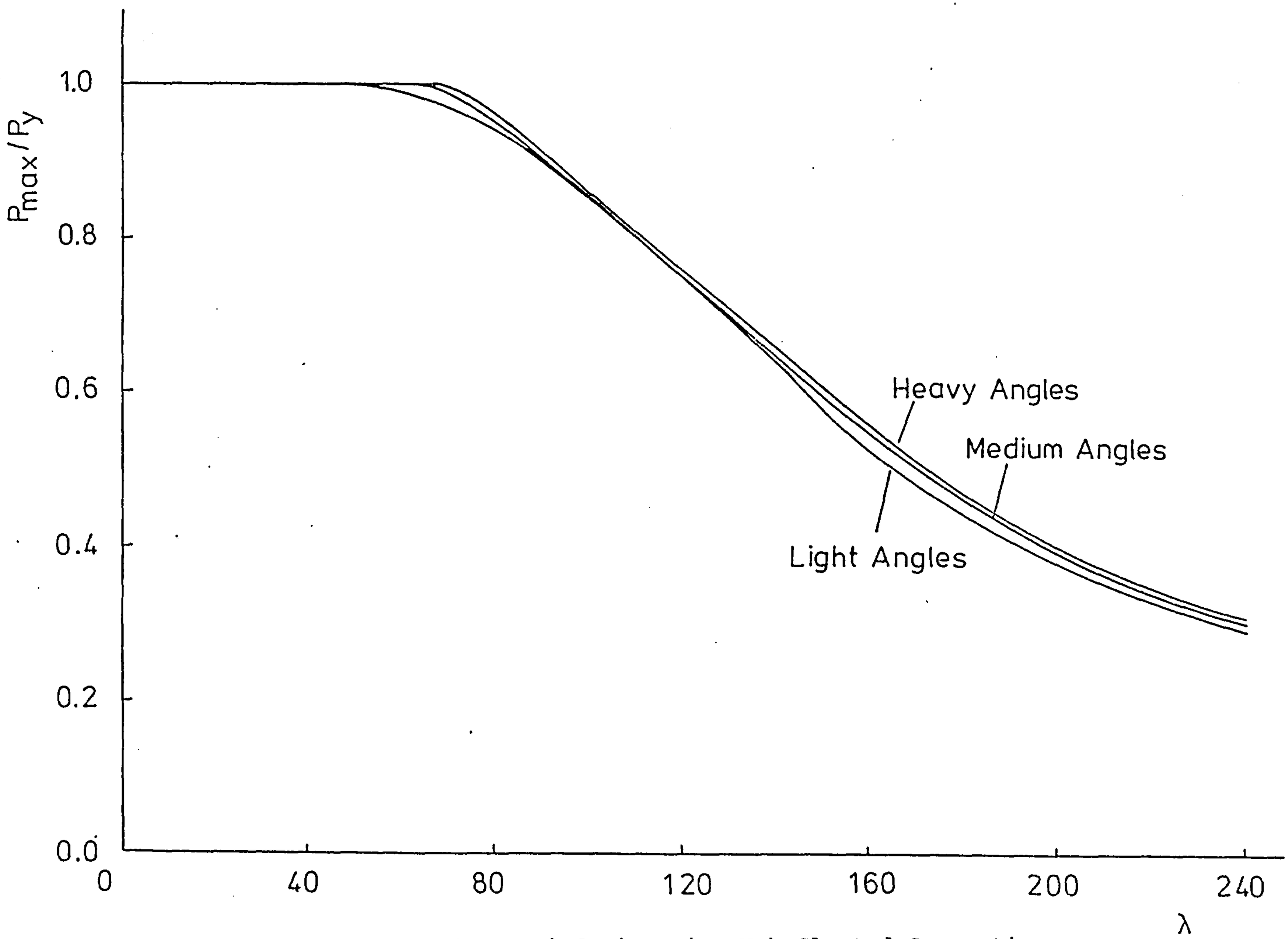

FIGURE 6.15 - Column Curves for Varied Dimension Web Cleated Connections

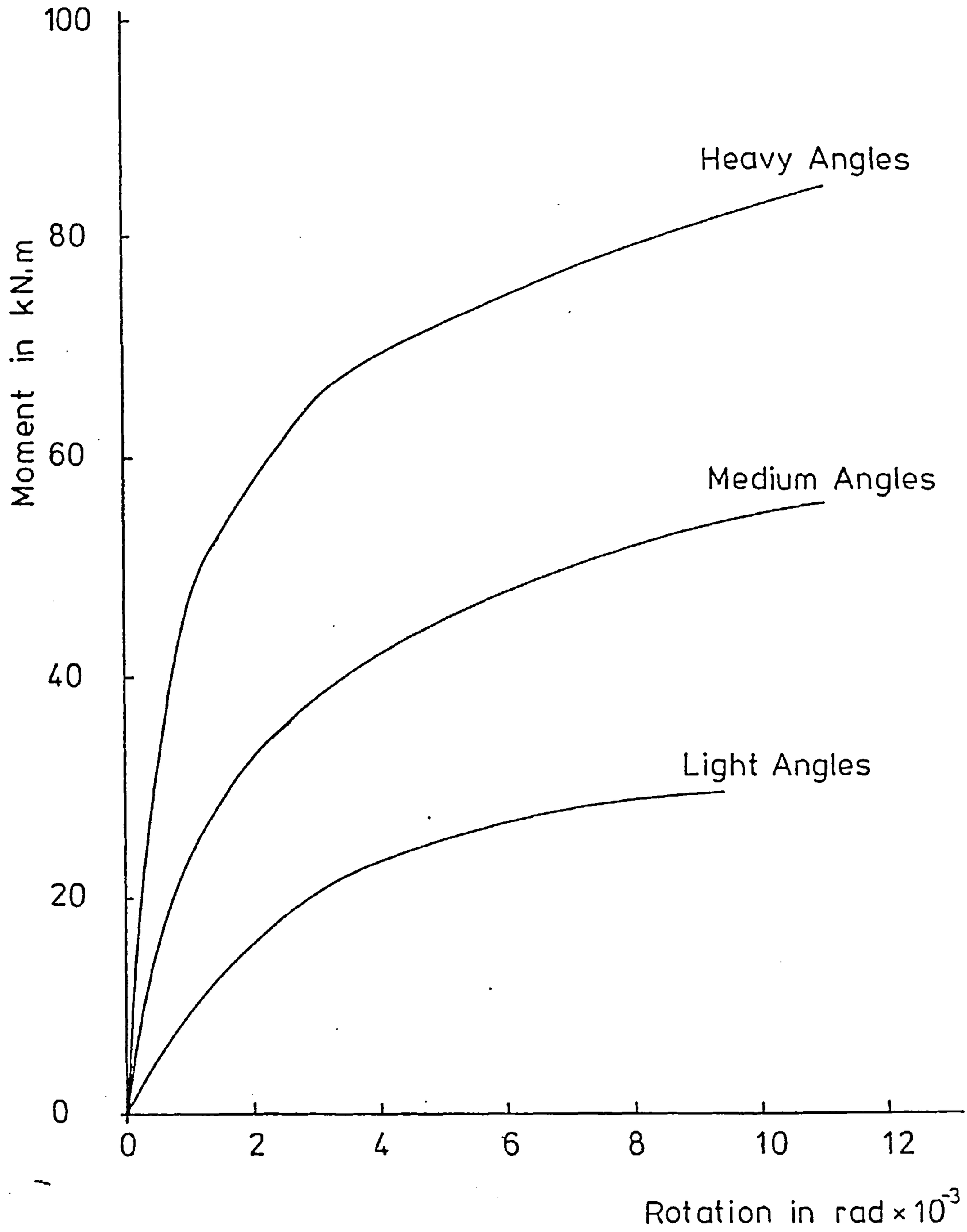

FIGURE 6.16 - Moment-Rotation Curves for Varied Dimension Bolted Flange Cleated Connections

and end plate connections. The resulting column curves for the more rigid connection tests are shown in Figure 6.17. For this more rigid connection type, connection dimensions have the most significant effect on column strength. The effect of the connection stiffness becomes important for all slendernesses greater than 100.

From the above three test series, of different connection types with varying connection dimensions, it can be seen that the influence of connection size becomes more significant as the general connection type stiffness increases.

6.5 Characteristics of the Column Section

6.5.1 Effect of section type

The effect of section type was investigated by considering the behaviour of a universal beam section, in addition to the universal column section used in the basic problem. A 305×127UB48 section with a major axis moment of inertia of 81.37×10^6 mm^4 was used for comparison with the 203×203UC60 used in the basic problem, which has a major axis moment of inertia of 53.83×10^6 mm^4. The universal beam section has a narrow flange shape while the universal column section is fairly square, the major axis moment of inertia is 18.6 times larger than the minor axis moment of inertia for the universal beam while the corresponding value for the universal column is only 2.6. Although the dimensions of the two

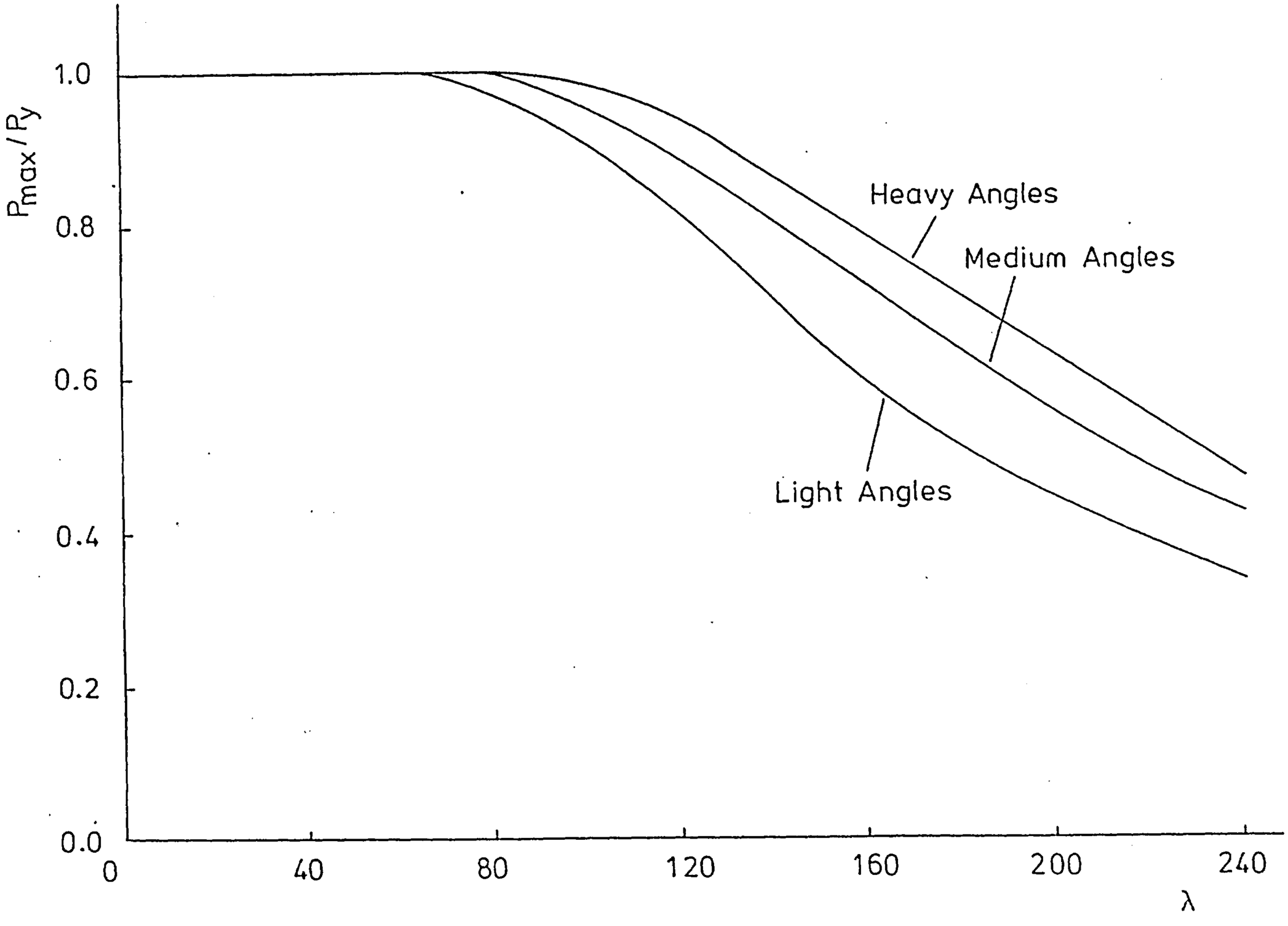

FIGURE 6.17 - Column Curves for Varied Dimension Bolted Flange Cleated Connections

sections are different, the same connection moment-rotation characteristics were applied.

Figure 6.18 shows a comparison of beam and column maximum load capacities over the full slenderness range; these are plotted using non-dimensional axes so that a direct comparison may be made. Up to a slenderness of 140, the two curves are exactly the same. For higher slendernesses the column section becomes slightly stronger, with an almost constant increase in strength of three per cent of P_y. This is due to the connection being relatively more flexible to the stiffer beam section. Despite this difference in load capacity in the higher slenderness range, the effect of different section types is not a significant factor.

Column curves for the same beam cross-section with the main connection types (web cleats, flange cleats and T-stubs) were produced and these are compared with the equivalent curves for the column section (previously shown in Figure 6.7) in Figure 6.19. From this, it can be seen, that agreement is close for beam and column cross-sections with the same end restraint conditions: These curves provide further evidence that the type of column section is not an important factor determining the shapes of column curve produced.

At this point it should be remembered that the analysis, which produced the above column curves,

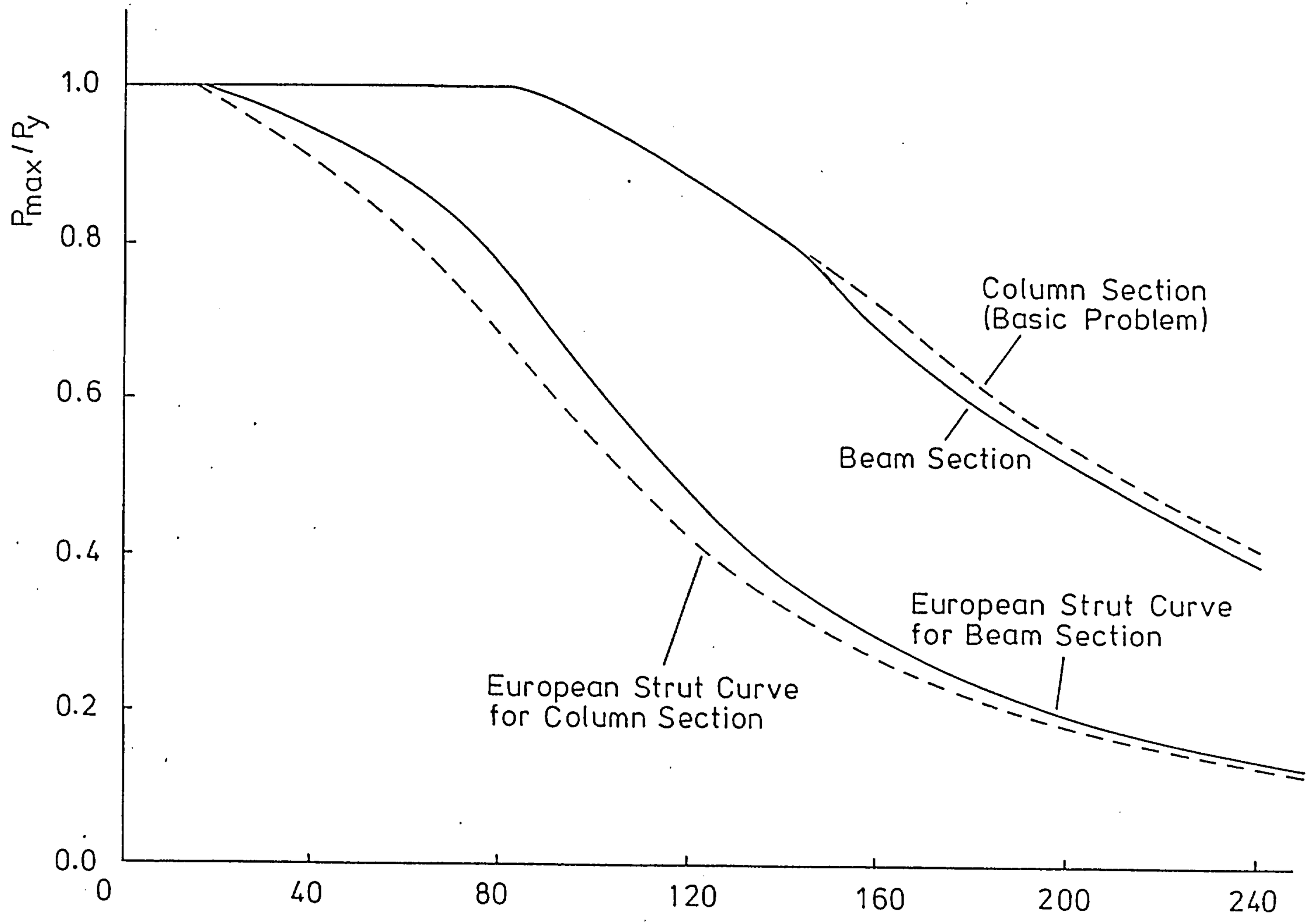

FIGURE 6.18 - Column Curves for the Comparison of Beam and Column Section Strength with Flange Cleated Connections

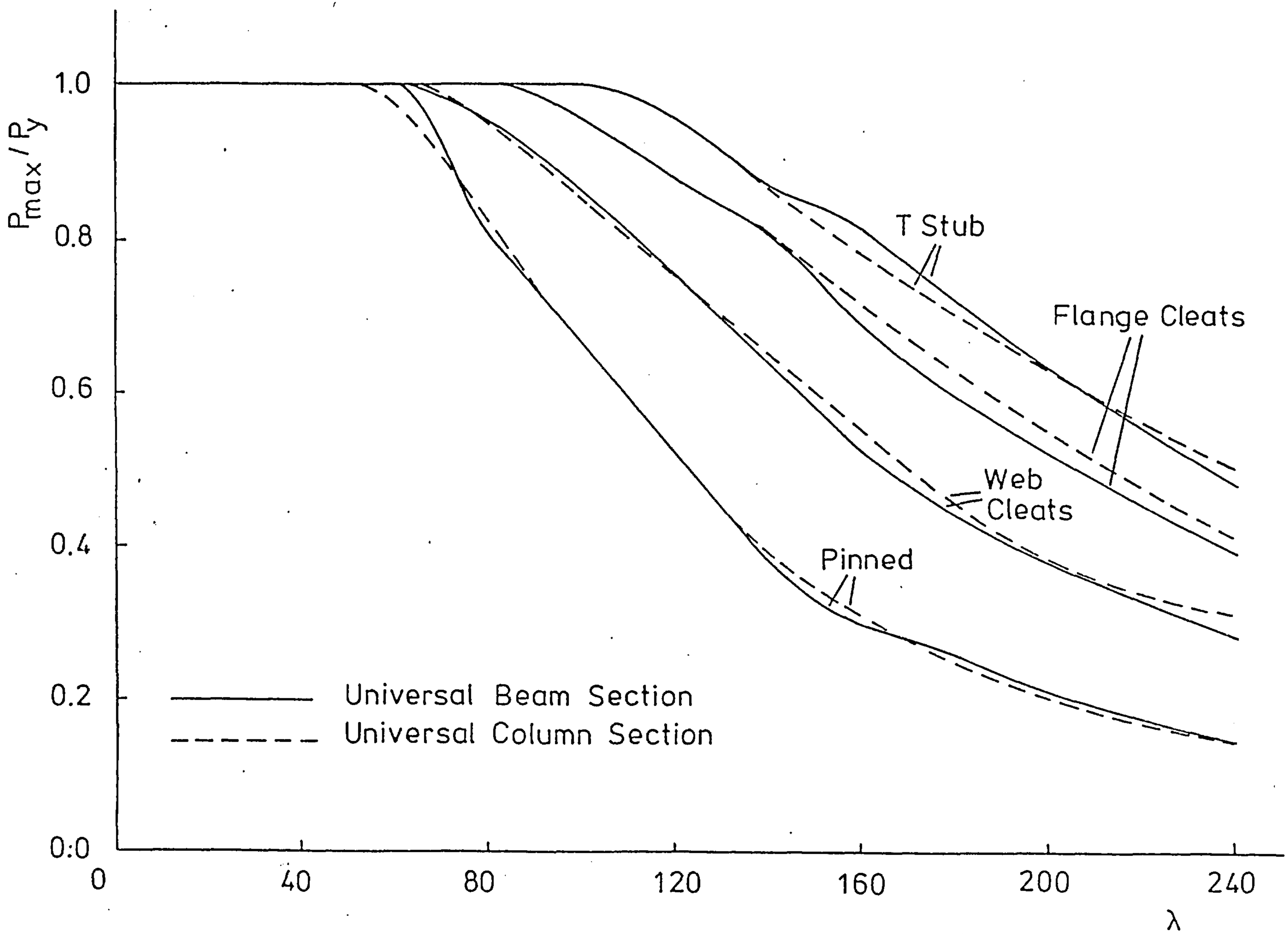

FIGURE 6.19 - Comparison of Column Curves for Beam and Column Sections with the Main Connection Types

considers only the in-plane behaviour of the member. The differences in the ratios of section major and minor bending stiffness suggest that section type would have a more important effect if three-dimensional behaviour was considered.

6.5.2 Effect of section bending axis

To examine the influence of the bending axis of the section on the behaviour of the column, the 203×203UC60 column was also analysed in minor axis bending. This effect is important as, in practice, members are often critical for bending in the plane of their minor axis. The end restraint characteristics for the flange cleated connection used in the basic problem were assumed. The same end connection arrangement is not physically possible due to the different orientation of the column flanges, however, the same end restraint behaviour is assumed for the purpose of comparison.

The results of the minor axis column case are compared with the major axis case in Figure 6.20. These results are plotted as non-dimensional maximum load capacity versus slenderness in the respective plane of bending, to enable direct comparison. For all slendernesses greater than 80 the minor axis column is relatively stronger, with the most significant strength differences occurring in the slenderness range between 80 and 140. This corresponds to the

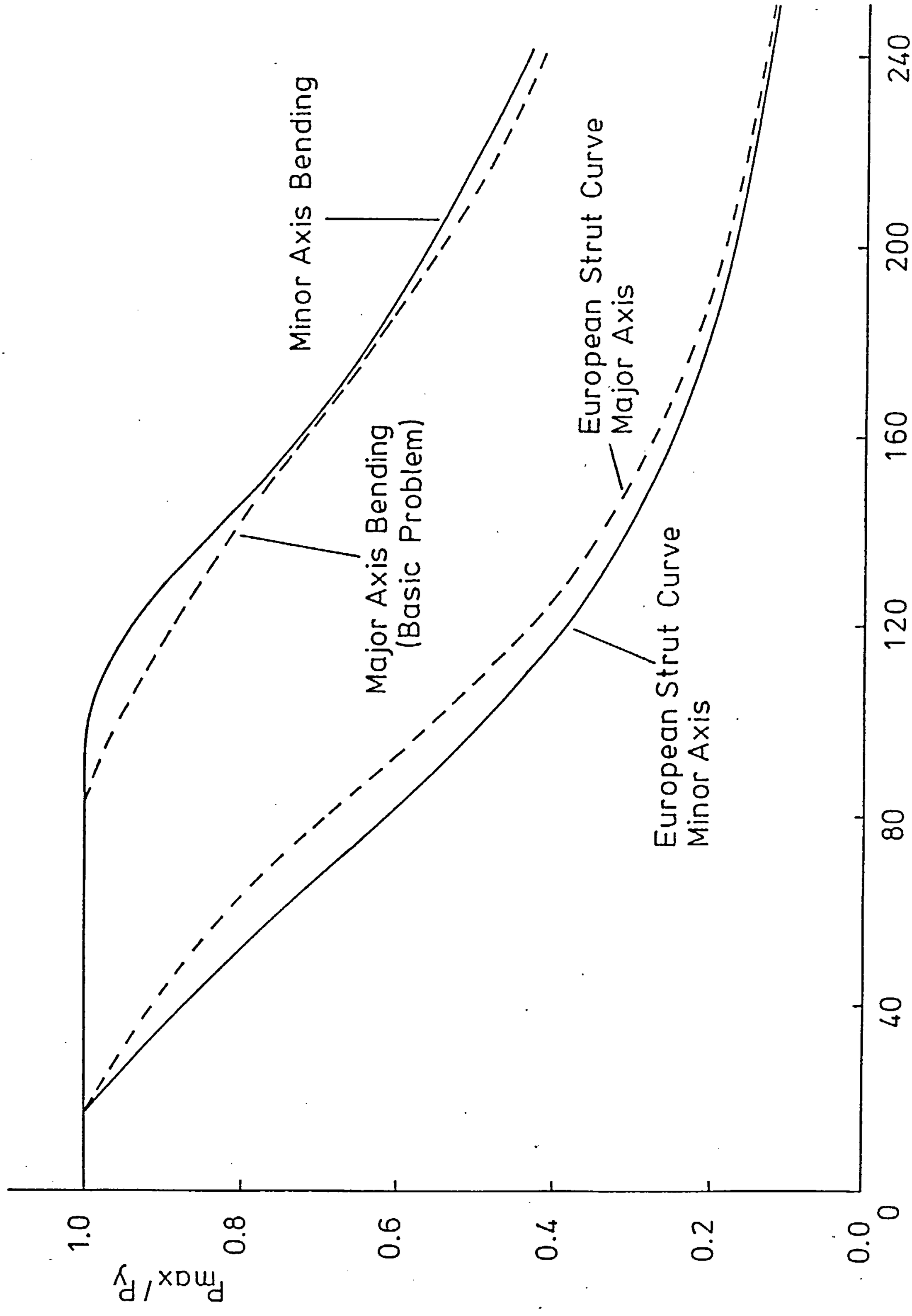

FIGURE 6.20 - Comparison of Column Curves for Major and Minor Axis Column Sections with Flange Cleated Connections

transition range of failure due to material yield and failure due to elastic instability. The greatest difference between the two column curves occurs at a slenderness of 120, where the minor axis column is 18.4 per cent of P_y stronger than the equivalent major axis column. For slenderness ratios greater than 140 the two column curves converge to each other. The column's minor axis moment of inertia is 20.41×10^6 mm^4 which is 2.6 times less than that of the major axis. This means that the end restraint conditions are relatively stiffer in the minor axis case when the same actual connection characteristic is used. This effect produces the stronger minor axis column curve.

Column curves for the minor axis column with end restraint provided by the four main connection types are shown in Figure 6.21. From these curves, it can be seen, that the presence of end restraint is important, however, the stiffness of the connection has a reduced influence on the column strength. The three column curves using the main connection types are nearer in value for the minor axis case than for the major axis case, of Figure 6.7, due to the relative increase in connection stiffness. This fact is more evident from the minor axis universal beam section column curves, Figure 6.22, using the same connection characteristics. Here, both the rigid and flexible connections have a similar effect on member

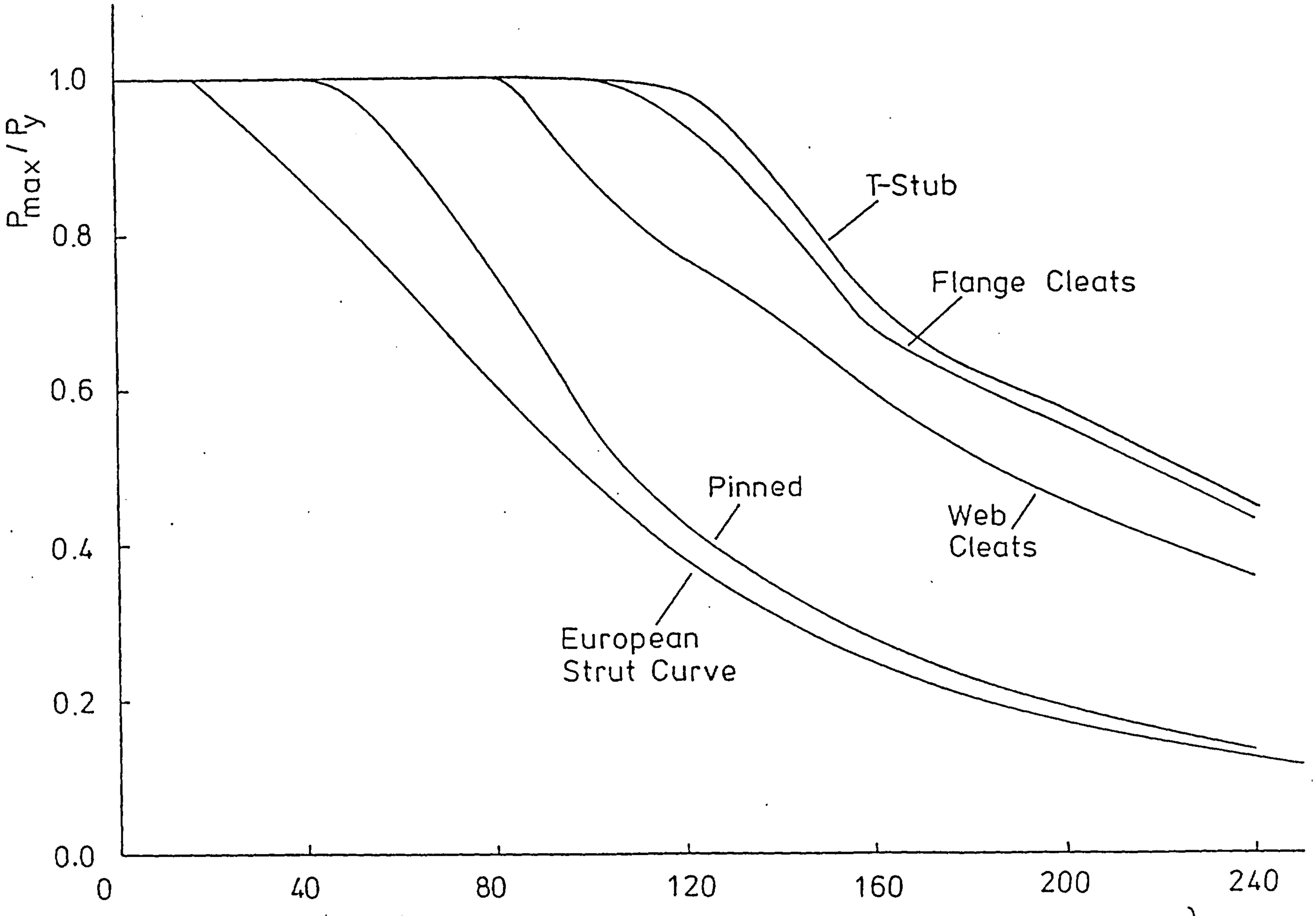

FIGURE 6.21 - Column Curves for Minor Axis Bending Column Section with the Main Connection Types

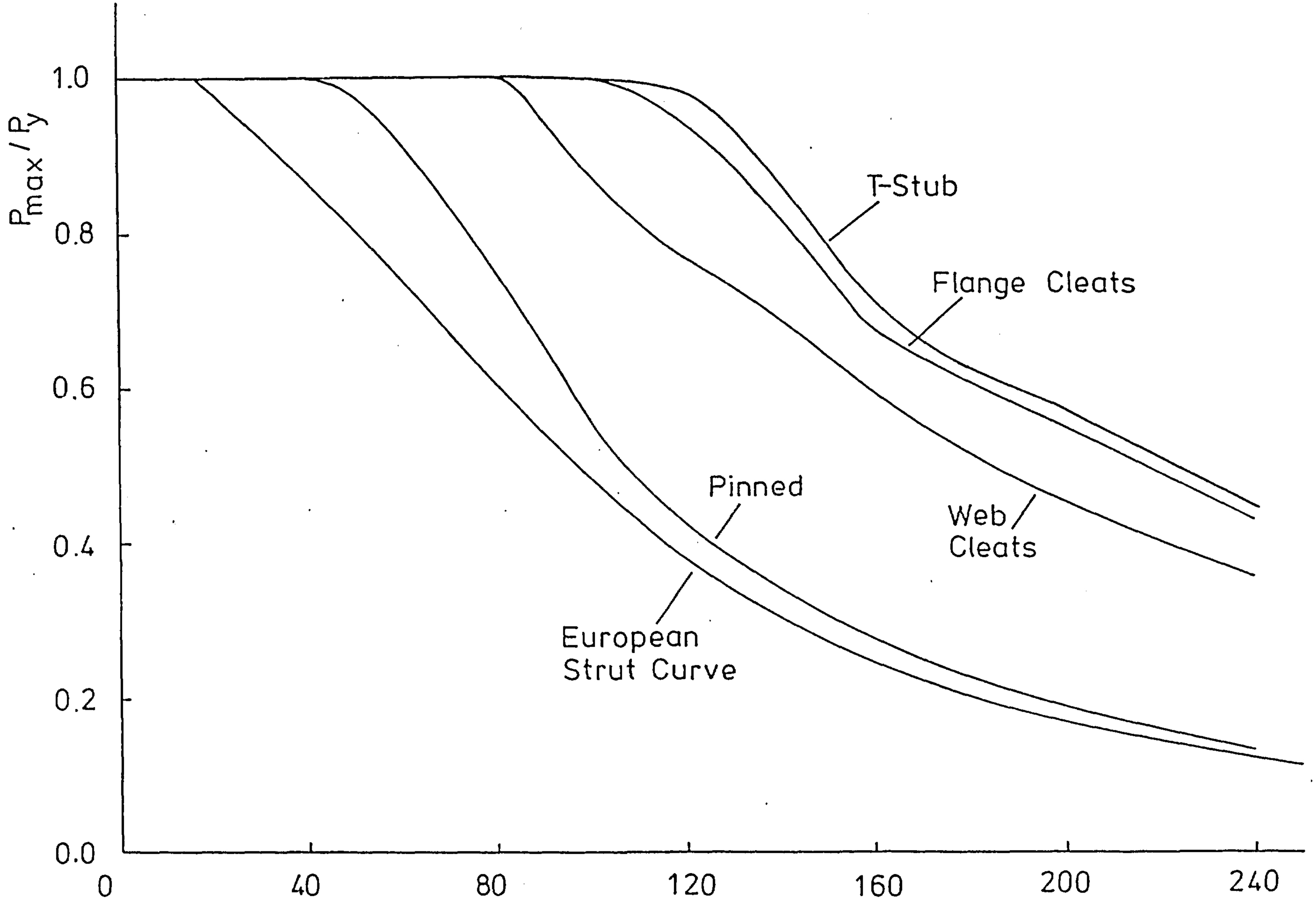

FIGURE 6.21 - Column Curves for Minor Axis Bending Column Section with the Main Connection Types

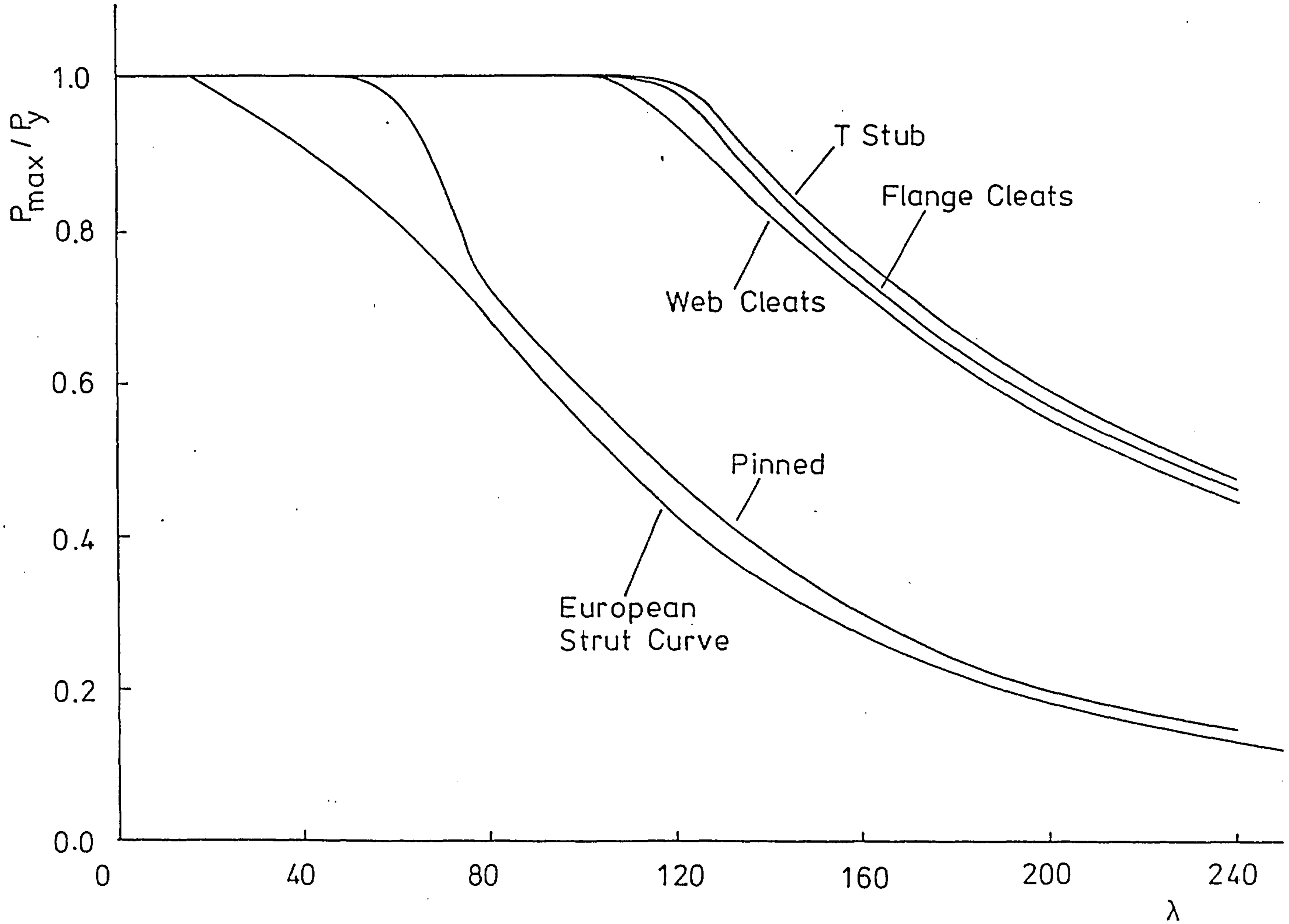

FIGURE 6.22 - Column Curves for Minor Axis Bending Beam Section with the Main Connection Types

behaviour and end restraint stiffness has reduced importance. This is a result of the minor axis beam stiffness being 18.6 times less than the major axis beam stiffness, producing relatively rigid connection characteristics from all connection types.

6.5.3 Effect of section size

To investigate the effect of the column section size, heavy and light universal column sections were compared with the medium column section used in the basic problem. A heavy section, of serial size 305×305UC158 with a moment of inertia of 357.66 × 10^6 mm^4, and a light section, of serial size 152×152UC23 with a moment of inertia 11.04 × 10^6 mm^4, were both assumed to have the same flange cleated connection characteristic as that used in the basic problem. Therefore, the ratio of the bending stiffnesses of the three sections is 6.64I:I:0.21I.

Typical load-deflection curves are shown in Figure 6.23a - c, which are plotted non-dimensionally so that comparison may be made. In all cases, the relative column deformation is reduced for the lighter sections and for the slender columns the lighter sections carry a relatively higher load. The full set of results in the form of column curves is illustrated in Figure 6.24, which shows that the semi-rigid end restraint has a more significant effect

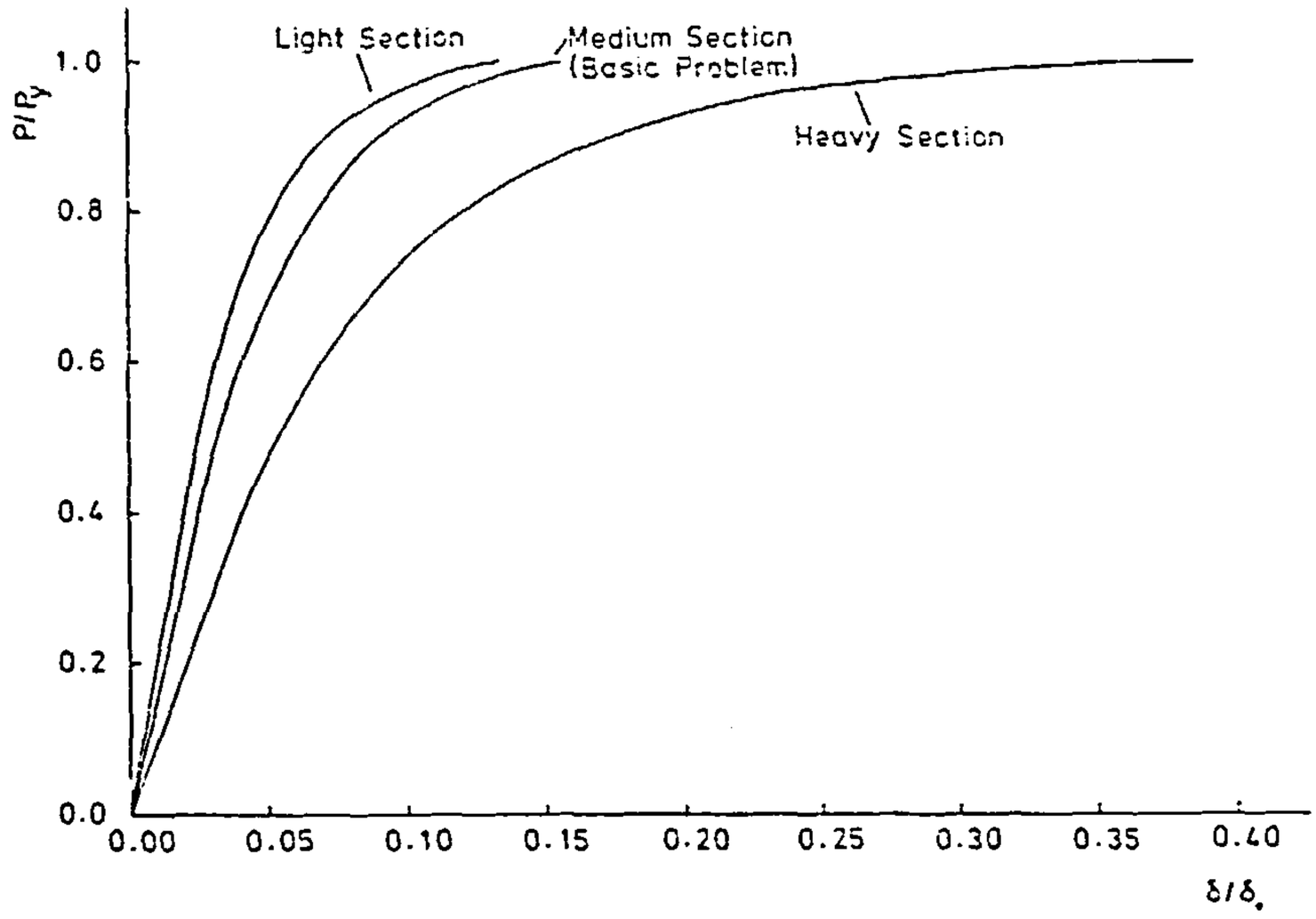

(a) $\dot{\lambda} = 40$

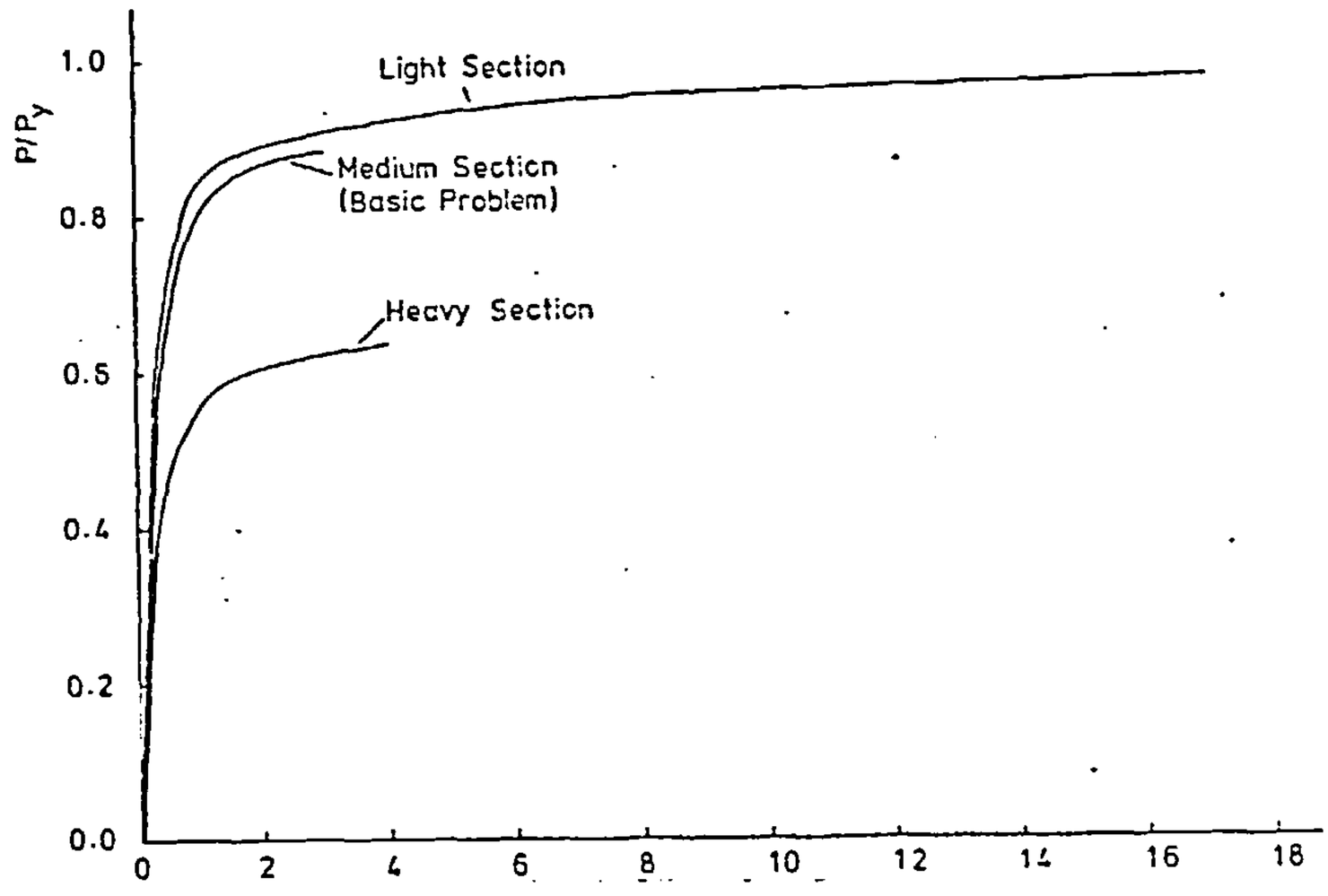

(b) $\lambda = 120$

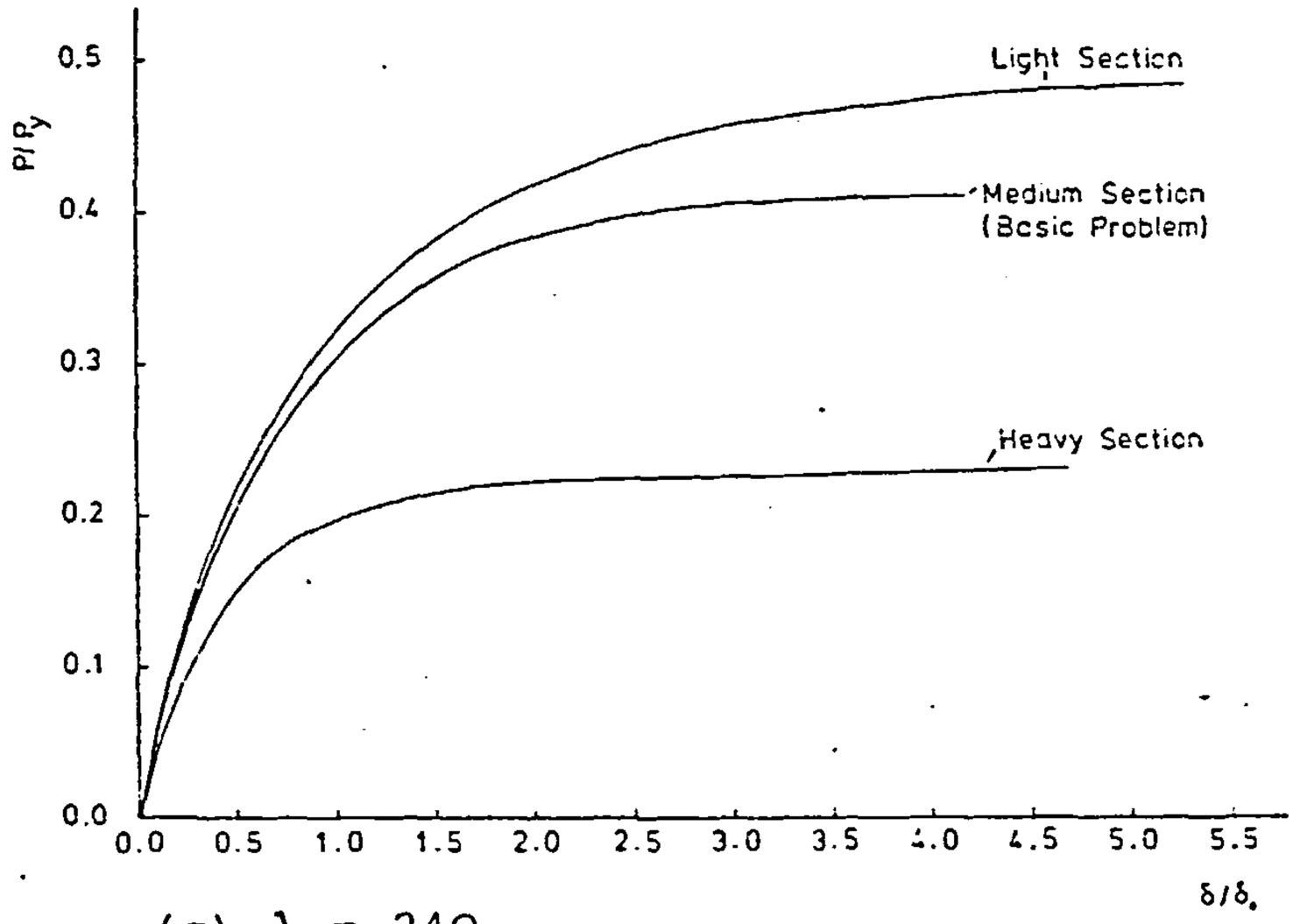

(c) $\lambda = 240$

FIGURE 6.23 - Typical Load-Deflection Curves for different Column Section Sizes

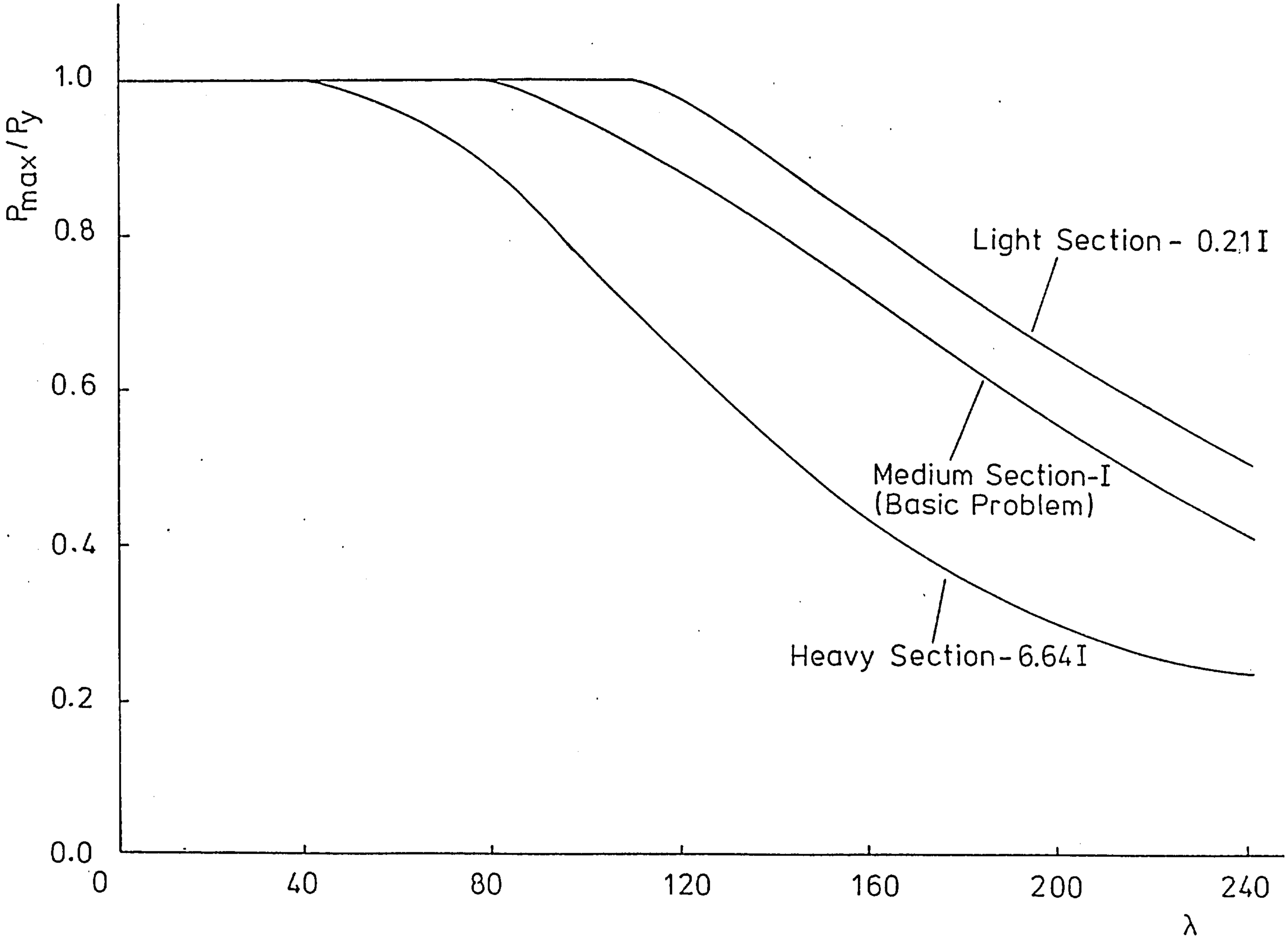

FIGURE 6.24 - Column Curves for different Column Section Sizes

as the section size reduces. Figure 6.24 also shows that lighter sections have greater relative load capacities over the full slenderness range.

The column section becomes relatively stronger as the section size reduces due to the relative increase in connection stiffness. The same connection characteristic is used for all three section sizes, however, resulting connection stiffnesses will be a greater proportion of the member stiffness for lighter sections than for heavier sections. This increases the relative stiffness of the lighter section's connection as compared with the connections of the heavier sections.

6.5.4 Effect of residual stress

Three different residual stress patterns were examined in addition to the parabolic pattern assumed in the basic problem. As an alternative for rolled sections the triangular initial stress pattern proposed by Lehigh University was used. Also used were the initial stresses resulting from welding during the fabrication of made up plate component sections. A discussion of the inclusion of these stress patterns is given in Section 4.7.3. In addition to the three realistic residual stress patterns, the ideal initially stress free condition was also assumed for the purpose of comparison.

The resulting column curves for the tests using flange cleated connection characteristics are shown in Figure 6.25. These results show that residual stresses influence column strength in the range of slendernesses from 80 to 200, outside this range the type of residual stress pattern has little effect. The greatest effect of the initial stress pattern occurs in the slenderness range from 120 to 160, where the column strength is reduced by at least five per cent of P_y for the parabolic stress pattern as compared to the initially stress free condition.

The influence of the type of residual stress pattern is more significant when the more flexible web cleated connection is used in the test instead of the more rigid flange cleated connection. Resulting column curves for the column with web cleated connections are shown in Figure 6.26, from which it can be seen that differing residual stress patterns have virtually no effect on column strength at low and high slenderness ratios. However, for low slenderness values the residual stress type does affect the load at which first yield within the section occurs. In this low slenderness range failure will occur when the section reaches its full squash load, while failure occurs due to elastic instability at high slenderness values. The greatest effect of the residual stress type occurs in the slenderness

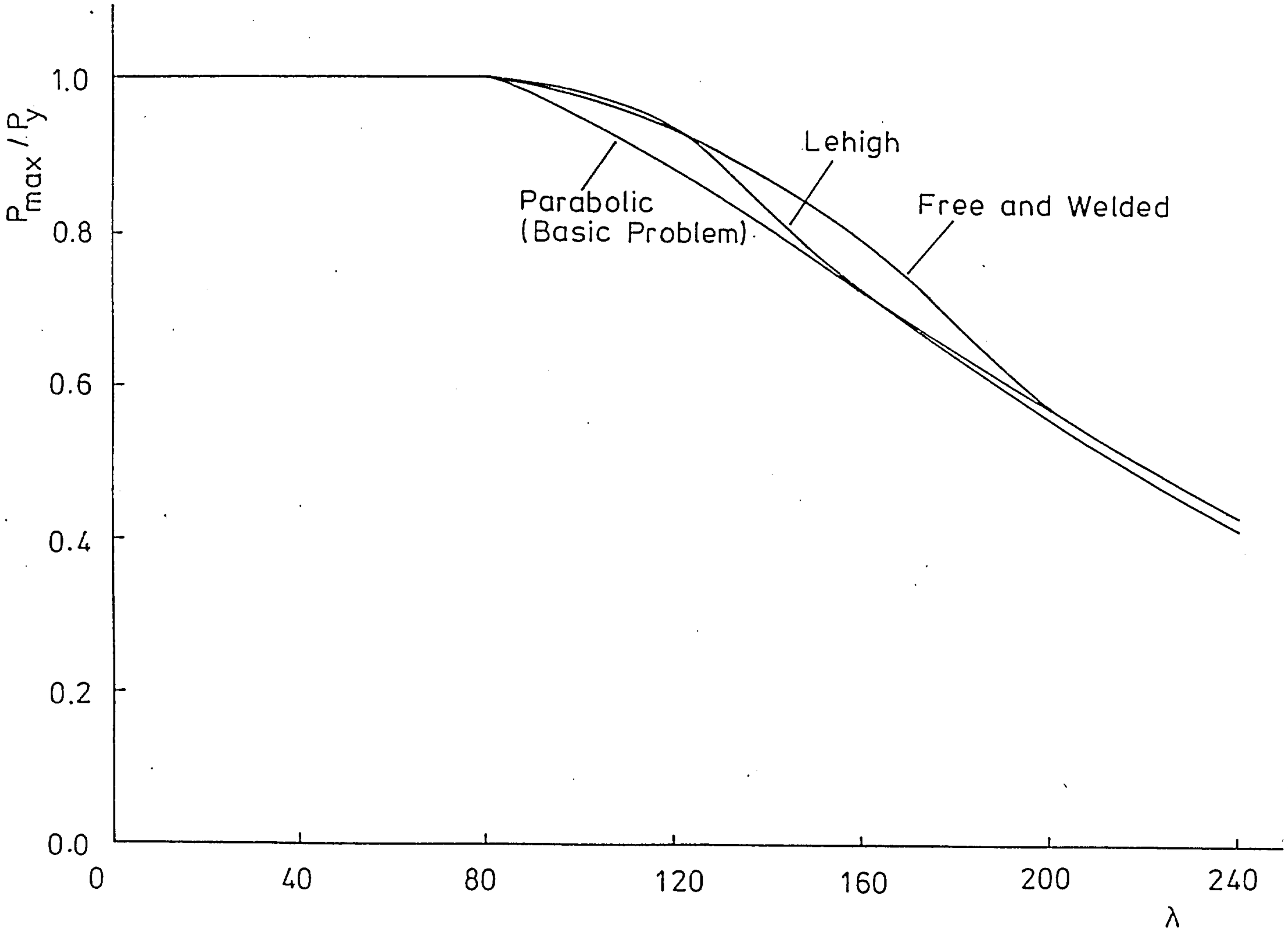

FIGURE 6.25 - Column Curves for different Residual Stress Patterns with Flange Cleated Connections

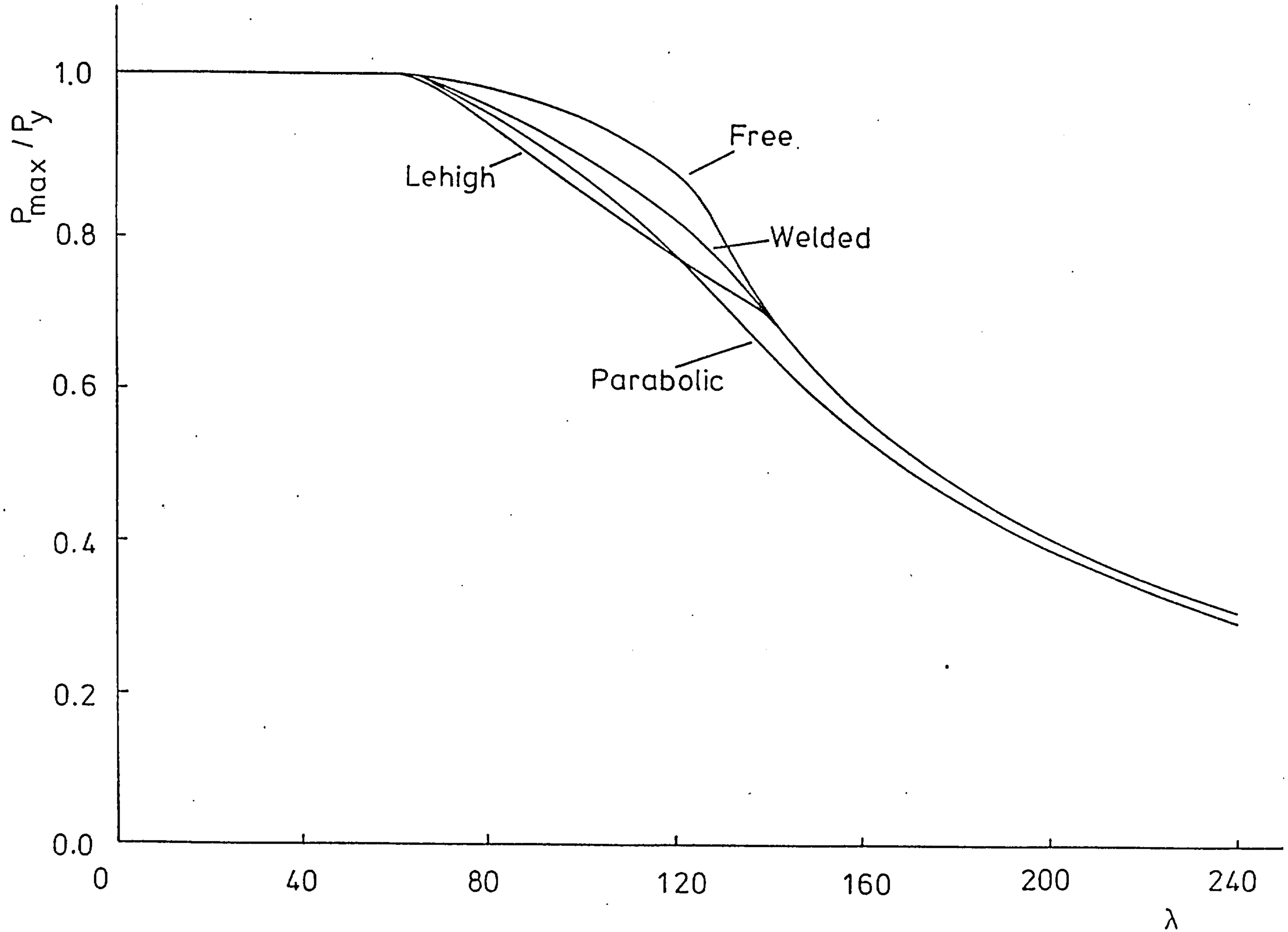

FIGURE 6.26 - Column Curves for different Residual Stress Patterns with Web Cleated Connections

range from 60 to 160. The parabolic stress distribution has the most significant strength reducing effect, with a maximum reduction of twelve per cent of P_y at a slenderness of 120. The effect of the Lehigh stress distribution is slightly less over the full range, while the welded stress distribution has a significantly smaller influence on column strength.

Typical load-deflection curves for the column tests with web cleated connections and the different initial stress patterns are shown in Figures 6.27a - c. At low slenderness values the residual stress type does not affect load capacity, however the column deflections increase with increased initial stress influence, as illustrated in Figure 6.27a for the slenderness value of 40. Load-deflection curves at a slenderness of 120 are shown in Figure 6.27b, which illustrates the strength reducing and deflection increasing effects of the different types of residual stress. The residual stress type has no effect on column deflections until the load level exceeds $0.5P_y$. For all tested slenderness values greater than 160 the load-deflection curves, for the different residual stress types, follow the same path, which is illustrated for a slenderness of 240 in Figure 2.27c.

Additional tests assuming ideal pinned connections and the four different residual stress patterns were also performed, the resulting column curves are shown in Figure 6.28. For the pinned column tests the

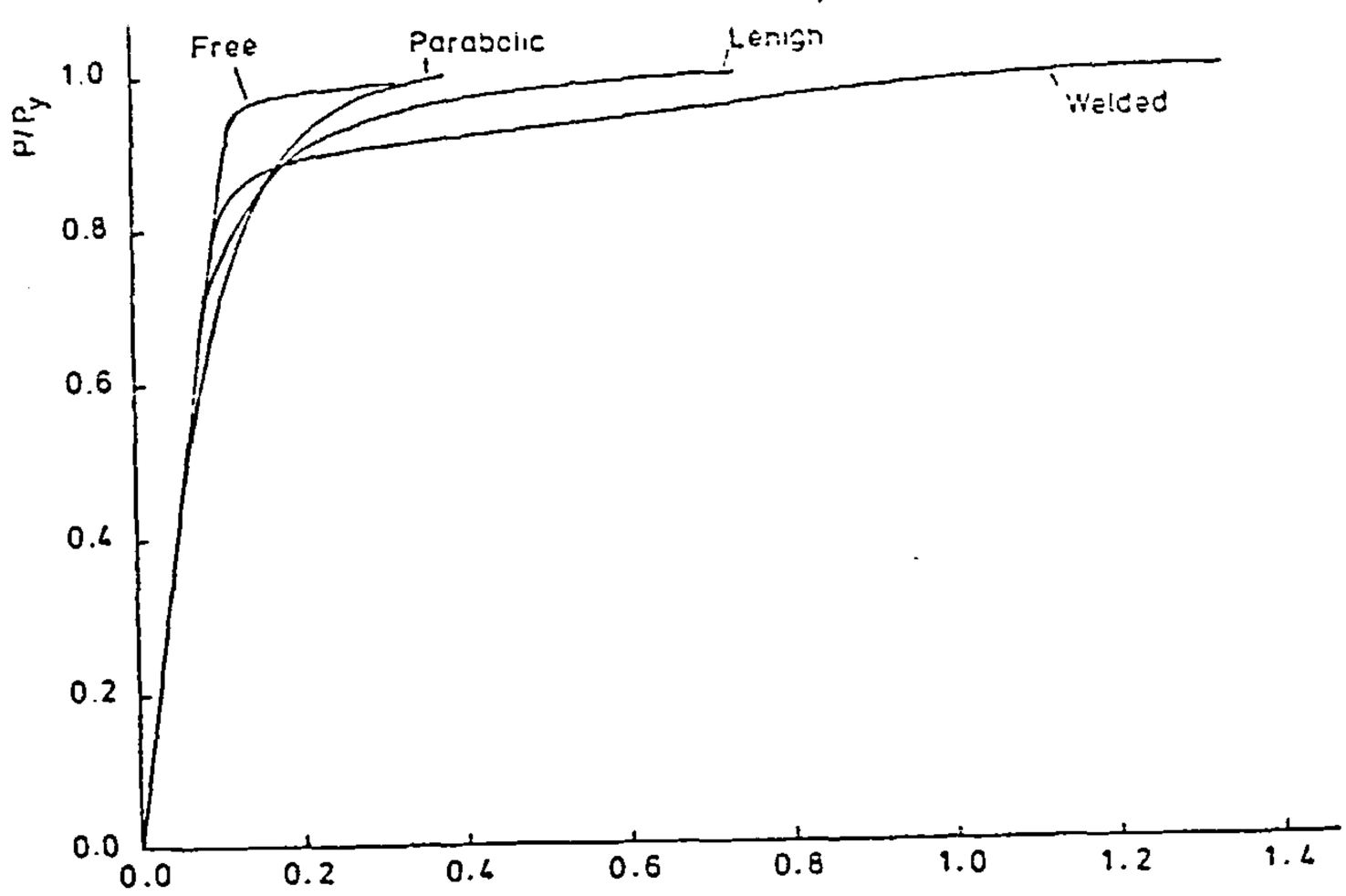

(a) $\lambda = 40$

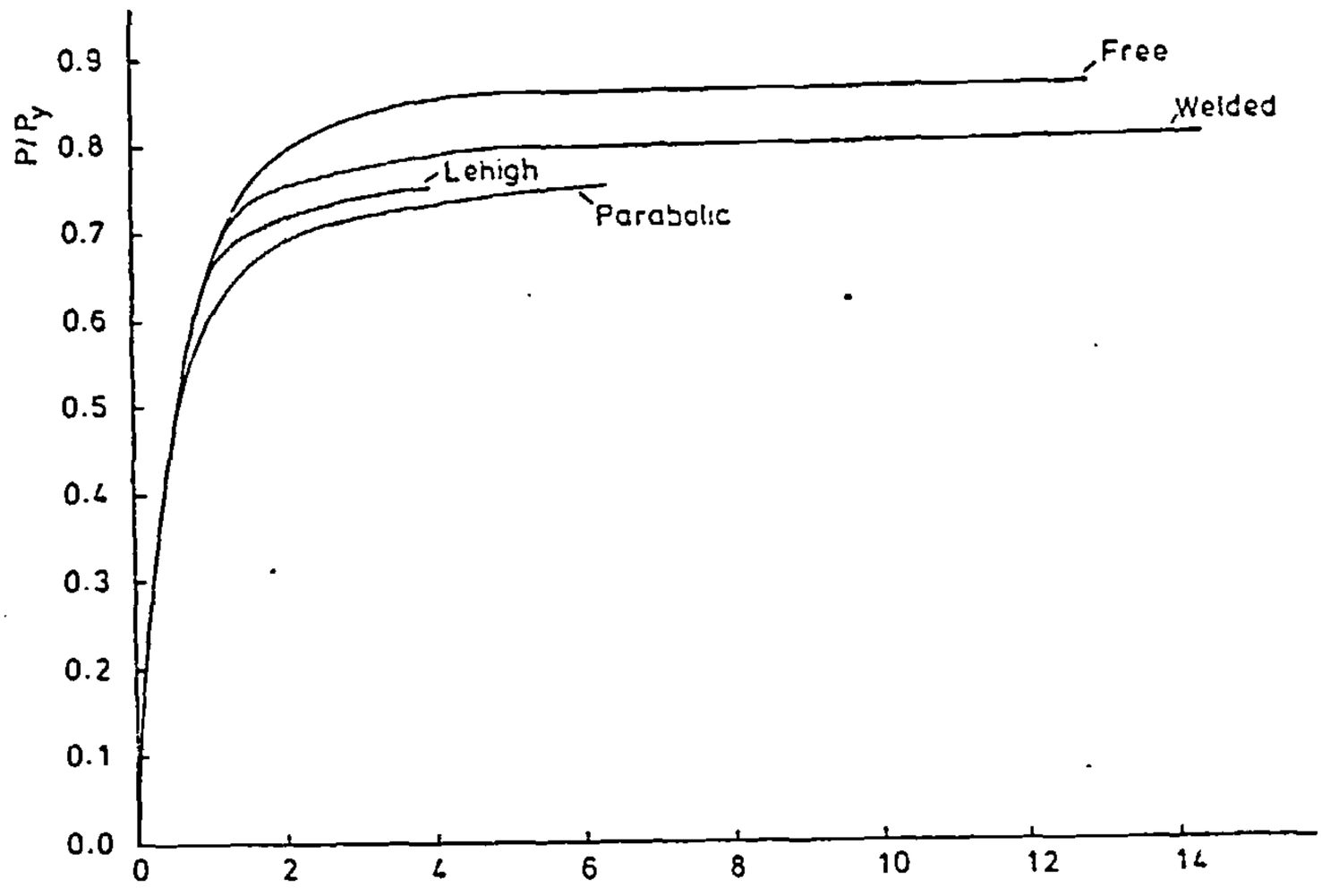

(b) $\lambda = 120$

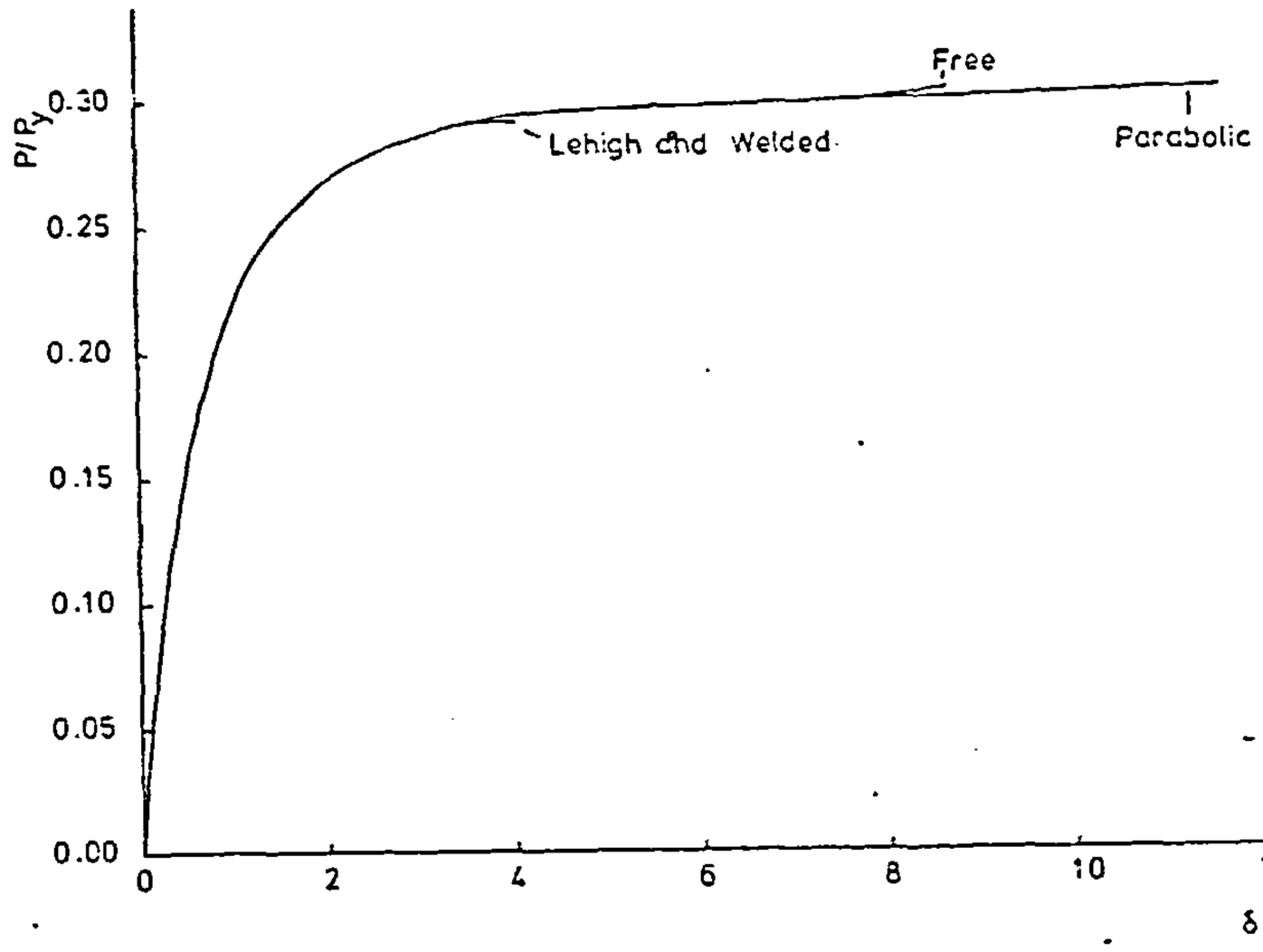

(c) $\lambda = 240$

FIGURE 6.27 - Typical Load-Deflection Curve for different Residual Stress Patterns with Web Cleated Connections

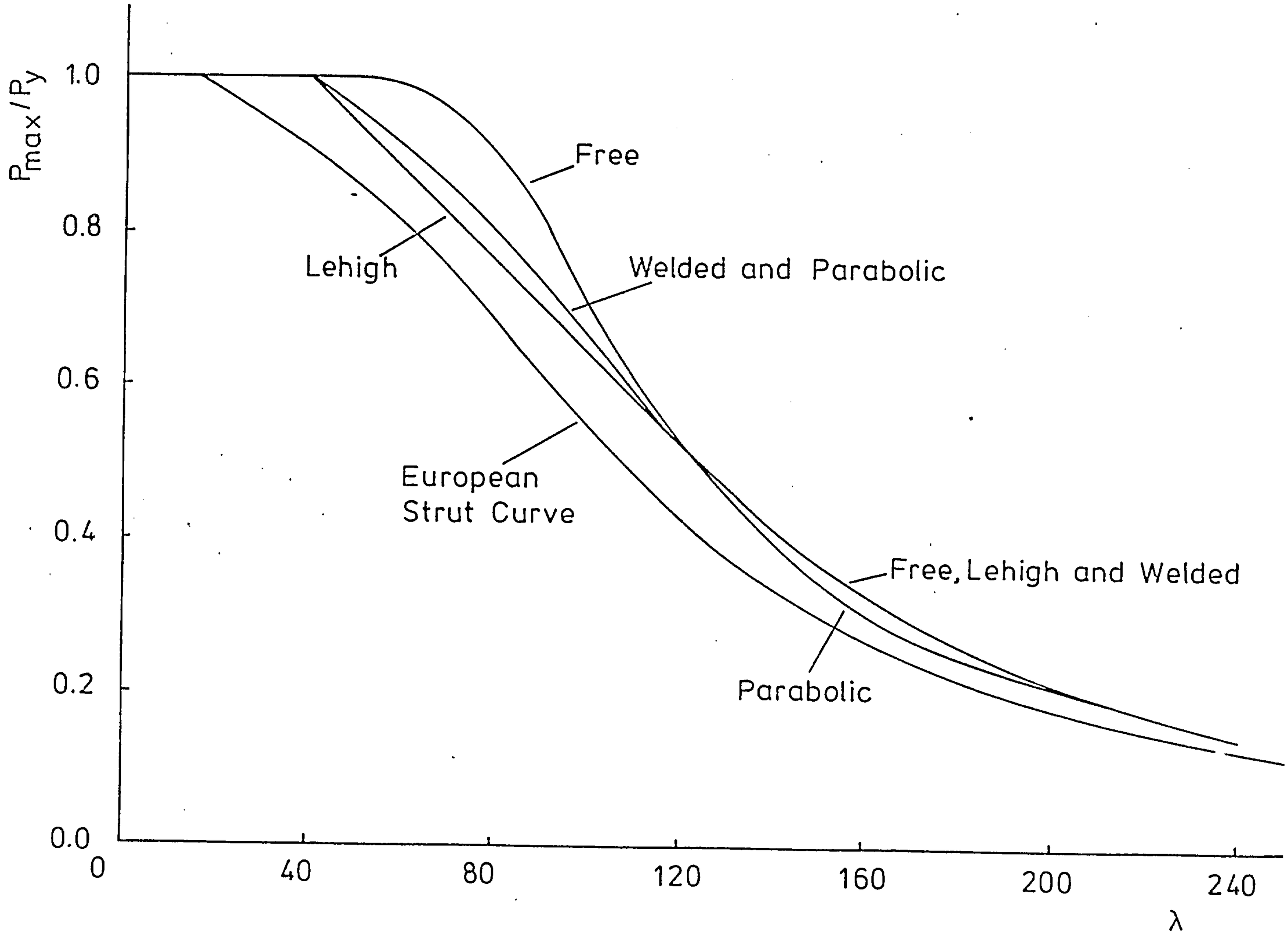

FIGURE 6.28 - Column Curves for different Residual Stress Patterns with Ideal Pinned Connections

residual stress pattern has the greatest influence in the lower slenderness range from 40 to 120, while the influence is small for all higher slenderness values.

It can be seen from Figures 6.25, 6.26 and 6.28, that the influence of residual stress type increases with slenderness as connection stiffness increases. The strength reducing influence of residual stresses has a more significant effect on the higher column slenderness values as the connection stiffness increases. This is due to the increased importance of material yield, along with the reduced significance of geometrical instability, as the end restraint stiffness is increased.

6.6 Characteristics of Geometrical Considerations

6.6.1 Effect of initial out-of-straightness

To investigate the effect of the initial out-of-straightness on the column strength, a series of tests were performed using different values of initial central deflection. In all cases the shape of the initial deflections were assumed to be that of a half sine-wave, with only the size of the initial deflections changing. In addition to the basic problem initial central deflection of L/1000, four other initial values were chosen to be L/5000, L/2000, L/500 and L/250. This range of initial values gives an even spread of initial

out-of-straightness from almost straight (L/5000) to the large imperfection state (L/250).

The results of this series of tests are given in the form of column curves in Figure 6.29. As would be expected, the increase in magnitude of initial out-of-straightness reduces the load carrying capacity of the column. Figure 6.29 shows that differing initial deflections produce parallel column curves, the height of which depends on the size of the initial deflections. The semi-rigid flange cleated connection is used in all tests, which produces column strengths in excess of the European Strut Curve value in all cases.

Typical load-deflection curves are given in Figure 6.30a - c, in which central deflections are non-dimensionalised with respect to the initial central deflection of the basic problem (L/1000). These load-deflection curves show that for all load levels the column deflections increase as the inital deflections increase. This would be expected, due to the reduced geometrical column stiffness caused by axial loads acting through increased lateral deflections off the column centre-line.

6.6.2 Effect of load eccentricity

To investigate the effects of eccentric load on the strength and behaviour of the column, a series of tests were performed with differing values of the end eccentricity of the axial load. In the basic problem the ideal case of zero eccentricity was assumed.

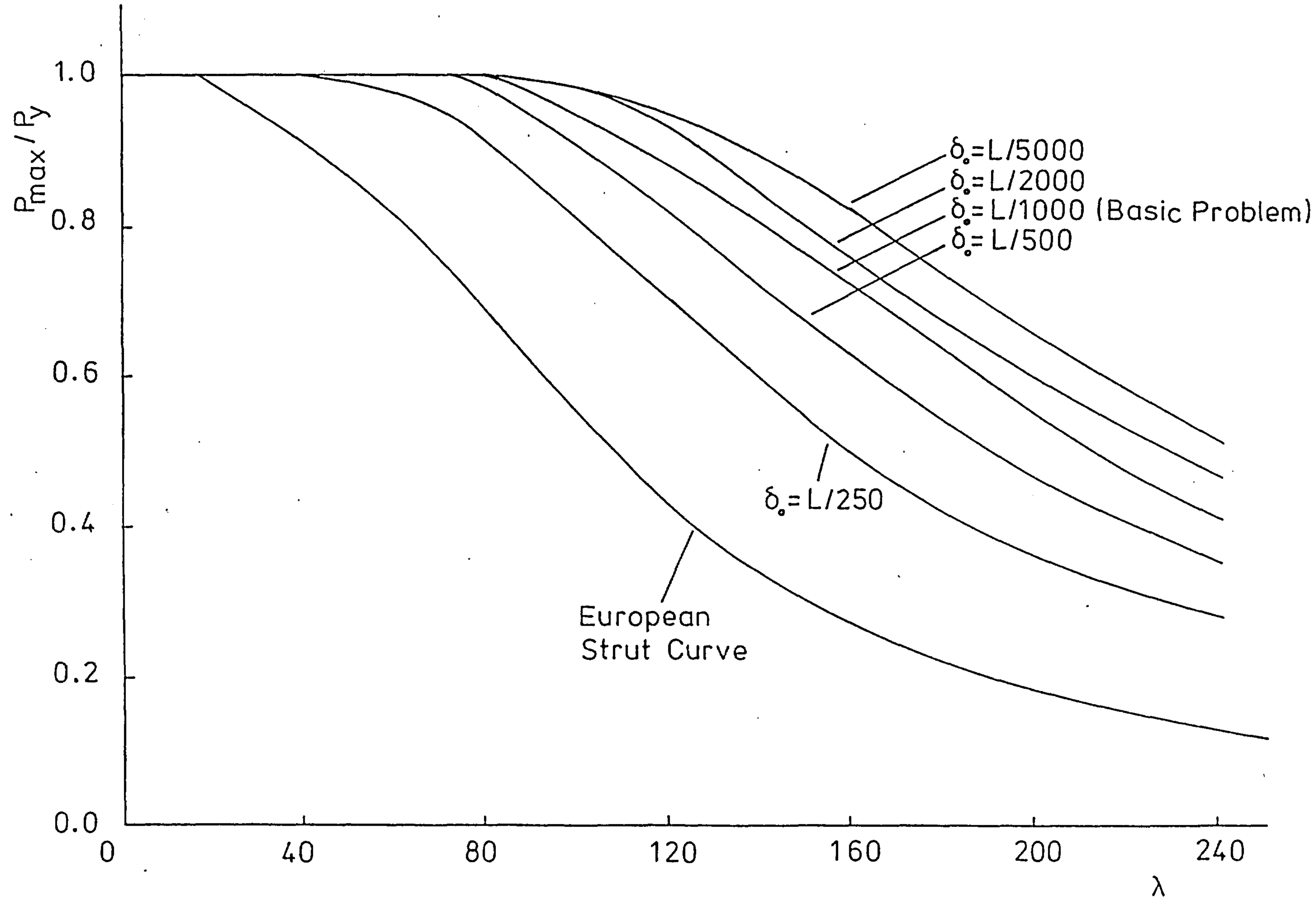

FIGURE 6.29 - Column Curves for different Initial Central Deflections

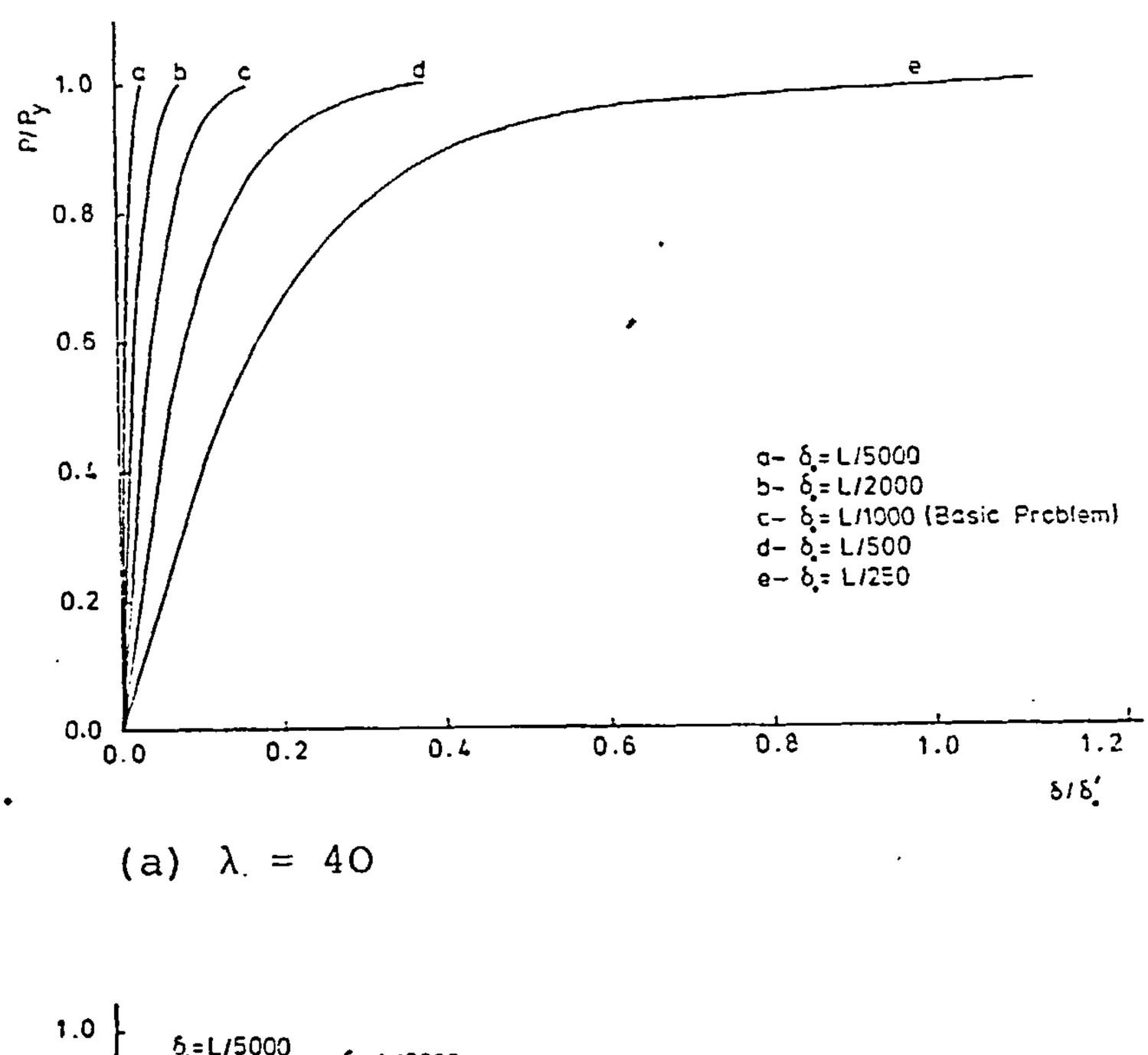

(a) $\lambda = 40$

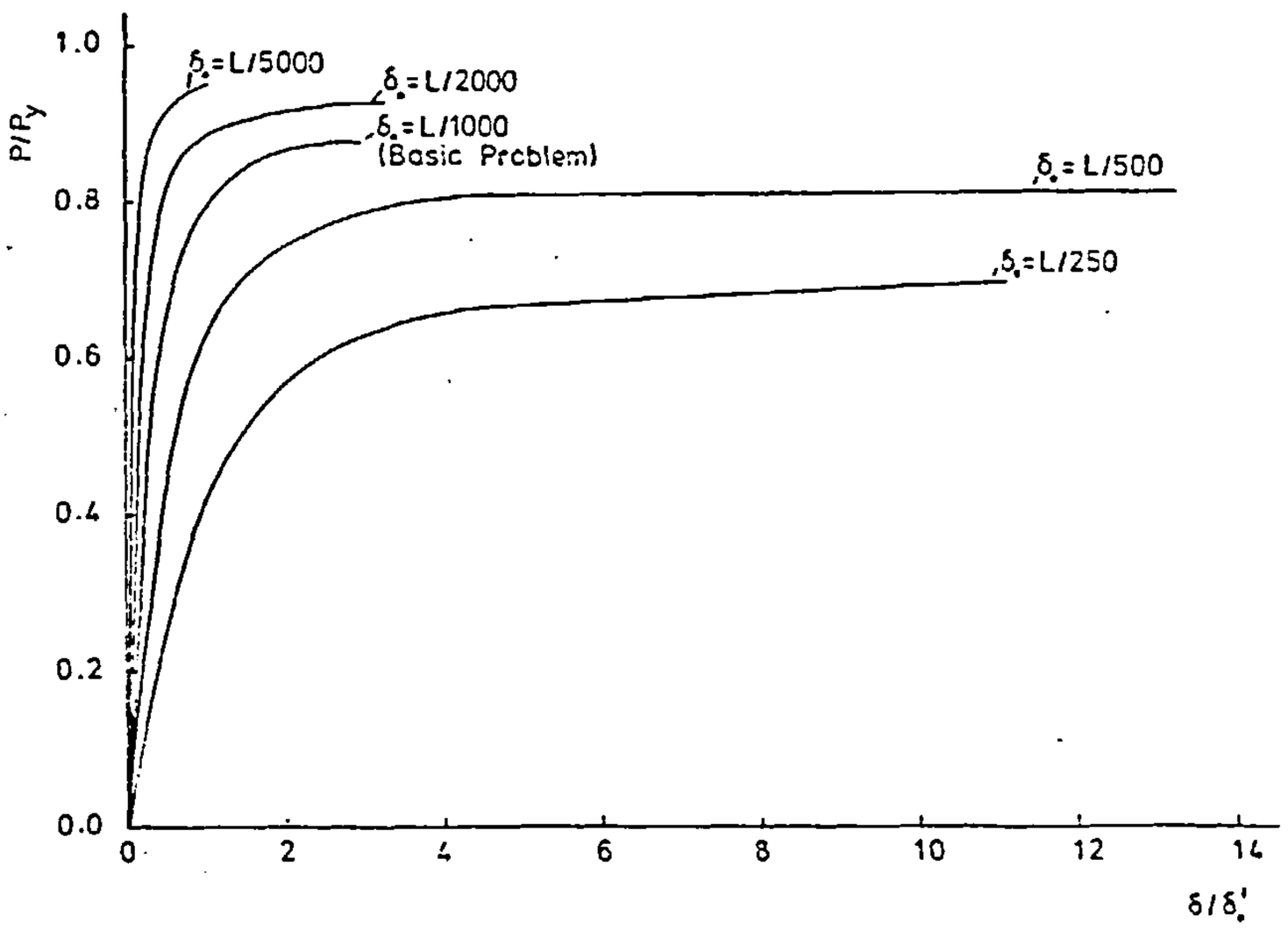

(b) $\lambda = 120$

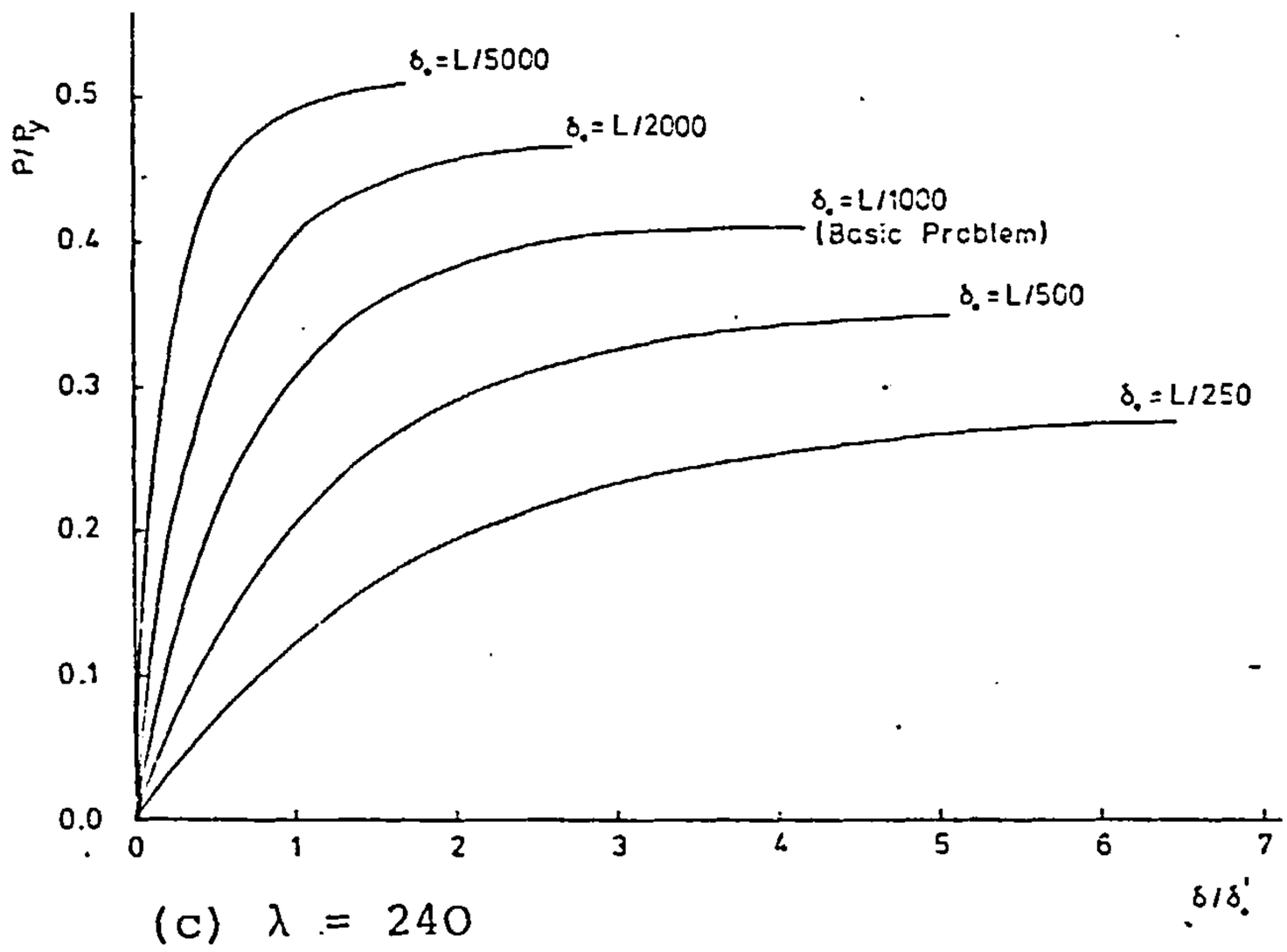

(c) $\lambda = 240$

FIGURE 6.30 - Typical Load-Deflection Curves for different Initial Central Deflections

Additional tests were performed on the flange cleated column with eccentricities equal to 10, 25, 50 and 100 mm.

The resulting column curves, presented in Figure 6.31, show that increasing eccentricity decreases the load carrying capacity of the column over the full slenderness range. The maximum eccentricity assumed reduces the load capacity of the column below the European Strut Curve values in the range of slendernesses from 50 to 105, for the flange cleated end connections. All other test eccentricities produce column strengths that satisfy the European Strut Curve with this end condition, it could be interpolated from Figure 6.31 that with an eccentricity of 79 mm the resulting column curve would just satisfy the European Strut Curve criteria on column strength.

Typical load-deflection curves are given in Figures 6.32a - c, which show that increased eccentricity of load reduces overall column stiffness due to the presence of increased end moment. It can also be seen that for any load level the resulting column deflections are increased with increased load eccentricity. Results also show that an increased eccentricity significantly reduces the column stability, with the instability criteria of failure occurring at lower slenderness values as the eccentricity increases.

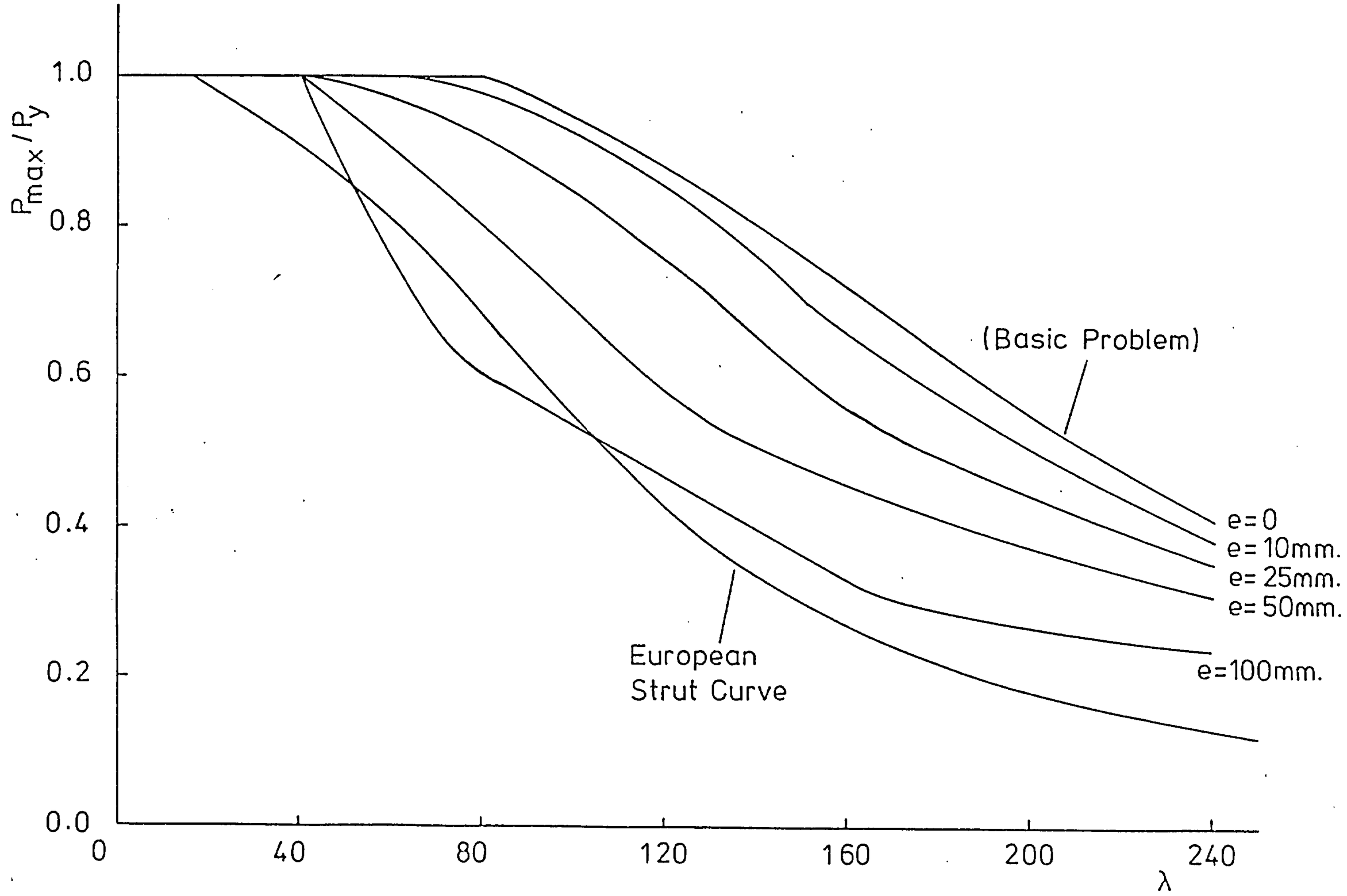

FIGURE 6.31 - Column Curves for different Load Eccentricities

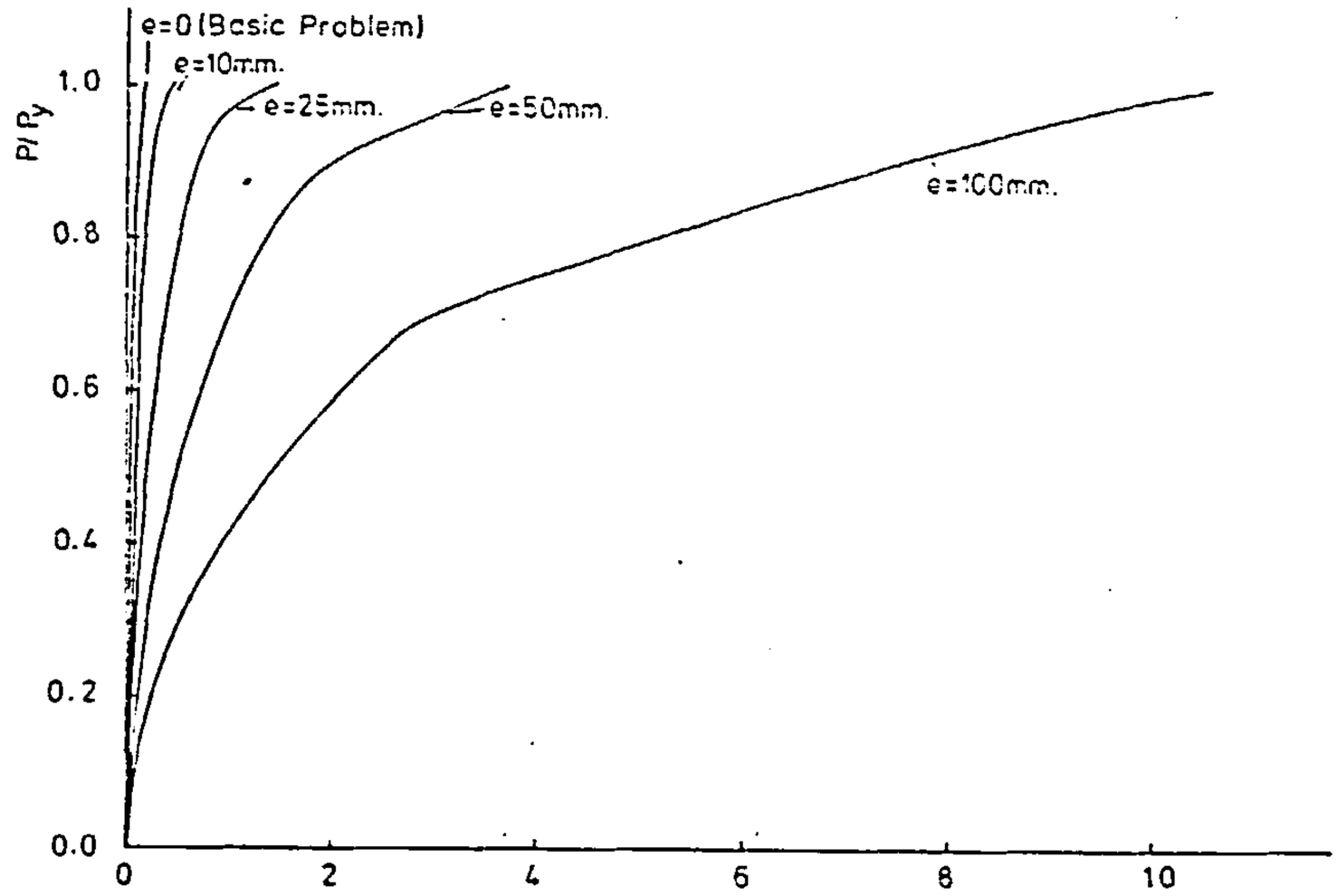

(a) λ = 40

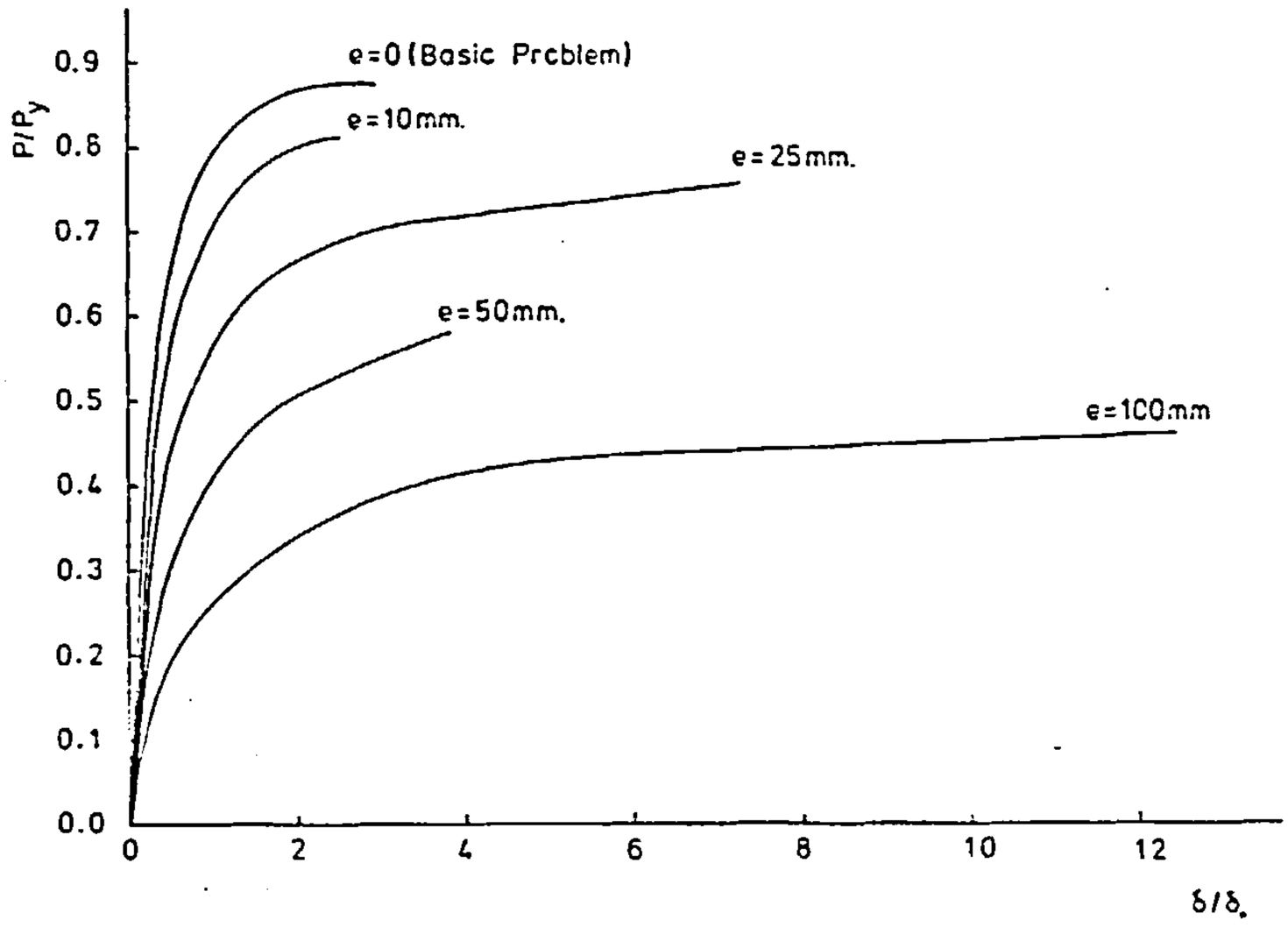

(b) λ = 120

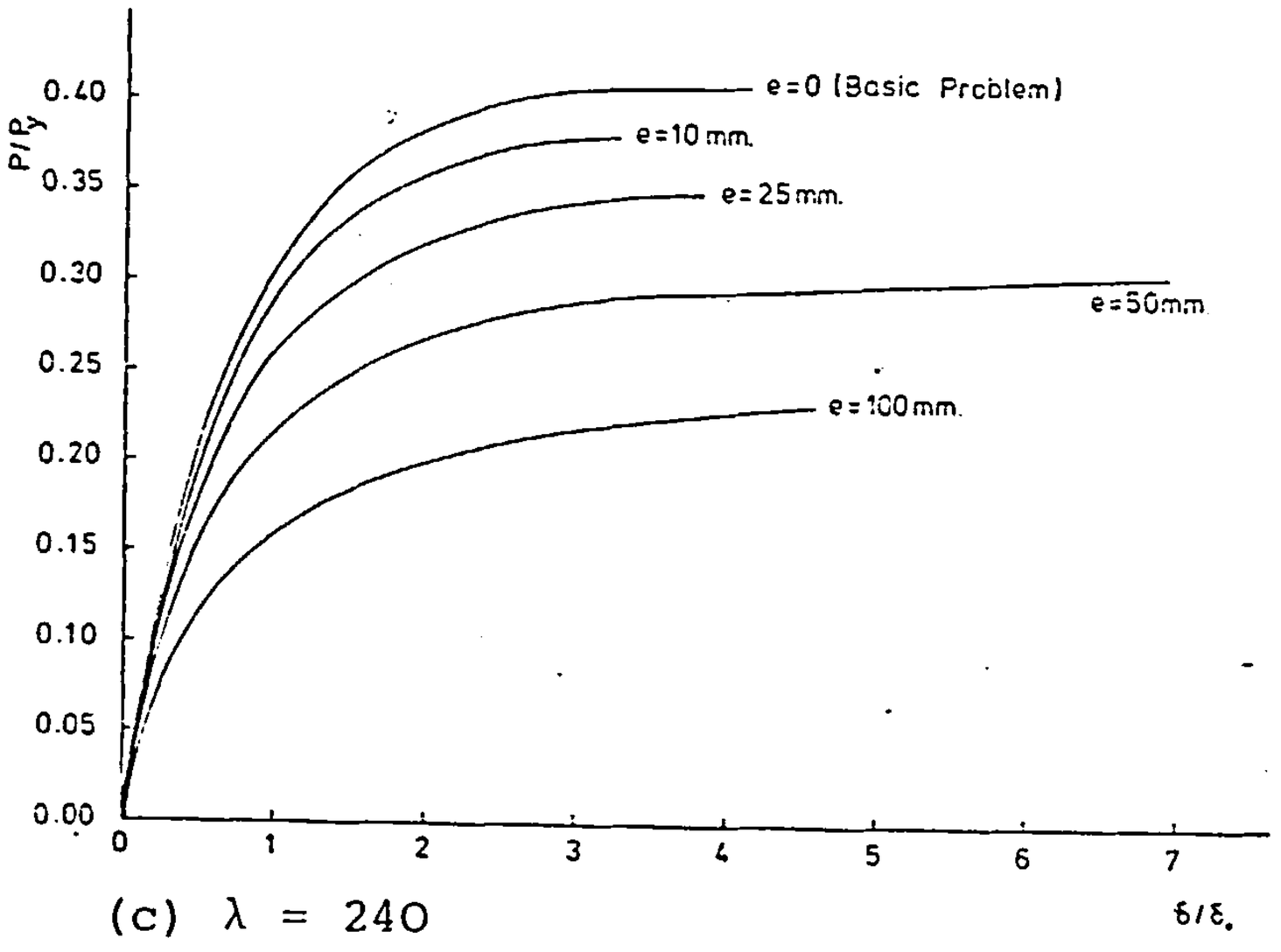

(c) λ = 240

FIGURE 6.32 - Typical Load-Deflection Curves for different Load Eccentricities

A notable feature, of the computer analysis of low slenderness columns with large end eccentricity values, is that excessive computer time was required for the solution. These extended job times are due to yield in the section caused by the large moments that exist in the section which require large numbers of equilibrium iterations to balance the internal and external member forces.

CHAPTER 7

General Discussion and Design Considerations

7.1 General Discussion of Parametric Study Results

A general trend that emerges from the results of the parametric study is the stiffening effect of different types of connection. In all cases an increase in restraint stiffness produces a corresponding reduction in column deflections at any given load level. This is accompanied by an increase in load carrying capacity, except in those cases where the column is so stocky that even when pin-ended it can attain its full squash load. Increased load capacity is developed due to the process of stiffening, resulting from the increased connection stiffness which increases the end restraint. This in turn reduces lateral deflections and so reduces the section's bending strains and stresses. These reduced section stresses delay the start of yield and allow the column to carry increased applied loads before the occurrence of failure, and so the column strength is increased.

Generally, the benefits of increased end restraint become more significant as the column becomes more slender. It was shown in Section 6.2.2 that the end restraint has the greatest effect in the range of slendernesses from 80 to 160. In all cases investigated the reduction in column deflections are illustrated by the typical load-deflection curves, while the increase in column strength over the whole slenderness range is summarised in the calculated column curves.

Variations in column stiffness have been shown to be due to different types of connection or different connection dimensions. Compared to the flange cleated connections used in the basic problem, the web cleated connections are less effective, whilst the end plate and T-stub connections produce stiffer column behaviour. The individual component dimensions of the connection, such as the connecting angle sizes, also influence the column behaviour. Connecting angle sizes influence the stiffness of the connection; this influence being important for the more rigid connection types than for the flexible web cleated connection types.

For any given connection, variation of the column section type, size and bending axis affects the relative stiffness of that connection. For example, a relatively smaller column section would have relatively stiffer connections when results are considered non-dimensionally.

The initial residual stresses present in the column have an appreciable effect on column strength at low slendernesses, while their effect is very small for very slender columns. The different types of residual stress pattern considered herein do not significantly affect column strength.

The effects of initial out-of-straightness and eccentricity of loading were considered in an investigation of geometrical imperfections in the parametric study. The presence of the increased end restraint

provided by the flange cleated connections, as compared to what would be expected for pin-ended cases, reduced the influence of these geometrical imperfections significantly. Variations of these imperfections result in fairly predictable changes in the behaviour of columns; increased out-of-straightness and increased eccentricity of load both reduce load carrying capacity.

7.2 The Effective Length of Columns

The concept of an effective column length is widely used in design as a method of allowing for different types of end conditions, therefore it is particularly instructive to consider the results of the parametric study, dealing with different types of end connections, in this context. The term effective length has been defined in a number of different ways (see for example reference 36). The approach adopted herein is believed to be that most frequently implied in codes of practice. The effective length (or more correctly the effective slenderness ratio) is defined as that length (slenderness) which gives the same strength on the basic column curve for pinned ends as the failure load for the actual column with its actual end restraints. The determination of effective length from this definition is shown by the construction on Figure 7.1 in which a horizontal line is drawn from the restrained column curve until it meets the basic

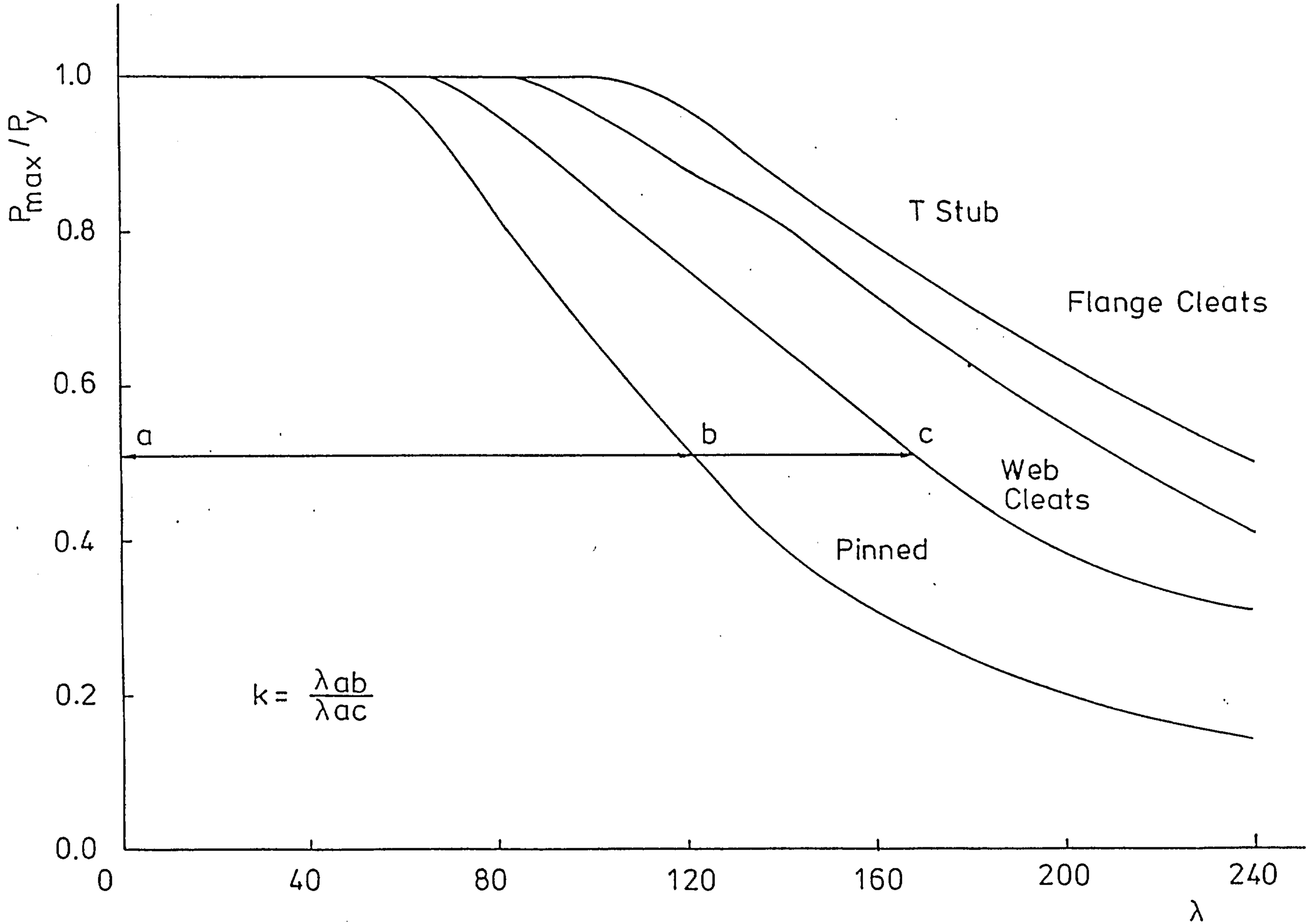

FIGURE 7.1 - Calculation of Effective Length Factors from Column Curves

curve. The effective length factor k is then obtained as the ratio of the pinned slenderness to the restrained column slenderness. It can clearly be seen from Figure 7.1 that, for a given end restraint condition, the effective length factor k need not necessarily be constant over the whole range of slendernesses.

Values of the effective length factor k obtained in this manner using the major axis bending column results with the four basic connection types of Figure 7.1 are given in Table 7.1. The most noticeable feature of these results is their consistency. In each connection case the effective length factor values vary very little over the range of slendernesses considered. The maximum deviation from the average k values occur at the extremes of high and low slendernesses. The consistency of these results is rather surprising since, as has been shown in Chapter 3, connection stiffness decreases with increasing end rotation. This would suggest that slender columns with larger deflections prior to failure might be expected to receive less restraint assistance. However, this effect is counteracted by the reduced significance of column material yield, which reduces the column stiffness in the lower slenderness ranges. This then allows the potentially greater effects of end restraint to be more fully utilised for the higher slenderness ranges.

TABLE 7.1 - Effective Length Factor for Basic Connection Types

MAXIMUM LOAD P/P_y	PINNED CONNECTION		WEB CLEATED CONNECTION		FLANGE CLEATED CONNECTION		T-STUB CONNECTION	
	Slenderness Ratio	Effective Length Factor	Slenderness Ratio	Effective Length Factor	Slenderness Ratio	Effective Length Factor	Slenderness Ratio	Effective Length Factor
0.3	161	1.00	246	0.652	-	-	-	-
0.4	138	1.00	193	0.713	243	0.565	-	-
0.5	123	1.00	170	0.725	208	0.590	237	0.519
0.6	109	1.00	149	0.732	185	0.590	207	0.527
0.7	95	1.00	130	0.736	164	0.581	181	0.528
0.8	80	1.00	110	0.728	142	0.563	155	0.513
0.9	71	1.00	90	0.795	115	0.622	132	0.541

An important feature of the results of Table 7.1 is that the effective length factors are significantly smaller than those generally accepted for design. The average effective length factors for the web cleated, flange cleated and T-stub connections, over the whole slenderness range, are 0.73, 0.59 and 0.52, respectively. These are much lower than the design values specified in codes of practice (1), which are 1.0 for the flexible web cleated connection and 0.7 for the more rigid flange cleated and T-stub connections. These results suggest the possibility of improved economy in column design by the use of lower effective length factors to account for the end restraint actually provided by the real end connections. However, it must be remembered that these results are based on the assumption that the semi-rigid connections are made to beams of infinite stiffness and that the column model is restricted to the no-sway situation. Therefore the calculated effective length factor will be a lower bound of the actual factors.

7.3 Column Stresses

The role of semi-rigid end restraint in reducing column deflections has already been discussed in Section 7.1. As a consequence of this the distribution of column stresses, and hence the spread of yield leading up to collapse, is also affected. The presence of initial residual stresses causes the first yield to

occur early in the loading range, due to the high compressive residual stresses in the flange tips. To study the influence of end restraint on the distribution of internal stresses and the point of first yield, it is better to consider the initially stress free column case.

In the case of the column with ideally pinned connections, yield occurs first at the column's mid-height for all values of slenderness. Failure follows almost immediately in the case of slender columns or after a limited amount of yielding for the more stocky columns. Although the end restraint stiffness of the flexible web cleated connections was insufficient to alter this pattern, their presence did reduce the stresses quite significantly as compared with the equivalent pin-ended case. The more rigid flange cleated and T-stub connections, however, caused first yield to occur more or less simultaneously at the mid-height and at the column ends in the lower slenderness ranges, while first yield was observed at the ends in the medium and higher slenderness ranges. These alterations in the internal stress distributions with increasing restraint stiffness leads to the higher load carrying capacities.

7.4 Comparative Study of Design Procedures

The method of choosing the effective length for a restrained column is very important in the design process. Several different methods of estimating the

effective length factor k are currently available to designers. The experimental results presented by Bergquist (45), together with the calculated results presented in Section 5.4, have been used as the basis for assessing the accuracy of some of these methods. The American W10×29 section of slenderness 189.7 with web cleated connections, as used in Section 5.4, is assumed in the following discussion.

Comparison of both effective length factors and non-dimensional peak loads, as determined by the various methods, are given in Table 7.2. All peak loads have been calculated using the SSRC column strength curve '2' (33) using the effective length factors determined by each method, with the exception of Bergquist's experimental peak load which is quoted directly. The design calculations producing the values of Table 7.2 are given in Appendix B. Existing American (2), British (1) and draft British (4) codes would require this column, with its flexible end restraint, to be designed as pin-ended with a maximum load capacity of 0.156 P_y which underestimates the actual load capacity by 37 per cent. This clearly indicates the possible improved economy of design that could be achieved, even if only the end restraint due to flexible connections were incorporated. One possibility might be to use reduced effective length factors.

TABLE 7.2 - Effective Length Factors and Peak Column Loads

Method of Determination	Effective Length Factor	$\frac{\text{Peak Load}}{\text{Squash Load}}$
Bergquist test result (45)	-	0.247
Calculated by author	0.747	0.253
SSRC - Rigid jointed (33)	0.645	0.315
SSRC - Pin jointed (33)	1.000	0.156
BS449: 1969 (1)	1.000	0.156
De Falco and Marino (34)*	0.660	0.305
Bergquist connection data (45)*	0.690	0.286
Peterson and Cermak (84)*	0.725	0.265

N.B. References marked by * refer to the source of the flexibility factor Z, which is used with Driscoll's alignment chart (35) and the SSRC nomograph (33).

Table 7.2 includes three methods modifying the normal SSRC alighment chart method, by the inclusion of a connection flexibility factor Z when the relative column stiffnesses are determined. These flexibility factors use the linear moment-rotation models which overestimate connection stiffness and become increasingly inaccurate as column end rotations increase. For this reason, these modified methods overestimate the peak load capacity by between seven and twenty-three per cent. This contrasts with the load calculated by the analytical program, with accurate allowance for the variable end restraint, which differs from the experimental value by less than 2.5 per cent. This calculated peak load is found using an effective length factor, calculated using the method described in Section 7.2, in conjunction with the SSRC nomograph.

CHAPTER 8

Conclusions

8.1 Summary

A review has been made of methods of incorporating semi-rigid end restraint into conventional methods of indeterminate frame analysis. This includes the treatment of frame stability and effective lengths. Reference is made to the important investigations into this subject.

An extensive review of the available connection moment-rotation data has been compiled. These moment-rotation data are available for several types of connection. However, the majority of these data are for outdated construction techniques. They also relate to column major axis bending, despite the fact that in practice column minor axis buckling is normally more critical.

The moment-rotation relationships were originally modelled by linear or bilinear functions although, more recently, curve fitting techniques have been used. End restraint models of experimental data using polynomial curve fits have been shown to be unsatisfactory. A more satisfactory method of representing connection behaviour using cubic B-spline curve fitting techniques has been proposed.

An analytical procedure has been developed to investigate the influence of "realistic" semi-rigid end restraint on the strength and behaviour of "real" steel columns. The analysis of the load-deflection behaviour, up to the maximum load level, is achieved

by means of an incremental finite element program. The effects of initial out-of-straightness, spread of material yield, initial residual stresses and eccentricity of loading are all included in the analysis. The influence of the end restraint is accounted for by modifying the appropriate terms in the overall stiffness matrix.

The validity of the developed program is verified by means of comparison with the experimental data reported by Bergquist (45). Agreement between the experimental and calculated results is shown to be acceptable, with the calculated maximum load overestimating the experimental failure load by less than ten per cent. It is recognised that this verification is based on a limited comparison, but no other data is available which reports both the column behaviour and the moment-rotation characteristics of the attached connections.

8.2 Observations of the Parametric Study

The following conclusions, based on the results of the parametric study, illustrate the important factors influencing the behaviour of columns with semi-rigid end restraint.

1) An increase in connection stiffness produces a corresponding reduction in column deflections at any given load level.

2) Increased connection stiffness considerably increases the column's maximum load capacity above the value that it would normally be designed to carry, except in those cases where the column is so stocky that even when pin-ended it can attain its full squash load.

3) The influence of the end restraint becomes more significant for slendernesses greater than 80.

4) The stiffness of the end restraint is dependent on the type of connection being used. Web cleated connections generally produce relatively flexible restraint, while the restraint provided by the T-stub connection is much greater. The more rigid connection types have a more significant effect on the column strength.

5) The connection stiffness also increases with an increase in the component dimensions of the connection. Moreover, the influence of connection size becomes more significant as the general connection stiffness increases.

6) The effects of different types of column section, whether universal columns or universal beams, is not an important factor. However, this seems likely to be a much more important effect if three-dimensional behaviour were being considered.

7) In the case of bending about the minor axis of the column, the end restraint conditions are relatively stiffer than for major axis bending when the same connection characteristic is used. Both rigid and flexible connections have a similar effect on minor axis behaviour due to minor axis member flexural stiffness being so much less than the major axis flexural stiffness. This means that relatively rigid connection characteristics exist for all types of connection.

8) Column sections become relatively stronger as section size reduces, when the same connection characteristic is used, due to the relative increase in connection stiffness.

9) The influence of the initial residual stress pattern is more significant with the more flexible connection types. The greatest effect of the residual stress type occurs in the slenderness range from 60 to 160. Outside this range there is little effect on column strength. However, at low slendernesses the residual stress levels do affect the load at which first yield within the section occurs.

10) Increased initial deflections increase general column deflections at all levels of loading. This significantly reduces column strength due to the reduced geometrical stiffness caused by axial loads acting through increased lateral deflections.

11) The effect of increasing the eccentricity of applied axial loads decreases the load carrying capacity of the column over the full slenderness range. Increased eccentricity also significantly reduces the column stability, with instability failures occurring at lower slenderness values as the eccentricity increases.

12) The presence of increased end restraint significantly reduces the influence of these geometrical imperfections.

13) The distribution of internal column stresses changes significantly as end restraint stiffness increases. For the more rigid connection types this may change the position of first yield from mid-height to the ends of the column.

14) The effective length factors of columns are reduced as the end restraint stiffness increases. For each connection type the effective length factors vary very little over the range of slendernesses considered.

This reduction in effective length factors suggests the possibility of improved economy in column design if semi-rigid end restraint is properly taken into account.

8.3 Recommendations for Future Work

The present investigation is restricted to the study of the in-plane behaviour of isolated members with

semi-rigid connections attached to rigid beams in a no-sway situation. This work requires development in the following areas:-

1) The inclusion of realistic beam stiffnesses is required in the analysis to account for the restraining effect of members attached at the column ends. The present analysis makes the simplifying assumption that the connections are made with rigid supports (infinitely stiff beams). A limited frame approach would enable beam stiffnesses to be included, which would give a better representation of the actual end restraint conditions of the column.

2) A study of the complete load-deflection behaviour of a column is necessary, the present analysis will only find the load-deflection relationship up to the maximum load value. Little information is available on this post-maximum load-deflection bahaviour. For isolated members this is only of academic interest, however, in the context of frame behaviour the complete load-deflection behaviour is important. After a member in a frame has reached its maximum load it will start to unload, the amount by which it unloads is important because this load will be redistributed to other members within the frame.

3) So far members have only been studied in isolation whereas the normal situation is within a structural frame system, from which members obtain their semi-rigid end restraint. The extension of the

analysis to semi-rigidly connected frames should be investigated. This would require the analysis to deal with both sway and no-sway situations.

4) This then leads to the field of frame stability as a possible area of investigation.

5) All work in the present investigation has been restricted to the in-plane behaviour of members. Studies of the influences of semi-rigid end connections on flexural-torsional bending and biaxial bending are required as little work has been done in these fields.

Before these effects can be properly studied the following experimental data is required:-

1) More up-to-date data relating to the connection techniques that are presently used in practice.

2) Data relating to other connection degrees of freedom; such as in-plane axial and shear deformations, and the out-of-plane lateral shear, twisting and lateral bending deformations. The extension of the analysis to include the effects of semi-rigid end restraint in these other degrees of freedom would only involve modification to the overall stiffness matrix, in a similar manner to that for semi-rigid flexural rigidity. It is the lack of experimental data that prevents these modifications from being implemented.

APPENDIX A

APPENDIX A

EXPERIMENTAL DATA DETAILS

This appendix contains details of the connections used in each test by the various experimenters listed in Tables 3.1, 3.2 and 3.3; the following types of connections are included:

1) Single Web Cleat

2) Double Web Cleats

3) Header Plate

4) Top and Seat Flange Cleats

5) End Plate without Column Stiffeners

6) End Plate with Column Stiffeners

7) Welded Top Plate and Seat Angle

8) T-Stubs

9) Combined Top and Seat Angle with Web Cleats

10) Combined T-Stubs with Web Cleats

N.B. All member sizes, in the following tables, are given in the units in which they were reported. Most reported data is in Imperial units, however, metric sizes are marked with an asterisk (*).

TABLE A.1 - Single Web Cleated Connection Data

Experimenter	Test No.	Beam Size	Column Size	Web Cleat Size	Type of Fastener
Johnston and Deits (39)	W13	18WF85	12WF92	$3 \times 2 \times \frac{1}{4} \times 12$	Welded
	W14	18WF47	12WF65	$3 \times 2 \times \frac{1}{4} \times 6$	Welded
	W15	12WF50	10WF45	$3 \times 2 \times \frac{1}{4} \times 6$	Welded
	W16	12WF25	10WF45	$3 \times 2 \times \frac{1}{4} \times 5$	Welded
Sommer (40)	21	18WF45	14WF38	$3\frac{1}{2} \times 3 \times \frac{3}{8} \times 9$	$\frac{3}{4}$ Bolts
	22	18WF45	14WF38	$3\frac{1}{2} \times 3 \times \frac{3}{8} \times 12$	$\frac{3}{4}$ Bolts
	23	24WF76	14WF38	$4 \times 3 \times \frac{3}{8} \times 15$	$\frac{3}{4}$ Bolts
	24	24WF76	14WF38	$4 \times 3 \times \frac{3}{8} \times 20$	$\frac{3}{4}$ Bolts

Experimenter	Series	Number of Specimens	Web Cleat Size	Number of Bolts
Lipson (41)	A1	11	$4 \times 3 \times \frac{3}{8} \times 4$	2-12 inclusive
	A2	5	$4 \times 3 \times \frac{3}{8} \times 4$	4, 6, 8, 10, 12
	A3	5	$4 \times 3 \times \frac{3}{8} \times 4$	2, 3, 7, 9, 11
	B	11	$4 \times 3 \times \frac{3}{8} \times 4$	2-12 inclusive
	C	11	$4 \times 3 \times \frac{3}{8} \times 4$	2-12 inclusive

N.B. Lipson (41) uses the same beam section (21WF62) and column section (1 in Plate) in all tests, varying only the number of bolts (3/4 in HSFG Bolts).

TABLE A.2 - Double Web Cleated Connection Data

Experimenter	Test No.	Beam Size	Column Size	Web Cleats Size	Type of Fastener
Batho + Rowan (8)	8	12 × 5 @ 30	12 × 8 @ 65	6 × $3\frac{1}{2}$ × $\frac{3}{8}$ × 9	$\frac{3}{4}$ Rivets
	9	12 × 5 @ 30	12 × 8 @ 65	6 × $3\frac{1}{2}$ × $\frac{1}{2}$ × 9	$\frac{3}{4}$ Rivets
	10	12 × 5 @ 30	12 × 8 @ 65	6 × $3\frac{1}{2}$ × $\frac{5}{8}$ × 9	$\frac{3}{4}$ Rivets
Rathbun (11)	1	6 I @ 12.5	9 × $\frac{1}{2}$ × 10 - Pl	6 × 4 × $\frac{3}{8}$ × $2\frac{1}{2}$	$\frac{7}{8}$ Rivets
	2	8 I @ 18.4	9 × $\frac{1}{2}$ × 12 - Pl	6 × 4 × $\frac{3}{8}$ × 6	$\frac{7}{8}$ Rivets
	3	8 I @ 18.4	$11\frac{3}{4}$ × $\frac{1}{2}$ × 13 - Pl	6 × 6 × $\frac{3}{8}$ × 6	$\frac{7}{8}$ Rivets
	4	12 I @ 31.8	9 × $\frac{1}{2}$ × 16 - Pl	4 × $3\frac{1}{2}$ × $\frac{3}{8}$ × 9	$\frac{7}{8}$ Rivets
	5	12 I @ 31.8	13 × $\frac{1}{2}$ × 16 - Pl	6 × 6 × $\frac{3}{8}$ × 9	$\frac{7}{8}$ Rivets
	6	18 I @ 54.7	9 × $\frac{3}{4}$ × 24 - Pl	4 × $3\frac{1}{2}$ × $\frac{3}{8}$ × 15	$\frac{7}{8}$ Rivets
	7	18 I @ 54.7	13 × $\frac{3}{4}$ × 24 - Pl	6 × 6 × $\frac{3}{8}$ × 15	$\frac{7}{8}$ Rivets

Continued . . .

TABLE A.2 - (Continued)(1)

Experimenter	Test No.	Beam Size	Column Size	Web Cleats Size	Type of Fastener
Munse, et. al. (28)	FK-4A	18WF50	12WF65	$6 \times 4 \times \frac{3}{8} \times 11\frac{1}{2}$	$\frac{3}{4}$ Rivets/Bolts
	FK-4B	18WF50	12WF65	$6 \times 4 \times \frac{3}{8} \times 11\frac{1}{2}$	$\frac{3}{4}$ Rivets/Bolts
	FK-4C	18WF50	12WF65	$6 \times 4 \times \frac{3}{8} \times 11\frac{1}{2}$	$\frac{3}{4}$ Rivets/Bolts
	FK-4R	18WF50	12WF65	$6 \times 4 \times \frac{3}{8} \times 11\frac{1}{2}$	$\frac{3}{4}$ Rivets
Mathison (42)	1	12WF27	10WF33	$4 \times 3\frac{1}{2} \times \frac{3}{8} \times 8\frac{1}{2}$	$\frac{3}{4}$ HT Bolts
	2	12WF27	10WF33	$4 \times 3\frac{1}{2} \times \frac{3}{8} \times 8\frac{1}{2}$	$\frac{3}{4}$ HT Bolts
	3	12WF27	10WF33	$4 \times 3\frac{1}{2} \times \frac{3}{8} \times 8\frac{1}{2}$	$\frac{3}{4}$ HT Bolts
	4	12WF27	10WF33	$4 \times 3\frac{1}{2} \times \frac{7}{16} \times 8\frac{1}{2}$	$\frac{3}{4}$ HT Bolts

Continued . . .

TABLE A.2 - (Continued) (2)

Experimenter	Test No.	Beam Size	Column Size	Web Cleats Size	Type of Fastener
Howe (43)	1	12WF27	10WF33	$4 \times 3\frac{1}{2} \times \frac{3}{8} \times 8\frac{1}{2}$	$\frac{3}{4}$ HSFG Bolts
	2	12WF27	10WF33	$4 \times 3\frac{1}{2} \times \frac{3}{8} \times 8\frac{1}{2}$	$\frac{3}{4}$ HSFG Bolts
	3	12WF27	10WF33	$4 \times 3\frac{1}{2} \times \frac{3}{8} \times 8\frac{1}{2}$	$\frac{3}{4}$ HSFG Bolts
	4	12WF27	10WF30	$4 \times 3\frac{1}{2} \times \frac{3}{8} \times 8\frac{1}{2}$	$\frac{3}{4}$ HSFG Bolts
Leon (44)	1	14WF30	10WF33	$4 \times 3\frac{1}{2} \times \frac{3}{8} \times 8\frac{1}{2}$	$\frac{3}{4}$ HSFG Bolts
	2	14WF30	10WF33	$4 \times 3\frac{1}{2} \times \frac{3}{8} \times 8\frac{1}{2}$	$\frac{3}{4}$ HSFG Bolts
	3	14WF30	10WF33	$4 \times 3\frac{1}{2} \times \frac{3}{8} \times 8\frac{1}{2}$	$\frac{3}{4}$ HSFG Bolts
	4	16WF36	10WF33	$4 \times 3\frac{1}{2} \times \frac{3}{8} \times 8\frac{1}{2}$	$\frac{3}{4}$ HSFG Bolts
	5	18WF50	10WF33	$4 \times 3\frac{1}{2} \times \frac{3}{8} \times 11\frac{1}{2}$	$\frac{3}{4}$ HSFG Bolts
	6	21WF62	10WF33	$4 \times 3\frac{1}{2} \times \frac{3}{8} \times 14\frac{1}{2}$	$\frac{3}{4}$ HSFG Bolts

Continued . . .

TABLE A.2 (Continued) (3)

Experimenter	Test No.	Beam Size	Column Size	Web Cleats Size	Type of Fastener
Lewitt, et. al. (38)	FK-3	12WF27	10WF49	$6 \times 4 \times \frac{3}{8} \times 8\frac{1}{2}$	$\frac{3}{4}$ Bolts/Rivets
	FK-4AB	18WF50	12WF65	$6 \times 4 \times \frac{3}{8} \times 11\frac{1}{2}$	$\frac{3}{4}$ Bolts
	FK-4AB-M	18WF50	12WF65	$6 \times 4 \times \frac{3}{8} \times 11\frac{1}{2}$	$\frac{3}{4}$ Bolts
	FK-4P	18WF50	12WF65	$6 \times 4 \times \frac{3}{8} \times 11\frac{1}{2}$	$\frac{3}{4}$ Bolts/Rivets
	WK-4	18WF50	12WF65	$6 \times 4 \times \frac{3}{8} \times 11\frac{1}{2}$	$\frac{3}{4}$ Bolts/Rivets
	FB-4	18WF50	12WF65	$4 \times 3\frac{1}{2} \times \frac{3}{8} \times 11\frac{1}{2}$	$\frac{3}{4}$ Bolts/Rivets
	FB-4A	18WF50	12WF65	$4 \times 3\frac{1}{2} \times \frac{3}{8} \times 11\frac{1}{2}$	$\frac{3}{4}$ Bolts/Rivets
	FK-5	21WF62	12WF65	$6 \times 4 \times \frac{7}{16} \times 14\frac{1}{2}$	$\frac{3}{4}$ Bolts/Rivets
	WB-10AB	18WF50	12WF65	$4 \times 4 \times \frac{7}{16} \times 29\frac{1}{2}$	$\frac{3}{4}$ Bolts
Bergquist (45)	A	W10 × 21	W10 × 29	$4 \times 3\frac{1}{2} \times \frac{1}{4} \times 8$	$\frac{7}{8}$ Bolts
	B	W10 × 21	W10 × 29	$4 \times 3\frac{1}{2} \times \frac{1}{4} \times 8$	$\frac{7}{8}$ Bolts/Welded
	C	W10 × 21	W10 × 29	$4 \times 3\frac{1}{2} \times \frac{1}{4} \times 8$	$\frac{7}{8}$ Welded/Bolts

TABLE A.3 - Header Plate Connection Data

Experimenter	Test No.	Beam Size	Column Size	Plate Size	Type of Fastener
Sommer (40)	5	18WF45	14WF38	15 × 6 × $\frac{1}{4}$	$\frac{3}{4}$ Bolts
	6	24WF76	14WF38	9 × 6 × $\frac{1}{4}$	$\frac{3}{4}$ Bolts
	7	24WF76	14WF38	12 × 6 × $\frac{1}{4}$	$\frac{3}{4}$ Bolts
	8	24WF76	14WF38	15 × 6 × $\frac{1}{4}$	$\frac{3}{4}$ Bolts
	9	24WF76	14WF38	18 × 6 × $\frac{1}{4}$	$\frac{3}{4}$ Bolts
	10	18WF45	14WF38	9 × 6 × $\frac{3}{8}$	$\frac{3}{4}$ Bolts
	11	18WF45	14WF38	12 × 6 × $\frac{3}{8}$	$\frac{3}{4}$ Bolts
	12	24WF76	14WF38	15 × 6 × $\frac{3}{8}$	$\frac{3}{4}$ Bolts
	13	24WF76	14WF38	9 × 6 × $\frac{3}{8}$	$\frac{3}{4}$ Bolts
	14	24WF76	14WF38	12 × 6 × $\frac{3}{8}$	$\frac{3}{4}$ Bolts
	15	24WF76	14WF38	15 × $7\frac{1}{2}$ × $\frac{3}{8}$	$\frac{3}{4}$ Bolts
	16	24WF76	14WF38	18 × $7\frac{1}{2}$ × $\frac{3}{8}$	$\frac{3}{4}$ Bolts
	17	24WF76	14WF38	12 × $7\frac{1}{2}$ × $\frac{1}{4}$	$\frac{3}{4}$ Bolts
	18	24WF76	14WF38	15 × $7\frac{1}{2}$ × $\frac{1}{4}$	$\frac{3}{4}$ Bolts
	19	24WF76	14WF38	12 × $7\frac{1}{2}$ × $\frac{1}{4}$	$\frac{3}{4}$ Bolts
	20	24WF76	14WF38	15 × $7\frac{1}{2}$ × $\frac{1}{4}$	$\frac{3}{4}$ Bolts

TABLE A.4 - Top and Seat Flange Cleated Connection Data

Experimenter	Test No.	Beam Size	Column Size	Top Cleat Size	Seat Cleat Size	Type of Fastener
Batho and Rowan (8)	1	12 × 5 @ 30	12 × 8 @ 65	4 × 4 × $\frac{1}{2}$ × 5	4 × 4 × $\frac{1}{2}$ × 5	$\frac{3}{4}$ Rivets
	2	12 × 5 @ 30	12 × 8 @ 65	4 × 4 × $\frac{3}{4}$ × 5	4 × 4 × $\frac{3}{4}$ × 5	$\frac{3}{4}$ Rivets
	3	12 × 5 @ 30	12 × 8 @ 65	4 × 4 × 1 × 5	4 × 4 × 1 × 5	$\frac{3}{4}$ Rivets
	4	12 × 5 @ 30	12 × 8 @ 65	4 × 4 × 1 × 5	4 × 4 × 1 × 5	$\frac{3}{4}$ Rivets
	5	12 × 5 @ 30	12 × 8 @ 65	6 × 6 × $\frac{1}{2}$ × 5	6 × 6 × $\frac{1}{2}$ × 5	$\frac{3}{4}$ Rivets
	6	12 × 5 @ 30	12 × 8 @ 65	6 × 6 × $\frac{3}{4}$ × 5	6 × 6 × $\frac{3}{4}$ × 5	$\frac{3}{4}$ Rivets
	7	12 × 5 @ 30	12 × 8 @ 65	6 × 6 × 1 × 5	6 × 6 × 1 × 5	$\frac{3}{4}$ Rivets
	16	12 × 5 @ 30	12 × 8 @ 65	6 × 6 × $\frac{3}{8}$ × 5	6 × 6 × $\frac{3}{8}$ × 5	$\frac{3}{4}$ HT Bolts
	17	12 × 5 @ 30	12 × 8 @ 65	6 × 6 × $\frac{1}{2}$ × 5	6 × 6 × $\frac{1}{2}$ × 5	$\frac{3}{4}$ HT Bolts
	18	12 × 5 @ 30	12 × 8 @ 65	6 × 6 × $\frac{3}{4}$ × 5	6 × 6 × $\frac{3}{4}$ × 5	$\frac{3}{4}$ HT Bolts
Rathbun (11)	8	12 I @ 31.8	6 × 1 × 24 - Pl	6 × 4 × $\frac{3}{8}$ × 6	6 × 6 × $\frac{3}{8}$ × 6	$\frac{7}{8}$ Rivets
	9	12 I @ 31.8	8 × 1 × 24 - Pl	6 × 4 × $\frac{3}{8}$ × 8	6 × 6 × $\frac{3}{8}$ × 8	$\frac{7}{8}$ Rivets
	10	12 I @ 31.8	14 × 1 × 24 - Pl	6 × 4 × $\frac{3}{8}$ × 14	6 × 6 × $\frac{3}{8}$ × 14	$\frac{7}{8}$ Rivets

Continued . . .

TABLE A.4 - (Continued)(1)

Experimenter	Test No.	Beam Size	Column Size	Top Cleat Size	Seat Cleat Size	Type of Fastener
Hechtman and Johnston (5)	2	12WF25	10WF49	$6 \times 4 \times \frac{5}{8} \times 6\frac{3}{4}$	$6 \times 6 \times \frac{1}{2} \times 6\frac{3}{4}$	$\frac{3}{4}$ Rivets
	5	18WF47	12WF65	$6 \times 4 \times \frac{1}{2} \times 12$	$6 \times 6 \times \frac{7}{8} \times 7\frac{1}{2}$	$\frac{3}{4}$ Rivets
	9	18WF47	12WF65	$6 \times 4 \times \frac{5}{8} \times 12$	$6 \times 6 \times \frac{7}{8} \times 7\frac{1}{2}$	$\frac{3}{4}$ Rivets
	10	18WF47	12WF65	$6 \times 4 \times \frac{3}{4} \times 12$	$6 \times 6 \times \frac{7}{8} \times 7\frac{1}{2}$	$\frac{3}{4}$ Rivets
	11	18WF47	14WF58	$6 \times 4 \times \frac{1}{2} \times 10$	$6 \times 6 \times \frac{7}{8} \times 7\frac{1}{2}$	$\frac{3}{4}$ Rivets
	16	12WF25	10WF49	$6 \times 4 \times \frac{1}{2} \times 6\frac{3}{4}$	$6 \times 6 \times \frac{1}{2} \times 6\frac{3}{4}$	$\frac{3}{4}$ Rivets
	17	12WF25	10WF49	$6 \times 4 \times \frac{1}{2} \times 6\frac{3}{4}$	$6 \times 6 \times \frac{1}{2} \times 6\frac{3}{4}$	$\frac{3}{4}$ Rivets
	18	12WF50	10WF49	$6 \times 4 \times \frac{1}{2} \times 8$	$6 \times 6 \times \frac{1}{2} \times 8$	$\frac{3}{4}$ Rivets
	20	14WF34	12WF34	$6 \times 4 \times \frac{5}{8} \times 12$	$6 \times 6 \times \frac{5}{8} \times 7\frac{1}{4}$	$\frac{3}{4}$ Rivets
	22	16WF40	12WF65	$6 \times 4 \times \frac{5}{8} \times 12$	$6 \times 6 \times \frac{3}{4} \times 7\frac{1}{2}$	$\frac{3}{4}$ Rivets

Continued . . .

Continued . . .

TABLE A.4 - (Continued)(2)

Experimenter	Test No.	Beam Size	Column Size	Top Cleat Size	Seat Cleat Size	Type of Fastener
Hechtman and Johnston (5) (Continued)	23	16WF40	14WF58	$6 \times 4 \times \frac{5}{8} \times 10$	$6 \times 6 \times \frac{3}{4} \times 7\frac{1}{4}$	$\frac{3}{4}$ Rivets
	24	18WF47	12WF65	$6 \times 4 \times \frac{5}{8} \times 12\frac{1}{2}$	$6 \times 6 \times \frac{7}{8} \times 7\frac{1}{2}$	$\frac{7}{8}$ Rivets
	25	21WF59	14WF87	$6 \times 4 \times \frac{3}{4} \times 14$	$6 \times 6 \times \frac{1}{2} \times 9\frac{1}{2}$	$\frac{7}{8}$ Rivets
	26	24WF74	14WF87	$6 \times 4 \times \frac{3}{4} \times 14$	$6 \times 6 \times \frac{1}{2} \times 9\frac{1}{2}$	$\frac{7}{8}$ Rivets
	31	24WF120	14WF87	$6 \times 4 \times \frac{7}{8} \times 14\frac{1}{2}$	Stiff Angle	$\frac{7}{8}$ Rivets
	32	21WF103	14WF87	$6 \times 4 \times \frac{7}{8} \times 14\frac{1}{2}$	Stiff Angle	$\frac{7}{8}$ Rivets
	35	12WF25	10WF49	$6 \times 4 \times \frac{5}{8} \times 8\frac{1}{2}$	$6 \times 6 \times \frac{1}{2} \times 8\frac{1}{2}$	$\frac{7}{8}$ Rivets
	36	18WF47	14WF58	$6 \times 4 \times \frac{5}{8} \times 11\frac{1}{4}$	$6 \times 6 \times \frac{7}{8} \times 11\frac{1}{4}$	$\frac{7}{8}$ Rivets
	37	18WF47	14WF58	$6 \times 4 \times \frac{5}{8} \times 11\frac{1}{4}$	$6 \times 6 \times \frac{7}{8} \times 11\frac{1}{4}$	$\frac{7}{8}$ Rivets

TABLE A.5 - End Plates without Column Stiffener Connection Data

Experimenter	Test No.	Beam Size	Column Size	End Plate Size	Type of Fastener
Sherbourne (46)	A1	15 × 5 @ 42	8 × 8 @ 35	$7 \times 18\frac{1}{2} \times 1\frac{1}{4}$	$\frac{3}{4}$ HT Bolts
Ostrander (47)	1	10WF21	8WF28	$6\frac{1}{2} \times 11 \times \frac{1}{2}$	Bolts
	3	10WF21	8WF28	$6\frac{1}{2} \times 11 \times \frac{3}{8}$	Bolts
	4	10WF21	8WF28	$6\frac{1}{2} \times 11 \times \frac{1}{4}$	Bolts
	9	10WF21	8WF28	$6\frac{1}{2} \times 11 \times \frac{3}{4}$	Bolts
	11	12WF27	8WF40	$7\frac{1}{2} \times 13 \times \frac{3}{8}$	Bolts
	12	12WF27	8WF40	$7\frac{1}{2} \times 13 \times \frac{1}{2}$	Bolts
	13	12WF27	8WF40	$7\frac{1}{2} \times 13 \times \frac{5}{8}$	Bolts
	17	12WF27	8WF24	$7\frac{1}{2} \times 13 \times \frac{3}{8}$	Bolts
	18	12WF27	8WF24	$7\frac{1}{2} \times 13 \times \frac{1}{2}$	Bolts
	19	12WF27	8WF24	$7\frac{1}{2} \times 13 \times \frac{5}{8}$	Bolts
	23	12WF27	8WF48	$7\frac{1}{2} \times 13 \times \frac{5}{8}$	Bolts

Continued . . .

TABLE A.5 - (Continued) (1)

Experimenter	Test No.	Beam Size	Column Size	End Plate Size	Type of Fastener
Bailey (48)	1	12 × 5 @ 32	8 × 8 @ 48	8 × $4\frac{1}{2}$ × 1	HSFG Bolts
	2	10 × 4 @ 17	8 × 8 @ 40	$6\frac{1}{2}$ × $4\frac{3}{8}$ × $\frac{3}{4}$	HSFG Bolts
	3	10 × 4 @ 19	8 × 8 @ 40	$6\frac{3}{4}$ × $4\frac{3}{8}$ × $\frac{3}{4}$	HSFG Bolts
Surtees and Mann (49)	C1	12 × 5 @ 25	8 × 8 @ 48	7 × 16 × $\frac{3}{4}$	$\frac{3}{4}$ HSFG Bolts
	C2	15 × 6 @ 40	10 × 10 @ 60	7 × $19\frac{1}{4}$ × $\frac{3}{4}$	1 HSFG Bolts
	C3	15 × 6 @ 40	10 × 10 @ 60	7 × $19\frac{1}{4}$ × $\frac{3}{4}$	1 HSFG Bolts
	C4	15 × 6 @ 40	10 × 10 @ 60	7 × $19\frac{1}{4}$ × 1	1 HSFG Bolts
	C5	15 × 6 @ 40	10 × 10 @ 60	7 × $19\frac{1}{4}$ × 1	1 HSFG Bolts
Zoetemeijer (50) *	2	IPE 300	HE200A	Not Reported	M20 HSFG Bolts
	9	IPE 300	HE200A	Not Reported	M20 HSFG Bolts
	10	IPE 300	HE200A	Not Reported	M20 HSFG Bolts
	20	IPE 400	HE300A	Not Reported	M22 HSFG Bolts
	21	IPE 400	HE300A	Not Reported	M22 HSFG Bolts
	22	IPE 400	HE300A	Not Reported	M22 HSFG Bolts

Continued . . .

TABLE A.5 - (Continued)(2)

Experimenter	Test No.	Beam Size	Column Size	End Plate Size	Type of Fastener
Zoetemeijer and Kolstein (51) *	1	HE240A	25 mm - Plate	240 × 230 × 25	M24 HSFG Bolts
	2	HE240A	25 mm - Plate	240 × 230 × 25	M20 HSFG Bolts
	3	IPE 400	25 mm - Plate	180 × 400 × 25	M24 HSFG Bolts
	4	IPE 400	25 mm - Plate	180 × 400 × 25	M16 HSFG Bolts
	5	IPE 300	25 mm - Plate	150 × 300 × 25	M24 HSFG Bolts
	6	IPE 300	25 mm - Plate	150 × 300 × 25	M16 HSFG Bolts
	7	IPE 400	HE240A	180 × 400 × 25	M24 HSFG Bolts
	8	IPE 400	HE240A	180 × 400 × 25	M24 HSFG Bolts
	11	IPE 400	HE240A	180 × 400 × 25	M24 HSFG Bolts
	12	IPE 400	HE240A	180 × 400 × 25	M24 HSFG Bolts
	13	IPE 300	HE240A	150 × 400 × 25	M24 HSFG Bolts
	14	IPE 300	HE240A	150 × 300 × 25	M24 HSFG Bolts
	17	IPE 300	HE240A	150 × 300 × 25	M24 HSFG Bolts
	18	IPE 300	HE240A	150 × 300 × 25	M24 HSFG Bolts
Grundy, et. al. (52) *	T-1	610UB113	310UC240	12 × 30 × 1	$\frac{7}{8}$ HSFG Bolts
	T-2	610UB113	310UC240	12 × 30 × $1\frac{1}{4}$	$\frac{7}{8}$ HSFG Bolts

TABLE A.6 - End Plates with Column Stiffener Connection Data

Experimenter	Test No.	Beam Size	Column Size	End Plate Size	Stiffener Size	Type of Fastener
Johnson, et. al. (53)	5	10 × $4\frac{1}{2}$ @ 25	8 × 8 @ 45	6 × $13\frac{1}{4}$ × $\frac{1}{2}$	3 × 8 × $\frac{1}{2}$	$\frac{3}{4}$ HT Bolts
Sherbourne (46)	A2	15 × 5 @ 42	8 × 8 @ 35	7 × 19 × $1\frac{1}{4}$	$3\frac{1}{2}$ × 7 × $\frac{5}{16}$	$\frac{3}{4}$ HT Bolts
	A3	15 × 5 @ 42	8 × 8 @ 35	7 × 19 × $\frac{3}{4}$	$3\frac{1}{2}$ × 7 × $\frac{5}{8}$	$\frac{3}{4}$ HT Bolts
	B1	15 × 5 @ 42	8 × 8 @ 35	7 × 19 × 1	$3\frac{1}{2}$ × 7 × $\frac{5}{16}$	$\frac{7}{8}$ HT Bolts
	B2	15 × 5 @ 42	8 × 8 @ 42	7 × 19 × $\frac{3}{4}$	$3\frac{1}{2}$ × 7 × $\frac{1}{2}$	$\frac{7}{8}$ HT Bolts
Ostrander (47)	2	10WF21	8WF28	$6\frac{1}{2}$ × 11 × $\frac{1}{2}$	3 × $7\frac{1}{8}$ × $\frac{3}{8}$	Bolts
	5	10WF21	8WF28	$6\frac{1}{2}$ × 11 × $\frac{1}{2}$	3 × $7\frac{1}{8}$ × $\frac{1}{4}$	Bolts
	6	10WF21	8WF28	$6\frac{1}{2}$ × 11 × $\frac{3}{8}$	3 × $7\frac{1}{8}$ × $\frac{1}{4}$	Bolts
	7	10WF21	8WF28	$6\frac{1}{2}$ × 11 × $\frac{1}{4}$	3 × $7\frac{1}{8}$ × $\frac{1}{4}$	Bolts
	8	10WF21	8WF28	$6\frac{1}{2}$ × 11 × $\frac{1}{4}$	3 × $7\frac{1}{8}$ × $\frac{3}{8}$	Bolts
	10	12WF27	8WF28	$6\frac{1}{2}$ × 11 × $\frac{3}{4}$	3 × $7\frac{1}{8}$ × $\frac{3}{8}$	Bolts
	14	12WF27	8WF40	$7\frac{1}{2}$ × 13 × $\frac{3}{8}$	4 × 7 × $\frac{1}{4}$	Bolts
	15	12WF27	8WF40	$7\frac{1}{2}$ × 13 × $\frac{1}{2}$	4 × 7 × $\frac{1}{4}$	Bolts
	16	12WF27	8WF40	$7\frac{1}{2}$ × 13 × $\frac{5}{8}$	4 × 7 × $\frac{1}{4}$	Bolts

Continued . . .

TABLE A.6 (Continued)(1)

Experimenter	Test No.	Beam Size	Column Size	End Plate Size	Stiffener Size	Type of Fastener
Ostrander (47) (Continued)	20	12WF27	8WF24	$7\frac{1}{2} \times 13 \times \frac{3}{8}$	$3 \times 7\frac{1}{8} \times \frac{1}{4}$	Bolts
	21	12WF27	8WF24	$7\frac{1}{2} \times 13 \times \frac{1}{2}$	$3 \times 7\frac{1}{8} \times \frac{1}{4}$	Bolts
	22	12WF27	8WF24	$7\frac{1}{2} \times 13 \times \frac{5}{8}$	$3 \times 7\frac{1}{8} \times \frac{1}{4}$	Bolts
	24	12WF27	8WF48	$7\frac{1}{2} \times 13 \times \frac{5}{8}$	$4 \times 6\frac{3}{4} \times \frac{1}{4}$	Bolts
Bailey (48)	4	12 × 5 @ 32	8 × 8 @ 40	$7 \times 4\frac{1}{2} \times 1\frac{1}{4}$	$\frac{5}{16}$ Stiffener	HSFG Bolts
	5	14 × 5 @ 26	8 × 8 @ 40	$7 \times 4\frac{1}{4} \times 1$	$\frac{5}{16}$ Stiffener	HSFG Bolts
	6	$14 \times 6\frac{3}{4}$ @ 45	8 × 8 @ 40	$8 \times 4\frac{5}{8} \times 1\frac{3}{8}$	$\frac{5}{16}$ Stiffener	HSFG Bolts
	7	$12 \times 6\frac{1}{2}$ @ 36	8 × 8 @ 40	$7\frac{1}{2} \times 4\frac{1}{2} \times 1\frac{1}{4}$	$\frac{5}{16}$ Stiffener	HSFG Bolts
	8	$8 \times 5\frac{1}{4}$ @ 20	8 × 8 @ 40	$6\frac{1}{2} \times 4\frac{1}{2} \times \frac{3}{4}$	$\frac{5}{16}$ Stiffener	HSFG Bolts
	9	$8 \times 5\frac{1}{4}$ @ 20	8 × 8 @ 40	$6\frac{1}{2} \times 4\frac{1}{2} \times \frac{3}{4}$	$\frac{5}{16}$ Stiffener	HSFG Bolts
	10	12 × 5 @ 32	8 × 8 @ 40	$7 \times 4\frac{1}{2} \times \frac{13}{16}$	$\frac{5}{16}$ Stiffener	HSFG Bolts
	11	14 × 5 @ 26	8 × 8 @ 40	$6\frac{1}{2} \times 4\frac{1}{4} \times \frac{7}{8}$	$\frac{5}{16}$ Stiffener	HSFG Bolts
	12	$12 \times 6\frac{1}{2}$ @ 36	8 × 8 @ 40	$7\frac{1}{2} \times 4\frac{3}{8} \times 1\frac{1}{16}$	$\frac{5}{16}$ Stiffener	HSFG Bolts
	13	$14 \times 6\frac{3}{4}$ @ 45	8 × 8 @ 40	$7\frac{1}{2} \times 4\frac{5}{8} \times 1\frac{1}{4}$	$\frac{5}{16}$ Stiffener	HSFG Bolts

Continued . . .

TABLE A.6 - (Continued)(2)

Experimenter	Test No.	Beam Size	Column Size	End Plate Size	Stiffener Size	Type of Fastener
Surtees and Mann (49)	C6	18 × 6 @ 55	10 × 10 @ 89	24 × 10 × $1\frac{1}{8}$	$\frac{1}{2}$ Stiffener	$1\frac{1}{8}$ HSFG Bolts
Zoetemeijer and Kolstein (51) *	9	IPE 400	HE240A	180 × 400	10mm Stiffener	M24 HSFG Bolts
	10	IPE 400	HE240A	180 × 400	10mm Stiffener	M24 HSFG Bolts
	15	IPE 300	HE240A	150 × 300	10mm Stiffener	M24 HSFG Bolts
	16	IPE 300	HE240A	150 × 300	10mm Stiffener	M24 HSFG Bolts
Packer and Morris(54) *	J1	254×102UB22	152×152UC37	368×152×15	Stiffener	M16 HSFG Bolts
	J2	254×102UB22	152×152UC37	368×152×15	Stiffener	M16 HSFG Bolts
	J3	254×102UB22	152×152UC37	368×152×15	Stiffener	M16 HSFG Bolts

TABLE A.7 - Welded Top Plate and Seat Connection Data

Experimenter	Test No.	Beam Size	Column Size	Top Plate Size	Seat Angle Size
Young and Jackson (10)	PA1	9 I 20.5	19 × 8 × 1 - Pl	$3 \times \frac{3}{8} \times 4\frac{1}{2}$	$5 \times 5 \times \frac{1}{2} \times 7$
	PA2	9 I 20.5	19 × 8 × 1 - Pl	$3 \times \frac{3}{8} \times 4\frac{1}{2}$	$5 \times 5 \times \frac{1}{2} \times 7$
	PB1	9 I 20.5	19 × 8 × 1 - Pl	$3\frac{1}{2} \times \frac{3}{8} \times 3\frac{1}{2}$	$5 \times 5 \times \frac{1}{2} \times 7$
	PB2	9 I 20.5	19 × 8 × 1 - Pl	$3\frac{1}{2} \times \frac{3}{8} \times 3\frac{1}{2}$	$5 \times 5 \times \frac{1}{2} \times 7$
	PC1	9 I 20.5	19 × 8 × 1 - Pl	$3 \times \frac{3}{8} \times 4$	$5 \times 5 \times \frac{1}{2} \times 7$
	PC2	9 I 20.5	19 × 8 × 1 - Pl	$3 \times \frac{3}{8} \times 4$	$5 \times 5 \times \frac{1}{2} \times 7$
	PD1	9 I 20.5	19 × 8 × 1 - Pl	$2\frac{3}{8} \times \frac{3}{8} \times 2\frac{3}{8}$	$5 \times 5 \times \frac{1}{2} \times 7$
	PD2	9 I 20.5	19 × 8 × 1 - Pl	$2\frac{3}{8} \times \frac{3}{8} \times 2\frac{3}{8}$	$5 \times 5 \times \frac{1}{2} \times 7$
	PE1	9 I 20.5	19 × 8 × 1 - Pl	$3\frac{1}{4} \times \frac{3}{8} \times 3\frac{7}{8}$	$5 \times 5 \times \frac{1}{2} \times 7$
	PE2	9 I 20.5	19 × 8 × 1 - Pl	$3\frac{1}{4} \times \frac{3}{8} \times 3\frac{7}{8}$	$5 \times 5 \times \frac{1}{2} \times 7$
Johnston and Deits (39)	W9	18WF47	12WF65	$6 \times \frac{5}{16} \times 11$	$6 \times 3\frac{1}{2} \times \frac{5}{8} \times 9$
	W10	18WF47	12WF65	$6 \times \frac{5}{16} \times 4$	$6 \times 3\frac{1}{2} \times \frac{5}{8} \times 9$

N.B. Pl - Plate

Continued . . .

TABLE A.7 - (Continued)(1)

Experimenter	Test No.	Beam Size	Column Size	Top Plate Size	Seat Angle Size
Brandes and Mains (55)	1	12WF25	10WF49	$5\frac{1}{2} \times \frac{3}{8} \times 7$	ST7WF21.5×$8\frac{1}{2}$
	2	12WF50	12WF65	$7 \times \frac{5}{8} \times 9$	ST13WF45.5×6
	3	12WF47	12WF65	$6 \times \frac{5}{8} \times 8$	ST9WF32×9
	4	12WF85	12WF65	$7\frac{1}{2} \times \frac{7}{8} \times 12$	ST15WF54×$7\frac{1}{2}$
	5	12WF85	12WF65	$7\frac{1}{2} \times \frac{7}{8} \times 12$	$8 \times 8 \times \frac{7}{8} \times 10$
	6	12WF85	12WF65	$7\frac{1}{2} \times \frac{7}{8} \times 12$	ST15WF54×$7\frac{1}{2}$
	7	12WF85	12WF65	$7\frac{1}{2} \times \frac{7}{8} \times 12$	ST15WF54×$7\frac{1}{2}$
	9	12WF85	12WF65	$7\frac{1}{4} \times 1 \times 12$	ST15WF54×$8\frac{1}{2}$
	10	12WF85	12WF65	$7\frac{1}{2} \times 1 \times 12$	$8 \times 8 \times 1 \times 10\frac{1}{2}$
	11	12WF85	12WF65	$6\&3 \times \frac{5}{16} \times 12$	Tee of Plates
					Continued . . .

Continued . . .

TABLE A.7 - (Continued)(2)

Experimenter	Test No.	Beam Size	Column Size	Top Plate Size	Seat Angle Size
Brandes and Mains(55) (Continued)	12	18WF85	12WF65	6&3 × $\frac{5}{16}$ × 12	Tee of Plates
	13	18WF70	12WF65	6&3 × $\frac{5}{16}$ × 12	6 × $3\frac{1}{2}$ × $\frac{3}{4}$ × 10
	14	18WF45	12WF65	6&3 × $\frac{5}{16}$ × 12	6 × $3\frac{1}{2}$ × $\frac{3}{4}$ × 9
	15	24WF74	14WF61	6&3 × $\frac{5}{16}$ × 12	Tee of Plates
	16	12WF85	12WF65	$10\frac{1}{2}$ × $\frac{3}{4}$ × 15	ST15WF54×$7\frac{1}{2}$
	17	12WF85	12WF65	$7\frac{1}{2}$ × $\frac{7}{8}$ × 12	ST15WF54×$7\frac{1}{2}$
	18	18WF85	12WF65	6&3 × $\frac{3}{8}$ × 12	Tee of Plates
Pray and Jensen (56)	1	14WF30	8 × 8WF	$6\frac{3}{4}$ × $\frac{3}{4}$ × $14\frac{3}{4}$	7 × 4 × $\frac{3}{4}$ × 9
Johnson (57)	4	10 × $4\frac{1}{2}$ @ 25	8 × 5 @ 28	$3\frac{1}{2}$ × $\frac{1}{2}$ × 4	4 × 4 × $\frac{1}{2}$ × 6
Johnson, et. al. (53)	6	10 × $4\frac{1}{2}$ @ 25	8 × 8 @ 45	8 × $\frac{1}{2}$ × $10\frac{1}{2}$	6 × $3\frac{1}{2}$ × $\frac{5}{8}$ × $5\frac{1}{2}$

TABLE A.8 - T-Stub Connection Data

Experimenter	Test No.	Beam Size	Column Size	T-Stub Size	Type of Fastener
Batho and Rowan (8)	13	12 × 5 @ 30	12 × 8 @ 65	ST15 × 6 @ 45	$\frac{7}{8}$ Rivets
	15	12 × 5 @ 30	12 × 8 @ 65	ST15 × 6 @ 45	$\frac{7}{8}$ Rivets
Rathbun (11)	13	12 I @ 31.8	9 × 1 × 22 - Pl	15G @ 99 × 9	$\frac{7}{8}$ Rivets
	14	12 I @ 31.8	14 × 1 × 22 - Pl	15G @ 99 × 14	$\frac{7}{8}$ Rivets
	15	16G @ 83	15 × 1 × 27 - Pl	24I @ 105.9×15	1 Rivets
	16	22G @ 101	15 × 1 × $39\frac{1}{2}$ - Pl	30G @ 204 × 15	1 Rivets
	17	22G @ 101	15 × 1 × $39\frac{1}{2}$ - Pl	30G @ 204 × 15	1 Rivets
	18	16G @ 83	14H @ 167	24I @ 105.9×15	1 Rivets

Continued . . .

TABLE A.8 - (Continued)

Experimenter	Test No.	Beam Size	Column Size	T-Stub Size	Type of Fastener
Douty (58)	D-1	14WF34	14WF150	18WF70	Bolts
	D-2	16WF40	14WF150	16WF40	Bolts
	D-3	21WF62	14WF150	21WF62	Bolts
Bannister((59)	a	10 × 8 BS	12 × 8 BS	24×7$\frac{1}{2}$ -Split I	$\frac{3}{4}$ Bolts
	b	10 × 8 BS	12 × 8 BS	24×7$\frac{1}{2}$ -Split I	$\frac{3}{4}$ Bolts
	c	10 × 8 BS	12 × 8 BS	24×7$\frac{1}{2}$ -Split I	$\frac{3}{4}$ Bolts
	d	10 × 8 BS	12 × 8 BS	24×7$\frac{1}{2}$ -Split I	$\frac{3}{4}$ Bolts
	e	10 × 8 BS	12 × 8 BS	24×7$\frac{1}{2}$ -Split I	
Zoetemeijer (50) *	8	IPE 300	HE200A	Not Reported	M20 HSFG Bolts
	12	IPE 400	HE300A	Not Reported	M22 HSFG Bolts
	19	IPE 400	HE300A	Not Reported	M22 HSFG Bolts
	23	IPE 400	HE300A	Not Reported	M22 HSFG Bolts

TABLE A.9 - Combined Top and Seat Angle with Web Cleats Connection Data

Experimenter	Test No.	Beam Size	Column Size	Top Angle Size	Seat Angle Size	Web Cleat Size	Type of Fastener
Batho and Rowan (8)	11	12×5@30	12×8@65	$6\times6\times\frac{1}{2}\times5$	$6\times6\times\frac{1}{2}\times5$	$6\times3\frac{1}{2}\times\frac{3}{8}\times9$	$\frac{3}{4}$ Rivets
	12	12×5@30	12×8@65	$6\times6\times\frac{1}{2}\times5$	$6\times6\times\frac{1}{2}\times5$	$6\times3\frac{1}{2}\times\frac{3}{8}\times9$	$\frac{3}{4}$ Rivets
Young and Jackson (10)	PJ1	18CB@47	12×1×42 - P1	$7\times\frac{3}{8}\times10\frac{5}{8}$	$7\times\frac{3}{8}\times10\frac{5}{8}$	$4\frac{1}{2}\times\frac{3}{8}\times6$	Welded
	PJ2	18CB@47	12×1×42 - P1	$7\times\frac{3}{8}\times10\frac{5}{8}$	$7\times\frac{3}{8}\times10\frac{5}{8}$	$4\frac{1}{2}\times\frac{3}{8}\times6$	Welded
	CJ1	18CB@47	12×12@110	$7\times\frac{3}{8}\times10\frac{5}{8}$	$7\times\frac{3}{8}\times10\frac{5}{8}$	$4\frac{1}{2}\times\frac{3}{8}\times6$	Welded
	CJ2	18CB@47	12×12@110	$7\times\frac{3}{8}\times10\frac{5}{8}$	$7\times\frac{3}{8}\times10\frac{5}{8}$	$4\frac{1}{2}\times\frac{3}{8}\times6$	Welded
Rathbun (11)	11	12I@31.8	9×1×24 - P1	$6\times4\times\frac{3}{8}\times9$	$6\times6\times\frac{3}{8}\times9$	$4\times3\frac{1}{2}\times\frac{3}{8}\times9$	$\frac{7}{8}$ Rivets
	12	12I@31.8	14×1×24 - P1	$6\times4\times\frac{3}{8}\times14$	$6\times6\times\frac{3}{8}\times14$	$4\times3\frac{1}{2}\times\frac{3}{8}\times9$	$\frac{7}{8}$ Rivets

TABLE A.10 - Combined T-Stub with Web Cleats Connection Data

Experimenter	Test No.	Beam Size	Column Size	T-Stub Size	Web Cleat Size	Type of Fastener
Batho and Rowan(8)	14	12×5@30	12×8@65	ST15×6@45	$6\times3\frac{1}{2}\times\frac{3}{8}$	$\frac{7}{8}$ Rivets
Young and Jackson (10)	PF1	18CB@47	12×1×42 - P1	$10\frac{5}{8}\times14\frac{1}{2}\times\frac{11}{16}\times12$	$4\frac{1}{2}\times\frac{3}{8}\times6$	$\frac{7}{8}$ Rivets
	PF2	18CB@47	12×1×42 - P1	$10\frac{5}{8}\times14\frac{1}{2}\times\frac{11}{16}\times12$	$4\frac{1}{2}\times\frac{3}{8}\times6$	$\frac{7}{8}$ Rivets
	CF1	18CB@47	12×12@110	$10\frac{5}{8}\times14\frac{1}{2}\times\frac{11}{16}\times12$	$4\frac{1}{2}\times\frac{3}{8}\times6$	$\frac{3}{4}$ Rivets
	CF2	18CB@47	12×12@110	$10\frac{5}{8}\times14\frac{1}{2}\times\frac{11}{16}\times12$	$4\frac{1}{2}\times\frac{3}{8}\times6$	$\frac{3}{4}$ Rivets
	PH1	18CB@47	12×1×42 - P1	$6\frac{5}{16}\times12\times\frac{7}{8}\times7\frac{1}{2}$	$4\frac{1}{2}\times\frac{3}{8}\times6$	Welded
	PH2	18CB@47	12×1×42 - P1	$6\frac{5}{16}\times12\times\frac{7}{8}\times7\frac{1}{2}$	$4\frac{1}{2}\times\frac{3}{8}\times6$	Welded
	CH1	18CB@47	12×12@110	$6\frac{5}{16}\times12\times\frac{7}{8}\times7\frac{1}{2}$	$4\frac{1}{2}\times\frac{3}{8}\times6$	Welded
	CH2	18CB@47	12×12@110	$6\frac{5}{16}\times12\times\frac{7}{8}\times7\frac{1}{2}$	$4\frac{1}{2}\times\frac{3}{8}\times6$	Welded

Continued . . .

TABLE A.10 - (Continued)

Experimenter	Test No.	Beam Size	Column Size	T-Stub Size	Web Cleat Size	Type of Fastener
Zoetemeijer (50) *	1	IPE 300	HE200A	Not Reported	Not Reported	M20 HSFG Bolts
	3	IPE 300	HE200A	Not Reported	Not Reported	M20 HSFG Bolts
	4	IPE 300	HE200A	Not Reported	Not Reported	M20 HSFG Bolts
	5	IPE 300	HE200A	Not Reported	Not Reported	M20 HSFG Bolts
	6	IPE 300	HE200A	Not Reported	Not Reported	M20 HSFG Bolts
	7	IPE 300	HE200A	Not Reported	Not Reported	M20 HSFG Bolts
	11	IPE 400	HE300A	Not Reported	Not Reported	M22 HSFG Bolts
	13	IPE 400	HE300A	Not Reported	Not Reported	M22 HSFG Bolts
	14	IPE 400	HE300A	Not Reported	Not Reported	M22 HSFG Bolts
	15	IPE 400	HE300A	Not Reported	Not Reported	M22 HSFG Bolts
	16	IPE 400	HE300A	Not Reported	Not Reported	M22 HSFG Bolts
	17	IPE 400	HE300A	Not Reported	Not Reported	M22 HSFG Bolts
	18	IPE 400	HE300A	Not Reported	Not Reported	M22 HSFG Bolts

APPENDIX B

APPENDIX B

CALCULATION OF EFFECTIVE LENGTH FACTORS

Basic Data

$\sigma_y = 345\ N/mm^2$, $E = 200\ kN/mm^2$

$I_c = 16.3\ in^4$, $I_g = 10.8\ in^4$

$L_c = 262\ in$, $L_g = 120\ in$

1. Calculated by Program Analysis

Maximum load capacity = 540.4 kN (0.284 P_y).

From Figure B.1 at a load level of 540.4 kN

$\lambda_{PIN} = 142$ and $\lambda_{WEB\ CLEATS} = 190$

$$\therefore \quad k = \frac{142}{190}$$

$$\underline{k = 0.747}$$

N.B. Figure B.1 shows column curves for a minor axis bending W10×29 section with both pinned and web cleated end condition. These have been calculated in the same way as column curves produced in the parametric study.

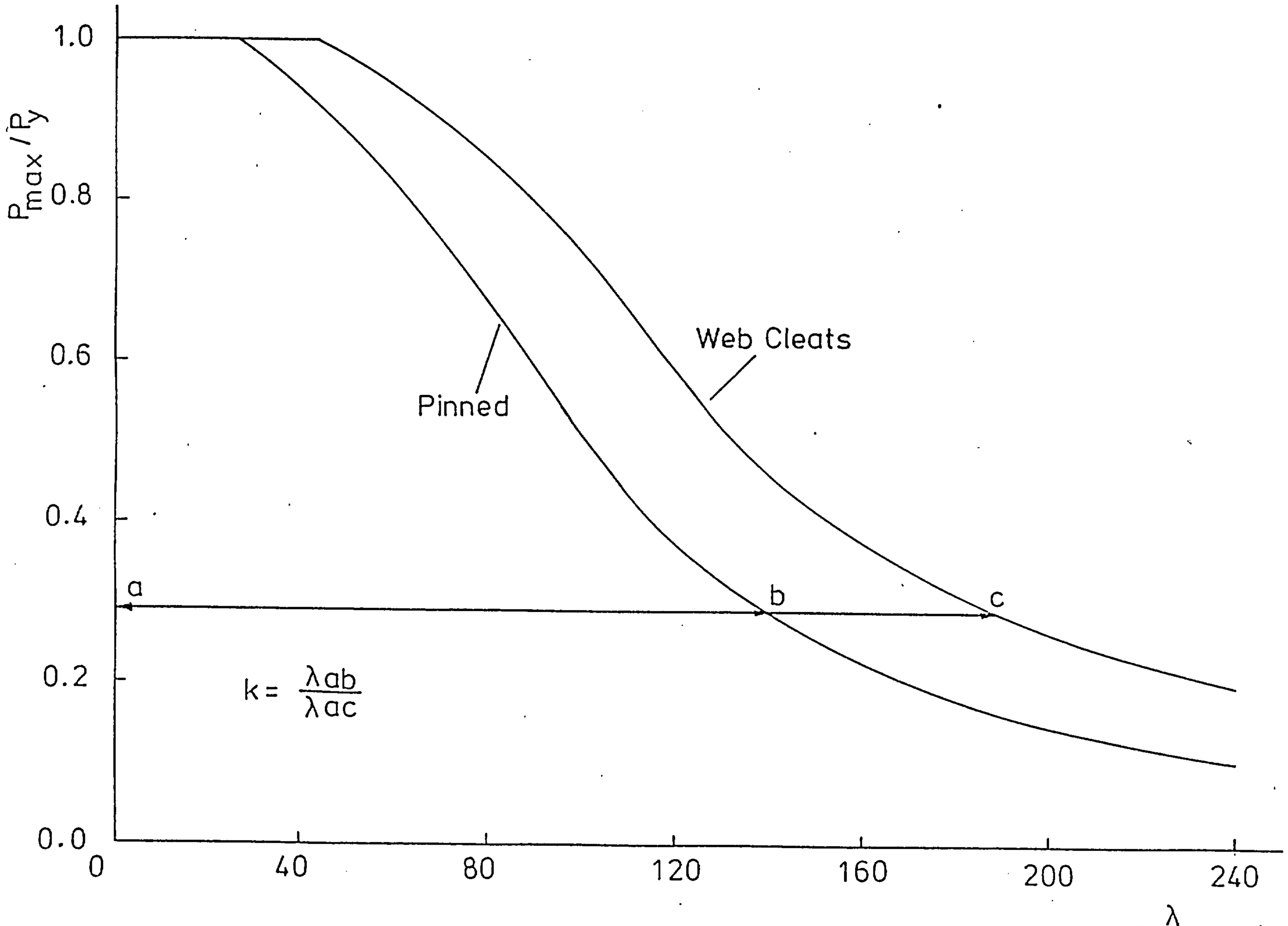

FIGURE B.1 - Column Curves for W10×29 Column Section with Pinned and Web Cleated Connections

$$\lambda' = \frac{kL}{\pi r}\sqrt{\frac{\sigma_y}{E}} \qquad \text{B.1}$$

$$\lambda' = \frac{0.747 \times 189.7}{\pi}\sqrt{\frac{345}{200000}}$$

$$\lambda' = 1.873$$

From SSRC Column Curve No. 2 (33)

$\sigma_u = 87.41\ N/mm^2$ Area = 5510 mm^2

$\therefore P_u = \underline{481.63\ kN}$ $(0.253\ P_y)$

2. <u>SSRC Alignment Chart - Rigid Jointed</u>

$$G = \frac{\Sigma(I_c/L_c)}{\Sigma(I_g/L_g)} \qquad \text{B.2}$$

$$G = \frac{(16.3/262)}{2(10.8/120)} = 0.346$$

From the SSRC sway prevented alignment chart

$$\underline{k = 0.645}$$

Substitute into equation B.1

$$\lambda' = 1.618$$

$$\therefore \underline{P_u = 0.315\ P_y}$$

3. SSRC Alignment Chart - Pin Jointed

When pin jointed $G = \infty$

$\therefore$ $k = 1.00$

Substitute into equation B.1

$$\lambda' = 2.508$$

$\therefore P_u = 0.156\ P_y$

4. BS 449: 1969

Column ends are restrained in position but not in direction

$\therefore$ Column to be designed as pin-jointed

$\therefore$ $k = 1.00$

As above: $\lambda' = 2.508$

$\therefore P_u = 0.156\ P_y$

5. De Falco and Marino (34) Modification

From table in reference 34 for a web cleated connection with three rows of fasteners the connection flexibility factor is:

$$Z = 3.1 \times 10^{-5} \text{ rad/kip-in}$$

For use in Driscoll's modification chart

$$C_p = \frac{I_g}{L_g} \times Z \times 10^5 \qquad B.3$$

$$C_p = \frac{10.8}{10} \times 3.1$$

$$C_p = 3.348$$

From Driscoll's chart for a braced frame

$$C_e = 0.87$$

Modified 'G' factor is then

$$G = \frac{\Sigma(I_c/L_c)}{C_e \Sigma(I_g/L_g)} \qquad B.4$$

$$G = \frac{0.346}{0.870}$$

$$G = 0.398$$

From SSRC alignment chart nomograph

$$\underline{k = 0.660}$$

Substitute into equation B.1

$$\lambda' = 1.655$$

$$\therefore P_u = 0.305\ P_y$$

6. Bergquist's Moment-Rotation Data

Flexibility factor of web cleated connection as measured experimentally by Bergquist (45).

$$Z = 0.94 \times 10^{-4} \text{ rad/kip-in}$$

Substitute in equation B.3

$$C_p = \frac{10.8}{10} \times 9.4$$

$$C_p = 10.152$$

Using Driscoll's braced frame chart

$$C_e = 0.67$$

Then in equation B.4

$$G = \frac{0.346}{0.670}$$

$$G = 0.516$$

From SSRC alignment chart nomograph

$$\underline{k = 0.690}$$

Substitute in equation B.1

$$\lambda' = 1.731$$

$$\therefore \underline{P_u = 0.286\ P_y}$$

7. Using Peterson and Cermak Flexibility Factor

In the discussion of Lother's (23) paper on elastic restraint equations Peterson and Cermak (84) proposed a method for calculating the flexibility factors of web cleated connections. For the connection being considered their method gives:

$$Z = 1.7 \times 10^{-4} \text{ rad/kip-in}$$

Substitute in equation B.3

$$C_p = \frac{10.8}{10} \times 17.0$$

$$C_p = 18.36$$

Using Driscoll's braced frame chart

$$C_e = 0.52$$

Which is then used in equation B.4

$$G = \frac{0.346}{0.520}$$

$$G = 0.665$$

From the SSRC alignment chart nomograph

$$\underline{k = 0.725}$$

Substitute in equation B.1

$$\lambda' = 1.818$$

$$\therefore \underline{P_u = 0.265 \cdot P_y}$$

REFERENCES

REFERENCES

1. BS449: 1969, "The Use of Structural Steel in Buildings", Part 2, B.S.I., London.

2. A.I.S.C., "Specification for the Design, Fabrication and Erection of Structural Steel for Buildings", A.I.S.C., New York, 1969.

3. A.S.1250, "Steel Structures", Standards Association of Australia, Sydney, 1975.

4. B.S.I., "Draft Standard Specification for the Structural Use of Steelwork in Building. Part I: Simple and Continuous Construction", B.S.I., London, 1977.

5. Hechtman, R. A. and Johnston, B. G., "Riveted Semi-Rigid Beam-to-Column Building Connections", Progress Report No. 1, Committee of Steel Structures Research, A.I.S.C., November 1947.

6. Wilson, W. M. and Moore, H. F., "Tests to Determine the Rigidity of Riveted Joints in Steel Structures", University of Illinois, Engineering Experimental Station, Bulletin No. 104, Urbana, U.S.A., 1917.

7. Steel Structures Research Committee, First Report, Department of Scientific and Industrial Research, H.M.S.O., London, 1931.

8. Steel Structures Research Committee, Second Report, Department of Scientific and Industrial Research, H.M.S.O., London, 1934.

9. Steel Structures Research Committee, Final Report, Department of Scientific and Industrial Research, H.M.S.O., London, 1936.

10. Young, C. R. and Jackson, K. B., "The Relative Rigidity of Welded and Riveted Connections", Canadian Journal of Research, Vol. 11, No. 1, pp. 62 - 100 and No. 2, pp. 101 - 134, Canada, 1934.

11. Rathbun, J. C., "Elastic Properties of Riveted Connections", Trans. A.S.C.E., Vol. 101, 1936, pp. 524 - 563.

12. Pippard, A. J. S. and Baker, J. F., "The Analysis of Engineering Structures", Arnold, 3rd Ed., London, 1936.

13. Cross, H., "Analysis of Continuous Frames by Distributing Fixed End Moments", Proc. A.S.C.E., Vol. 56, No. 5, 1930, pp. 919 - 928.

14. Johnston, B. G. and Mount, E. H., "Analysis of Building Frames with Semi-Rigid Connections", Trans. A.S.C.E., Vol. 107, 1942, pp. 993 - 1019.

15. Gere, J. M., "Moment Distribution", D. Van Nostrand, New York, 1963.

16. Stewart, R. W., "Analysis of Frames with Elastic Joints", Trans. A.S.C.E., Vol. 114, 1947, pp. 17 - 39.

17. Sourochnikoff, B., "Wind Stresses in Semi-Rigid Connections of Steel Framework", Trans. A.S.C.E., Vol. 115, 1950, pp. 382 - 402.

18. Lightfoot, E. and Baker, A. R., "The Analysis of Steel Frames with Elastic Beam-Column Connections", Golden Jubilee Congress Symposium on the Design of High Buildings", Hong Kong University Press, 1961, pp. 205 - 217.

19. Monforton, A. R. and Wu, T. S., "Matrix Analysis of Semi-Rigidly Connected Frames", Journal of the Structural Division, A.S.C.E., Vol. 89, ST6, December 1963, pp. 13 - 42.

20. Livesley, R. K., "Matrix Methods of Structural Analysis", Pergamon Press, 1st Ed., Oxford, 1975.

21. Gere, J. M. and Weaver, W., "Analysis of Framed Structures", D. Van Nostrand, Princeton, 1965.

22. Johnston, B. G. and Hechtman, R. A., "Design Economy by Connection Restraint", Engineering News-Record, 10 October 1940, pp. 74 - 77.

23. Lothers, J. E., "Elastic Restraint Equations for Semi-Rigid Connections", Trans. A.S.C.E., Vol. 116, 1951, pp. 480 - 502.

24. Huang, J. Y., "Derivation of an Elastic Restraint Equation for the Split Beam Semi-Rigid Beam-Column Connection", Masters Thesis, College of Engineering, Oklahoma State University, 1958.

25. Yu, S. Y., "The Derivation of an Equation for the Elastic Restraint of the Top and Seat Angle Type of Semi-Rigid Connection", Masters Thesis, College of Engineering, Oklahoma State University, 1953.

26. Yu, W. W., "The Derivation of an Elastic Restraint Equation for the Combined Top and Seat with Web Angle Semi- Rigid Beam-Column Connection", Masters Thesis, College of Engineering, Oklahoma State University, 1955.

27. Munse, W. H., "Fifty Years of Riveted, Bolted and Welded Steel Construction", Journal of the Construction Division, A.S.C.E., Vol. 102, CO3, September 1976, pp. 437 - 447.

28. Munse, W. H., Bell, W. G. and Chesson, E., "Behaviour of Riveted and Bolted Beam-to-Column Connections", Journal of the Structural Division, A.S.C.E., Vol. 85, ST3, March 1959, pp. 25 - 50.

29. Fisher, J. W. and Struik, J. H., "Guide to Design Criteria for Bolted and Riveted Joints", J. Wiley and Sons, New York, 1974.

30. Halldorsson, O. P. and Wang, C. K., "Stability Analysis of Frameworks by Matrix Methods", Journal of the Structural Division, A.S.C.E., Vol. 94, ST7, July 1968, pp. 1745 - 1760.

31. Przemieniecki, J. S., "Theory of Matrix Structural Analysis", McGraw Hill, New York, 1968.

32. Romstad, K. M. and Subramanian, C. V., "Analysis of Frames with Partial Connection Rigidity", Journal of the Structural Division, A.S.C.E., Vol. 96, ST11, November 1970, pp. 2283-2300.

33. Johnston, B. G. (Ed.), "Guide to Stability Design Criteria for Metal Structures", 3rd Ed., J. Wiley, New York, 1976.

34. De Falco, F. and Marino, F. J., "Column Stability in Type 2 Construction", A.I.S.C. Engineering Journal, Vol. 3, No. 2, April 1966, pp. 67 - 71.

35. Driscoll, G. C., "Effective Length of Columns with Semi-Rigid Connections", A.I.S.C. Engineering Journal, Vol. 13, No. 4, October 1976, pp. 109 - 115.

36. Wood, R. H., "Effective Lengths of Columns in Multistorey Buildings", The Structural Engineer, Vol. 52, No. 7, Part 1, July 1974, pp. 235 - 244.

37. Lightfoot, E. and Le Messurier, A. P., "Elastic Analysis of Frameworks with Elastic Connections", Journal of the Structural Division, A.S.C.E., Vol. 100, ST6, June 1974, pp. 1297 - 1309.

38. Lewitt, C. W., Chesson, E. and Munse, W. H., "Restraint Characteristics of Flexible Riveted and Bolted Beam-to-Column Connections", University of Illinois, Engineering Experimental Station Bulletin, No. 500, January 1969.

39. Johnston, B. G. and Deits, G. R., "Tests of Miscellaneous Welded Building Connections", The Welding Journal, Vol. 21, January 1942, pp. 5 - 27.

40. Sommer, W. H., "Behaviour of Welded Header Plate Connections", Masters Thesis, University of Toronto, Ontario, Canada, 1969.

41. Lipson, S. L., "Single-Angle Welded-Bolted Connections", Journal of the Structural Division, A.S.C.E., Vol. 103, ST3, March 1977, pp. 559 - 571.

42. Mathison, W., "Moment-Rotation Characteristics of Semi-Rigid, High Tensile Bolted Connections", Masters Thesis, McGill University, Montreal, Canada, August 1959.

43. Howe, J. W., "Moment-Rotation Characteristics of Semi-Rigid High Tensile Bolted Connections - II", Masters Thesis, McGill University, Montreal, Canada, April 1961.

44. Leon, E. V., "Moment-Rotation Characteristics of Semi-Rigid High Tensile Bolted Connections - III", Masters Thesis, McGill University, Montreal, Canada, April 1961.

45. Bergquist, D. J., "Tests on Columns Restrained by Beams with Simple Connections", Report No. 1, American Iron and Steel Institute Project No. 189, Department of Civil Engineering, University of Texas, Austin, Texas, January 1977.

46. Sherbourne, A. N., "Bolted Beam-to-Column Connections", The Structural Engineer, Vol. 39, June 1961, pp. 203 - 210.

47. Ostrander, J. R., "An Experimental Investigation of End Plate Connections", Masters Thesis, University of Saskatchewan, Canada, 1970.

48. Bailey, J. R., "Strength and Rigidity of Bolted Beam-to-Column Connections", Conference on Joints in Structures, Paper A4, University of Sheffield, U.K., 1970.

49. Surtees, J. O. and Mann, A. P., "End Plate Connections in Plastically Designed Structures, Conference on Joints in Structures, University of Sheffield, U.K., 1970.

50. Zoetemeijer, P., "A Design Method of the Tension Side of Statically Loaded, Bolted Beam-to-Column Connections", Stevin Laboratory, Technical University of Delft, Netherlands, Vol. 20. No. 1, 1974.

51. Zoetemeijer, P. and Kolstein, M. H., "Geboute Balk-Kolomvertindingen met Korte Kopplaat", Stevin Laboratory, Technical University of Delft, Netherlands, Report 6-75-20, 1975 (in Dutch).

52. Grundy, P., Thomas, I. R. and Bennetts, I. D., "Beam-to-Column Moment Connections", Journal of the Structural Division, A.S.C.E., Vol. 106, ST1, January 1980, pp. 313 - 330.

53. Johnson, L. G., Cannon, J. C. and Spooner, L. A., "High Tensile Preloaded Bolted Joints", British Welding Journal, Vol. 7, No. 9, September 1960, pp. 560 - 569.

54. Packer, J. A. and Morris, L. J., "A Limit State Design Method for the Tension Region of Bolted Beam-Column Connections", The Structural Engineer, Vol. 55, No. 10, October 1977, pp. 446 - 458.

55. Brandes, J. L. and Mains, R. M., "Report of Tests of Welded Top-Plate and Seat Connections", Welding Journal, March 1944, pp. 146 - 165.

56. Pray, R. F. and Jensen, C., "Welded Top Plate Beam-Column Connections", Welding Journal - Welding Research Supplement, Vol. 35, July 1956, pp. 338 - 347.

57. Johnson, L. G., "Tests on Welded Connections between I-Section Beams and Stanchions", British Welding Journal, Vol. 6, January 1959, pp. 38 - 46.

58. Douty, R. T., "Strength Characteristics of High Strength Bolted Connections with Particular Application to the Plastic Design of Steel Structures", Ph.D. Thesis, Cornell University, U.S.A., 1964.

59. Bannister, A., "Moment-Angle Change Relationships for Certain Connections Incorporating Friction Grip Bolts", Civil Engineering and Public Works Review, Vol. 61, Nos. 719 and 720, June 1966, pp. 755 - 758, July 1966, pp. 873 - 878.

60. Krishnamurthy, N. and Graddy, D. E., "Correlation between 2- and 3-Dimensional Finite Element Analysis of Steel Bolted End-Plate Connections", Computers and Structures, Vol. 6, Nos. 4 and 5, August and October 1976, pp. 381 - 389.

61. Krishnamurthy, N., "Steel Bolted End-Plate Connections", Proceedings of the International Conference on Finite Element Methods in Engineering, Adelaide, Australia, December 1976, pp. 23.1 - 23.16.

62. Krishnamurthy, N., "A Fresh Look at Bolted End-Plate Behaviour and Design", A.I.S.C. Engineering Journal, Vol. 15, No. 2, April 1978, pp. 39 - 49.

63. Krishnamurthy, N., Huang, H. T., Jeffrey, P. K. and Avery, L. K., "Analytical M-θ Curves for End-Plate Connections", Journal of the Structural Division, A.S.C.E., Vol. 105, ST1, January 1979, pp. 133 - 145.

64. Lipson, S. L. and Haque, M. I., "Elastic-Plastic Analysis of Single-Angle Bolted-Welded Connections using the Finite Element Method", Computers and Structures, Vol. 9, No. 6, December 1978, pp. 533 - 545.

65. Lionberger, S. R., "Statics and Dynamics of Building Frames with Nonrigid Connections", Ph.D. Thesis, Stanford University, U.S.A., 1967.

66. Lionberger, S. R. and Weaver, W., "Dynamic Response of Frames with Nonrigid Connections", Journal of the Engineering Mechanics Division, A.S.C.E., Vol. 95, EM1, February 1969, pp. 95 - 114.

67. Kennedy, D. J. L., "Moment-Rotation Characteristics of Shear Connections", A.I.S.C. Engineering Journal, Vol. 6, No. 3, October 1969, pp. 105 - 115.

68. Frye, M. J., "Analysis of Frames with Flexible Connections", Masters Thesis, University of Manitoba, Winnipeg, Canada, 1971.

69. Frye, M. J. and Morris, G. A., "Analysis of Flexibly Connected Steel Frames", Canadian Journal of Civil Engineering, Vol. 2, No. 3, September 1975, pp. 280 - 291.

70. Cox, M. G., "The Numerical Evaluation of B-Splines", Journal of the Institute of Maths Applications, Vol. 10, 1972, pp. 134 - 149.

71. Hayes, J. G., "Numerical Methods for Curve and Surface Fitting", The Institute of Mathematics and its Applications, May/June, 1974, pp. 144 - 152.

72. Zienkiewicz, O. C., "The Finite Element Method", McGraw-Hill, 3rd ed., London, 1977.

73. Rockey, K. C., Evans, H. R., Griffiths, D. W. and Nethercot, D. A., "The Finite Element Method - A Basic Introduction", Crosby Lockwood Staples, London, 1975.

74. Nath, B., "Fundamentals of Finite Elements for Engineers", The Athlone Press, London, 1974.

75. Gallagher, R. H. and Padlog, J., "Discrete Element Approach to Structural Instability Analysis", Journal of the American Institute of Aeronautics and Astronautics, Part 2, Vol. 1, No. 6, June 1963, pp. 1437 - 1439.

76. Ersvik, O. and Alpsten, G., "Experimentell Undersokning av Knäckhållfastheten has bredflänsprofiler HE200A Ritade på Olika Sätt", Stålbyggnadsinstitutet, Sweden, Report 19:3, December 1970 (in Swedish).

77. Nethercot, D. A., "Residual Stresses and their Influence upon the Lateral Buckling of Rolled Steel Beams", The Structural Engineer, Vol. 52, No. 3, March 1974, pp. 89 - 96.

78. Young, B. W., "Residual Stresses in Hot-Rolled Sections", Department of Engineering, University of Cambridge, CUED/C - Struct./TR. 8, 1971.

79. Dorn, W. S. and McCracken, D. D., "Numerical Methods with FORTRAN IV Case Studies for Engineers", J. Wiley, New York, 1972.

80. Jones, S. W., "Semi-Rigidly Restrained Column Analysis Program", Department of Civil Structural Engineering, University of Sheffield, October 1980.

81. Bergan, P. G. and Soreide, T., "A Comparative Study of Different Numerical Solution Techniques as Applied to a Nonlinear Structural Problem", Computer Methods in Applied Mechanics and Engineering, Vol. 2, 1973, pp. 185 - 201.

82. Timoshenko, S. P. and Gere, J. M., "Theory of Elastic Stability", McGraw Hill, 2nd Ed., New York, 1961.

83. Dwight, J. B., "Use of Perry Formula to Represent the New European Strut-Curves", Department of Engineering, Cambridge University, Technical Report No. CUED/C-Struct/TR-30, 1972.

84. Peterson, D. F. and Cermak, J. F., discussion of "Elastic Restraint Equations for Semi-Rigid Connections", by J. E. Lothers, Trans. A.S.C.E., Vol. 116, 1951, pp. 496 - 499.